DOE/ER/13000--T12

STANFORD SYNCHROTRON RADIATION LABORATORY

ACTIVITY REPORT FOR 1988

ABOUT THE STANFORD SYNCHROTRON RADIATION LABORATORY

SSRL is a national facility supported primarily by the Department of Energy for the utilization of synchrotron radiation for basic and applied research in the natural sciences and engineering. It is a user-oriented facility which welcomes proposals for experiments from all researchers.

The synchrotron radiation is produced by the 3.5 GeV storage ring, SPEAR, and the 15 GeV storage ring, PEP, operated by the Stanford Linear Accelerator Center (SLAC). SPEAR is dedicated to the production of synchrotron radiation during 50% of its operations time or about 4 months per year. The remainder of the time synchrotron radiation may be used parasitically during colliding beam runs for high energy physics experiments. Operation on PEP is generally parasitic.

SSRL currently has 25 experimental stations on the SPEAR and PEP storage rings. There are 180 active proposals for experimental work from 130 institutions involving approximately 700 scientists. There is normally no charge for use of beam time by experimenters.

Additional information for prospective users is contained in the booklet "User Guide". Further information about the facility may be obtained by writing or telephoning Katherine Cantwell at SSRL, SLAC Bin 69, PO Box 4349, Stanford, CA 94309-0210 - telephone (415)926-3191.

This report summarizes the activity at SSRL for the period January 1, 1988 to December 31, 1988.

SSRL is operated by the Department of Energy,
Office of Basic Energy Sciences, Division of Chemical Sciences.
Support for research by SSRL staff is provided by that Office's Division
of Materials Science. The SSRL Biotechnology Program is supported by the National Institutes of Health,
Biomedical Resource Technology Program, Division of Research Resources.

Stanford Synchrotron Radiation Laboratory
1988 ACTIVITY REPORT

TABLE OF CONTENTS

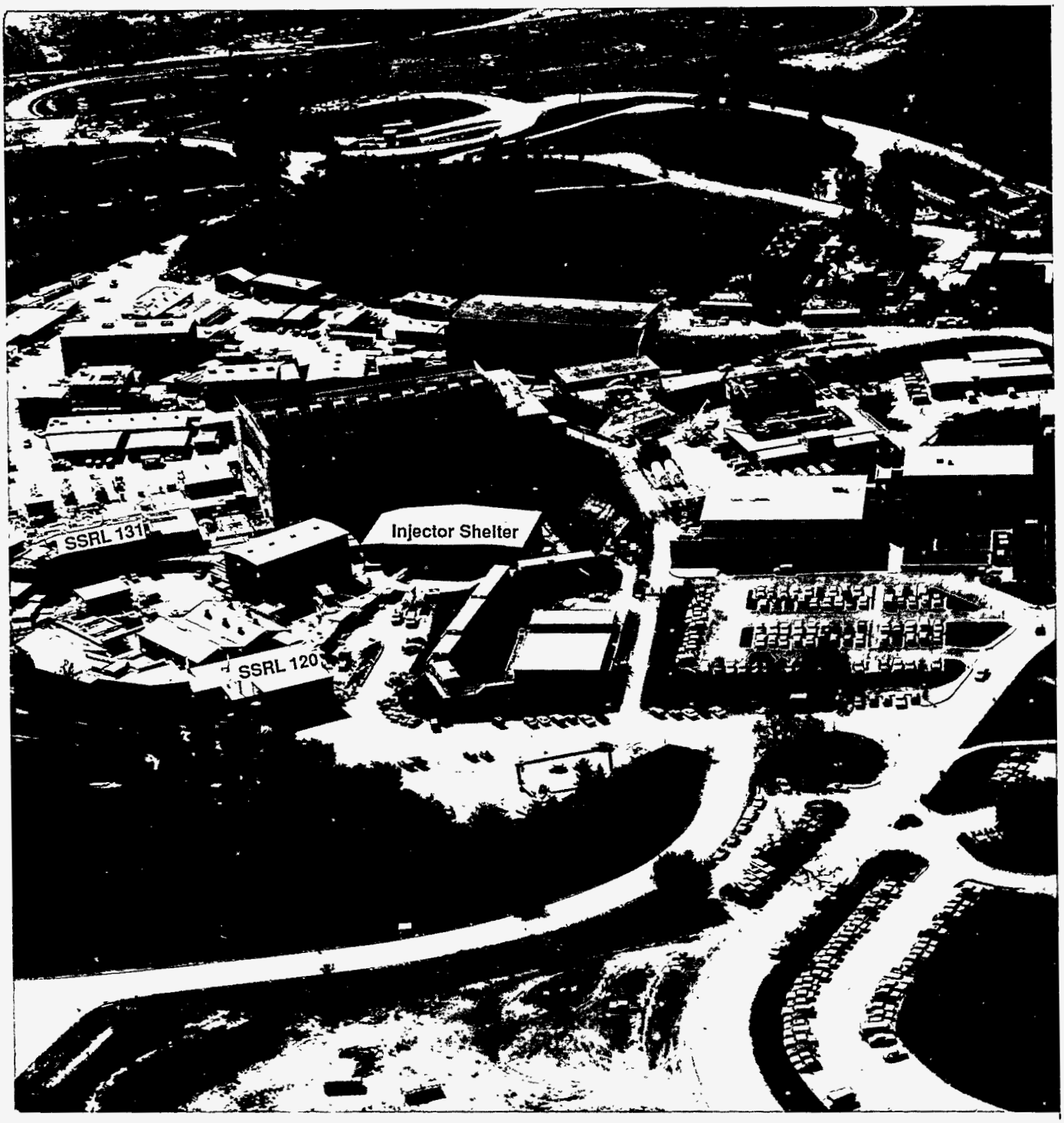

Overview of SSRL

-Photo by Joe Faust

The SPEAR ring is shown on the left side of the picture. SSRL has 23 stations housed in the two building (131, 120) adjacent to the north and south arcs of the ring. The large white building in the center is the shelter for the new 3 GeV injector. The building (LOS) on the far right houses the scientific, administrative and engineering staffs.

ACTIVITY REPORT 1988

INTRODUCTION

For SSRL operations, 1988 was a year of stark contrasts. The first extended PEP parasitic running since the construction of our two beam lines on that storage ring took place in November and December. Four experiments, discussed below, were performed and detailed operational procedures which allowed synchrotron radiation and high energy users to coexist were established. SSRL anticipates that there will be significant amounts of beam time when PEP is run again for high energy physics.

On the other hand, activity on SPEAR consisted of brief parasitic running on the VUV lines in December when the ring was operated at 1.85 GeV for colliding beam experiments. There was no dedicated SPEAR running throughout the entire calendar year. This is the first time since dedicated SPEAR operation was initiated in 1980 that there was no such running. The decision was motivated by both cost and performance factors, as discussed in Section 1 of this report.

Fortunately, SLAC and SSRL have reached an agreement on SPEAR and PEP dedicated time charges which eliminates the cost volatility which was so important in the cancellation of the June-July dedicated SPEAR run. As discussed in Section 2, the 3 GeV SPEAR injector construction is proceeding on budget and on schedule. This injector will overcome the difficulties associated with the SLC-era constraint of only two injections per day. SSRL and SLAC have also embarked on a program to upgrade SPEAR to achieve high reliability and performance. As a consequence, SSRL's users may anticipate a highly effective SPEAR by 1991, at the latest. At that time, SPEAR is expected to be fully dedicated to synchrotron radiation research and operated by SSRL. Thus, major advances in SSRL's ability to serve the community are anticipated.

FACILITY DEVELOPMENT

As implied above, the highest priority development project at SSRL is the 3 GeV injector, coupled with SPEAR improvement itself. Section 2 describes progress in its construction and presents many photographs of its components. Described as well in Section 2 are theoretical studies of low emittance SPEAR configurations as well as a variety of analyses of PEP. A major conclusion of the latter is that PEP could be brought to a high performance level for synchrotron radiation production at a cost of approximately $6.5M. A similar analysis of SPEAR is presently being performed.

Section 3 describes improvements to SSRL's experimental facilities. For the most part, these constitute improvements to, and upgrades of, existing beam lines. Among them, the completion of the Beam Line 5 monochromator stands out as a major addition to the Laboratory's capabilities. Also described are two branch lines, 6-1 and 10-1, which are presently under development, as well as improvements of the general support facilities.

Chapter 5 describes the second PEP Workshop held on November 2, 1988 as well as the 15th Annual SSRL Users Conference which was held on October 27-28, 1988.

EXPERIMENTAL PROGRESS REPORTS

The highlights of the past experimental year were the four experiments performed on PEP. These are described in detail in the Experimental Progress Reports 1096Mp, 2013M, 2035B and 8003M.

The first of these (1096 Mp) is an in-situ, time-resolved study of organometallic vapor phase epitaxy (OMVPE) using grazing incidence x-ray scattering (GIXS). GIXS is important for this purpose because the relatively high pressures present in the OMVPE chamber prevent application of other surface structure techniques like LEED, which require high vacuum. In this work, PEP's high brightness made the time resolution possible. It was also extremely valuable to have the isolation from other experimenters which PEP's single experiment facilities provide.

Progress Report 2013M describes a photoelectron spectroscopy study of Kr correlation satellites which was performed to support a more extensive program to determine an improved upper limit on the neutrino mass.

The initiation of time-resolved small-angle X-ray scattering studies on PEP is discussed in Progress Report 2035. These experiments sought to measure potential structural changes on a 10-100 millisecond time scale associated with the photocycling of bacteriorhodopsin in purple membrane, which functions as a light-driven proton pump. As part of a collaboration with KEK, a Fuji imaging plate was brought over from Japan for tests in time resolved mode. These experiments were later continued at SPEAR on Beam Line 4-2.

Progress Report 8003M describes a program to elucidate the physics of the dynamical diffraction of X-rays by nuclei at resonance. In this experiment, subtle frequency shifts of the effective transition energies were observed as the Bragg incidence angle was varied, an effect now explainable by an energy-dependent diffraction formalism.

Arthur Bienenstock
Director

I LABORATORY OPERATIONS

There was no dedicated synchrotron radiation experimental time in 1988 and only very limited parasitic time. On the bright side, the first experience with running PEP for synchrotron radiation in a mode parasitic with the high energy physics occurred. The staff of the laboratory directed its efforts to numerous improvement and maintenance projects in the absence of beam time.

Cancellation of the June-July Dedicated Run - Initially a dedicated run had been planned for the June-July, 1988 period. SSRL, in an unprecedented move, decided to cancel this run. This decision was based on three factors. (1) Due to the lower than anticipated LINAC use by the SLAC High Energy Physics program the cost of the June run would have been over $11,000 per shift. SSRL would not have been able to afford more than 70 shifts. (2) To turn on the storage ring, which had been idle since December, and start 22 user groups on line in a period of 70 shifts was judged to be inefficient. (3) SPEAR performance in the last run, late1987, had been very poor. There was reason to anticipate that the June run would also be poor. The entire SPEAR ring had been vented, a circumstance which would have led to short lifetimes for most of the short run. June was a critical time in the development of the SLAC Linear Collider (SLC) and SSRL anticipated that there would be little support for SPEAR operations available from SLAC. Finally, SSRL knew that funding for FY 1989 was low and would not allow use of all the shifts available. By using the carryforward created by not running in June, two substantial dedicated runs could be anticipated in 1989.

PEP Parasitic Running - In the first operation of PEP since 1986 four synchrotron radiation experiments (85 user shifts) were run on the two SSRL beam lines this fall, with exciting results (see Experimental Progress Reports 1096Mp, 2013M, 2035B, and 8003M). Colliding beam physics work commenced in October and shortly before Thanksgiving SSRL opened its PEP beam lines. Aside from the experimental results, much of the achievement of this run was in establishing detailed operational procedures which allowed synchrotron radiation and high energy users to coexist on PEP. This bodes well for future PEP runs.

When PEP was running well in the colliding beam mode at 13.5 GeV typical beam currents were 19 mA at the top of the fill, dropping to 13 mA in 2-4 hours, at which point more particles were injected. The injections took about 20 minutes. The ring was operated in a 3 bunch mode, giving synchrotron light pulses separated by 2.5 microsecs. Measured flux rates at the sample using a Si(111) crystal were 10^{11} to 10^{13} per second in the 10-15 KeV range. These fluxes are comparable to those found at the multipole wiggler Beam Lines 6 and 10 on SPEAR in a dedicated mode. However, the divergence characteristics of the PEP beam are superior to those found on SPEAR by about a factor of five.

The PEP beam can be focused to a spot with a vertical FWHM of less than 0.5 mm, and a horizontal FWHM of less than 2 mm. The PEP focal spot looks much cleaner than the focal spot on a SPEAR beam line, and the flux density in the 10-15 KeV range is about a factor of ten higher than can be achieved at the multipole wiggler beam lines on SPEAR. It is anticipated that there will be PEP parasitic running available again in the late spring of 1989.

SPEAR Parasitic Running - Parasitic running on the SPEAR VUV lines occurred in December 1988. The storage ring was operating at 1.85 GeV for colliding beam experiments. The 111 delivered user shifts were used by 7 groups to commission equipment, train students and obtain data.

Operations Division Activities - Beam line maintenance and improvement activities and coordinating the move of personnel and equipment from the Building 120/131 complex to the new LOS building were the main focus of the Operations Division in 1988. When the June run was cancelled, a number of improvement activities were initiated. These included the rebuilding/upgrading of Beam Line 2, installation of Beam Line 6-1, modification of Beam Line 6-2, completion of Beam Line 5, fabrication of new hutches, and outfitting of the Building 120 office and user lounge areas. The Operations Division also lent assistance to the injector project by coordinating the removal of Building 101 and supplying extra manpower. The vacuum group within the Operations Division is heavily involved in the development of the injector vacuum system.

The Operations Division had their first experience with running SPEAR and PEP simultaneously during the fall of 1988. The long distances between the PEP beam lines and SPEAR made this particularly challenging.

Figure 1 is a listing of the characteristics of the 25 SSRL experimental stations.

Figure 1 **CHARACTERISTICS OF SSRL EXPERIMENTAL STATIONS**

SSRL presently has 25 experimental stations 23 of which are located on SPEAR and two on PEP. 12 of these stations are based on insertion devices while the remainder use bending magnet radiation.

	Horizontal Angular Acceptance (mrad)	Mirror Cut Off (keV)	Monochromator	Energy Range (eV)	Resolution ΔE/E	Approximate Spot Size HgtxWdth (mm)	Dedicated Instrumentation
INSERTION DEVICES STATIONS							
WIGGLER LINES - X-RAY							
End Stations							
4-2 (8-Pole)							
Focused	4.6	10.2	Double Crystal	2800-10200	~5×10^{-4}	2.0 x 6.0	
Unfocused	1.0		Double Crystal	2800-45000	~10^{-4}	2.0 x 20.0	
6-2 (54-Pole)							
Focused	2.3	22	Double Crystal	2800-21000	~5×10^{-4}	2.0 x 6.0	
Unfocused	1.0		Double Crystal	2800-45000	~10^{-4}	2.0 x 20.0	
7-2 (8-Pole)							Six-circle Diffractometer
Focused	4.6	10.2	Double Crystal	2800-10200	~5×10^{-4}	2.0 x 6.0	
Unfocused	1.0		Double Crystal	2800-45000	~10^{-4}	2.0 x 20.0	
10-2 (31-Pole)							
Focused	2.3	22	Double Crystal	2800-21000	~5×10^{-4}	2.0 x 6.0	
Unfocused	1.0		Double Crystal	2800-45000	~10^{-4}	2.0 x 20.0	
Side Stations							
4-1	1.0		Double Crystal	2800-45000	~5×10^{-4}	2.0 x 20.0	
4-3							Two-circle Diffractometer,
Focused	1.0		Double Crystal	2800-45000	~5×10^{-4}	0.5 x 20	Vertically focussing mirror
Unfocused	1.0		Double Crystal	2800-45000	~10^{-4}	2.0 x 20.0	
7-1	1.0		Curved Crystal	6000-13000	~8×10^{-4}	0.6 x 3.0	Rotation Camera
7-3	1.0		Double Crystal	2800-45000	~10^{-4}	2.0 x 20.0	
UNDULATOR LINES - VUV/SOFT X-RAY							
5 multiple undulators	1.5		Rowland Circle-Multiple Grating	10-1200	$\Delta\lambda$ = .013-.13Å	6.0 x 8.0*	Commissioning in Progress
6-1			6m SGM	150-600	$\Delta\lambda = \geq .055$Å		Commissioning in Progress
UNDULATOR LINES - X-RAY							
PEP 1B							
Focused	1.7	22	Double Crystal	12000-22000	2×10^{-5}	0.5 x 3	
Unfocused	FULL		Double Crystal	12000-42000	~10^{-5}	0.6 x 6.0	Six-circle Diffractometer
PEP 5B							
Focused	1.7	22	Double Crystal	12000-22000	2×10^{-5}	0.5 x 3	
Unfocused	FULL		Double Crystal	12000-20000	~10^{-5}	0.6 x 6.0	
BENDING MAGNET STATIONS							
X-Ray							
1-4	2.0		Curved Crystal	6700-10800	0.3×10^{-3}	0.25 x 0.5	Small Angle Scattering Detector
1-5	1.0		Double Crystal	2800-30000	~10^{-4}	3 x 20	Area Detector/CAD-4
2-1(Focused)	4.8	8.9	Double Crystal	2800-8900	~5×10^{-4}	1 x 4	
2-2	1.0 - 6.1		None	3200-30000		4 x 22	
2-3	1.0		Double Crystal	2800-30000	~5×10^{-4}	3 x 20	
VUV/Soft X-Ray							
1-1	2.0		Grasshopper	64-1000	$\Delta\lambda$ = .1-.2 Å	1.0 x 1.0	
1-2	4.0		6m TGM	8-180	$\Delta\lambda$ = .06-3 Å	1.0 x 2.0	
3-1	2.0		Grasshopper	25-1000	$\Delta\lambda$ = .05-2 Å	1.0 x 1.0	
3-2	4.0		Seya-Namioka	5-40	$\Delta\lambda$ = .2-6 Å	2 x 7	
3-3	8-10	4.5	UHV Double Crystal (Jumbo)	800-4500	~5×10^{-4}	1.5 x 2.5	
3-4	0.6		Multilayer	0-3000	White or $\Delta\lambda/\lambda$ = .6%	2 x 8	Vacuum Diffractometer/ Lithography Exposure Station
8-1	12		6m TGM	8-180	$\leq 6\times10^{-3}$	$\leq$ 1mm²	Angle Resolved e-Spectrometer
8-2	5		6m SGM	50-1000	$\Delta\lambda$ = .01-.03 Å	$\leq$ 1mm²	Angle Resolved e-Spectrometer

II ACCELERATOR PHYSICS PROGRAM

The highest priority of the SSRL Accelerator Physics program is to increase the reliability and performance of SPEAR for synchrotron radiation research. Within that priority, the greatest emphasis is being placed on the construction of the 3 GeV SPEAR Injector, since lack of on-demand injection is the main impediment to both reliable operation and the additional machine physics required to analyze and improve SPEAR. Some effort is also being devoted to the exciting development of PEP as a synchrotron radiation source.

THE 3 GEV INJECTOR

The construction of an independent, dedicated 3 GeV injector synchrotron for SPEAR was funded by the DOE in mid-January, 1988. During the year most of the activities were concentrated on the following:

- clearing of the site
- conceptual design and specifications of the equipment shelter, of the radiation shielding, of the electrical and mechanical utilities, and of the safety systems
- conceptual specifications of the magnet power supplies
- detailed design of the bending magnets, vacuum chambers
- procurement of the Linac modulators

The location of the injector ring is shown in Figure 2.

The decision was made to use a White circuit at 10 Hz for the magnet power supplies. Originally a computer controlled supply ramping at 2 Hz was assumed. While such a system is used for existing and proposed boosters in other laboratories, it became increasingly clear that at SLAC the pulsating

Figure 2

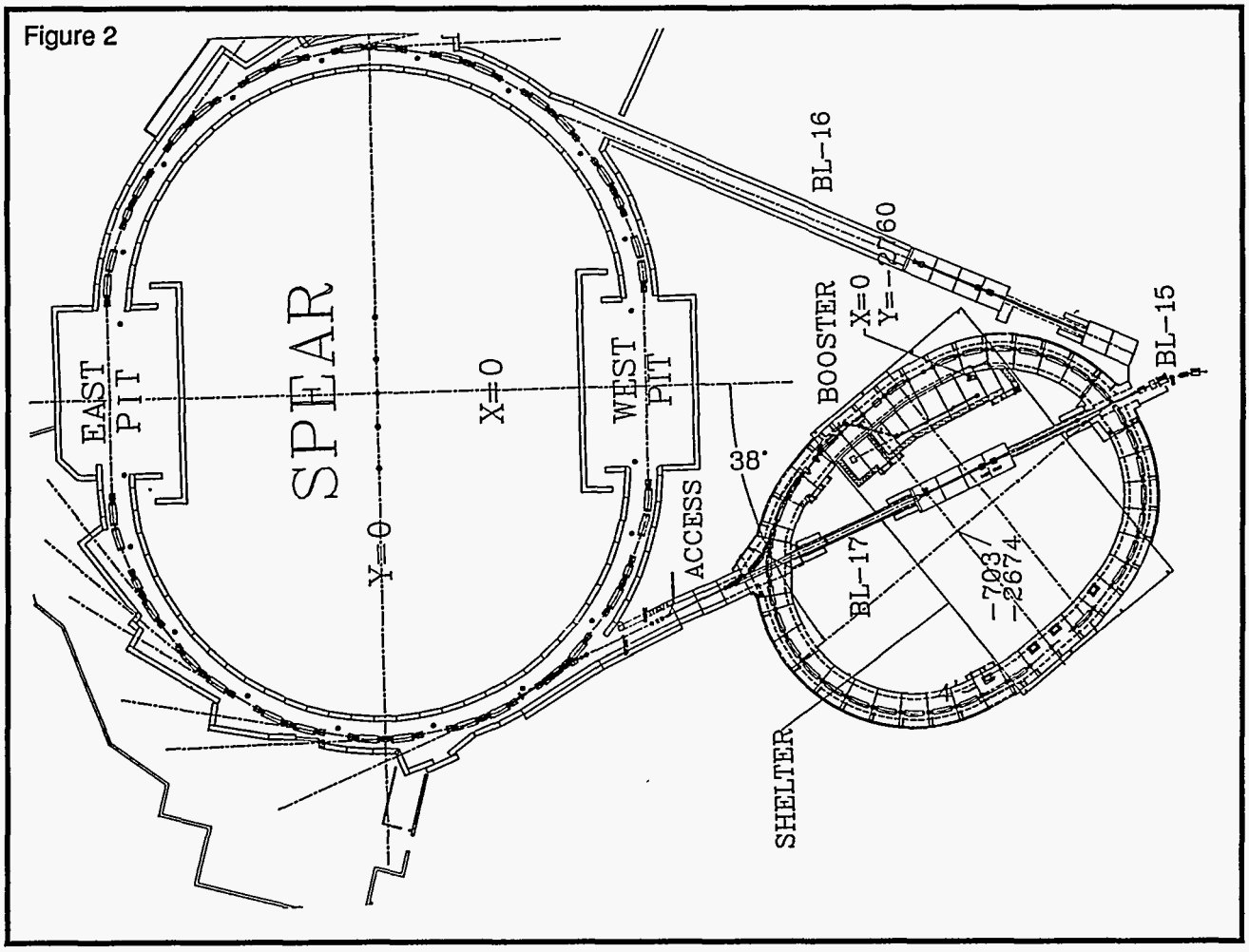

3 GeV Booster Synchrotron for SPEAR

electric load on the mains could cause unacceptable perturbations which would interfer with the operation of the SLC. A beneficial effect of this decision is a factor of five higher injection rate into SPEAR, compared to a booster cycling at 2 Hz. In addition, no modifications of the present power supplies are required should a positron option be implemented later.

Site clearing was started in February 1988, and the site contract for storm drainage, paving, grading, a 133 meter ring slab, and beam line support piers was awarded in June. Work was finished in September 1988. The shielding, roof blocks and equipment shelter contracts were placed in July (Figures 3, 4 and 5). Beneficial occupancy of the equipment shelter occurred on schedule in January 1989 and installation of the electrical, mechanical and safety systems began.

Figure 3

January 1988

Site of the 3 GeV Booster before clearing. The building on the far left (101) was demolished to make room for the 133 m ring.

Figure 4

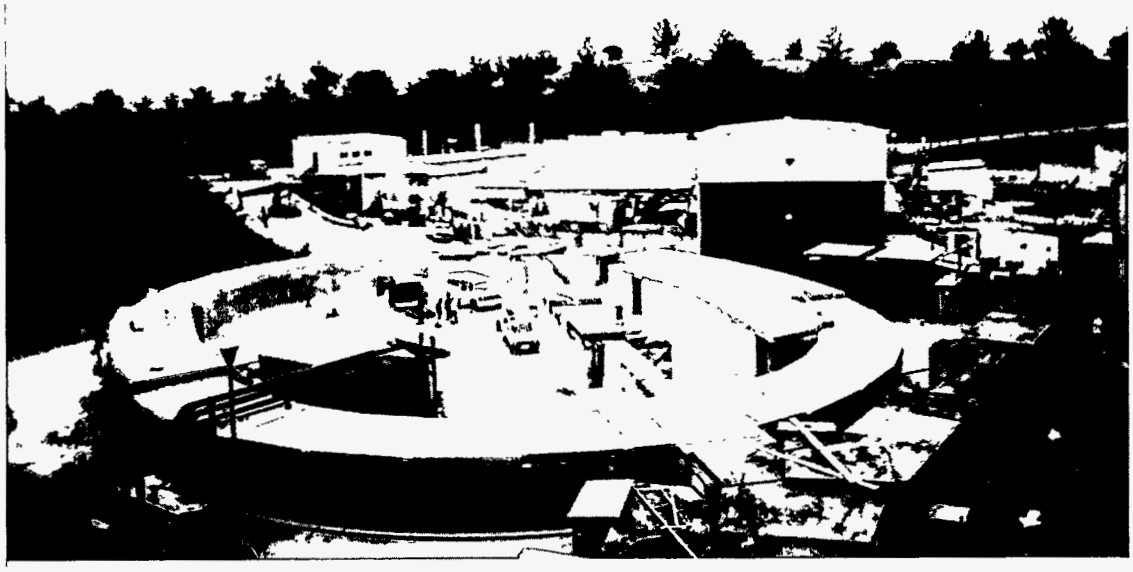

September 1988

Completion of the housing for the booster which is built around the present SPEAR electron injection line.

Figure 5

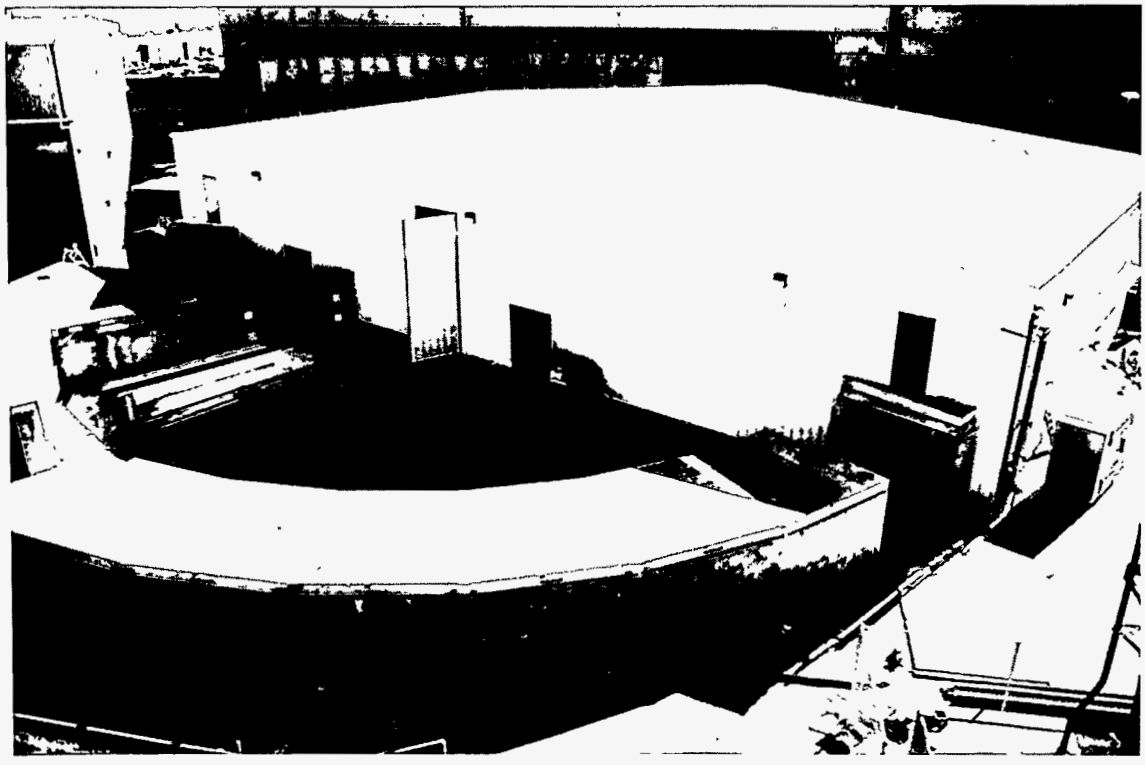

December 1988

Completion of the shelter for the controls, linac and accelerator physics experimental area.

Design and procurement of the main booster components, including magnets, supports, vacuum chambers and linac modulators was undertaken in 1988.

A three-block bending magnet prototype (Figures 6 and 7) was constructed to evaluate the characteristics of three different types of steel under the cycling conditions required for the booster. In parallel a power supply able to cycle this magnet to 15 kGauss at a cycling rate of up to 15 Hz was completed. The main goal of the high power magnet test was to establish the heating properties during cycling; specifically, to compare the heating of the more cost effective 1005 steel with more expensive transformer steel. Tests were performed that led to the choice of 1005 steel for the booster, with a cycling rate of not more than 15 Hz. While the transformer steel is more heat resistant, it was found that the heating of the 1005 steel is well within acceptable limits, even for fields as high as 14 kGauss. In general, at 3 GeV a field of only 8 kGauss is needed.

Figure 6

Stacking the Bending Magnet Blocks for the Prototype

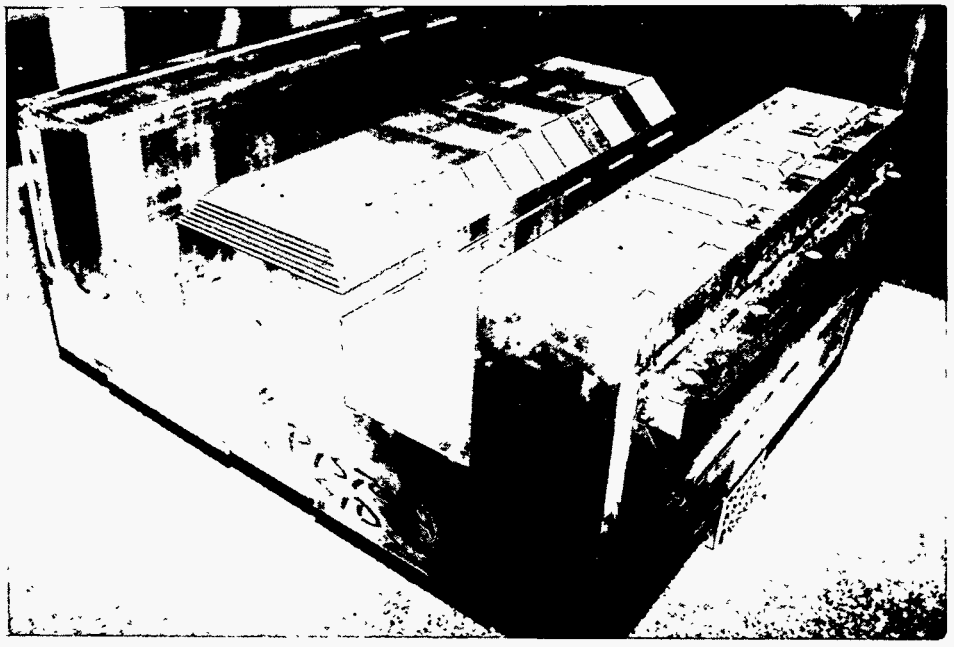

Figure 7

Prototype Bending Magnet Block for the Injector

A prototype of the thin walled stainless steel vacuum chamber has been developed, fabricated and successfully tested (Figures 8 and 9). The 0.33 mm stainless steel tube was strengthened against collapse from atmospheric pressure by a series of external ribs. Pressure tests showed that the complete chamber could withstand an external pressure up to 10 atmospheres, giving a generous safety factor for its use in the booster.

Figure 8

Thin Walled Vacuum Chamber Segment

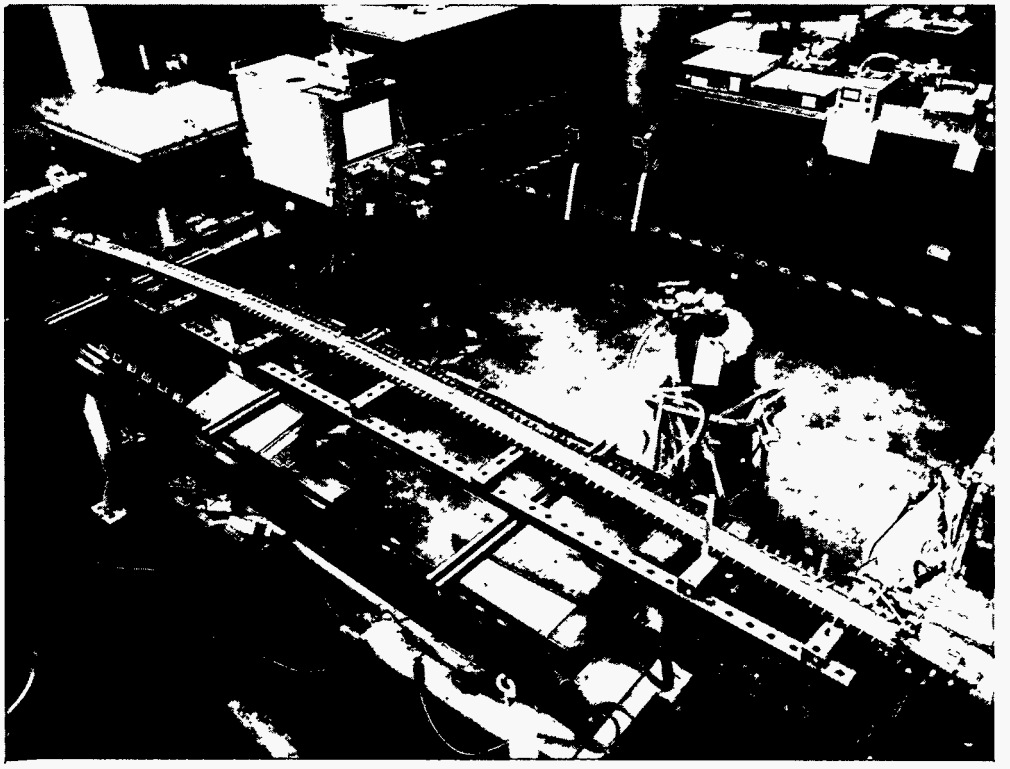

Figure 9

Full Scale Vacuum Chamber Prototype for the Injector

The designs of the ring vacuum chamber, flanges, bellows, ceramic rings for electrical insulation of the vacuum chamber, pumps etc. were finalized. All production steps for the fabrication of the final thin walled vacuum chamber have been exercised, evaluated and confirmed during the construction and vacuum test of two full scale girder chambers (Figure 10).

The charging supply for the first linac modulator has been completed and the first modulator is expected to be completed by early 1989.

A surplus SPEAR RF cavity had been refurbished for use in the booster synchrotron. This refurbishing included the addition of tuning devices, vacuum pumps and higher order mode protection.

The design of the injection/ejection systems was started during July 1988 and is expected to be finished early next year.

The main goal for next year is to fabricate all the main booster components and install them by the end of next year. After a systems test period over the first 3 months of 1990, commissioning of the complete booster is scheduled for April 1990. Project completion is expected by September 1990.

SPEAR STUDIES

During 1988 there was no machine physics available at SPEAR and work on SPEAR was restricted to theoretical studies and R&D work on low emittance configurations. Specific studies were directed toward a practical low emittance configuration that could be implemented after installation of a third injection kicker. Lower beam emittance than now available can be achieved by operating SPEAR with stronger quadrupole fields. In this case, however, injection with the present injection components is very difficult. A third kicker magnet as part of the injector project will make injection into such lower emittance configurations much simpler. *(See SSRL 1985 Activity Report, page III-1.)* Continued studies are required to determine the practically achievable low emittance in SPEAR.

Figure 10

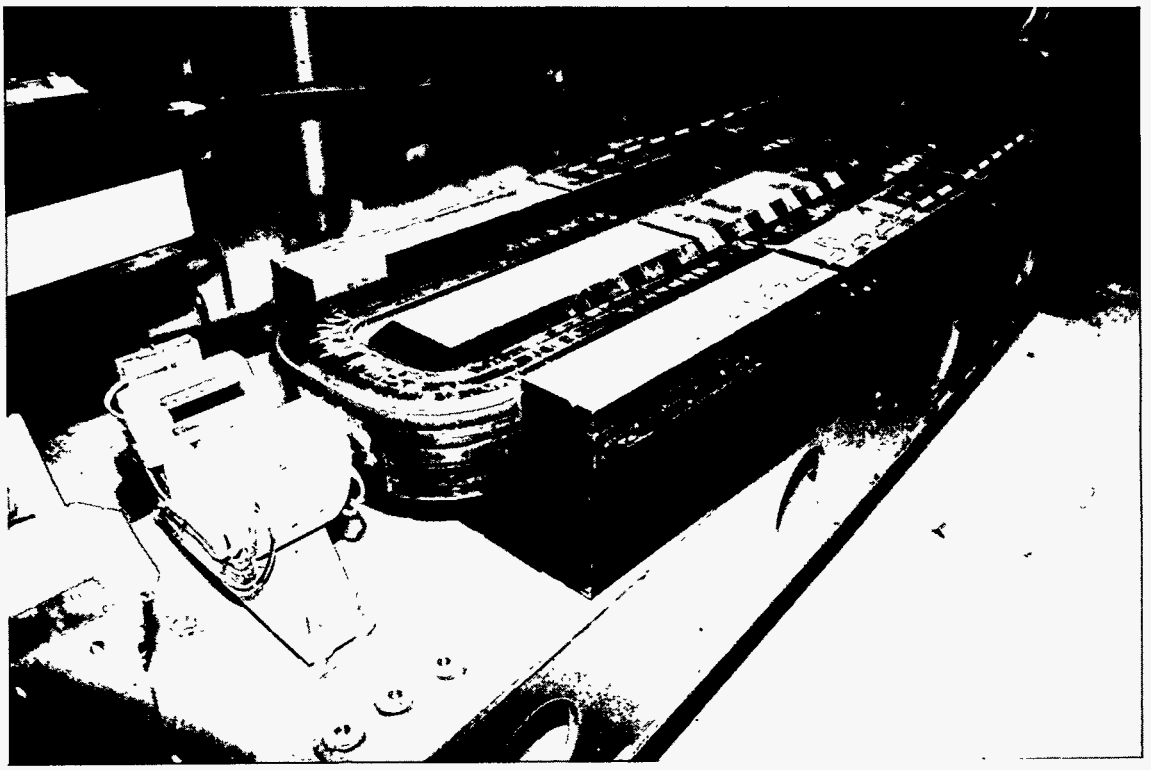

Final Booster Girder

PEP STUDIES

PEP Injector Project - As part of the Linear Collider project the SLAC linac has been upgraded to 50 GeV and extensively modified, reducing its availability and suitability as an injector to SPEAR and PEP. A study of a possible alternative injector to PEP has been carried out. Injection to PEP would be provided by upgrading the 3 GeV SPEAR injector, now in construction, to enable it to operate at 5 GeV and bringing this beam to the existing PEP electron injection line via a 240 meter long transfer line as shown in Figure 11. After injection at 5 GeV, PEP would generally be ramped to 6-10 GeV for most dedicated operation now anticipated. Although less desirable than full energy injection, this scheme provides the quickest and least costly path to achieving injection to PEP independent of the SLAC linac. *[See "A 5 GeV Injector for PEP", H.-D. Nuhn, R. Boyce, R. Gould, H. Winick, B. Youngman and R. Yotam, to be published in the Proceedings of the 1989 Particle Accelerator Conference and SSRL ACD note 66.]*

Figure 11

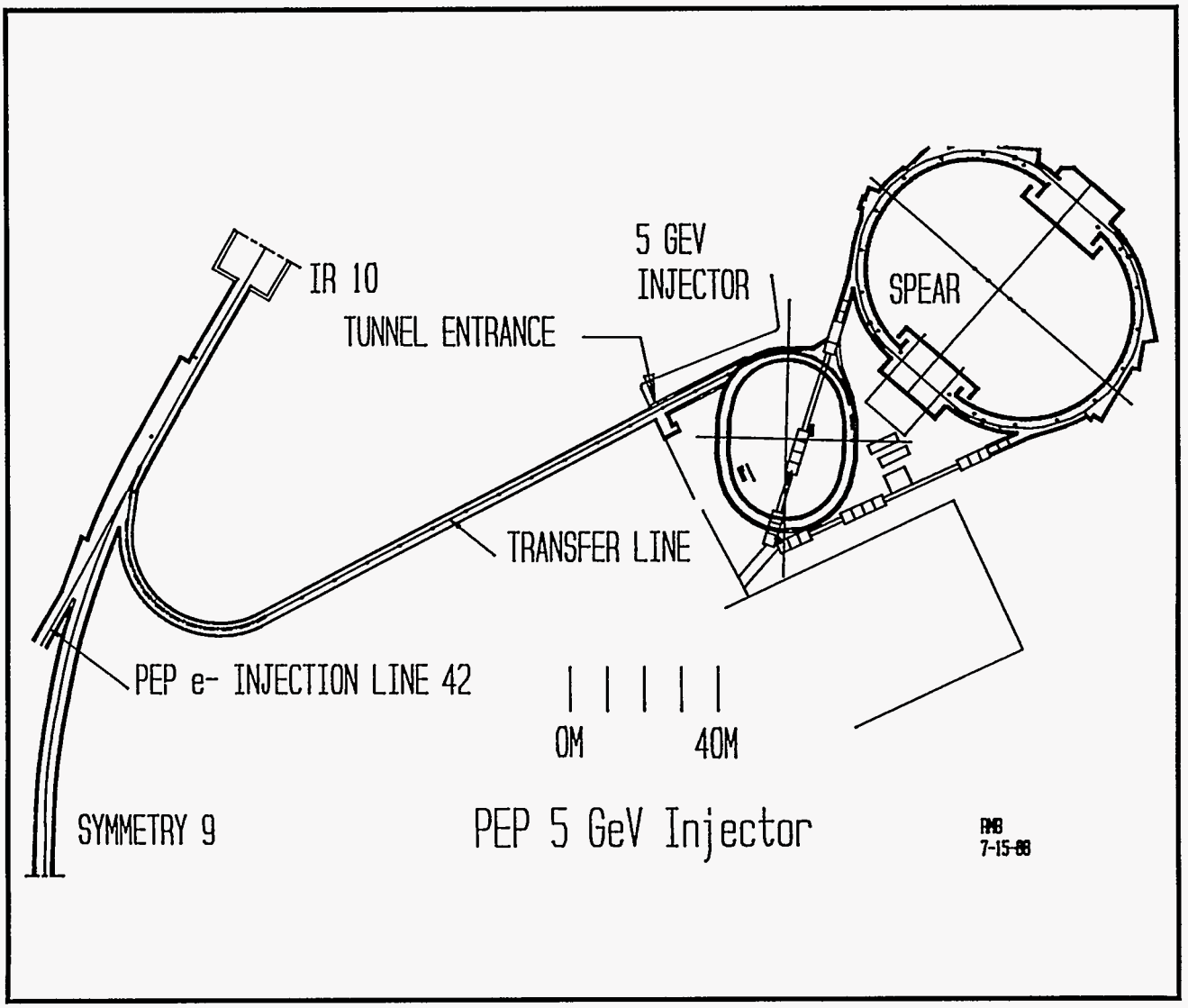

Studies of High Current in PEP - During dedicated operation of PEP for synchrotron radiation research a stored current of 50-100 mA is desired in the low emittance optics at 6-10 GeV. During the December 1987 dedicated low emittance tests *(see 1987 Activity Report)*, stable stored currents of 15-20 mA were achieved at 7.1 GeV. (The highest stored current achieved was 33 mA, but stability and reproducibility were poor at the higher levels.) Multi-bunch longitudinal instabilities were identified as the cause of the limitation on current. This was addressed at the November 2, 1988 Workshop on Accelerator Physics Issues Relating to the Use of PEP as a Synchrotron Radiation Source *(see Chapter 5)*. A main conclusion of this workshop was that a feedback system could be built to raise the threshold for these instabilities, as has been done at other laboratories. Work on the design of such a feedback system was started after the workshop. In an 8 hour study of multi-bunch operation of PEP at 13.6 GeV a total current of 65 mA of electrons was achieved in the high energy physics optics. This is the highest current yet achieved in PEP. The maximum current was limited by heating problems in the RF system rather than instabilities.

Interest in developing the high current, multi-bunch capabilities of PEP is also coming from the high energy physics community (in connection with future B-Factories and higher luminosity for the present PEP colliding beam program) and from the nuclear physics community (in connection with their proposal to use the stored beam in PEP interacting with gas jet or cold cluster targets located in the ring itself). Collaborations are forming between SSRL and these groups on feedback systems and further studies.

Improvements and Additions to PEP - A study was carried out, in collaboration with SLAC physicists and engineers, on the improvements necessary to existing components of PEP to improve its reliability as a synchrotron radiation source and on the additions necessary to more fully exploit its potential. The components studied include the RF system, beam position monitoring system, vacuum system, computer control system, alignment system, magnet power supplies and orbit correction system. Additions to PEP that were studied include damping wigglers, beam lines and an upgrade to the SPEAR 3 GeV injector to reach 5 GeV. The total cost of improvements needed to optimize synchrotron radiation performance is estimated at about $6M. This is exclusive of major additions (beam lines, damping wigglers and a new injector. A report on this work has been distributed. *["PEP as a Dedicated Synchrotron Radiation Source", R. Boyce, R. Gould, H.-D. Nuhn, H. Winick, R. Yotam and B. Youngman, SSRL ACD Note 67.]*

Parasitic Operation of PEP - During the Fall of 1988 synchrotron radiation experiments were carried out on the two operational undulator beam lines on PEP during colliding beam runs. In order for this parasitic operation to be compatible with the high energy physics experiment, studies were carried out on electron orbits and photon beam steering to arrive at operational modes that permitted photon beams to be properly steered into the experimental stations without adverse effect on the high energy experiment. These studies were carried out in collaboration with SLAC accelerator physicists and with the cooperation of the high energy experimental group.

Circular Polarization from PEP - A study is being carried out on obtaining very high energy circular polarized radiation from the center pole of the 3-pole emittance control wigglers now installed in PEP. A report is in preparation. Figure 12 shows one of the results.

Figure 12

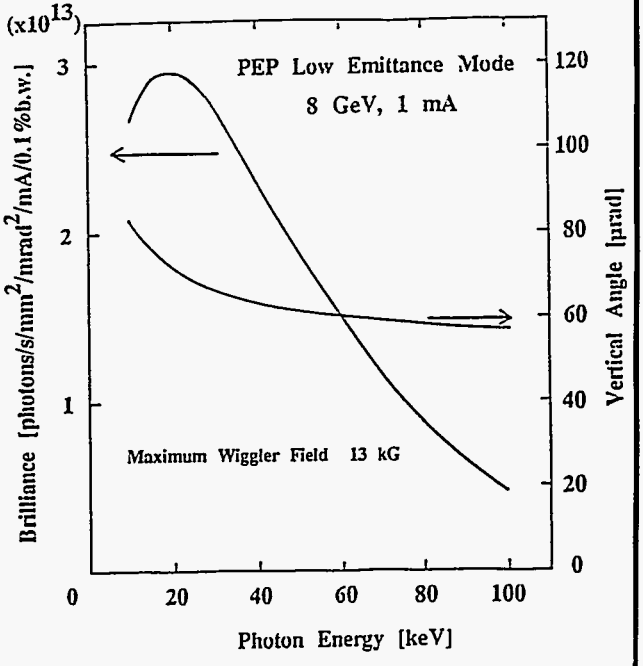

GENERAL ACCELERATOR PHYSICS ACTIVITIES

Theoretical work in Accelerator Physics is carried out by Stanford University graduate students under the direction of Helmut Wiedemann.

Low Emittance Storage Ring Modes - Practical limits in the design of ultra-low emittance storage rings are encountered due to nonlinear aberrations in the beam dynamics. These aberrations limit the area of beam stability also called dynamic aperture. This dynamic aperture can be made infinite in the ideal case of proper placement of infinitely thin sextuples around the ring. In practice, the finite thickness of strong sextuples causes a large reduction of the dynamic aperture. Using the algebraic manipulation program REDUCE, the trajectory through the sextuples and focusing elements was approximated in terms of the most convenient coordinates. The most important aberration terms in the horizontal plane were determined, and corrected by including octupolar fields in the appropriate places. After inserting the octupolar fields into the model lattice of the ring, the horizontal dynamic aperture, calculated by numerical tracking, was increased by 30%.

A low emittance focusing configuration has been developed and optimized for PEP. The linear optics was improved to achieve higher photon beam brightness. Introduction of long damping wigglers can reduce this low beam emittance to much lower values of less than 1 n-meter at 6 GeV. The nonlinear effects of these damping wigglers are being studied and sextuple distributions are being developed to assure a large dynamic aperture while correcting the chromaticities. Experiments have been conducted to determine the nonlinear effects of the existing wiggler magnets on the particle beam in SPEAR.

Studies of High Brightness Electron Sources - Progress was made developing tools for the design of a high brightness electron source including space charge effects. The simulation program MASK was adapted to run on SSRL's VAX 8810 computer, which included developing new post-processing software. MASK will be used to optimize the shape of the RF gun cavity to be used as the electron source for the 3 GeV SPEAR injector. Post-processing for the program SUPERFISH was improved to allow easier examination of the accelerating and focusing fields in the cavity for various shapes. A program was developed to confirm the results of MASK in the low space-charge limit.

Joanne Marchetti left SSRL in September to take a position in the Dean of Research's Office. Joanne had been at SSRL as Herman Winick's secretary for over 10 years.

III EXPERIMENTAL FACILITIES

Experimental facilities at SSRL are of two types: general facility stations and participating research team (PRT) stations. General facility stations have been funded by various government agencies, principally the DOE, NIH and NSF and are open to the user community on a competitive basis for 100% of their operating time.

SSRL has three operational PRTs with a fourth in the process of developing a branch line. All present PRTs are three-party collaborations with SSRL as one of the parties. The two outside institutions receive 2/3 of the available beam time while the other third is reserved for the SSRL general users. The PRT arrangements are for a 3 year period. Renewal is based on a review by an ad hoc committee, appointed by the Stanford University Dean of Research, which considers scientific merit, contributions to graduate student education and to the SSRL user community.

The three PRTs are EXXON/Lawrence Berkeley Laboratory/SSRL (Beam Line 6), University of California/National Laboratories (with LLNL as the lead lab)/SSRL (Beam Lines 8 and 10) and Xerox/ Stanford University/SSRL (Beam Line 5). An IBM/ The Center for Materials Research (Stanford University)/SSRL collaboration is presently constructing a side station on Beam Line 10 in a PRT mode.

X-RAY FACILITIES

Improvements to Existing Facility Lines - There are 13 x-ray stations located on six beam lines at SSRL. Two of these are PRT lines (wiggler lines 6 and 10) . The other 11 are SSRL facility stations. Of the facility lines, two (Beam Lines 4 and 7) have wigglers as sources for six stations and the other two (Beam Lines 1 and 2), serving five stations, have bending magnet sources.

Beam Line 2 Rework - A major effort during the last year was the complete reworking, in partnership with IBM San Jose, of Beam Line 2. Beam Line 2, built in 1976, has 3 branch lines. Station 2-2 (focused x-ray), 2-3 (which has been used primarily as a facility characterization port for the last few years) and 2-4, a white radiation line. Recent advances in techniques utilizing polychromatic beam (topography, powder diffractometry) motivated a redesign which allows a broader fan of radiation to the white radiation port and, in particular, provides more space for these experiments without compromising the other two branch lines.

The branch lines were redesignated in the upgrading process to conform to the standard SPEAR notation. The focused line is now 2-1, the white radiation line is 2-2, while the unfocused line remains 2-3.

Reconstruction was completed in December. The white radiation port now receives 6.1 milliradians of beam. A permanent pinhole camera was installed between stations 2-2 and 2-3 to provide constant monitoring of the beam position at the source point. This opens up much of the time on station 2-3, which had previously been used primarily for this purpose, for EXAFS studies.

New instrumentation was developed for the white radiation line (2-2), specifically a larger hutch with two permanent tables is now available. The front table translates vertically. Two precise double-axis diffractometers were installed on the second table in the back of the hutch. They will be used for monochromatic plane wave topography and high resolution goniometry measurements. This station is now equipped with a CAMAC crate, NIM bin and microVAX II computer.

Branch Line 4-2 Improvement Program - A new focused silica mirror was ordered, coated, tested and installed on 4-2. Because of the complications associated with the January 1989 start up, only a brief examination of the quality of the focus was made. A nominal vertical size of 500 microns (FWHM) was measured, on par with the best focus ever measured on this beam line.

Branch Line 4-3 Improvement Program - A new downward reflecting vertically focusing mirror has been installed downstream of the monochromator. SSRL staff have made preliminary measurements of the vertical focus size, in conjunction with Bill Warburton, the beam line steward. At a 5.5 mrad angle of incidence, a vertical size of 110 microns (FWHM) was measured. Since this mirror only focuses in one dimension, the mirror cutoff can be choosen to suit the needs of the user. The vertical focus for a larger range of incidence angles will be measured during the summer 1989 run.

Branch Line 7-2 - As with 4-2, a new fused silica mirror was installed on 7-2. SSRL staff measured the vertical focus as nominally 500 microns. We are pleased to report that we now have a focus comparable to the best that has been measured on 4-2 for the first time in the history of 7-2. In addition, substantial heat damage to the vertical entrance aperture of the mirror was observed during the installation of the new mirror. The entire mirror aperture system was rebuilt with new slides and motors and the cooling system was upgraded to match that on 4-2.

PEP 1B - The six-circle diffractometer was installed in PEP 1B. The instrument is now fully provided with beam path hardware, slits, detectors, and electronics.

Figure 13

Microchannel grooved crystal assembly

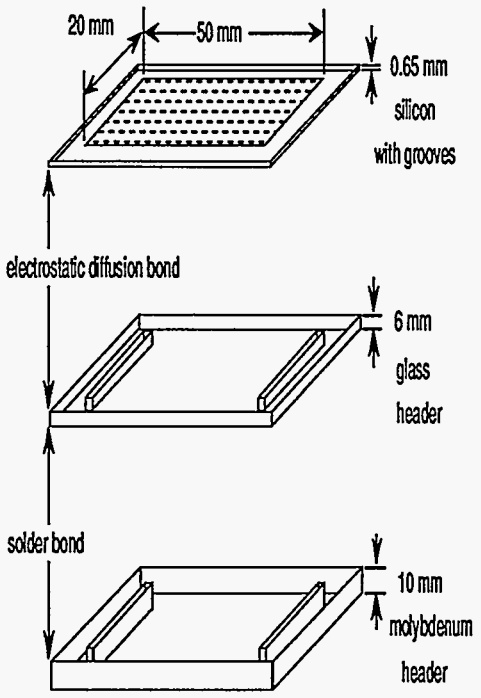

General X-ray Facility Improvements

Monochromator Cooling Project - SSRL has entered into a collaborative project with LLNL to develop a water-cooled monochromator capable of absorbing 1-2 kW of synchrotron radiation power without distortion. The technique borrows from recently developed semiconductor technology, whereby a thin, grooved wafer is bonded to a glass substrate which serves as a hydraulic header.

A prototype monochromator was fabricated and tested with a conventional x-ray generator for flatness. These tests have indicated that the crystal deformation upon bonding to the glass header can be kept within acceptable limits.

Figure 13 shows the microchannel grooved crystal assembly.

VUV FACILITIES

There are currently ten VUV or soft x-ray beam lines at SSRL. Four of these facilities were built by PRTs, and the general user community has access to 33% of the time on these lines. The facilities being scheduled for users are: two TGM's (1-2 and 8-1), two grasshopper monochromators (1-1 and 3-1), a Seya-Namioka monochromator (3-2), an in-vacuum double crystal monochromator (3-3), a SGM (8-2) and the lithography/optics line (3-4). Construction has been completed on Beam Line 5 and Station 6-1. Both are being commissioning. The long shutdown in 1988 allowed many improvement projects to be undertaken in the VUV facilities.

Branch Line 1-1 - Elliptical focusing mirrors were purchased for both grasshopper monochromators, the first of which has been installed with the expected improvement in flux. The mirror is a profiled piece of selected float glass which is bent to give an elliptical figure. This figure produces a smaller spot size at the entrance slit than the original spherical mirror. The initial results from Branch Line 1-1 indicate an improvement in flux by about a factor of 3. The size of the focus has been reduced from 90 microns to 40 microns. Further improvement to 25 microns may be possible, with additional increase in flux through the monochromator. The second mirror will be installed in Branch Line 3-1 during 1989.

Branch Line 1-2 - Commissioning was completed during the December parasitic run on this TGM. The optics were aligned and evaluated. Two of the three gratings, the 288 and 822 l/mm, operated as expected. Poor results (during the installation of the new mirror) were obtained from the 2400 l/mm grating. Thus, the beam line is operating very well from 7 eV to 90 eV. The Mo mirror is the original polished copper flat installed more than fifteen years ago. It has a built in a cant which cannot be fully compensated with the current design. Plans are being made to replace this mirror to achieve an increase in throughput by a factor of two or three.

Branch Line 3-2 - An all metal, bakeable, pneumatically controlled exit valve was installed on this 18° line. This allows the valve to be interlocked, protecting the vacuum in the monochromator from accidental venting of the user's chamber. A valve controller was designed and tested for control and local interlocking of these valves. Ten out of the twelve VUV experimental stations now have similar systems.

Branch Line 3-4 - The lithography/optics beam line was further improved this year to expand the flexibility for studying optical properties of materials and detectors. The end station controls have been completely redesigned and a Macintosh based data acquisition system added. A new valve interlock system was designed, constructed, installed and tested, making the beam line more user friendly and fool proof. A calorimeter was installed for making absolute flux measurements. The fine adjustments on the monochromator are now controlled by in-vacuum motors, replacing the micrometers, and interfaced to the control computer.

General VUV Facility Improvements

VUV Data Acquisition Developments - MicroVAXes have been installed on Beam Line 5 and Station 1-2 and a development system has been installed in the LOS VUV lab. The EXP data collection program, which has been in use for several years on the PDP 11/34's, has been upgraded to work on the microVAX systems. This configuration was used to take data on Branch Line 1-2 both off-line (no beam) and during the December parasitic run. Monochromator interface programs are being developed for all the VUV beam lines and the microVAX systems will be installed as these routines are completed.

On Branch Line 3-4, the Lithography/Optics station, a Macintosh is operating with Labview based data collection and control software developed to meet the needs on this highly flexible beam station.

Upgrade of the Perkin-Elmer Chamber - Work started this year to upgrade the Perkin-Elmer UHV experimental chamber to incorporate the following features:

- A transfer mechanism, including a separate chamber to allow faster exchange of samples;
- A sample carousel inside the main chamber which positions samples with a simple rotation in front of different sample treatment devices such as an evaporator, a sputter gun, an annealer, and a LEED analyzer; and
- A new manipulator allowing two rotations and three linear motions of samples.

The sample holder is of the standard SSRL design. The manipulator head includes an electron bombardment heater capable of heating samples up to more than 1400°C without affecting the surrounding detectors. The shielding of the heater as well as the high temperature durable metals and insulators chosen for all parts in direct and indirect contact with the samples will result in a lower sample contamination in contrast to common heater performances.

The design for the upgrade of the Perkin-Elmer chamber was finished in 1988, and the transfer arm and two sets of manipulator heads have been completed. The precision fabrication of parts from insulator materials and high temperature durable metals was accomplished by SSRL's technical staff. All parts (except an independent pump unit for the transfer chamber) are expected to be ready for the dedicated run in June 1989.

BIOTECHNOLOGY FACILITIES

The research and user support in the Biotechnology Division at SSRL are funded jointly by the NIH Division of Research Resources and the core SSRL DOE operations budget. Two specialized branch lines for protein crystallography (1-5 Area Detector and 7-1 Rotation Camera) exist as well a variety of supporting equipment and instrumentation.

Facilities for Protein Crystallography - A new, commercially built, multi-wire area detector to replace the original area detector on 1-5 was received and installed in 1988. The upgrade to a microVAX II GPX workstation control system for the detector facility was completed. The system now operates with significantly enhanced performance and functionality. A write-once, multiple-read 0.8 Gb optical disk was added for reliable high volume data archiving.

On the Rotation Camera line, which is used to measure x-ray diffraction data photographically, the x-ray optics were replaced providing a significant enhancement in throughput. In addition, a low temperature cryostat capable of cooling the protein crystal sample to 80°K during data collection was designed and constructed.

Facilities for X-ray Absorption Spectroscopy - The low temperature (4K) Oxford cryostat was upgraded with a reliable turbo-pump system and is now routinely available to users. Substantial progress was made in developing new HgI_2 array detectors for EXAFS studies of dilute materials. A fully functional five-element array with better than 300 eV resolution per element has been constructed and tested at SSRL. The array is controlled through a microVAX by software that can also set gain and window levels on the amplifiers and single-channel analyzers.

The "rapid turnaround" station for XAS measurements is being implemented to provide the means for users to study a variety of chemical, biological and materials problems without the need to write a lengthy proposal or commit a large amount of time to developing an EXAFS program. New motorized alignment rails have been constructed and assembled and will be used in three x-ray hutches. The design, fabrication and testing of a new system that provides for in-situ electrochemistry of samples simultaneous with XAS measurements at low energies (2-3 KeV) has been completed.

Facilities for Small Angle Scattering - The SAXS camera system underwent a major upgrade (including motorization of the goniometers and tilt stages) to provide capability under microVAX control for three different types of experiments: 1) scattering from protein solutions, 2) diffraction from oriented membranes, and 3) diffraction from thin layers and monolayers of proteins or peptides. A time-resolved imaging plate detection system is being evaluated at SSRL in collaboration with scientists from KEK.

Henry Bellamy, Mike Soltis and Zofia Rek of the SSRL Biotechnology Staff.

Improvements to Existing PRT Facilities

Beam Line 5 (Xerox/Stanford University/SSRL) - During 1988, progress was concentrated on the final steps of monochromator construction. By the end of 1988, the monochromator with a complete set of optics was fully assembled, optically aligned, tested in air with visible light under computer control, pumped down, and baked out to achieve an ultra high vacuum of $1x10^{-10}$ Torr. In addition, progress has been made in development of the beam line and SPEAR computer software in order to enable asynchronous control of the multi-undulator source from the beam line microVax workstation. During the first quarter of 1989, commissioning of Beam Line 5 began with first undulator light through the monochromator on January 20, 1989. All testing and operation of the beam line to date indicate that mechanical and optical alignment tolerances have been met.

Much of 1988 was devoted to assembly of the critical "main shaft" of the monochromator. This assembly is especially difficult due to the critically tight tolerance of the bearing runout, the complexity of an integral Codling slit/mirror, and the additional complication of water cooling. Mechanical adjustments and measurements of the entrance and exit Codling slit/mirror to the specified minimum of a 10 micron optical opening were confirmed by measurements made during grating alignment with visible light. Negligible bearing runout for the entrance Codling slit/mirror was confirmed during photon energy scanning operation of the monochromator in early 1989 using the undulator source.

Optics installation, visible light alignment, and testing of grating positioning occurred midyear in 1988. Results from this work indicate that proper focusing of visible light at zero-order was achieved by all four gratings. These results imply that the monochromator will be capable of achieving the ultimate predicted resolution [*see SPIE 582, 251(1985)*]. Unfortunately, a minor mechanical failure prevented small slit (high resolution) operation of the monochromator during operation of the storage ring in winter 1989. Therefore, ultimate resolution has yet to be verified.

Shown in Figure 14 is the total current yield from gold as the monochromator is scanned in photon energy.

Figure 14

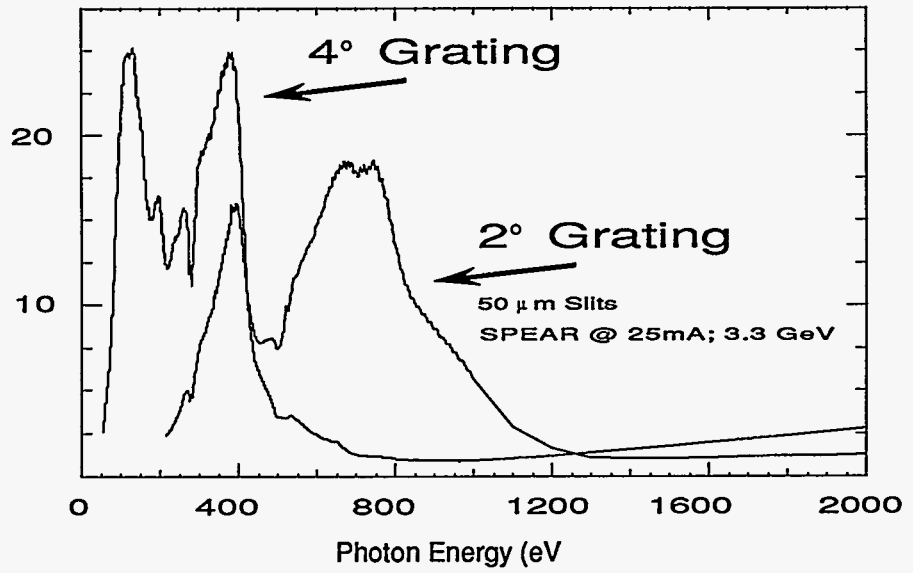

The spectrum was taken using the 2° grating at a resolution of about 0.07 Å (50 micron slits). The 4° grating spectrum was at a resolution of about 0.15 Å (50 micron slits). The undulator is tuned to an energy of 410 eV (70 mm gap, 15 period undulator). The undulator fundamental can be seen as the peak in yield at about 400 eV, and the undulator second harmonic gives rise to an intensity peak at about 700 eV. The structure in the yield spectra at energies below the fundamental is due primarily to the dependence of the reflectivity of the beam line optics on photon energy. With the 15 period undulator tuned to 150 eV (fundamental), an estimated factor of 50 increase in flux over the SSRL grasshopper monochromators (operating at identical resolution and beam current) is observed at 150 eV. Evident in the figure is the differing performance of the two gratings, which is due primarily to the blaze condition. The 2° grating is blazed for optimum operation at 600 eV, while the 4° grating is blazed for optimum 210 eV operation. Note the low contribution of scattered light, as evidenced by the low value of total yield above 1000 eV.

Operation of Beam Line 5 is critically dependent on computer control due to the large number of independent (eleven) motions of the monochromator and undulator system. The setup and up-to-air testing of the monochromator was performed under PDP 11/73 control of a slave Z80 microprocessor system. Conversion of the monochromator control software from the PDP 11/73 to a microVAX workstation (the current SSRL beam line computer standard) was initiated, with use of this system during the beam line commisioning phase.

During the January-March 1989 experimental run, operation of the multi-undulator was restricted to a fixed gap (70 mm) and a single insertion device (15 period) while efforts were concentrated on monochromator debugging/commissioning. Horizontal orbit compensation as a function of gap for the 15 period device was measured. Unstable storage ring operation during the last several weeks of the run prevented planned tests of the effect of undulator gap scanning on orbit stability.

The effect of the changing intensity of the undulator emission on the beam line vertical steering monitor was studied. Due to unwanted and non-symmetric emission from the nearby bend magnets, the vertical steering monitor signal can become biased. This problem is due to the changing relative contribution of the bend magnet radiation to the total current measured in the steering monitor as the undulator emission is varied by changing the gap. The bend magnet contribution to the total signal was investigated and found to introduce an error signal which is about 3% of the steering signal at minimum gap (k=4.2, 15 period device). As the gap opens and the undulator-derived steering signal diminishes, the error signal fraction increases. At a gap of 70 mm (k=1.5, 15 period device) the error signal fraction has increased to 10% of the steering monitor current. Further study is required to better understand the quantitative effect of this error signal on the vertical positioning of the undulator beam.

Beam Line 8 (UC/National Labs/SSRL) - I_o monitors for both Beam Lines 8-1 and 8-2 were upgraded using the new SSRL design. The new I_o section is shorter and features improved slits and a channeltron-amplified mesh arrangement. In addition, voltage is applied to nonintercepting wire loops that help clean the input beam of low energy stray electrons. A translatable diode detector was also installed downstream of each entrance slit section to aid in adjusting the prefocusing optics.

A new set of prefilters was added to Branch Line 8-2 using new hardware that holds up to seven filters. The present assortment includes Mg, Cu, Ni, Fe, Ag and C filters made at either Luxel or LLNL. A vanadium filter will be added soon. This installation was aided by a new gate valve which permitted faster turn-around.

Several improvements were made to the new multipurpose chamber designed for use on Branch Line 8-2. By means of a differentially-pumped 1500 Å Al window, this chamber will make possible a variety of experiments in the 500-1100 eV region at pressure of ~10^{-6} Torr with quick turn-around. Improvements include provisions for easier alignment of the chamber, the addition to the vacuum system of a front-end RGA, and I_o monitor mounted near a new Huber adjustable entrance slit, a translatable filter holder, and a NBS-style diode featuring a Au cathode that can be inserted into the beam near the chamber exit. A computer-coupled Klinger rotation stage for experiments on layered synthetic microstructures will be installed for use during the first dedicated run in 1989.

Apparatus for positioning and aligning the two VSW chambers for Branch Lines 8-1 and 8-2 was also constructed.

Beam Line 10 (UC/National Labs/SSRL) - A high front hutch (8'x7'x10') for Branch Line 10-2 was designed and construction completed in early September. The hutch has white-light capabilities for energy dispersive experiments in both scattering and absorption studies and can accommodate an adjustable 66" x 48" table (in fabrication) with walking space along both sides.

During the first 1989 dedicated run characterization of the beam line will be completed by measuring the following parameters as a function of ring current, wiggler field, and photon energy for focused and unfocused conditions: (a) horizontal and vertical beam profile using both a pin hole approach and CCD imaging, (b) flux measurements, (c) power curves, and (d) monochromator resolution. Comprehensive documentation for operating the various beam line components such as mirror, entrance slit, filters, wiggler field, monochromator, etc. will also be developed.

In the spring, meetings were held to discuss how to provide 1-3 keV coverage for the PRT. A phased approach was considered consisting of :

1) upgrading Branch Line 10-2 by the addition of a differential pumping section to allow removal of the beryllium windows upstream and operation of a HV monochromator;

2) modifying the present monochromator for cooled operation in high vacuum; and

3) constructing a new branch line, 10-3, specifically for the 1-3 keV range.

In July, work began on the first phase with the goal of initial operation during the fall parasitic run when the thermal load would be minimized by the low storage-ring energy. The standard monochromator rotary feedthrough was modified to a HV feedthrough. A water-cooled differential pumping section to be operated in conjuction with a LN cold trap was designed, built, and installed. Initial tests of the differential pump showed that a pressure ratio of 4-5 decades can be maintained which allows operation of the monochromator at $5x10^{-6}$ Torr. Unfortunately, operation of insertion devices was not permitted during the fall parasitic run and no tests of the beam line were made.

Cooling of the monochromator crystals in HV is necessary for full wiggler operation without the Be windows. Until this is completed, for soft x-ray mode operation during dedicated beam time the Beam Line 10 insertion device will be used as an undulator. The undulator acts as a low-pass filter and reduces the thermal load on the first crystal by a factor of 200 from normal wiggler operation. Multilayers will be used during initial experiments because of their good thermal stability. (Their large bandpass will also improve flux for experiments where energy resolution is not critical.) Although the 1-3 keV flux in undulator mode is less than that in wiggler mode, such operation will allow valuable experience to be gained during dedicated time while upgrading of the monochromator continues.

In 1988 an agreement was concluded with an IBM/CMR PRT to construct and operate Branch Line 10-1 for an initial four-year period. As a part of the agreement, a mirror tank will be installed that is sufficient for mirrors for both Branch Line 10-1 and a possible future soft x-ray Branch Line 10-3.

PRT Facilities Under Development

Branch Line 6-1 (LBL/EXXON/SSRL) - Station 6-1 is a new, VUV branch line using radiation from the 54-pole wiggler. During 1988 fabrication was completed, and the components were installed at SSRL and aligned without beam. This beam line consists of a high resolution and high flux Spherical Grating Monochromator (SGM). A Rowland circle geometry, with a large radius of 55 m, is maintained with moveable entrance and exit slits. The complete photon energy range (50 eV-1000 eV) will finally be covered by three gratings.

The first optical component, a water-cooled plane mirror (8.7 m from the wiggler source) horizontally reflects a part of the intense wiggler beam by 5.6 degrees. Next, a toroidal mirror, at 16.15 m, deflects the beam 5 degrees vertically, while focusing vertically on the entrance slit and horizontally on the exit slit. The source is demagnified by three at the entrance slit and by 0.7 at the exit slit. A large grating chamber may accommodate three water-cooled gratings.

A single fused silica grating (600 l/mm) from Ferranti Astron was installed (with no cooling). It is gold plated as are all the other optical surfaces. The high quality of this grating (very small slope error and surface roughness) has been confirmed by the observation of an unusually low contribution from stray light. The polishing of four metal grating blanks has been completed by Perkin Elmer. Two of the blanks will be ruled in the coming months.

Branch Line 10-1 (IBM/Stanford University/SSRL) - A new PRT has been formed by IBM and Stanford's Center for Material Research (CMR) to build and operate a soft x-ray beam line (100-1000 eV). The University of California/National Labs PRT has agreed with the IBM/CMR PRT and SSRL that this new beam line will be built as a side station on the Beam Line 10 wiggler and be designated Branch Line 10-1. The monochromator and experimental station will be between 10-2, the x-ray end station, and 8-2, the spherical grating monochromator (SGM) beam line.

The layout of Branch Line 10-1 (Figure 15) is similar to the LBL built SGM, Branch Line 6-1. The first mirror is a horizontally deflecting flat. The second mirror is a vertically deflecting toroid with the image focused in the tangential plane on the entrance slit of

Figure 15

Beam Line 10-1 Layout

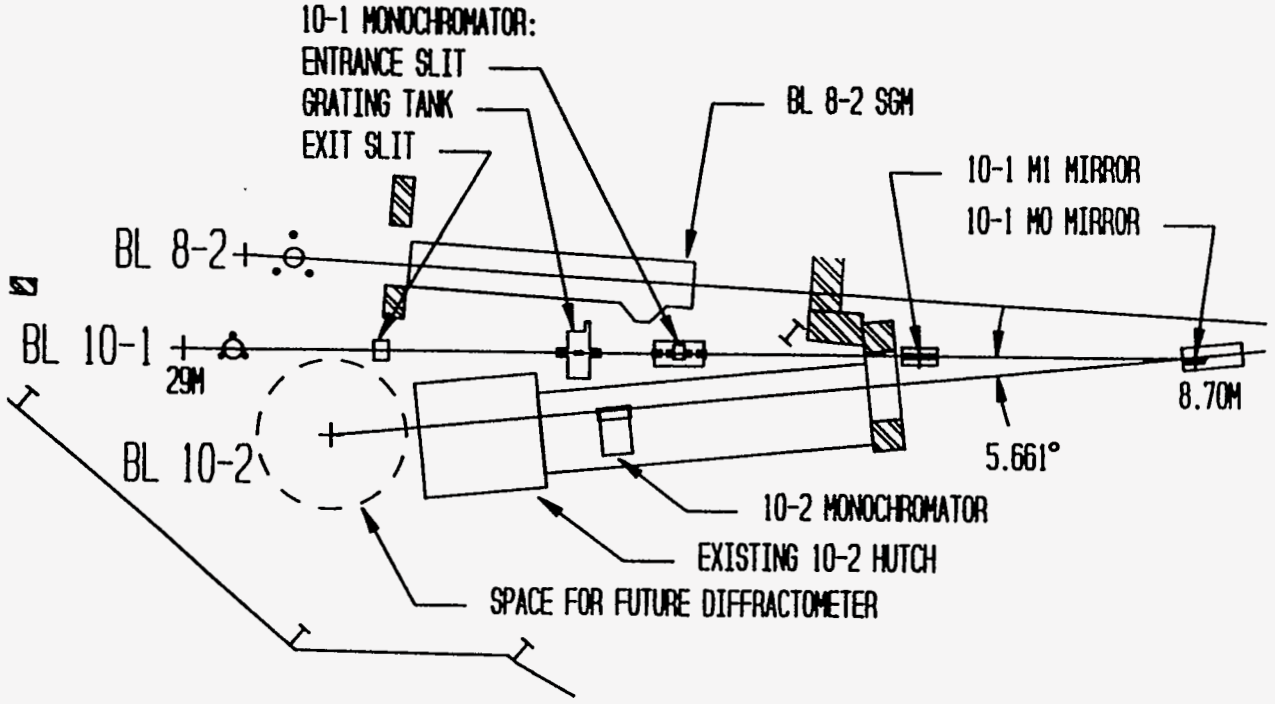

a SGM and in the sagittal plane on the exit slit. Both mirrors will be silicon carbide and cooled from the sides. The monochromator is a 6 meter SGM with a moveable entrance slit. The slit jaws will be water cooled. The two silicon carbide gratings will be cooled from the sides. For suppression of higher order light there will be two interchangeable refocusing mirrors, one will be coated with gold and the other nickel. Each will have a different angle of incidence.

Designs have been progressing toward the goal of installing all in-alcove components during the 1989 August-September shutdown. All the optical components have been ordered and have delivery dates before mid July 1989. The monochromator is to be delivered during the summer of 1989. Commissioning should start during the first run of FY 1990.

SUPPORT FACILITIES

Computational Facilities - During 1988 the upgrade of the SSRL computer system was completed with the replacement of the VAX 11/780 and 11/750 computers by a VAX 8810 computer system. This has resulted in a performance increase of more than a factor of four. The first of the beam line computer system upgrades to a microVAX II GPX workstation was accomplished. This is the first step that will lead eventually to replacements of all the aging PDP-11/34 computer systems. The increase in performance is significant and will permit on-line data analysis to be performed concurrently with data acquisition and provide for much enhanced graphics.

A variety of new software and database systems were developed including: "layered" data acquisition code that allows different types of experiments to be controlled by almost identical software. Databases to maintain records of engineering drawings at SSRL and to maintain correspondence with proposal referees; and an 'on-line' stockroom inventory program was developed to handle stock issues for users and staff. The VAX motors program that provides the VAX-CAMAC interface was completed and debugged and will be used on several stations during the Winter, 1989 run. The high level user interface for the data acquisition package, (called MIDAS) is currently under development and test. An application package for XAS data collection will be tested during the summer 1989 run.

Mirror Coating Facility - The SSRL Large Optics Coating Facility was moved to the new Metro-Mirror

Laboratory in the LOS building. The system has gone through some changes to improve the quality of the thin film coatings. A new five crucible e-Gun and five position shutters were installed. The new e-Gun allows materials to be selected for coating without opening the lower half of the chamber. This quick turn around means that better coating pressures can to be maintained. A new optics cleaning facility under a hepa filter has also been installed to assure particle free cleaning.

Twelve mirrors were coated in 1988. Eight of these were for other laboratories, such as NSLS, ORNL and Los Alamos. Platinum, gold, nickel and rhodium have been evaporated at pressures of $5x10^{-8}$ Torr during coating.

User/Staff Cleanroom - The old vacuum group cleanroom in Building 131 is being setup for the use of users and staff. This room has several benches, an ultra sonic cleaner, spot welder and a limited number of clean tools for work on manipulators and detectors in a clean environment.

Biochemical Laboratory - Only a few changes were made to the laboratory in 1988. These include the addition of a microfuge for small volume samples and an ultracentrifuge rotor with swinging buckets.

SSRL staff celebrating the completion of a rebuilt Beam Line 2

IV ENGINEERING

The SSRL Engineering group, both mechanical and electrical, provides support to laboratory operations and developmental activities. Beam line design and modification is a continuing major effort. In 1988 the group played a major role in the design and construction of SPEAR Beam Lines 5, 8, 10, 6-1 and PEP Beam Line 1B, plus a major rebuilding of Beam Line 2. Major support was also provided to the 3 GeV injector now in construction and to a design study for the upgrade of this injector to 5 GeV level so that it could serve as an injector to PEP via a new transfer line.

MECHANICAL ENGINEERING

Thermal-Structural Analysis - Finite element analyses techniques have been used to calculate the temperature and stress distributions in the SPEAR supercrotch, the fixed and moving masks on Beam Lines 4 and 7, the beryllium windows on Beam Lines 6 and 10, the differential pumping system newly installed on Beam Line 10-2, and to estimate the stresses in a proposed flexible vacuum chamber with variable height.

The results of the window temperature calculations correlated well with measured temperature distributions on a test window (heated with an electron beam welder) using an infrared camera.Some temperature measurements were taken on the Beam Line 7 (8-pole wiggler) supercrotch exposed to bending magnet radiation plus the fringes of the wiggler beam. These measurements show very small temperature rises. A higher temperature rise, and higher stress, is expected if the wiggler beam is missteered toward the crotch. It is planned to study this under controlled conditions with intentionally missteered beams. The measured temperatures will then be compared with those predicted by finite element analysis. This should provide a better basis for setting limits on SPEAR current as a function of electron energy and wiggler field. This project is being carried out in collaboration with members of the SSRL X-ray Group.

Injector Magnet Tests - The Mechanical Engineering Group assisted the Injector Group in the design of the bend magnet support system. Vibrational modes were calculated, and design suggestions made to increase the fundamental vibrational frequency of the support beam. Assistance was given in measuring vibrational frequencies in prototype assemblies. Deflections and stresses of proposed beams were predicted. Calculations were made of the heating effects in magnet windings. Assistance was given to develop procedures for bonding magnet laminations.

ELECTRICAL ENGINEERING

Beam Line Control Systems - A major activity of the Electrical Engineering group is the design, construction, maintenance and improvement of the many electronic systems for SSRL beam lines. These include vacuum controls, photon beam steering and stabilization controls, personnel protection interlock systems, communications (audio, video, data), insertion device controls and experimental station electronics. The group provides continuous support of these systems during operational periods.

In 1988 the EE group design activities included the implementation of control systems for two new SPEAR beam lines: Beam Line 5 and Branch Line 6-1. Installation of these control systems was completed and the various controls were tested.

A control logic was designed and implemented for Branch Line 10-2 to allow the operation of this branch line in both hard x-ray and soft x-ray modes. The controls included the interlocks required to operate the differential pump section, cold trap module, and the in-vacuum monochromator. In the hard x-ray mode the differential pump section, which operates in vacuum, is separated from the in-helium monochromator by a beryllium window module. In the soft x-ray mode, the beryllium window is removed, and the monochromator is operated in vacuum.

Beam Line Steering and Stabilization - The upgrade of the SPEAR steering control system was completed (see description in SSRL Activity Report for 1987). The new steering control system was tested in operation and performed as designed.

Experimental Station Electronics - A new V/F (voltage to frequency) converter was developed and tested. The new unit includes two V/F channels and is packaged in a NIM module. The circuit includes a commercial monolithic synchronous voltage to frequency converter. Each channel has a switch which allows the input signal to be buffered (unity gain) or amplified by 10. A new I/F (current to frequency) converter was developed and tested.

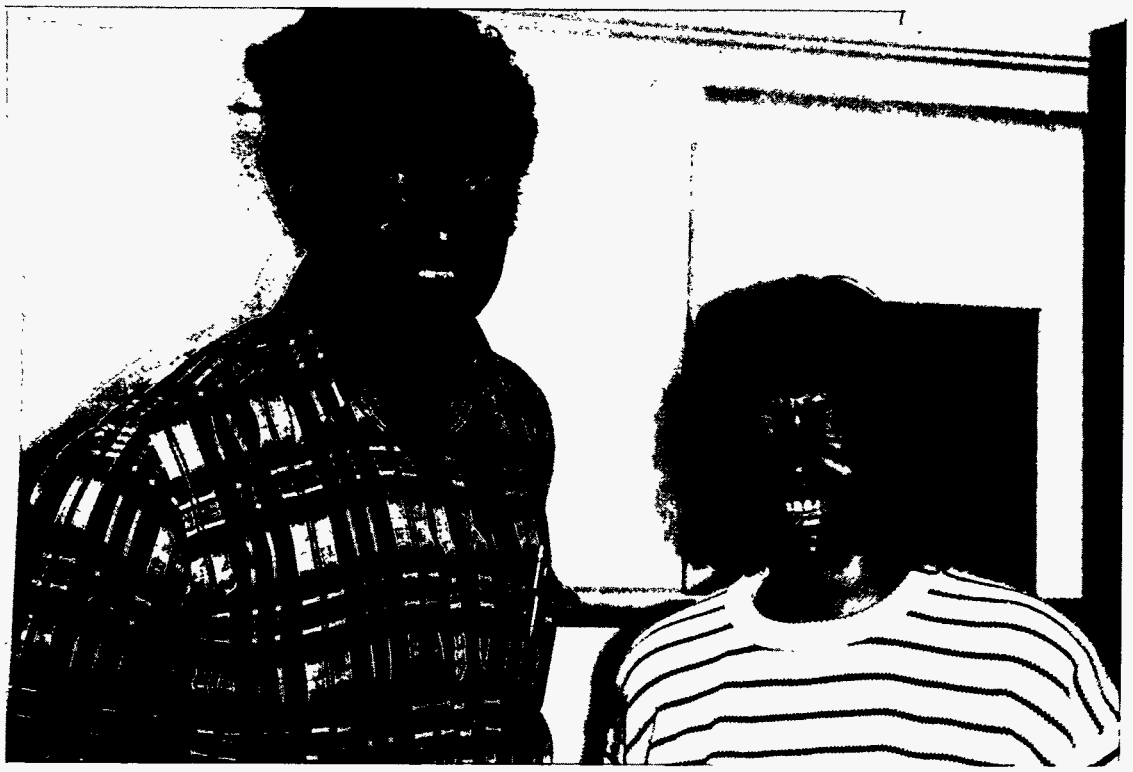

Richard Boyce, SSRL Engineering Staff and Zofia Rek, SSRL Scientific Staff at the Beam Line 2 Celebration. Richard was lead designer on the project and Zofia the scientific coordinator.

Bill Parrish, IBM and Katherine Cantwell, SSRL looking at the new 2-2 Hutch. The redevelopment of Beam Line 2 was a joint venture with IBM.

V CONFERENCES AND WORKSHOPS

2nd PEP WORKSHOP

On November 2, 1988, SSRL conducted a Workshop on Accelerator Physics Issues Relating to the Use of PEP as a Synchrotron Radiation Source. The 48 registered participants included accelerator physicists from laboratories in the U.S. (ANL, BNL, Cornell, LBL, LLNL, SLAC, SSRL and Wisconsin), Europe (CERN, ESRF), Japan (JAERI, the Photon Factory and Riken) and Taiwan (SRRC). The workshop was chaired by H. Winick and H.-D. Nuhn.

The main objective of the workshop was to review the results of the December 1987 dedicated low emittance run on PEP and to plan future accelerator physics studies as well as additions and modifications to PEP to fully exploit its potential as a synchrotron radiation source.

Five working groups were formed to make specific recommendations for future studies and PEP modifications. A main objective of the workshop was to develop approaches to the attainment of stable stored beam currents of 50-100 mA in low emittance mode at electron energies around 6-10 GeV. The first two of the working groups were directly relevant to this. The Executive Summary of the workshop proceedings *(available from SSRL as report 88/06)* contains the following review of working group activities:

Feedback Systems, Tune Splitter Techniques, Higher Harmonic Cavities: (S. Kramer, ANL) The consensus of the workshop was that a wide-band longitudinal feedback system was the most effective approach to raising the levels of stable stored current in PEP in dedicated low emittance operation towards the desired 50-100 mA. It may be necessary to also implement a transverse feedback system to reach the highest levels. This is because calculated rise times for transverse instabilities, although longer than for longitudinal instabilities, are still short compared to the damping time due to synchrotron radiation emission at electron energies around 6-10 GeV in PEP. The transverse feedback system could be implemented after tests are made with the longitudinal system and the need for the transverse system is definitely known.

Consideration might also be given to the use of a narrow band feedback system and tune splitting as was success fully tested on PETRA by R. D. Kohaupt and the use of a higher harmonic (Landau) cavity.

Damping of Higher Cavity Modes, Impedance Reduction: (G. Nicholls, ANL) Significant reduction in the higher mode impedance of the PEP RF cavities and other components could be achieved, particularly if PEP were to become a dedicated synchrotron radiation source. Such reductions would result in an increase in the threshold currents for instabilities, leading to more stable and larger stored currents.

Removing 2/3 of the present RF cavities should result in a reduction of ring impedance by about a factor of 2. However it would also result in a reduction of the top energy of the ring from about 16 GeV to about 11 GeV. In addition, the lower RF voltage available would limit the ability to achieve very short bunches using the RF overvoltage technique. Other approaches could be considered such as damping antennas to suppress higher cavity modes, mode management with adjustable blank off flanges as has been used at the Photon Factory and new cavities that would suppress higher modes by design.

In general, these approaches have drawbacks compared to feedback systems which are likely to achieve more significant gains with less cost and complexity and without some of the trade-offs. Reduction of higher mode impedances is however attractive when used in combination with a feedback system to achieve even higher performance levels.

Low Energy Injection and Ramping: (E. Rowe, Wisconsin) Until now there has been no need to develop low energy injection and ramping for PEP. With the possibility that the SPEAR 3 GeV injector, now in construction, could be upgraded to 5 GeV and used as a PEP injector, it becomes important to consider this. At lower energy, instability thresholds will set in at even lower currents so that it will be necessary to raise these thresholds. Based on

experience with other rings (e.g., Aladdin, NSLS, SPEAR) it should be straightforward to inject and ramp 50-100 mA in PEP after some experience has been gained and with suitable increase in the thresholds for instabilities such as may be expected with the implementation of feedback systems.

Low Emittance Configurations: (J. Safranek, SSRL) Further emittance reduction by increasing the horizontal focussing does not seem attractive. An improvement to the present low emittance lattice could be made by reducing the dispersion function at the symmetry straight sections. This would reduce the dispersion contribution to the source size for the present undulator beams. This becomes more important as the emittance is reduced since, eventually, the source size at these locations would be dominated by the dispersion. A low emittance lattice could be developed that would be optimized for damping wigglers. With 100 meters of damping wigglers the emittance of PEP could be reduced to about 1 nm-rad at 6 GeV.

Short Bunches: (L. Rivkin, SLAC) PEP offers unique opportunities to achieve short bunches. Several techniques have been considered including pulse compression, excitation of quadrupole oscillations, high RF voltage and lattice modifications. Standard deviation bunch lengths as short as 1.6 ps at 6 GeV appear to be attainable.

The workshop provided much information and many ideas that will be of immense help to SSRL in planning for the development of PEP as a synchrotron radiation source. Although PEP was the central focus of the workshop, it is clear that the experience on PEP and the discussions at the workshop had much relevance to other light sources. In addition, the multi-laboratory participation in the workshop, as was also the case in the December 1987 dedicated low emittance run, gave the participants an opportunity to meet their counterparts from other laboratories, often for the first time, and made for an exciting and stimulating experience for all.

15th Users' Conference

The 15th Annual SSRL Users Conference was held October 27 and 28, 1988. It was chaired by Marjorie Olmstead (University of California-Berkeley) and John Arthur of the SSRL staff.

Even though the beam time at SSRL was limited during the last year, exciting research was accomplished, as evidenced by the invited scientific talks presented at the meeting. Piero Pianetta of SSRL described the first operation of a photoemission microscope, the result of a collaboration between SSRL, Stanford, and Surface Science Laboratories. Chemical identification via soft x-ray photoemission spectroscopy with a spatial resolution of better than 5 microns was demonstrated. Another talk by Walt Ellis of Los Alamos National Laboratory described studies of resonant photoemission from shallow levels in high-temperature superconductors and related oxides. These measurements give important information about the atomic origin of the states near the Fermi level which contribute to or inhibit superconductivity. Tom Russell from the IBM Almaden Research Center described soft x-ray reflectivity studies of polymer films, which probed the effects of sample preparation on the phase separation of polymer mixtures. The use of hard x-rays for microtomography was discussed by John Kinney from Lawrence Livermore National Laboratory. He showed that the technique can rapidly and non-destructively produce three-dimensional images of samples, giving both structural and chemical detail with a resolution of several microns.

An Abstract Book of the invited talks and posters is available from SSRL (SSRL report 88/04).

Lawrence Pan, Anne Borg and Paul King, members of the SSRL VUV group at the Users Conference Poster Session.

Users and staff enjoying lunch

VI SSRL ORGANIZATION

SSRL FUNCTIONAL ORGANIZATION

The SSRL administration is divided into seven functional areas each headed by a senior staff member. These are: X-ray, VUV, Biotechnology, Accelerator Physics, Operations, Engineering and Administration. In addition, each experimental station and piece of specialized instrumentation is the responsibility of an SSRL staff member. The charts which follow depict these responsibilities and the functional organization of SSRL.

SSRL EXPERIMENTAL STATIONS
RESPONSIBLE PERSONNEL

BRANCH LINE	RESPONSIBLE SCIENTIST/ENGINEER
1-1 (Grasshopper)	I. Lindau, F. Senf
1-2 (TGM)	I. Lindau/M. Rowen
1-4 (SAS)	S. Brennan/H. Tompkins
1-5 (Bend Magnet X-ray)	G. Brown/T. Troxel
2-1 (Bend Magnet X-ray)	G. Brown/T. Troxel
2-2 (White Radiation)	Z. Rek
2-3 (Bend Magnet X-ray)	G. Brown/T. Troxel
3-1 (Grasshopper)	I. Lindau, F. Senf
3-2 (SXR- 18 degree)	I. Lindau/F. Coffman
3-3 (SXR-Jumbo)	I. Lindau/M. Rowen
3-4 (Lithography)	P. Pianetta
4-1 (Wiggler)	G. Brown/T. Troxel
4-2 (Wiggler)	G. Brown/T. Troxel
4-3 (Wiggler)	S. Brennan/H. Tompkins
5 (Undulator)	I.Lindau/F. Coffman
6-1 (SGM)	F. Senf,P. Heimann *(LBL)*
6-2 (Wiggler)	J. Arthur/T. Troxel D. Moncton *(EXXON)*, P. Ross*(LBL)*
7-1 (Rotation Camera)	P. Phizackerley, M. Soltis
7-2 (Wiggler)	S. Brennan/H. Tompkins
7-3 (Wiggler)	G. Brown/T. Troxel
8-1 (SGM)	M. Rowen,G. Tirsell *(LLNL)*
8-2 (TGM)	M. Rowen,S. Williams (UCLA)
10-2 (Wiggler)	S. Brennan/J. Wong (LLNL)
PEP 1B	G. Brown/T. Troxel
PEP 5B	G. Brown/T. Troxel

INSTRUMENTATION/FACILITY RESPONSIBILITIES

MATERIALS DIFFRACTOMETER: *S. Brennan/H. Tompkins*
PERKIN-ELMER SAMPLE CHAMBER: *F. Senf*
VG SAMPLE CHAMBER: *F. Senf*
AREA DETECTOR: *P. Phizackerley, H. Bellamy*
CAD-4 DIFFRACTOMETER: *M. Soltis*
COMPUTER SYSTEMS: *T. Cox*
7-2 SPECTROMETER: *S. Brennan/H. Tompkins*
BIOCHEMISTRY LABORATORY: *B. Hedman/R. Mayer*
DARKROOMS: *M. Soltis, Z. Rek*
BEAM LINE STEERING: *R. Hettel*
EXAFS EQUIPMENT AND SOFTWARE: *B. Hedman/R. Mayer*
SAS CAMERA (BIOLOGY): *S. Wakatsuki*
EXAFS CONSULTANT: *B. Hedman*
SCATTERING CONSULTANT: *S. Brennan*
RT-11 SOFTWARE CONSULTANT: *S. Brennan*
TOPOGRAPHY EQUIPMENT: *Z. Rek*
RAPID TURN AROUND EXAFS FACILITIES: *B. Hedman/R. Mayer*
MIRROR COATING/METROLOGY LABORATORY: *D. Ernst*

SSRL DEVELOPMENT PROJECTS - RESPONSIBLE PERSONNEL

STATION 6-1	*F. SENF (SSRL), W. MCKINNEY (LBL)* *R. YOTAM (SSRL)/J. CHIN (LBL)*
3 GeV SPEAR INJECTOR-	*H. WIEDEMANN*
STATION 10-1	*I. LINDAU (STANFORD), J. STOHR (IBM),* *M. ROWEN (SSRL)/J. MONTGOMERY (SSRL)*

SSRL Organization Chart

March 1989

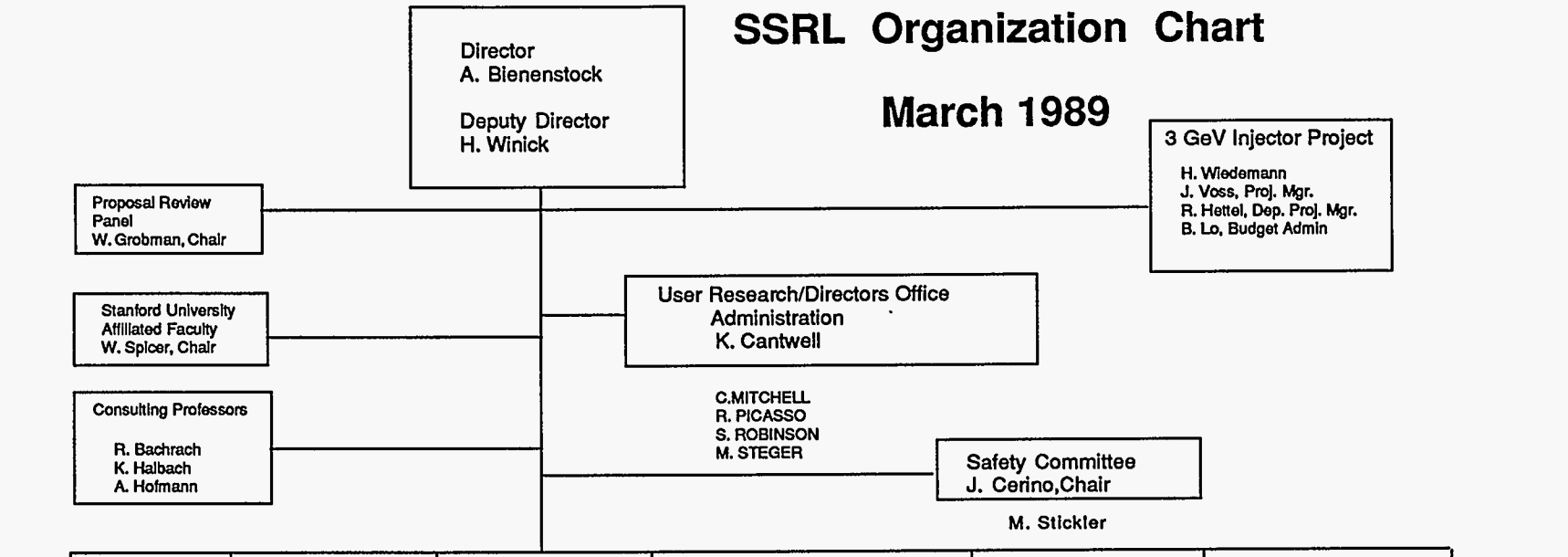

J. ARTHUR
A. BIENENSTOCK
S. BRENNAN
P. CAPEDER
G. KERR
H. PRZYBYLSKI
S. RUBY
A. TISCARENO
H. TOMPKINS
C. TROXEL, JR.
T. TROXEL

B. BURDICK
R. CARR
F. COFFMAN
G. HUSEK
R. MORRIS (SEL)
B. PATE
P. PIANETTA
M. ROWEN
F. SENF
R. TATCHYN
C. TROXEL
*A. WALDHAUER

H. BELLAMY
B. HEDMAN
R. MAYER
P. PHIZACKERLEY
Z. REK
M. SOLTIS

COMPUTER RESOURCES

A. COX, Mgr
J. HAYWARD
A. WINSTON

M. BALTAY
J. CERINO
C. CHAVIS
R. HETTEL
T. HOSTETLER
G. JOHNSON
J. KWONG
J. LEONARD
B. LO
J. MELLO
H.-D. NUHN
J. SEBEK
J. VOSS
J. WEAVER
H. WINICK

BUSINESS ADMINISTRATION

M. BOWMAN, Mgr
M. BRUCE-HEMENWAY
L. CRUM
L. DUNN

PERSONNEL ADMINSTRATION

S. LOVGREN, Mgr
L. DUNN

ELECTRONICS

R. YOTAM, Mgr
R. GAROUTTE
R. HETTEL
M. HORTON
R. ORTIZ
J. YANG

MECHANICAL

B. YOUNGMAN, Mgr
R. BOYCE, Dep Mgr
M. DORMIANI
J. MONTGOMERY

M. STICKLER, Admin
C. TROXEL, Mgr
C. TANIGUCHI (Stockroom)

OPERATORS

D. DAY, Supervisor
P. BOYD
K. CULLER
J. DUNN
D. ERNST
D. NEAR
D. ROSITCH
B. SILVERS
T. YOTT

PLANT

A. FILIPPI

VACUUM

H. MORALES, Supervisor
M. NALLS
T. NEAL

*Sabbatical

SSRL ADVISORY BOARDS

PROPOSAL REVIEW PANEL

A main task of the Proposal Review Panel is the review and rating of scientific proposals to SSRL based largely on reports obtained from outside (non-panel) referees. The panel met on January 8 and 9, 1988 and on July 15 and 16, 1988 at SSRL and rated the new proposals which had been received in September, 1987 and March, 1988 respectively.

As of December 31, 1988 SSRL has received a total of 2076 proposals of which 180 are presently active.

The Proposal Review Panel meets twice yearly, generally in June and January. Deadlines for receipt of proposals for consideration at the next meeting are the first of September and the first of March of each year. Two PRP members, Charles Cantor, Columbia University (Biology) and Bob Batterman, Cornell University (Materials) left the panel after the July meeting.

The panel members in 1988 were:

Biology Sub-panel
Don Engelman, Yale University
Wayne Hendrickson, Columbia University
William Orme-Johnson, MIT

Materials Sub-panel
G.Slade Cargill, IBM Research Center
Howard Birnbaum, University of Illinois
Russell Chianelli, Exxon
Denis McWhan, AT&T Bell Laboratories

VUV Sub-panel
Charles Fadley, University of Hawaii
Warren Grobman, IBM Watson Research Center (Chairperson)
Torgny Gustafsson, Rutgers University

SCIENCE POLICY BOARD

The Science Policy Board reviews all aspects of SSRL operation, development and plans for the future. It reports to Stanford University President Donald Kennedy. The Board met once during this reporting peroid, on April 27-29, 1988. The members at the time of the meeting were:

B. McDaniel, Cornell University *(Chairperson)*
P. Chaudhari, IBM
E. Ginzton, Varian Laboratories
W. Kohn, University of California
W. Orme-Johnson, MIT
Y. Petroff, LURE
F. Schwettman, Hewlett-Packard
P. Wolff, MIT

SSRL USERS ORGANIZATION

Members of the Executive Committee of the SSRLUO were appointed at the 15th Annual SSRL Users Group Meeting as following:

Marjorie Olmstead, UC-Berkeley *(Chairperson)*
Stephen Laderman, Hewlett-Packard *(Vice-Chair)*
Troy W. Barbee, Jr., LLNL
Frank (Bud) Bridges, University of California
Ross Bringans, XEROX
Gordon Brown, Stanford University
Louis Terminello, Lawrence Berkeley Laboratory
Al Thompson, LBL
Trevor Tyson, Stanford University
Stan Williams, University of California
Joe Wong, LLNL *(Past-Chairperson)*
Katherine Cantwell, *(Secretary - SSRL Liaison)*

The Users Organization Executive Committee meets peroidically throughout the year to consider and advise on matters pertinent to user interests at the Laboratory.

VII EXPERIMENTAL PROGRESS REPORTS

BIOLOGY PROPOSALS

VUV PROPOSALS

Hal Tompkins (left) and John Arthur (right) of the SSRL X-ray staff in front of the groups' x-ray generator.

Duty Operator, Don Rositch

X-RAY ABSORPTION STUDIES OF DISORDERED SYSTEMS

E.D. Crozier, N. Alberding, K.R. Bauchspiess, D.T. Jiang
Physics Department, Simon Fraser University
Burnaby, B.C., Canada V5A 1S6

R. Ingalls, J. Freund and B. Houser
Physics Department, University of Washington
Seattle, Wash., 98195, U.S.A.

Surfaces

Obtaining quantitative details of the structure of interfacial regions is a difficult experimental problem, yet of fundamental interest. It is of particular importance in device-physics application where the interface of interest may be buried beneath a passivating layer. In our studies we use the glancing-incidence EXAFS technique in which the depth or interface is selected by simply choosing the correct angle of incidence.

In this reporting period we have continued our analysis of Ni films prepared by molecular beam epitaxy. Ni epitaxially grown on the (001) face of iron single crystals shows interesting magnetic and structural properties. Although the first 6 ML (monolayers) of Ni have not been shown to be ferromagnetic, additional layers exhibit large cubic in-plane magnetic anisotropy. LEED and RHEED analysis show that the first 6 ML of Ni have the bcc structure of the substrate. LEED has been unable to determine the structure of the thicker films. RHEED patterns show some b.c.c. features but with additional spots which are not yet explained. It has been unclear whether the unusual magnetic properties are caused by a novel crystal structure or by a normal crystal structure with defects.

Our samples were 6 ML and 37 ML of Ni epitaxially grown on the Fe single crystal (001) surface in a MBE chamber at room temperature. An Al layer, about 75 Å, was deposited on the top at 130K to prevent oxidation. The FMR results confirmed that the Ni in the Al-covered Ni(37 ML)/Fe(001) sample has similar magnetic behavior to the Ni not covered with Al. Fluorescence EXAFS data were collected at glancing-incident angles. The Fourier transform magnitude of the 37 ML sample is shown in Fig. 1.

Comparison of layers vs bulk Ni samples

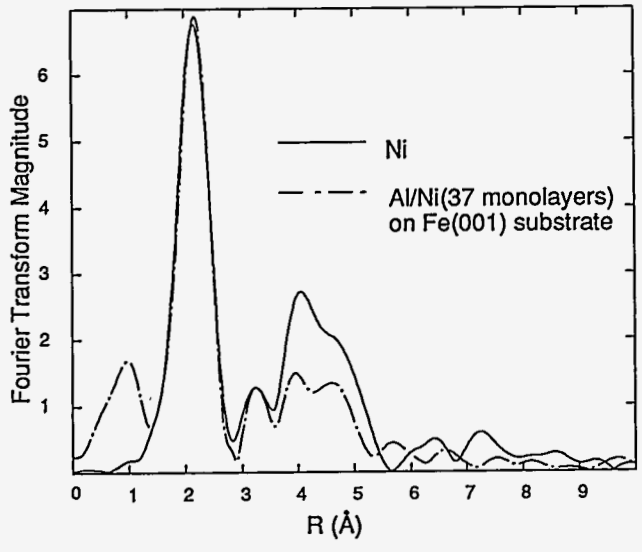

Our curve fits, to both the filtered k-space data, and to the real and imaginary parts of the Fourier transform, show that the first- and second-shell Ni-Ni distances differ by only 0.016±0.01 Å and 0.013±0.05 Å from f.c.c. Ni metal. The ratio of the number of neighbors in the two shells is 0.50±0.05. For a f.c.c. lattice the ratio would be 0.5 and for b.c.c., 0.75. Thus the local structure is nearly identical with that of pure f.c.c. Ni. However, the amplitude of the 3rd and 4th shells are significantly smaller. In contrast, the Fourier transform of the 6 ML Ni sample spectrum differs substantially from that of bulk Ni (Fig. 2).

Fitting this shell to Al phases gives a distance of 2.48±0.02 Å, which could indicate the quenched tetragonal Al_3Ni_2 alloy. Thus substantial intermixing of the Al overlayer with the 6 layers of Ni may occur[1].

Comparison of 6 Monolayer and Bulk Nickel

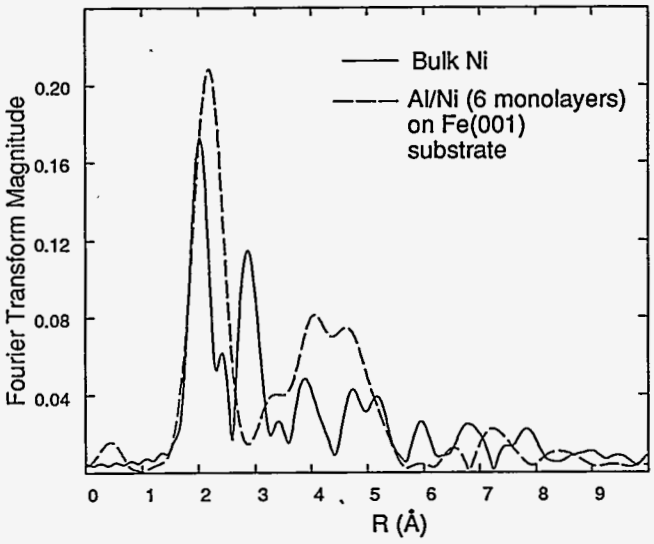

Valence Transition in SmSe

SmSe undergoes an isostructural pressure-induced continuous mixed valence transition. We investigated the valence transition as a function of pressure at 77K where the temperature-dependent part of the EXAFS Debye-Waller factor is reduced so that possible structural disorder can be readily detected. For maximum R-space resolution the Se K-edge EXAFS was measured up to 24 $Å^{-1}$. Our previous work[2] indicated an anomaly in the Debye-Waller factor in the region of the phase transition. During this reporting period we have extended our analysis procedures to try to determine if this anomaly can be interpreted as being due to a splitting of the nn Se-Sm distance into two Se-Sm distances according to the different ionic radii of the rare earth ion.

For the analysis we used theoretical backscattering amplitudes and phases, calculated from first principles[3] and employed a curved-wave formalism. One-shell fits to the Se-Sm co-ordination were improved by including a second Sm coordination shell. The goodness of fit, corrected for the increased number of variable parameters, was improved by a factor of ~2.5, making the addition of a second Sm shell significant. The difference between the two Sm distances is approximately 0.11 Å which was confirmed by a beating analysis[2] . We obtain Gaussian pair distribution functions, shown in Fig. 3 for several pressures. In the transition region two peaks are resolved. This may indicate that SmSe is perhaps not homogeneously mixed valent or it could indicate that the Sm atoms may indeed relax with a time constant like that of the valence fluctuations (~10^{-13} s).

Pair Distribution Functions

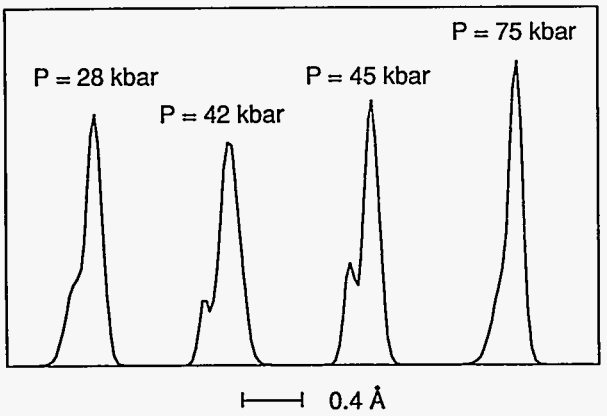

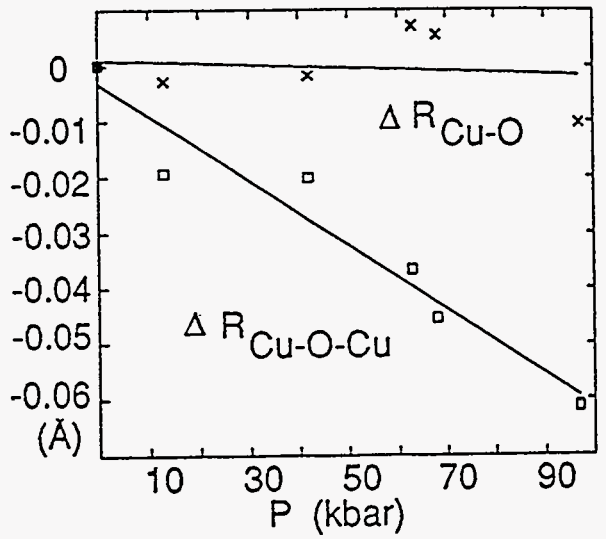

[1]D.T. Jiang, N. Alberding, A.J. Seary, B. Heinrich, E.D. Crozier, Physica B. (to be published).

[2]K.R. Bauchspiess, E.D. Crozier, R. Ingalls, J. Phys. (Paris) Colloq. **47**, C8-975 (1986)

[3]K.R. Bauchspieß, E.D. Crozier, R. Ingalls, Physica B (to be published)

[4]N. Alberding, K.R. Bauchspiess, J.M. Tranquada, R. Ingalls and E.D. Crozier, Physica,B.(to be published).

High T_c Superconductivity

A valid theory of high T_c must predict the observed increase in T_c with pressure. The theory will require detailed knowledge of the crystal structure. X-ray diffraction studies have suggested that pressure causes a monotonic compression of the lattice parameters, without producing any structural changes in the unit cell. However, for perovskite-like structures phase transitions are difficult to detect by x-ray diffraction.

During our November 1987 run we explored the pressure dependence of the EXAFS spectra of two high T_c superconductors. Our analysis of $YBa_2Cu_3O_{7-\delta}$ strongly suggests that the oxygen bridges between copper atoms bend with the application of pressure. Strong beating among the Y, Ba and Cu shells makes the analysis complex, and the evidence of chain bending is mainly from reduction of the amplitude of the Cu-O-Cu multiple scattering amplitude. This year we continued with the analysis of $La_{1.85}Sr_{0.15}CuO_{4-y}$ in collaboration with J.M. Tranquada. In this case, the La and Cu peaks are more easily isolated and are not as intricately intertwined as in the Y-Ba-Cu case. Here the EXAFS spectra indicate that, as pressure is increased, the Cu-Cu distance shortens more than twice as much as the Cu-O distance decreases. Again the Cu-O bonds seem to bend with pressure. For $La_{1.85}Sr_{0.15}CuO_{4-y}$ our results indicate that the Cu-O-Cu bond angle is 164° ± 10° at 90 kbar. This implies that with pressure the Cu-O octahedra rotate and the consequent change in the electronic structure should be included in theoretical treatment of the high temperature superconductivity.[4]

X-RAY ABSORPTION AT HIGH PRESSURES

R. Ingalls and J. Freund

Physics Department, University of Washington, Seattle WA

and

E. D. Crozier

Physics Department, Simon Frazer University, Burnaby, B. C., Canada

We have examined copper as a pressure calibrant for extended x-ray absorption fine structure (EXAFS) measurements of solids under pressure.[1] We find that copper is an excellent pressure marker if great care is taken both in the theoretical formulation of the EXAFS-formula (cumulant expansion) and in the data analysis (Fourier transforms). The two standard single-shell data analysis techniques, the ratio method and parameter fitting, give perfectly compatible results which confirms the usefulness of McKale's new curved wave EXAFS amplitude and phase tabulations.[2]

When the pressure induced nearest neighbor (nn) distance reductions are thus extracted from the EXAFS spectra an isothermal equation of state (E.O.S.) is required in order to express the results in terms of pressures. We have searched the literature carefully for appropriate two- and three-parameter E.O.S. which can be written both in the usual form $p = f(V/V_0)$ and in the form $V/V_0 = f(p)$, where V/V_0 is the relative volume and p the pressure. The latter form is necessary for further data interpretation. We find about a dozen of these E.O.S., have invented two new ones and compared all of them.[3] It turns out that compression data of most materials found in the literature are fitted very well with our new E.O.S.

With the conversion from nn distance reductions to pressures accomplished we estimate that the accuracy of our pressure calibration is about 0.5 GPa which compares favorably with the standard techniques in x-ray scattering work. We have therefore used copper as a pressure standard with many other samples, including amorphous germanium.

We have just completed the data analysis of amorphous germanium and find two interesting results: (1) Contrary to some reports we can *not* find a phase transition to a crystalline form of germanium up to 8.9 GPa. (2) We have calculated the bulk modulus of the Ge-*bonds* (as opposed to the *bulk* of the material, including voids) and find that it is larger than for crystalline Ge. We are now working on two- and three-body potential calculations in order to explain this difference.

References

1. J. Freund and R. Ingalls, Phys. Rev. B., (submitted)

2. A. G. McKale, et. al. J. Am. Chem. Soc., **110**, 3763 (1988).

3. J. Freund and R. Ingalls, J. Phys. Chem. Solids, (in press)

Acknowledgements

This work was supported in part by the U. S. Department of Energy and the National Sciences and Engineering Research Council of Canada.

The W(001) Phase Transition; A Synchrotron X-ray Diffraction Study

I.K. Robinson, A.A. MacDowell
AT&T Bell Laboratories, Murray Hill, NJ 07974

M.S. Altman, P.J. Estrup
Brown University, Providence, RI 02912

K. Evans-Lutterodt, J.D. Brock, R.J. Birgeneau
MIT, Cambridge, MA 02139

INTRODUCTION

W(001) has been identified as an interesting candidate for surface phase transition studies. Previous LEED work [1] has deduced that the low temperature ordered phase consists of two equivalent domains. In one domain the surface tungsten atoms are displaced from their bulk positions in the (110) direction, and the other domain has displacements in the $(1\bar{1}0)$ direction. Furthermore, within each domain the displacements order in an antiferromagnetic fashion, leading to the zig-zag chains on the surface. This structure can be described as $(\sqrt{2} \times \sqrt{2})R45^\circ$ with two atoms in the unit cell, and gives rise to half order diffraction peaks that have no bulk contribution. The choice of the (1.5,1.5) peak dictates that the scattering observed comes from only one of the two domains, the domain with momentum transfer parallel to the displacement vector. LEED and helium diffraction studies of the surface diffraction peaks have concluded that there is a reversible phase transition at approximately 200K.

RESULTS

The surface diffraction peak we studied (see Figure 1) was commensurate at all temperatures within our experimental accuracy of ≈1%, in the measured temperature range from 140K to 360K. This is in agreement with LEED data, but in disagreement with helium scattering measurements [3] suggesting that the half order peak is commensurate in the ordered phase, but becomes incommensurate above the transition temperature.

The x-ray diffraction half widths below 200K are approximately constant, but not resolution limited, corresponding to a finite domain size. Above 200K we observe critical scattering, and the half widths vary smoothly with temperature, from a half width of $6 \times 10^{-3}\text{Å}^{-1}$ to $9 \times 10^{-1}\text{Å}^{-1}$ in the longitudinal direction. This is a direct manifestation of the disordering of the $(\sqrt{2} \times \sqrt{2})R45$ reconstruction above the transition temperature.

The integrated intensity is conserved across the transition (see Figure 2) confirming that this is a disordering of the $(\sqrt{2} \times \sqrt{2})R45^\circ$ phase, and that the short range structure does not change dramatically through the phase transition.

The half widths in the direction parallel to the displacement vector are smaller than in the perpendicular direction, with $\xi_\parallel \approx 0.6\xi_\perp$.

The two correlation lengths (inverse half widths) diverge isotropically with temperature, i.e. $\nu_\perp = \nu_\parallel$, with $\xi_\parallel = \xi_{\parallel 0} t^{-\nu_\parallel}$.

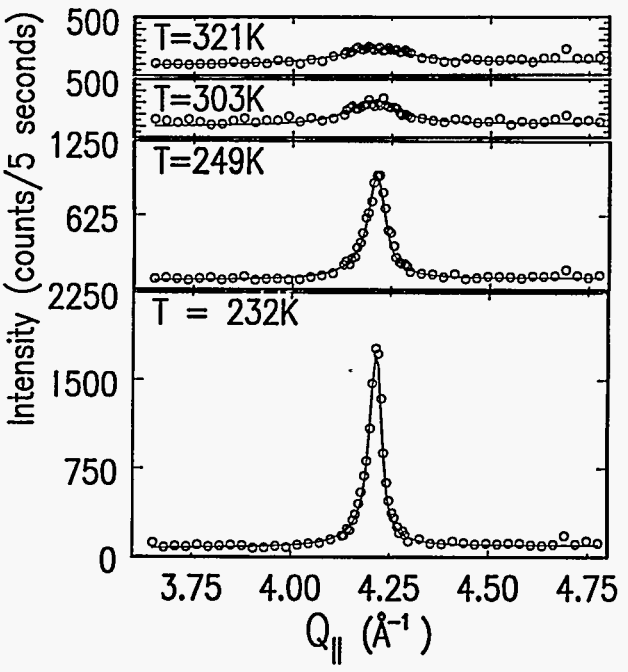

Figure 1: Longitudinal scans through the $(\frac{3}{2}, \frac{3}{2})$ peak.

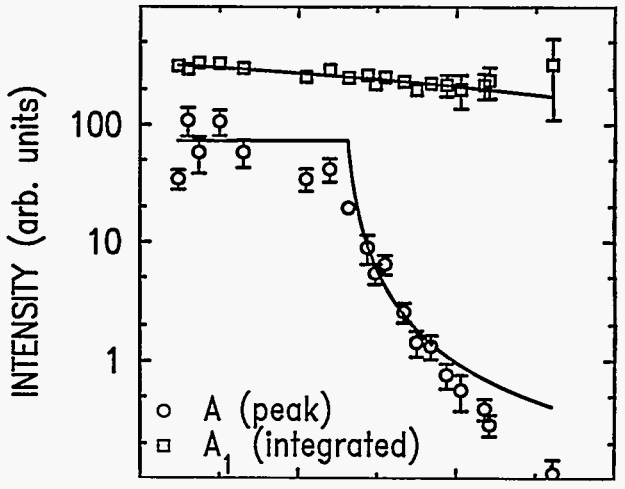

Figure 2: Comparison of peak intensity (A), and integrated intensity (A_1) as function of temperature.

References

[1] M.K. Debe, D.A. King, Phys. Rev. Lett. 39, 708 (1977); T.E. Felter, R.A. Barker, P.J. Estrup, Phys. Rev. Lett. 38, 1138 (1977); J.F. Wendelken, G.C. Wang, Phys. Rev. B32, 7542 (1985)

[2] G.Y. Hu, S.C. Ying, Physica A 140, 585 (1987)

[3] H.J. Ernst, E. Hulpke, J.P. Toennies, Phys. Rev. Lett. 58, 1941 (1987); J. Lapujoulade, B. Salanon, Surf. Sci. 173, L613 (1986).

COSTER-KRONIG TRANSITION PROBABILITIES IN METALS

S. L. Sorensen,[1] R. Carr,[2] S. J. Schaphorst,[1] S. B. Whitfield,[1] and B. Crasemann[1]

[1]Department of Physics and Chemical Physics Institute, University of Oregon, Eugene, Oregon 97403

[2]Stanford Synchrotron Radiation Laboratory, Stanford, California 94305

INTRODUCTION

Coster-Kronig transitions are Auger transitions in which a vacancy is transferred among subshells within a single inner shell of an atom or molecule. These low-energy radiationless transitions are exceedingly fast, causing large hole-state level widths and taxing the limits of perturbative theoretical approaches. Coster-Kronig rates are very sensitive to transition energy and wave-function overlap, and hence, to details of the atomic model including the effects of relativistic and quantum electrodynamic corrections.

Coster-Kronig transition rates are very difficult to measure because of their low energy. It is considerably easier to measure the "bulk" Coster-Kronig yield, defined as the total probability that a vacancy in atomic subshell i is transferred to subshell j of the same shell.

The experiment tested a new method which is useful in measuring Coster-Kronig yields in lighter elements. Previously measured transition rates existed only for heavy elements (Z>54) and generally only for L_2 decay because the accepted method relies on coincident detection of two decay products. There are no x rays which originate with a vacancy in the L_1 subshell leaving the L_2 shell vacant. The coincident method is valuable for measuring only the $f_{2,3}$ transition probabilities.

The photoionization method can yield values for the Coster-Kronig transition rates which can be compared with trends predicted by theoretical atomic models.

EXPERIMENTAL METHOD

Target samples were evaporated <u>in situ</u> onto an aluminum substrate. Radiation from the JUMBO double-crystal monochromator was tuned to ionize selected L subshells of the target elements. The incident photon flux was monitored by measuring photoelectrons ejected from a gold grid placed near the entrance of the target chamber. Auger spectra from the samples were recorded by means of a double cylindrical-mirror electron analyzer.

In order to measure the rate f_{23} of vacancy transfer from the L_2 to the L_3 subshell, the L_3-$M_{4,5}M_{4,5}$ Auger-electron spectrum was recorded when only the L_3 subshell was photoionized, and again, when both L_2 and L_3 subshells were ionized. Comparison of Auger-line intensities in the two cases, normalized to the same incident photon flux and taking into account the respective L subshell photoionization cross sections,[1] makes it possible to deduce f_{23}. An analogous procedure, based on measurements of L_2-$M_{4,5}M_{4,5}$ Auger spectra, permits determination of f_{12}.

Each data set was fitted to a set of peaks described by 4 continuously varying parameters. The analysis is complicated by the satellites which arise during the ionization procedure, either from multiple ionization or from spectator vacancies created by a transition taking place before the Auger decay. One not previously identified satellite in the silver $L_{2,3}$-$M_{4,5}$ Auger spectra is shown by an arrow. Calculations were carried out in order to identify the spectator vacancy which caused the shift in Auger energy. The $M_{4,5}$ vacancy which is left after an L_x-$L_y M_{4,5}$ Coster-Kronig transition takes place is responsible for the shift in the energy of the Auger line.

The $L_{2,3}$-$M_{4,5}M_{4,5}$ Auger spectra of Ag are shown in Fig. 1. The main peaks of the multiplet group are labelled in the figure. Figure 2 shows the results from the analysis of the four metals in the context of the previously measured transition rates. Theoretical values were calculated by Chen et al.[2] The agreement with theoretical predictions is good for $f_{2,3}$ while the measured values of L_1 Coster-Kronig yields are smaller than predicted by ~30%.

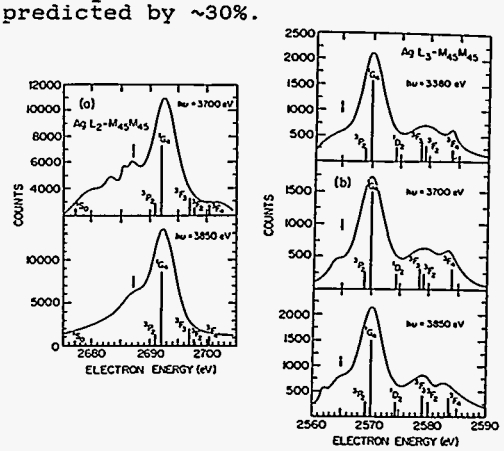

Figure 1. (a) Fitted Ag L_2-$M_{4,5}M_{4,5}$ Auger spectra excited with x rays of 3700, and 3850 eV energy. (b) Fitted Ag L_3-$M_{4,5}M_{4,5}$ Auger spectra excited with x rays of 3380, 3700, and 3850 eV energy.

The analysis is difficult for very light metals because the splitting between the L_1 and $L_{2,3}$ subshells is very small, making it difficult to accurately distinguish the L_2-$M_{4,5}M_{4,5}$ Auger peaks from the L_3-$M_{4,5}M_{4,5}$ group. This contributes to the large errors in the measured values of f_{12} in nickel and copper.

Results include Coster-Kronig transition probabilities f_{ij} that have not previously been measured and that play an important role in characterizing the dynamics of inner-shell electron reorganization following ionization.[3] The theoretical values for f_{1j} are consistently higher than the measured rates. This suggests that there are effects which are important in the calculation which must be included. Many-body effects including correlations with the continuum must be included in a multiconfiguration calculation to take account of these effects.

ACKNOWLEDGMENTS

We gratefully acknowledge the technical assistance and advice of Matt Richter, Michael Rowen, Ann Waldhauer, and Joseph Woicik. We thank W. Jitschin for help and advice in the initial stages of this work. This research is supported in part by National Science Foundation Grant PHY-85 16788 and Air Force Office of Scientific Research Grant AFOSR-87-0026. The experiment was performed at SSRL which is supported by the Department of Energy through the Office of Basic Energy Sciences and the National Institutes of Health through the Biotechnology Resources Program.

REFERENCES

1. J. H. Scofield, Lawrence Livermore National Laboratory Report No. UCRL-51326 (1973) and At. Data Nucl. Data Tables 14, 121 (1974).

2. M. H. Chen, B. Crasemann, and H. Mark, Phys. Rev. A 24, 177 (1981).

3. W. Bambynek, B. Crasemann, R. W. Fink, H.-U. Freund, H. Mark, C. D. Swift, R. E. Price, and P. Venugopala Rao, Rev. Mod. Phys. 44, 716 (1972).

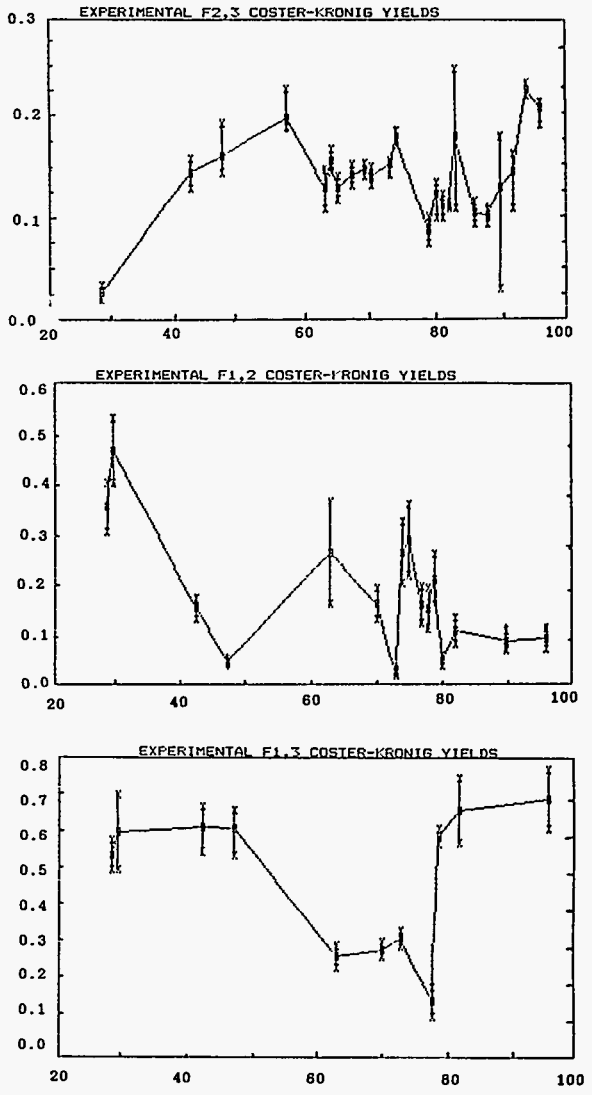

Figure 2. Measured Coster-Kronig transition rates for Ni, Cu, Mo, and Ag in the context of all previously measured rates.

XAS INVESTIGATION OF THE Nb SITE IN NATURAL PYROCHLORES AND SAMARSKITES

Proposal No. 1049Mp

R.B. GREEGOR*, F.W. LYTLE*, B.C. CHAKOUMAKOS**, G.R. LUMPKIN**, J.K. WARNER** and R.C. EWING**
*The Boeing Company, Seattle, WA 98124
**Department of Geology, University of New Mexico, Albuquerque, NM 87131

INTRODUCTION

Minerals of the pyrochlore group (Fd3m, Z=8) have the general formula $A_{1-2}B_2O_6Y_{0-1}$, where A=Ca, Na, U, Th, REE, Y, Ba, Sr, Pb; B=Nb, Ta, Ti, Zr, Sn, Fe; and Y=O, OH, F. Three subgroups are defined on the basis of the major B-site cations: microlite (Ta-rich), pyrochlore (Nb-rich) and betafite (Ti-rich). Samarskite is a complex Ti-Nb-Ta oxide whose stoichiometry approximates $A_3B_5O_{16}$, where A=Ca, U, Th, REE, Pb, Fe(2+); and B=Nb, Ta, Ti, Sn, W, Zr, Fe(3+). The variable chemistry and large stability field of these minerals lead to several interesting applications including use as a constituent of polyphase radioactive waste forms. Both pyrochlore and samarskite often occur in the aperiodic metamict (radiation damaged) state due to alpha decay/recoil nuclei damage created by 238 U and 232 Th. Previously we used x-ray absorption spectroscopy to investigate the Ti site in complex AB_2O_6 oxides, and the Ti, U and Ta site in $A_2B_2O_6Y$ pyrochlores. We extend our investigations here to the Nb B site in pyrochlores and samarskites.

EXPERIMENTAL DETAILS

Complete electron microprobe analyses of the pyrochlore [1] and samarskite [2] are given elsewhere. The pyrochlores contain 2.9-26 wt.% UO_2, 0.2-2.7 wt.% ThO_2, and have calculated doses of 3-90 x 10^{16} alphas/mg (3-94 dpa). The samarskites contain 8-14 wt.% UO_2, 0.3-2.0 wt.% ThO_2, and have doses of 8-60 x 10^{16} alphas/mg (9-65 dpa). All samples are x-ray and electron diffraction amorphous. Splits of the samples were annealed in air (pyrochlores) or in a 96% Ar, 4% H mixture (samarskites) at 1000C for one hour. Polycrase ($LaNbTiO_6$), euxenite ($YNbTiO_6$), manganotantalite ($MnTaNbO_6$) and niobium oxide (Nb_2O_5) were used as standards for empirical (Nb-O) phase determination and general comparison. These samples were taken to the Stanford Synchrotron Laboratory (SSRL) where the x-ray absorption measurements were performed. At SSRL the Nb K-edges were measured using a fluorescent detector on wiggler beam lines equipped with Si(111) or Si(220) double crystal monochromators.

RESULTS

Results of the x-ray absorption near edge structure (XANES) measurements of the Nb K-edge at 18985.6 eV (zero of energy in plots) are shown in Figures 1a and 2a. The doublet at the top of the absorption rise becomes better resolved after the samples have been annealed. The loss of resolution in the doublet of the metamict samples can be attributed to a greater distribution of bond lengths in the first and more distant coordinating atoms around the Nb. The increase in the pre-edge feature for pyrochlores is related to loss of site symmetry in the radiation damaged state. Increase in the L_1 pre-edge feature was also observed for the metamict samples at the Ta B-site in pyrochlores. Note that some of the annealed samples retain distortion at the Nb site as evidenced by the presence of the pre-edge feature. In particular, the annealed samarskites show a pre-edge feature which is even larger than the pre-edge feature for the metamict samples. For the pyrochlore group the radiation damaged spectra resembled Nb_2O_5 and the annealed spectra resembled the polycrase standard spectra. In polycrase (orthorhombic, aeschynite structure type), Nb occurs in a single octahedral site with Nb-O bond lengths ranging from 1.92 to 2.16 A [3]. The structure of Nb_2O_5 is monoclinic with a large unit cell (a=21.16A, b=3.822A, c=19.35A; B=119.83) in which Nb occupies 14 distinct octahedral sites and one tetrahedral site. Nb-O bond lengths in Nb_2O_5 range from 1.65 to 2.26A [4].

The K^2, phase corrected Fourier transforms of the Nb K-edge EXAFS are shown in Figures 1b and 2b. Comparison of the Fourier transforms for annealed and metamict samarskite samples indicates major disruption of the periodicity beyond ~3 A in the metamict samples. In contrast, there is only a slight reduction in magnitude of the 2.0 A Nb-O peak in metamict samarskites. Futhermore, there is no significant difference between the mean Nb-O bond lengths of crystalline and metamict samarskite. The Fourier transforms for annealed and metamict pyrochlore also indicate that the periodicity beyond ~3 A is largely disrupted in the metamict state. In addition, the transforms for the metamict pyrochlores exhibit a significant reduction in the magnitude of the Nb-O peak at 1.9-2.1 A with the emergence of a distinct shoulder at ~2.3 A.

The difference in the near neighbor radiation response of samarskite and pyrochlore may be related to the bond ionicity. Higher Nb valence in the pyrochlore groups (as indicated by the XANES edge position) implies increased electronegativity and reduced Pauling bond ionicity as compared to the samarskites. It has been shown that compounds with lower ionicity are more subject to amorphization than those with higher ionicity [5]. For example, NbO (ionicity > .59) retains its crystallinity under ion bombardment while Nb_2O_5 (ionicity=.59) becomes amorphous. The lower Nb valence in the samarskites suggests higher Pauling bond ionicity making the near neighbor bonds more resistant to radiation damage.

ACKNOWLEDGEMENTS

This work was supported by the U.S. Department of Energy, Office of Basic Energy Sciences.

REFERENCES

[1] G.R. Lumpkin, Ph.D. Dissertation, Dept. of Geology, University of New Mexico (1988).
[2] J.K. Warner, Master Thesis, Geology Department, Univ. New Mexico, 1988.
[3] D. Fauquier and M. Gasperin, Bull. Soc. Fr. Mineral. Cristallogr. 93, 258 (1970).
[4] B.M. Gatehouse and A.D. Wadsley, Acta Cryst. 17, 1545 (1964).
[5] H.M. Naguib and R. Kelly, Radiation Effects 25, 1 (1975).

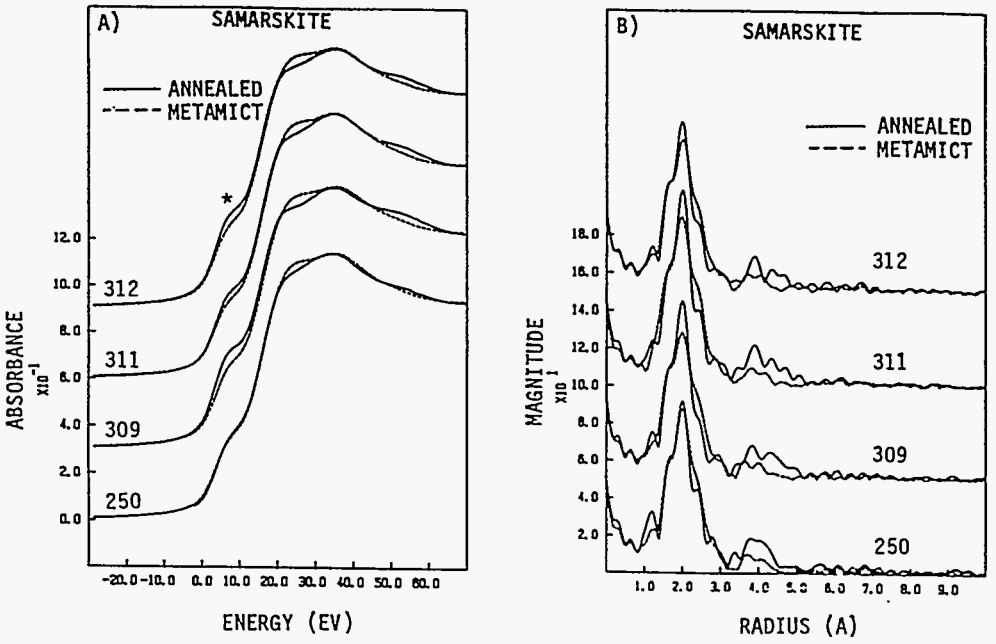

Figure 1. XANES and Fourier transforms for annealed and metamict samarskite.

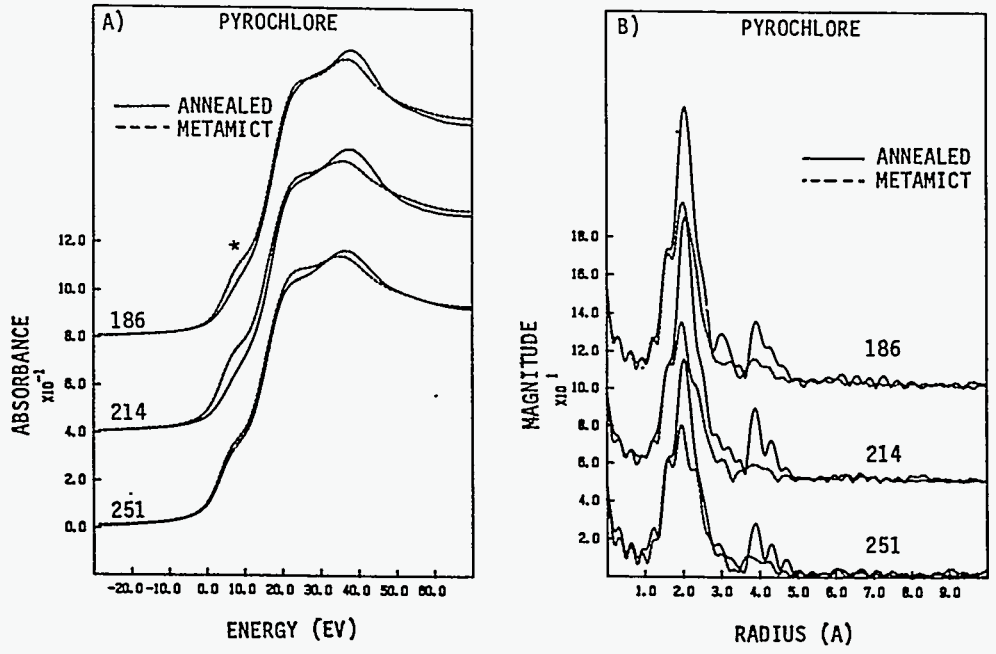

Figure 2. XANES and Fourier transforms for annealed and metamict pyrochlore.

Structural Investigations of WGe Multilayers and Amorphous WGe Alloys

Marybeth Rice
Department of Electrical Engineering
Stanford University

Arthur Bienenstock
Stanford Synchrotron Radiation Laboratory

In December of 1987 we performed Anomalous X-ray Scattering and EXAFS experiments on WGe multilayers with the aim of understanding the atomic arrangements in these materials as a function of atomic composition and layer spacing. Our intention was to determine how chemical interactions effect the observed structures by comparing our multilayers to the already well characterized MoGe multilayer system[1]. The WGe and MoGe systems are nearly identical in all respects except for chemical affinity of the component atoms. The MoGe system has four compounds in its equilibrium phase diagram while WGe has none.

We discuss here samples with nominal bilayer compositions of 30 Å W/30 Å Ge, 20 Å W/20 Å Ge, and 10 Å W/10 Å Ge. These samples, like the MoGe samples, were fabricated by magnetron sputter deposition with the substrates rotating directly beneath the targets sequentially. These samples should all contain 60 atomic % W, but are in fact composed of 70 to 80 atomic % W. This discrepancy is due to the resputtering of freshly deposited Ge atoms by neutral Argon atoms (from the sputtering gas) that rebound from the W sputtering target and hit the sample as it moves into the line of the W target[2]. The resputtering of W atoms as the samples move under the Ge target is negligible in comparison due to the ineffectiveness of the much less massive Ge atoms in reflecting neutral A atoms. The fraction of W in the samples increased as the bilayer spacing decreased since the A atoms have enough energy to penetrate very thin Ge layers and rebound again off the under lying W layer thus knocking out Ge atoms both on the way in and on the way out.

In the 30 Å W/30 Å Ge, 20 Å W/20 Å Ge, 10 Å W/10 Å Ge sequence of samples there is a trend from amorphous to crystalline structures as the bilayer spacing decreases. The 30 Å W/30 Å Ge sample is uniformly and completely amorphous, the 10 Å W/10 Å Ge sample exhibits varying degrees of crystallinity with an amorphous background and the 20 Å W/20 Å Ge sample exhibits both crystalline regions with amorphous background and purely amorphous regions. (Small crystallites in the reflection scan of the 30 Å W/30 A Ge sample are not part of the sample; they come from the residue of etchant used to free the film from the substrate). This trend is the opposite of what one might expect. In MoGe, MoSi, and WC multilayer systems[1,3,4] with metal and nonmetal layers of nearly equal spacing, the films exhibit crystallinity when the bilayer is thick but become amorphous as the bilayer spacing decreases. In the thin bilayer regime the structure of the multilayer approaches that of the amorphous alloy. Exactly the opposite trend is seen here. However, as discussed in above, these multilayers are all much richer in W than planned. A WGe alloy with 70 or 80 atomic percent W is probably outside the amorphous range of the material. It is likely that WGe alloys with high concentrations of W are phase separated into c-W and a-WGe regions. In these multilayers the W concentration increases as the bilayer spacing decreases due to the resputtering effects described above. So, as the bilayer gets thinner the amorphous alloy structure becomes inaccessible. There is not enough Ge in these multilayers to incorporate all of the W into an amorphous alloy even when the layers get thin enough so that atomic interactions at the interface dominate the structure of the film.

The amorphous structure present in the 30 Å W/30 Å Ge, 20 Å W/20 Å Ge, 10 Å W/10 Å Ge multilayers looks almost the same in each. This amorphous structure bears a striking resemblance to that of a-$Mo_{65}Ge_{35}$[5]. It is less similar to that of a-$Mo_{42}Ge_{58}$[5] though still close. This indicates that these multilayers contain a W rich a-WGe alloy. Amorphous Ge is not apparent in these scans. The first three peaks of a-Ge occur right where the valleys of the WGe multilayers occur.

Information about how the c-W is incorporated into the films can be gathered from a comparison of the sizes of the crystallites parallel to the layers (transmission geometry) and perpendicular to them (reflection geometry). In the 20 Å W/20 Å Ge and 10 Å W/10 Å Ge multilayers the W peaks look very sharp both in transmission and reflection. Calculations of the crystallite sizes using the Scherrer equation show that they extend for about 100 Å both in the layer plane and perpendicular to it. This means that the W crystallites extend beyond the thickness of the layers in the direction perpendicular to the layer planes. This coherency of the W crystallites through many layers could be caused by the Ge layers assuming the same structure as the W layers or it could be the result of W crystallites punching through the Ge layers.

The W crystallites in the 20 Å W/20 Å Ge and 10 W Å/10 Å Ge films appear in the diffraction scans with an amorphous background. These peaks look very different from the peaks of the 30 Å Mo/10 Å Ge and 20 Å Mo/10 Å Ge multilayers (of similar atomic composition- 70 to 80 % metal) which exhibit Ge epitaxy. The epitaxial MoGe multilayers have sharp Mo peaks with asymmetric sidebands. This appearance is typical of strained superlattices. No sidebands appear on the W peaks of the WGe multilayers.

If the coherency of the W crystallites beyond the layer spacing is due to Ge epitaxy, the Ge bond length in these regions will be very similar to the c-W bond length of 2.74 Å. The a-Ge bond length is 2.45 Å, and the W-Ge bond length in a-WGe (if it is similar to the Mo-Ge bond length in a-MoGe, which is strongly suggested) is ~2.60 Å[5]. The Ge-Ge bond length in Mo rich a-MoGe alloys is very long though. In a-$Mo_{65}Ge_{35}$ it is 2.75 Å. This means that a Ge-Ge bond length of ~2.74 Å does not definitively identify epitaxy. EXAFS modeling at the Ge edge of the WGe multilayers should indicate which of these bond lengths is present. The distances obtained for both Ge and W backscatters are very short (~2.5 Å) and do not resemble the distances obtained from EXAFS fits to a-$Mo_{65}Ge_{35}$[5]. The EXAFS data do not indicate the presence of epitaxy. However, the limitations of the technique could miss epitaxy if it were present with a-Ge.

To further investigate the epitaxy question a Transmission Electron Microscopy (TEM) cross section of the crystalline part of the 20 Å W/20 Å Ge film was prepared by ion milling. The Ge layers look broken. W appears to be breaking through the Ge layers to form large crystallites. Fringes from the c-W can be seen in the images. These fringes are not as strong or as intense as they would be if the Ge was also crystalline and in the same structure as the W[6].

In the 30 Å W/30 Å Ge, 20 Å W/20 Å Ge, 10 Å W/10 Å Ge sequence of multilayers the structure changes from

a completely amorphous, modulated WGe alloy to a combination of c-W and a-WGe as the bilayer spacing decreases. Given the general trend with bilayer spacing seen here and the lack of evidence for Ge epitaxy, it seems likely that the Ge, in very thin layers, balls up on the W in a-WGe islands. The next W layer to be deposited will then contact W from the previous bilayer in the places where there is incomplete Ge coverage. This allows the W to form crystallites that span ~100 Å both parallel and perpendicular to the layer plane. When the Ge layer is thicker the islands merge and there is complete coverage of the underlying W layer. The next W layer to be deposited does not touch the W of the previous bilayer and crystal growth is inhibited.

The critical thickness for complete coverage of W by Ge must occur at value very close to those present in the 20 Å W/20 Å Ge multilayer. In this multilayer there are apparently regions of complete coverage of the W by Ge as well as regions of incomplete coverage. The thickness of the film, and of the individual layers, varies across the sample because parts of the substrate are closer to the target during fabrication than others. In the 30 Å W/30 Å Ge multilayer, the Ge layer is thick enough everywhere to completely cover the W beneath it.

These samples contain less Ge than planned, so the 20 Å W/20 Å Ge multilayer is very similar in bilayer spacing and atomic percent metal to the 20 Å Mo/10 Å Ge multilayer. The structures of these films are very different. The chemical interactions between the metal and the semiconductor apparently influence the structure of these films.

References

1 L. C. Wilson and A. I. Bienenstock, MRS Proceedings, (1987).

2 R. Bruce, S. Eicher and W. D. Westwood, J. Vac. Sci. Tech. **A6**, 1642, (1988); D. W. Hoffman and J. S. Badgley, J. Vac. Sci. Tech., **A5**, 1791, (1987).

3 A. K. Petford-Long, M. B. Stearns, C. H. Chang, S. R. Nutt, D. G. Stearns, N. M. Ceglio, and A. M. Hawryluk, J. Appl. Phys., 61, 1422 (1987).

4 J. B. Kortright, SSRL Activity Report (1987).

5 J. B. Kortright and A. I. Bienenstock, Phys. Rev. B, 37, 2979, (1988).

6 K. Holloway, private communication.

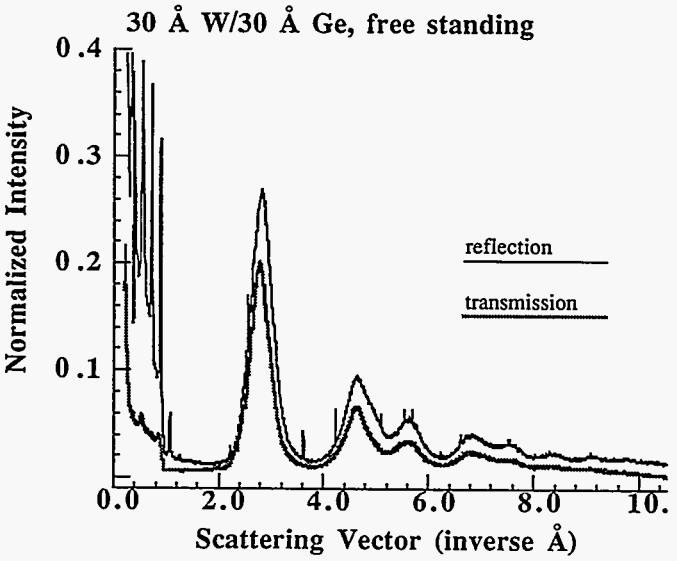

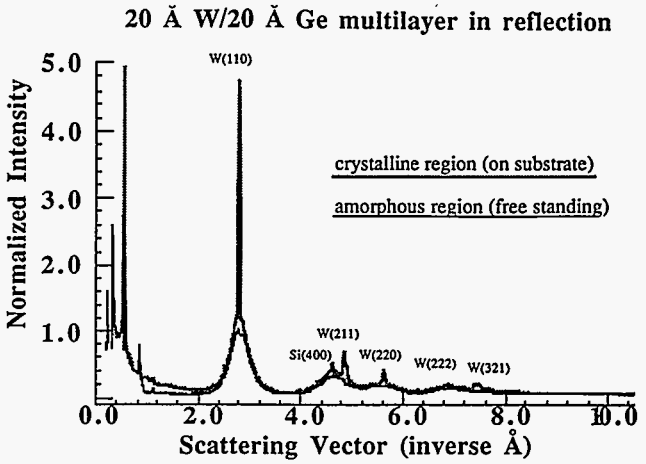

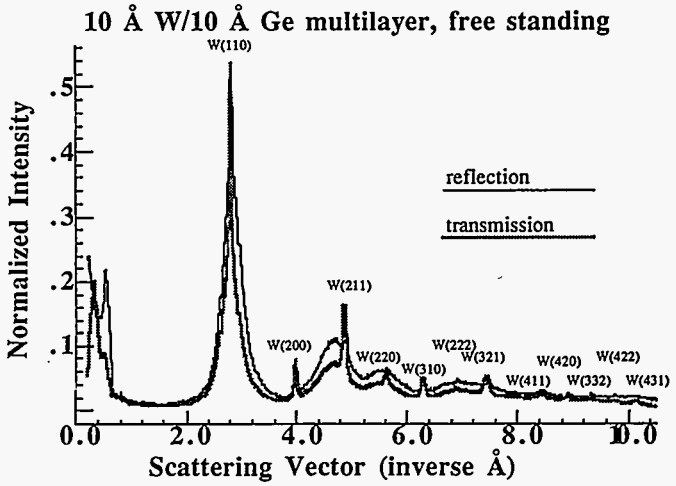

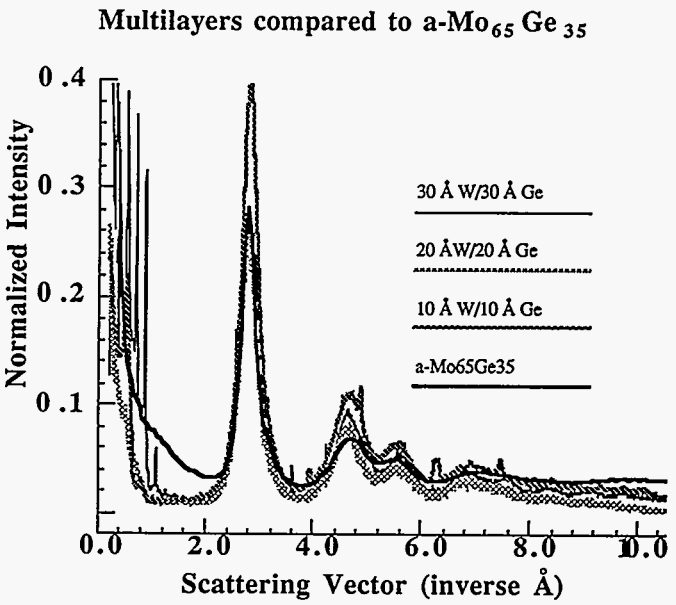

EXAFS SPECTROELECTROCHEMISTRY OF CONDUCTING POLYMERS: COPPER POLY-3-METHYLTHIOPHENE

R.C. Elder and William R. Heineman
Department of Chemistry, University of Cincinnati
Cincinnati, OH 45221-0172

Electrically conducting polymers especially those macromolecules having extended π-electron systems have been intensely studied in recent years. Of particular interest are conjugated π-electron polymers doped with charge transfer complexes exhibiting semiconducting of metallic properties[1]. We have been investigating the polymer poly-3-methylthiophene which can be electropolymerized onto a platinum electrode yielding a conductive film. These films, however, when exposed to ambient conditions lose their conductivity and electrode activity after a few weeks[2]. This polymer can also be synthesized by transition metal induced polymerization of 3-methyl-2,5-dilithothiophene and 3-methyl-2,5-dibromothiophene at 0° C in dry THF solution[3]. The use of anhydrous cupric chloride yields the best results. When the resulting polymer is doped with iodine and exposed to moisture, this polymer displays very good conductivity (up to 40 S/cm) and an extraordinary degree of stability. The bulk copper concentration is about 30% by weight copper as measured by atomic absorption analysis. This polymer prepared under the same conditions using different transition metals yielded poor conductivities ($\sim 10^{-7}$ S/cm)[4].

We have investigated the chemical and structural form of the copper ions in this insoluble polymer matrix using EXAFS. The polymer samples which were provided by the groups of Professors Harry B. Mark and Hans Zimmer were presumed to be cross-linked by copper coordination to the sulfur atoms of the thiophene rings. This would provide a 4 coordinate copper-sulfur environment[4]. Polymers containing copper were synthesized using anhydrous Cu(I) (material 1) and Cu(II) (material 2) and both have been examined via EXAFS and XANES studies.

EXPERIMENTAL

EXAFS spectra were measured on beamline IV-3 by using an ion chamber, fluorescence detector. The solid Cu poly-3-methylthiophene polymers were diluted with Coffeemate (TM) and packed into aluminum sample holders. The beam size was 1.5 x 15 mm. Cu-S parameters were developed using copper(II)bis(N,N-diethyldithiocarbamate) or $Cu(dtc)_2$, and those for Cu-N were available from copper(I)bis(2,9-dimethyl-1,10-phenanthroline) tetrafluoroborate or $Cu(DMP)_2BF_4$.

RESULTS

The XANES spectra of both 1 and 2 were measured. 2 displays two distinct peaks at 8982.8 and 8997.4 eV and a shoulder at 8989.0 eV. These features are also observed for 1, however, at different relative intensities and slightly shifted to 8983.2, 8998.6 and 8989.4 eV respectively.

The EXAFS Fourier transforms of 1 and 2 were computed and in each there is only one intense peak indicating one main backscattering shell. The maximum in the amplitude function of the back transformed, filtered EXAFS data occurs at 5.6 and 5.1 K for 1 and 2 respectively. This maximum for $Cu(DMP)_2BF_4$, the Cu-N model compound, occurs at 5.6 K as compared to the Cu-S model compound, $Cu(dtc)_2$, which does not reach its maximum until 7.2 K. Copper metallothionein, another sulfur coordinated complex, has an envelope maximum at 6.5 K. This indicates that the backscatter is not sulfur but an element in the row above it in the periodic table, most likely oxygen from the water absorbed by the polymer.

Curve fitting of the filtered EXAFS data further disproves the coordination of the copper centers to sulfur. Using the empirical parameters derived from solid $Cu(dtc)_2$ in the attempt to fit the Cu-poly-3-methylthiophene data to a sulfur coordination yielded unreasonable results for bond length and phase shift. The resulting bond length for the data was of 2 1.98 Å which is too short for a Cu-S bond which is on average 2.3 Å. The value of ΔE_0 from this fit was 26 eV and the coordination number was 4.2. The fit for 1 was equally bad. In this case the bond length was a bit more reasonable, 2.15 Å, however, the coordination number was -4.9 and ΔE_0 was 48 eV. Curve fitting of the filtered EXAFS data using nitrogen parameters to model oxygen as the backscatterer yielded much better results. Since we did not have data on a Cu-O model compound, we used the empirical parameters derived from solid $Cu(dmp)_2BF_4$ the Cu-N model compound. Fitting 1 showed a Cu-O bond length of 1.97 Å with a coordination number of 3.7 and a ΔE_0 of -2.5 eV. 2 displayed the same bond length of 1.97 Å, a coordination number of 2.3, and a ΔE_0 of -5.86 eV. The similarity in edge structure and bond lengths suggests that the copper centers are in similar environments and may have the same oxidation state.

The use of EXAFS has shown that the copper centers in copper poly-3-methylthiophene are not bonded to the sulfur atoms in the thiophene ring, but rather they are most likely coordinated by water present in the polymer matrix. This is demonstrated by the more reasonable empirical fits obtained modeling the EXAFS data to a Cu-O instead of a Cu-S model. The amplitude maxima in the filtered EXAFS data also support this conclusion.

ACKNOWLEDGEMENTS

This work was supported by Air Force Grant AFOSR-88-0089. The X-ray spectroscopy and calculations reported here were performed by Dr. Lee R. Sharpe.

REFERENCES

1. R.J. Waltman, J. Bargon, Can. J. Chem., 64, 76-95 (1986).

2a. R.J. Waltman, J. Bargon and A.F. Diaz, J. Phys. Chem. 87, 1459-1463 (1983).

2b. G. Tourillon and F. Garnier, J. Electrochem. Soc.: Electrochemical Science and Technology, Vol. 130, No. 10, 2042-2043 (1983).

3. A. Amer, et al., Journal of Polymer Science: Polymer Letters Edition, Vol. 22, 77-82 (1984).

4. A. Czerwinski, et al., J. Electrochem. Soc.: Electrochemical Science and Technology, Vol. 134, No. 5, 1158-1164 (1987).

APPLICATION OF X-RAY SCATTERING TO THE *in situ* STUDY OF ORGANOMETALLIC VAPOR PHASE EPITAXY

P.H. Fuoss D.W. Kisker, G. Renaud and K.L. Tokuda
AT&T Bell Laboratories, Holmdel, N.J. 07733
S. Brennan
Stanford Synchrotron Radiation Laboratory, Stanford, CA.94309
J.L. Kahn
Physics Department, Stanford University, Stanford, CA.94305

INTRODUCTION

Chemical vapor deposition (CVD) processes have become well established for preparing thin films of III-V and II-VI semiconductors such as GaAs and ZnSe. Despite the technological importance of these materials, little is known about the detailed mechanisms of these growth processes. In addition to chemical reactions which occur in the vapor phase, growth involves reactions and diffusion which occur on the surface of the growing material as well as structural changes induced in the material as growth proceeds.

In contrast, UHV techniques such as molecular beam epitaxy (MBE) and chemical beam epitaxy (CBE) have been studied using *in situ* electron based analytical techniques including: reflection high energy electron diffraction (RHEED), Auger electron spectroscopy and x-ray photoemission spectroscopy (XPS). Unfortunately, due to the high gas pressures used in CVD growth processes, *in situ* electron based techniques cannot be employed. Despite the lack of probes, great progress has been made in understanding CVD processes by phenomenological studies of relationships between growth parameters and material properties. A detailed understanding of the microscopic processes occurring during CVD will enhance our understanding and control of these processes.

In principle, x-ray scattering and spectroscopy techniques are well suited to studying these near atmospheric pressure processes, but advances in this area have been limited both by the lack of suitable x-ray sources and by the difficulty of integrating the growth and measurement experiments. We have developed equipment and techniques to perform *in situ* x-ray scattering studies of the structure of surfaces during OrganoMetallic Vapor Phase Epitaxial (OMVPE) growth using the extremely bright undulator radiation from the PEP storage ring.

Our initial experiments have used the grazing incidence x-ray scattering (GIXS) approach to study the growth of ZnSe epitaxial films grown on GaAs by OMVPE, using diethylselenium and diethylzinc as source compounds. The use of GIXS to study *in situ* growth processes is well established for ultra-high vacuum monolayer growth[1] and for analysis of surface and interface structures of grown films.[2] GIXS can analyze 1) the crystal structure of the surface and thin film, 2) study size distributions of islands and 3) analyze defect structures on the surface and in the thin, growing film.

SYSTEM DESIGN

The goal of performing in situ x-ray scattering, while growing material using OMVPE techniques, requires a careful blending of techniques and a special design of both the OMVPE reactor and the x-ray diffractometer. A particularly troublesome problem is providing a large aperture window which allows the full range of structures to be studied and which is protected from CVD deposition. Even a small amount of deposits would rapidly degrade the transmission of the incident and diffracted beams.

Our reactor system is shown in Figure 1. The basic unit of construction is a 4" OD stainless steel tube with 6" OD ultra-high vacuum flanges. The diffracted beam window consists of 0.5mm thick beryllium brazed to a monel flange. A separate beryllium window for the incident beam is mounted on the 2 3/4" flange which comes perpendicularly out of the window spool piece. These windows are configured so that diffracted beams can be observed over an angle of 120° in the plane of the substrate and 40° normal to the substrate. The system is designed to protect the Be windows from deposition by focussing the reactive gases onto the

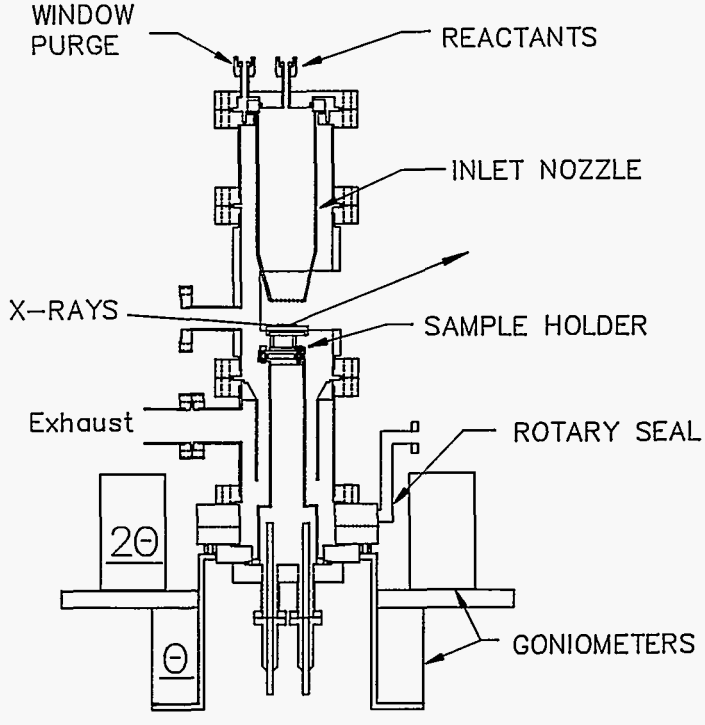

Fig. 1: An overall drawing of our special-purpose OMVPE reactor. The details are described in the text.

sample and by establishing a non-reactive gas flow along the outside wall. In addition to the non-reactive wall flow, the Be window assembly is protected from deposition and overheating by a thin aluminum shield.

The specially constructed, remote controlled gas handling system (CVD Equipment, Inc.) is capable of supporting three organometallic sources. All of the switching valves are interfaced to a separate programmable controller, which can communicate with the central data acquisition computer. This, coupled with dynamic pressure balancing between the vent/run lines, allows systematic studies of interrupted growth. It also allows for the growth of high quality superlattices.

The entire reactor, diffractometer and gas handling equipment, is enclosed in a single 3' wide by 6' long cabinet mounted on wheels. The control electronics are contained in a separate cabinet for remote control of all gas flow and sample temperature. Installation is rapid requiring only: 1) connecting the cables between the control cabinet to the reactor, 2) attaching the N_2 and H_2 supply lines and 3) providing exhaust. This process takes ~30 minutes and enables efficient timesharing operation of a synchrotron beamline.

We have installed this system on PEP Beamline 5B at the SSRL. Si(111) crystals were used to monochromatize a 9.4 KeV x-ray beam. A flux of 2.5 x10^{10} photons/sec was observed into a 0.1mm x 1.5mm entrance slit. (The incident spot size was 1.7 mm horizontally by 0.8 mm, FWHM.)

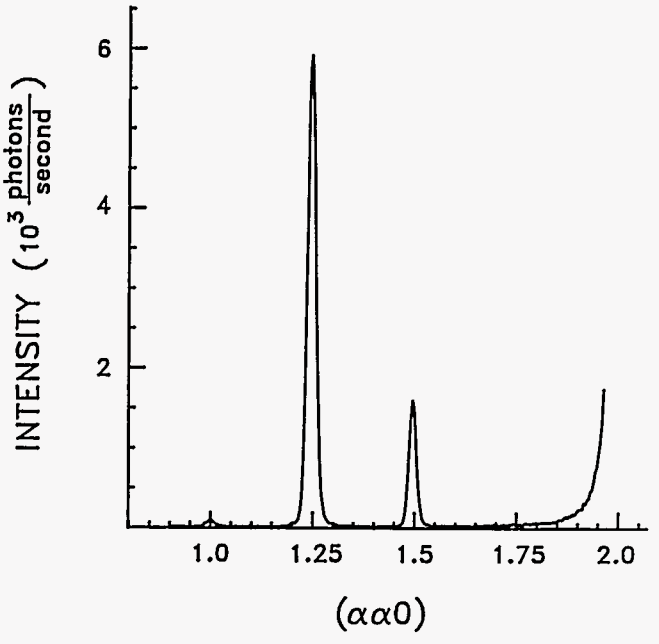

Fig. 2: Data along the (110) azimuth from a GaAs (001) surface prepared at 500 C in 100 torr of flowing H_2.

EXPERIMENTAL RESULTS

The system was used to study the growth of ZnSe on the GaAs (001) surface. Three principle experiments were performed. First, we studied the structure of the GaAs (001) surface at elevated temperature in 100 Torr of flowing H_2. Typical results of this study are shown in Figure 2. A [4x2] reconstruction was found with the four-fold reconstruction direction along the top Ga bonds. The two-fold direction of this reconstruction was extremely weak and the surface rapidly transformed to a [4x1] pattern. This [4x1] reconstruction was stable for several hours in flowing H_2 at 250-400 C. In addition, an [8x1] reconstruction was occasionally observed which appears to be correlated with incomplete oxide removal.

The second experiment consisted of examining the surface reconstructions of the growing ZnSe layer. This surface had a clear [2x1] reconstruction (see Figure 3) with the two-fold axis

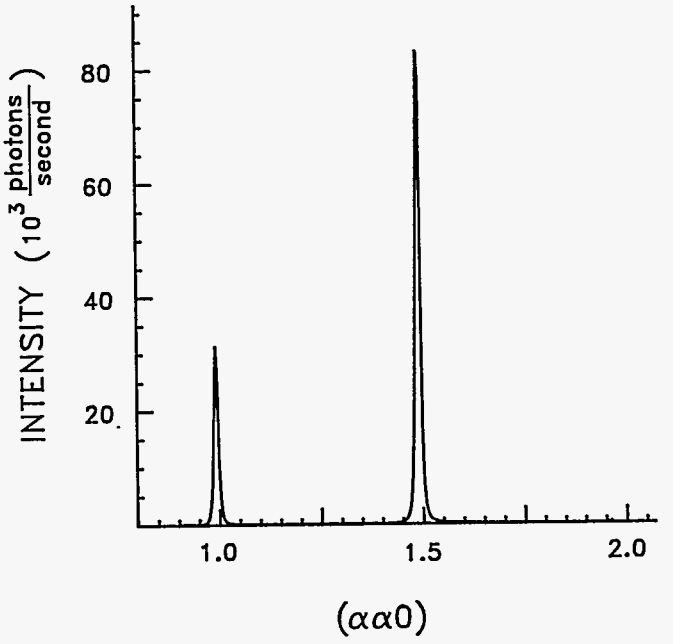

Fig. 3: Data along the (110) azimuth from a grown ZnSe (001) surface. Note that the ZnSe reconstruction peaks are narrower than the GaAs reconstruction peaks. This suggests larger domains on the ZnSe surface.

along the Ga top bonds of the GaAs substrate. Peak count rates of 10^5 were observed from this surface. Finally, we examined the effects of changing the growth parameters on various diffraction peaks and on the specular reflectivity. Figure 4 shows the specular reflectivity at the (0,0,1/2). It is clear that the intensity immediately falls when the Se organometallic is turned on, stabilizes at a low value when it is turned off, increases when the Zn organometallic is added and stabilizes at a high value when the Zn channel is turned off. It is tempting to ascribe these oscillations to the alternate growth of complete Se and Zn layers. However, other explanations are possible (e.g. saturation of the surface with the Se organometallic followed by reaction with Zn) and a definitive explanation awaits further analysis.

FUTURE POSSIBILITIES

With these initial experiments we have established the feasibility of using x-ray based analytical tools for the *in situ* analysis of CVD systems such as OMVPE processes. Our current results demonstrate that we have excellent surface sensitivity, low backgrounds, and high signal levels. Having such an analytical tool at our disposal, we can now proceed to the study of a wide range of challenging systems. Starting with ZnSe, we extend our studies of growth transients using reflected beam intensities (cf. RHEED oscillations), establish the presence of layer by layer growth processes if they exist, and characterize the extent of surface roughness as a function of growth parameters such as temperature, pressure, growth rate, source compounds, etc. In addition, because the ZnSe/GaAs system is slightly lattice mismatched, we will be able to monitor the development of strain in the overlayer, which will then be relieved by the formation of misfit dislocations at the substrate interface. The *in situ* study of this process should give valuable insight into the kinetics of lattice relaxation in mismatched systems.

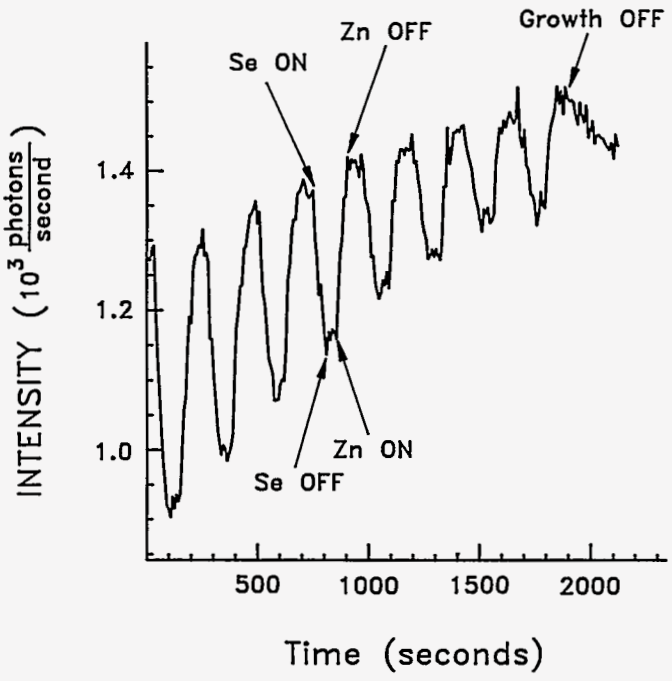

Fig. 4: The (0,0,1/2) specular reflectivity of the ZnSe surface during alternate flows of Et_2Se and Et_2Zn. These data were taken at a growth temperature of 450 C.

There are many interesting problems in other systems as well. One such problem is the growth of CdTe-ZnTe superlattices. We have studied growth in this system[3] and find that the coherency and defect structure of the final superlattice is very sensitive to the thickness of the CdTe layer and to growth conditions. The superlattice is very sensitive to thickness of the CdTe layer and to growth conditions. It would be straightforward to extend the capabilities we are developing for the ZnSe canse to analyze the growth of these superlattices. Another example would be the study of the initial stages of growth of GaAs on silicon, where the structural details of the interface apparently control the resulting film properties.

In summary, coupling the brightest x-ray source with proven x-ray scattering techniques, we have developed a powerful tool for *in situ* analysis of CVD systems. We expect the understanding gained by the application of this tool will lead to the development of new CVD techniques and methods.

ACKNOWLEDGEMENTS

The authors gratefully acknowledge the help of the large number of SSRL personnel who worked very hard to make this first experiment happen. They include J. Cerino, D. Day, H. Przybylski, R. Silvers, C. Troxel and T. Troxel. In addition, several Bell Labs colleagues contributed through discussions and support, including L.J. Norton, R. D. Feldman, A. Ourmazd, C. V. Shank and A. M. Glass. Support for one of us (S.B.) is provided by the Dept. of Energy Office of Basic Energy Sciences. Work was done at Stanford Synchrotron Radiation Laboratory which is supported by the Dept. of Energy, Office of BES, Div. of Chem./Mat. Sci.

REFERENCES

1. W. C. Marra, P. H. Fuoss and P. Eisenberger. Phys. Rev. Lett. **49**, 1169(1982).

2. W. C. Marra, P. Eisenberger and A. Y. Cho. J. Appl. Phys. **50**, 6927(1979).

3. D. W. Kisker, P. H. Fuoss, J. J. Krajewski, P. Armithiraj, S. Nakahara and J. Menendez. J. of Crystal Growth. **86**, 210(1987).

LOCAL ATOMIC STRUCTURE of HIGH T_c SUPERCONDUCTORS

J. B. Boyce
Xerox Palo Alto Research Center, Palo Alto, CA 94304, USA

F. G. Bridges
Physics Department, University of California, Santa Cruz, Santa Cruz, CA 95059, USA

T. Claeson
Physics Department, Chalmers University of Technology, 41296 Gothenburg, Sweden
and

T. H. Geballe
Department of Applied Physics, Stanford University, Stanford, CA 94305, USA

The local structure of $Y_1Ba_2Cu_3O_y$ determined using x-ray absorption fine structure (XAFS) agrees well with the long-range order given by diffraction results for both oxygen-rich, orthorhombic (y=6.98 and 6.87) and oxygen-deficient, tetragonal (y=6.15) compounds. The x-ray absorption near-edge structure supports the conclusion that, as y=7 goes to y=6, the O is removed from the chains and the chain Cu atoms, Cu(1), becomes monovalent with a linear O-Cu-O structural configuration and a $3d^{10}$ electronic configuration, as in Cu_2O. For the XAFS analysis, structural standards were determined, and these standards worked well not only for the Cu first-neighbor O environment but also for the Cu second-neighbor metal-atom environment out to 4Å. A detailed multipeak analysis reproduced the XAFS spectra well and yielded structural parameters that agree with diffraction. The temperature dependence of the structural parameters shows only a smooth variation, with no significant anomalies. The Cu-X distances have a negligible to a small positive change with temperature, consistent with the lattice expansion. The exception is the Cu-Ba distances which change substantially; the Cu(1)-Ba distance increases and the Cu(2)-Ba distance decreases. This indicates that the Ba moves away from the Cu(1)-O chains and toward the Cu(2)-O planes with increasing temperature and that anharmonicity plays a role. This motion is larger for the oxygen-depleted compound than for the fully-oxygenated material. The in-plane Cu-O first neighbor vibrations exhibit no significant softening with temperature. They agree well with a harmonic, Einstein oscillator model which shows that the Cu-O bonds are tightly bound (characteristic Einstein temperatures Θ_E = 596 ± 20 K) and are slightly softer by 6% in the oxygen-deficient, tetragonal material.

We have also made XAFS measurements for a series of Co and Fe substituted samples of $YBa_2Cu_3O_{7-\delta}$ (YBCO). Our analysis of the first and second neighbor environments indicates that the Co atoms primarily replace the Cu in the chain sites, the Cu(1) atoms, in YBCO, but many of these Co(1) sites and their neighboring oxygen sites are highly distorted. The first neighbor Co-O peak consists of ~3.5 oxygen at 1.8Å and ~1.3 oxygen at 2.4Å, while the second neighbor multi-peak in the XAFS data is unexpectedly low in amplitude. Structure in this peak is inconsistent with a simple gaussian broadening and indicates that several Co(1)-Ba distances exist. We propose an aggregation of the Co atoms into distorted, zigzag chains along the <110> directions, with some of the Co displaced off-center by ~0.45Å along a perpendicular <110> direction. This model is consistent with the second neighbor XAFS data, provides an explanation for the tetragonal structure, and accommodates excess oxygen within the Co chains. The Fe data suggest that similar chains also exist in the Fe substituted samples. There are, however, some differences between the local environments of the Fe and Co. The primary difference is that a small but significant number of Fe atoms occupy the Cu(2) plane sites while no appreciable number of Co atoms are found on the Cu(2) sites in the more dilute samples. Finally, near-edge measurements on the Co and Fe K-absorption edges indicate that the valence is primarily +3, but a mixture of valences exists. For Co the edge position corresponds to a mixture of +2 and +3 valences, while Fe exists in a mixture of +2, +3, and +4 states.

INVESTIGATION OF THE VALENCE OF Pr IN $YBa_2Cu_3O_7$

F. W. Lytle*, R. B. Greegor*, Joe Wong# and E. M. Larson#
*The Boeing Co., Seattle, WA 98124
#Lawrence Livermore National Laboratory, Livermore, CA 94550

INTRODUCTION

Most rare earth (RE) elements can be substituted for Y in $YBa_2Cu_3O_7$ (YBC) with little effect on the superconducting properties; however, Pr does interfere with the superconductivity.(1-3) An obvious possible reason is that Pr is valence 4 rather than valence 3 as are the other REs. Reports have claimed pure valence 3(4) and mixed 3 and 4 valence.(5) The valence of Pr is important in that it is a key to the mechanism of superconductivity. We examined the samples of Dalichaouch et al.(6) The spectra were measured in the e-yield mode with Si(220) crystals and a vertical divergence of 5×10^{-5} radians.

RARE EARTH L-ABSORPTION SPECTRA

Because of the dipole selection rules $\Delta J = 0, \pm 1$ and $\Delta S = 0$ the edge resonances of $L_{1,2,3}$ x-ray absorption edges are the transitions 2s to np, $2p_{1/2}$ to $nd_{3/2}$ and $2p_{3/2}$ to $nd_{3/2,5/2}$, respectively.(7) Note that the different transitions will each project different final states. The $L_{2,3}$ XANES are usually very similar in appearance although the shape and relative intensity of the edge resonances must be related to the admixture of $d_{3/2}$ and $d_{5/2}$ final states. The Pt edges are the classic example of this effect.(7) The relative intensity of the two resonances can be used to assess the spin-orbit splitting of the 5d states(7,8) and the effect has also been observed experimentally in other 5d elements and Re compounds.(9)

The relative intensity and energy position of the L_3 edge resonance in a series of compounds of the same element have long been used as indicators of valence and of bond ionicity. However, these simple concepts no longer have meaning for the RE $L_{2/3}$ edges which split into complicated spectra. The transition is not just 2p to 5d but involves the 4f electrons as well. This occurs because of two related factors: 1) The 4f electrons which are normally spatially located inside the 5d and 6s shells become comparable in energy and position with the 5d

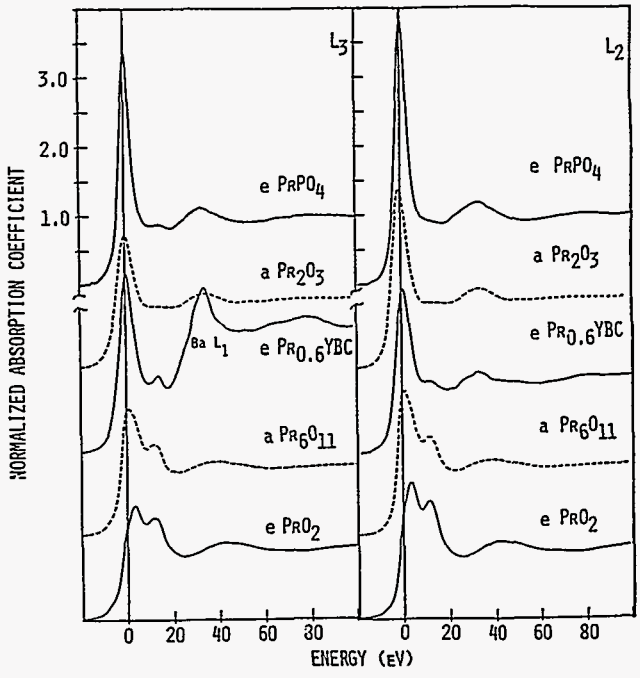

Fig. 1. Pr $L_{2,3}$ edge spectra in reference compounds and in PrYBC. The e or a designation indicates normal absorption or e-yield data.

electrons and hybridize with them. The resulting orbital has a double well potential(10) which produces rich, complicated spectra which are extremely sensitive to chemical environment. 2) The 4f hybrid orbital is sensitive to the presence and specific location of the core hole, i. e. the spectrum observed does not necessarily reflect the ground state of the compound. Details of the electronic state differ depending upon the depth of the core level used for observation.(11) Detailed theories(12-14) have been presented based upon the configuration interaction of the core hole and final state electrons plus the interaction between the 4f and 5d electrons.

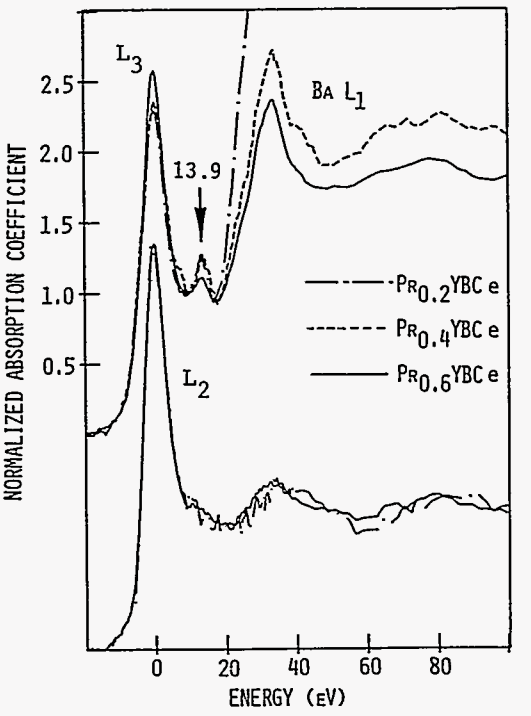

Fig. 2. Comparison of Pr $L_{2,3}$ spectra for three concentrations of Pr in YBC.

RESULTS AND DISCUSSION

Examples of $L_{2,3}$ spectra for compounds with Pr valence 3, 4 and mixed 3/4 valence are shown in Fig. 1. Note the complicated spectra for the valence 4 compounds, whereas the valence 3 edge resonance is a single peak; however, in all the compounds (except PrYBC) the L_2 and L_3 edges are very similar. The separate data for the PrYBC compounds is shown in Fig. 2. The obvious difference is the peak at 13.9 eV on the L_3 edge. This feature is also concentration dependent with the most intensity for the lowest concentration sample. Since this peak is found on the L_3 edge and not on the L_2 edge it implies that the peak is due to a state with approximately $d_{5/2}$ symmetry without a corresponding $d_{3/2}$ density. This effect is similar to that of Pt (7) or, to a lesser degree, Au (9) where more intense transitions occur on the L_3 edge than the L_2. In these 5d metals the effect occurs because of the narrowing of the d-band which lowers the $d_{3/2}$ states with respect to the $d_{5/2}$;hence, the $d_{3/2}$ levels are filled first and transitions occur at the L_3 edge which do not occur at the L_2. Without an accurate model or more relevant reference compounds it is difficult to specify the cause of this effect in PrYBC except to note that x-ray spectroscopy proves the unfilled Pr valence band has more $d_{5/2}$ character than $d_{3/2}$ and the effect may be due to a narrowing of the valence band. This effect is unique among our small collection of RE reference compounds and may imply a unique spin-orbit configuration at the Pr sites in YBC. We emphasize that it is not simply a case of mixed valence as in Pr_6O_{11} where the Pr $L_{2,3}$ spectra could be simulated by summing Pr_2O_3 and PrO_2 spectra in the stoichiometric ratio. This could not be done for the $L_{2,3}$ edges in PrYBC.

REFERENCES

1. D. W. Murphy, S. Sunshine, R. B. van Dover, R. J. Cava, B. Batlogg, S. M. Zahurak and L. F. Schneemeyer, Phys. Rev. Lett. 58, 1898 (1987).

2. K. N. Yang, Y. Dalichaouch, J. M. Ferreira, B. W. Lee, J. J. Neumeier, M. S. Torikachvili, H. Zhou, M. B. Maple, and R. R. Hake, Sol. St. Comm. 63, 515 (1987).

3. Z. Fisk, J. D. Thompson, E. Zirngiebl, J. L. Smith and S. W. Cheong, Sol. St. Comm. 62, 743 (1987).

4. E. E. Alp, G. K. Chenoy, L. Soderholm, G. L. Goodman, D. G. Hinks, B. W. Veal, P. A. Montano and D. E. Ellis, preprint.

5. S. Horn, J. Cai, S. A. Shaheen, Y. Jeon, M. Croft, C. L. Chang and M. L. den Boer, Phys. Rev. B36, 3895 (1987).

6. Y. Dalichaouch, M. S. Torikachvili, E. A. Early, B. W. Lee, C. L. Seaman, K. N. Yang, H. Zhou and M. B. Maple, Sol. St. Comm. 65, 1001 (1988).

7. L. Mattheiss and R. Dietz, Phys. Rev. B22, 1663 (1980).

8. V. V. Nemoshkalenko, V. N. Antonov, W. John, H. Wonn and PZiesche, Phys. Stat. Sol. b111, 11 (1982).

9. F. W. Lytle, Ber. Bunsenges. Phys. Chem. 91, 1251 (1987).

10. K. R. Bauchspiess, W. Boksch, E. Holland-Moritz, H. Launois, R. Pott and D. Wohlleben in "Valence Fluctuations in Solids", ed. by L. Falicov, W. Hanke and M. Maple, North-Holland, 1981, p.417.

11. G. Kaindl, G. K. Wertheim, G. Schmeister and E. V. Sampathkumaran, Phys. Rev. Lett. 58, 606 (1987).

12. O. Gunnarsson and K. Schonhammer, Phys. Rev. B28, 4315 (1983).

13. T. Jo and A. Kotani, J. Mag. Mag. Mat 52, 396 (1985) and references therein.

14. A. Bianconi, A. Morelli, H. Dexpert, R. Karnatak, A. Kotani, T. Jo and J. Petiau, Phys. Rev. B35, 806 (1987).

PHOTOELECTRON SPECTROMETRY OF CORRELATION SATELLITES IN KR AS AN AID TO DETERMINING THE NEUTRINO REST MASS

R. Bartlett, T.J. Bowles, R.G.H. Robertson, W. Trela, D.L. Wark, J.F. Wilkerson
Los Alamos National Laboratory

George S. Brown
Stanford Synchotron Radiation Laboratory

Bernd Crasemann, Stacey L. Sorensen, Scott Whitfield
University of Oregon

David A. Knapp, John Henderson
Lawrence Livermore National Laboratory

INTRODUCTION

Whether the neutrino has a non-zero rest mass is one of the major outstanding problems in modern particle physics. A non-zero neutrino mass would have important consequences for models of the evolution of the universe and would be the first indication of physics beyond the Standard Model. One can obtain from tritium beta decay a sensitive test of the mass of the electron anti-neutrino by looking near the endpoint for small departures of the electron spectrum from the shape expected for zero mass. However, the total instrument resolution including source effects such as backscattering, energy loss and decays to different atomic final states distort the spectrum near the end point. The curvature induced by these effects is opposite to the curvature induced by neutrino mass, and must be precisely corrected for before a value for the neutrino mass can be derived from a measured spectrum. It is especially important to measure accurately any tails that are present because of their large contribution to the resolution-induced spectral distortion.

The Los Alamos group has constructed an experiment[1] that minimizes source-related contributions to the total resolution function by the use of a gaseous molecular tritium source. The gaseous source eliminates backscattering and surface contaminants, minimizes energy loss in the source, and places the tritium in the molecular environment with the most accurately known final-state effects. The total resolution function of the source and spectrometer is measured with the use of K-conversion electrons from the 32.15-keV transition in ^{83m}Kr, which is recirculated through the source in the same manner as the T_2 gas. In order to deduce the true instrumental resolution it is necessary to know the shake-off and shake-up contributions to the Kr electron spectrum. Our knowledge of these correlation effects, which are analogous to the final-state effects in tritium, was previously obtained from a combination of outer-shell photoionization experiments and calculations[2]. Measurements with the Los Alamos spectrometer, however, showed indications of a larger continuum and a smaller contribution from the 3d shake-off lines than expected. The inability to unambiguously assign this tail to the Kr line itself or to the total resolution function of the spectrometer would limit the sensitivity of the Los Alamos experiment far above the expected value of 10 eV.

THE EXPERIMENT

In order to reduce the uncertainties associated with the Kr internal conversion lineshape we measured the electron spectrum from an analogous process, namely photoionization of the K shell of natural Kr. These two processes differ only in the replacement of a virtual photon by a real one, and to first order should produce the same satellite spectrum. X-rays from the PEP 5B beamline were monochomatized using Si(111) Bragg reflections at 15225 and 17025 eV and Si(333) reflections at 15225 eV. These energies were chosen to place the 1s line and its correlation satellites at energies clear of Auger lines. The x-rays illuminated a gas jet target, the resulting photoelectrons were then energy analyzed in a double cylindrical mirror analyzer (CMA) equipped with a stage of pre-retardation[3]. The resolution was dominated by the divergence in the x-ray beam. It was 18 eV FWHM for the 17025 eV data. The total resolution for the Si(333) data was about 7 eV FWHM.

Scanning the spectrum was accomplished by varying the retardation voltage. The resulting efficiency variation of the CMA was measured by observing the diagram line at fixed photon energy for various values of the pass energy E_p. The efficiency was found to vary approximately as $(E_p/E_k)^n$, where E_k is the outgoing electron kinetic energy[3] and n was experimentally determined to be 2.0 ± 0.2 (2.5 ± 0.3) for the 15225 eV (17025 eV) data. These uncertainties include the effects from the variation of the channel electron multiplier efficiency with electron energy and the fact that the efficiency did not vary strictly as a power law. Count rates at the photopeak were of order 100 to 300 s^{-1} for the Si(111) data and 30 s^{-1} for the Si(333) data. Background was measured by lowering the photon energy to place the diagram line below the region of interest. Backgrounds not associated with the beam (mainly dark current in the electron multiplier) were made negligible by using the time structure of the PEP beam. An offline experiment was carried out to look for a scattering tail associated with a strong line in the CMA. A photoemissive source was placed at the object position in front of the CMA, no scattering tail was observed below the monoenergetic line to a level less than 0.5% integrated over the entire spectrum.

Preliminary analysis of the data was done by simply convolving the SSRL photoionization spectra with a Gaussian having a width adjusted to match the slightly worse resolution of the LANL conversion line data. Such a procedure is adequate to establish whether or not the continuum features of both spectra

are the same. The comparison (Fig. 1) reveals that they are indeed the same to a high degree, confirming that the unexpected continuum observed in with the LANL spectrometer is associated with atomic effects in the Kr atom. Fig. 2 shows a comparison between the Si(333) result and the prediction available before this work[2] (again convolved with a Gaussian to match the experimental width). The positions and intensities of the satellites near the diagram line agree remarkably well with the data, but as expected the continuum further from the peak is not given by the calculation.

CONCLUSIONS

We have confirmed that a continuum feature is present in the electron spectrum from internal conversion and photoionization of Kr, and qualitatively confirmed the absence of a tail on the total resolution function of the LANL tritium beta decay experiment. Further analysis is being done to establish quantitatively the maximum tail allowed by the data. At present we do not know the origin of this continuum feature, but note that a very similar feature has been seen in 1s photoionization of Ne[4]. We speculate that it arises from the direct collision of the ejected 1s electron with an orbital electron in the same atom. That process is indistinguishable in the final state from the usual shakeup and shakeoff one, and would therefore be coherent with it. We are continuing analysis of the data in order to extract all the quantitative information available about the shakeup and shakeoff spectrum, and are attempting to produce a theoretical understanding of the observed features.

REFERENCES

1. J.F. Wilkerson et al., Phys. Rev. Lett. 58, 2023 (1987).

2. R.G.H. Robertson, Proceedings of the VIII Moriond Workshop, "Tests of Fundamental Laws in Physics," Les Arcs, Savoie, France, (in press). D.A. Knapp, Ph. D. Thesis, Princeton University (Los Alamos Report LA-10877-T; unpublished).

3. P.W. Palmberg, J. Electron Spectr. and Related Phen. 5, 691 (1974).

4. S. Svensson et al., Phys. Rev. Lett. 58, 2639 (1987).

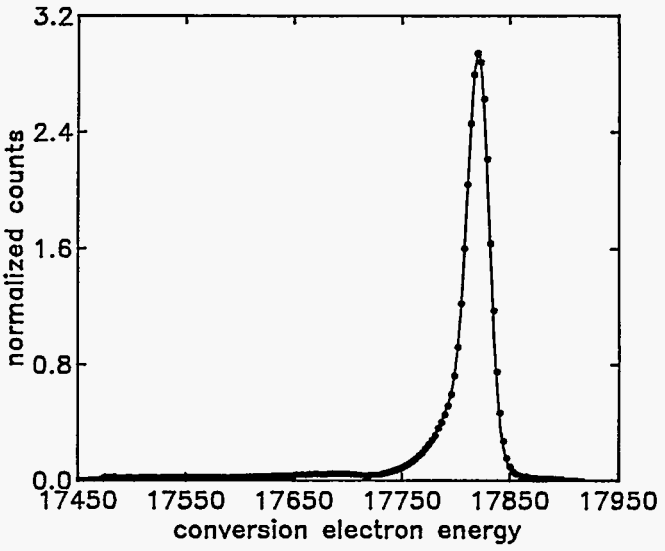

Fig. 1. Comparison between electron spectra from 1s photoionization of Kr (line) measured at SSRL and internal conversion (points) measured at LANL.

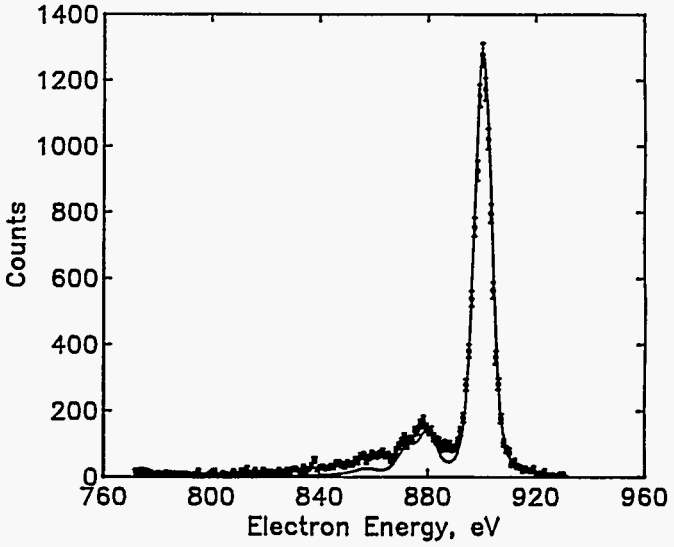

Fig. 2. Comparison between calculated electron spectrum for 1s photoionization of Kr (line) and the Si(333) data (points).

INVESTIGATION OF THE 'JOIN' BETWEEN XANES AND EXAFS

F. W. Lytle and R. B. Greegor, The Boeing Co., Seattle WA 98124

INTRODUCTION

We noticed that the second derivative of XANES data is useful for separating and identifying complex spectra. This is illustrated in Fig. 1. In panels ABC and DEF a 5 eV width unit arctangent is compared to a 5 eV width unit Lorentzian. Panels AD show each function centered at 0 eV, BE show the first derivative and CF show the second derivative. Panels GHI show the same sequence for a sum spectrum. Note that the major component of the 2nd derivative of a positive Lorentzian is a narrow, symmetrical, negative-going peak which maintains the same relative intensity and position as the original Lorentzian. The arctangent in the 2nd derivative has diminished so much in amplitude as to be almost negligible compared to the Lorentzian. Of course this is related to the relative 'sharpness' of the two functions. The 5 eV values were chosen as typical by fitting freely varying functions to typical 5d element spectra. In the following we show spectra carefully aligned on a common energy scale along with their 2nd derivatives in order to display the spectra and their separate multiplet components.

RESULTS AND DISCUSSION

To compare L_1 with $L_{2,3}$ spectra we begin by noting the difference in symmetry of the initial state wave functions, 2s vs 2p, where the 2s does not have a node at the origin and

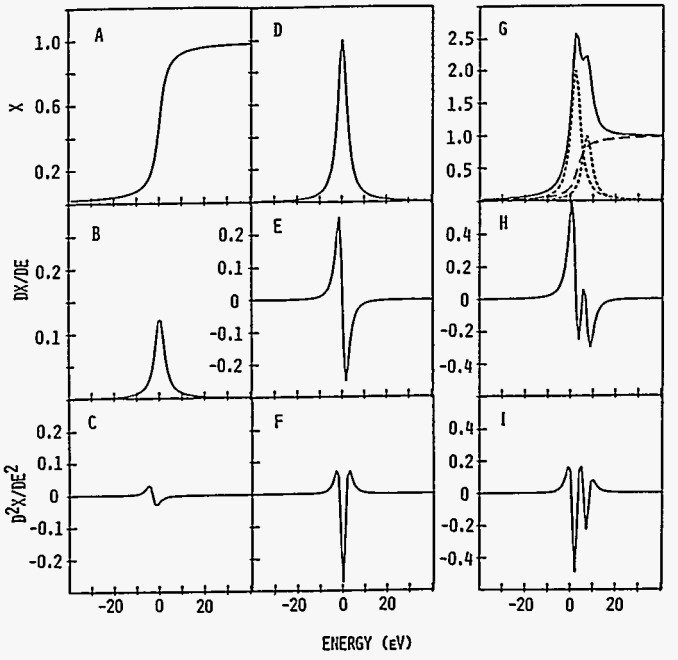

Fig. 1. Model spectra for 5 eV wide A) Arctangent, D) Lorentzian and G) sum of two Lorentzians plus arctangent, BEF) their 1st derivatives and CFI), their 2nd derivatives.

the 2p electron does. This causes the pi difference in phase between the s and p EXAFS phase shifts.(1) This is graphically demonstrated in Fig. 2C where the L_1 EXAFS of Pr_2O_3 (dashed line) has been inverted (pi phase shift) and overplotted on the L_3 spectrum. To account for the slight difference in slope of the two phase shifts the $L_{1,3}$ spectra were normalized in energy to the peaks at 32 and 270 eV which resulted in multiplying the L_1 energy scale x 0.95. The match of the two EXAFS spectra is a convincing argument of the common origin of the details of the fine structure down to 20 eV. This is a general result and has been

observed for many sets of $L_{1,2\ or3}$ edges. In Fig. 2A the XANES of the L_3 and the inverse of the L_1 Pr_2O_3 spectra are overplotted to illustrate the 'join' between the EXAFS and XANES. The L_1 energy scale has been multiplied by 0.95. The spectra were lined up on the first peak in the 2nd derivative in Fig. 2B where the L_1 spectrum has not been inverted. The coincidence in energy of the EXAFS and XANES features over the full range in energy show that the EXAFS may be used to place the onset of the absorption edge of $L_{1,2\ or3}$ on a common energy scale which is necessary for identification of the origin of peaks common to both edges. By inverting the L_1 spectra and plotting as in Fig. 1A and D the origin of the large dip which occurs after $L_{2,3}$ edge resonances is made clear. It is simply the first,big EXAFS bump out of phase by pi with the K or L_1 edges. The dip corresponds to the first big peak above the edge in K or L_1 spectra. In the region below 20 eV there are large differences between the $L_{1,3}$ spectra caused by the differences in the symmetries accessible by the dipole transition operating on each edge. From the perspective of the 2s or 2p initial states these are the separate symmetry projected density of final states of the compound. In order to confirm the identity of the peaks identified with the transitions 2p to 5d and 2s to 5d, the spectra of Re_2O_7 in Fig. 2DEF were chosen. The identification of 1s to 3d transitions common in K edges is well known.(2,3) This prepeak is very small for elements in environments with inversion symmetry and grows in intensity as the environment is distorted or

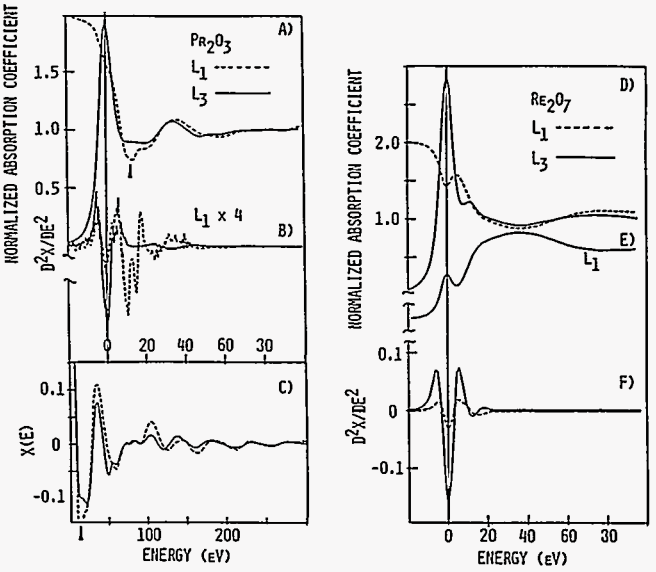

Fig. 2.

Illustration of the relationship between L_1 and L_3 spectra. In A) the inverted Pr_2O_3 L_1 spectrum is compared with the L_3. Note the close similarity above 20 eV. In C) the inverted L_1 EXAFS is compared with the L_3. In B) the 2nd derivatives of L_1 and L_3 are compared. Note that the edge features of $L_{1,3}$ line up at E = 0 when the EXAFS is aligned. In D) the inverted L_1 edge of Re_2O_7 is compared with the L_3, in E) the normal representation of the L_1 edge is shown and in F) the 2nd derivative of $L_{1,3}$ is compared.

the inversion symmetry is removed. The transition becomes dipole allowed and intense in tetrahedral coordination and has been treated theoretically and experimentally.(2,3) This effect is evident in the L_1 spectrum (Fig. 2E) of the tetrahedrally coordinated Re_2O_7. The peak at E = 0 is much larger than in the distorted octahedral coordination of Pr_2O_3 where it was necessary to enlarge the scale to make the peak visible(Fig. 2B). In Fig. 2D the L_1 spectrum has been inverted and overplotted on the L_3 spectrum to show the energy match of the peaks at E = 0 and the EXAFS. The 2nd derivatives (not inverted) are shown plotted to a common ordinate scale in Fig. 2 F. The $L_{1,3}$ spectra of a number of compounds in our data library has been compared in this way to verify that lining up on the EXAFS can be

used to identify the $L_{1,3}$ common transitions and that the 2s to 5d transition varies in intensity with the crystallographic environment of the absorbing element. In the perfect octahedral coordination of BaO it was barely visible, increasing to that shown for tetrahedral Re_2O_7.

1. B. K. Teo and P. A. Lee, J. Am. Chem. Soc. 101, 2815 (1979).

2. F. W. Kutzler et al., J. Chem. Phys. 73, 3274 (1980).

3. Joe Wong et al., Phys. Rev. B30, 5596 (1984).

Shallow and deep donors in $Ga_{1-x}Al_xAs$ semiconducting alloys

T.M. Hayes and D.L. Williamson
Physics Department
Colorado School of Mines, Golden, CO 80401

P. Gibart
Laboratory for Solid State Physics and Solar Energy, CNRS
Sophia Antipolis, 06560 Valbonne, France

Heavily n-doped $Ga_{1-x}Al_xAs$ alloys are of great interest for device applications. For $x < 0.2$, there are several preferred doping elements yielding shallowly bound donor states. For larger x, however, a deep level state appears for each of these dopants, called a DX center.[1] The solution of the resultant serious device problems has been impeded substantially by the absence of direct microscopic structural knowledge of the DX center due to the low concentration of dopants in the materials of interest, typically 10^{17} to 10^{19} cm^{-3}. In particular, there is a great deal of interest in the possibility of a large lattice relaxation associated with the neutral DX center. Addressing this issue, we have undertaken to examine the Sn environment in a variety of Sn-doped $Ga_{1-x}Al_xAs$ alloys using fluorescence detection x-ray absorption spectroscopy (XAS).

In the 1987 Activity Report, we reported the results of preliminary analysis of Sn K-shell fluorescence EXAFS data from samples of GaAs and $Ga_{0.7}Al_{0.3}As$ doped with 5×10^{18} cm^{-3} Sn and held at 80 K. To obtain neutral DX centers, the $Ga_{0.7}Al_{0.3}As$ sample had been cooled in the dark from 300 K to 80 K in approximately 1 minute. We discovered subsequently that many of the individual data files which we had added together to improve signal-to-noise from these dilute samples contained unusually large noise. Eliminating those improved the quality of the summed data files substantially. The Fourier transforms of the resulting spectra are shown in Fig. 1.

These spectra have been compared in detail with each other and with that from ordered $ZnSnAs_2$, in which each Sn atom is surrounded by four As atoms at 2.60 Å. We conclude that each Sn atom in the doped samples has four As neighbors at ~2.58 Å, but note that the nearest-neighbor (NN) peak in the radial distribution function does not have a simple Gaussian shape. While there are slight differences between NN peaks in the two doped samples, there is no evidence of a large shift in NN distance associated with the neutral DX center in $Ga_{0.7}Al_{0.3}As$, thereby eliminating the possibility of a large dilatory lattice relaxation in this sample. An angular distortion consistent with Mössbauer spectroscopy results[2] would of course be possible. Measurements of the Sn donor site under different doping conditions and with different illumination and thermal histories are in progress.

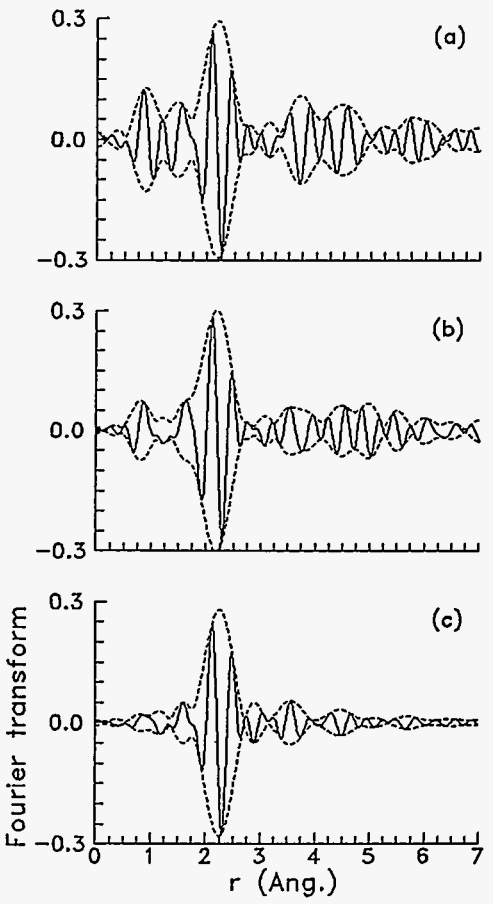

Fig.1. The real part (solid line) and the magnitude (dashed line) of the Fourier transform of the extended fine structure, $k\chi(k)$, on the Sn K-shell absorption of (a) GaAs and (b) $Ga_{0.7}Al_{0.3}As$ doped with $\sim5\times10^{18}$ cm^{-3} Sn and of (c) ordered $ZnSnAs_2$ at 80 K. The data were transformed using a square window with final-state electron momentum k between 2.8 and 10 $Å^{-1}$, broadened by convolution with a Gaussian of half-width 0.5 $Å^{-1}$.

1. D.V. Lang, in Deep Centers in Semiconductors, ed. by S.T. Pantelides (Gordon and Breach, New York, 1985), p. 489

2. P. Gibart, D.L. Williamson, B. El Jani and P. Basmaji, Phys. Rev. B 38, 1885 (1988)

Search for Ultra-fast, Luminous, Heavy-atom Scintillators

W.W. Moses and S.E. Derenzo,
Donner Laboratory and Lawrence Berkeley Laboratory,
University of California, Berkeley, CA 94720

1 Introduction

The ideal scintillation crystal for gamma detection has not been found. Such a crystal would have high density, high light output, short decay time, and would be both colorless and easy to work with. The first three entries in Table 1 list the properties of the three most common scintillating crystals. BGO ($Bi_4Ge_3O_{12}$) is very dense, but has low light output and a long decay time. Barium fluoride (BaF_2) has a short decay time, but is has low density and light output, and emits light in the short-wave UV region. Sodium iodide (NaI[Tl]) is luminous, but has a slow decay time, low density, and is hygroscopic.

The study in progress is part of a systematic search for new and better scintillators. At the Stanford Synchrotron Radiation Laboratory (SSRL), we make rapid measurements of the fluorescent decay time and light output of a large number of powdered samples. At the Synchrotron Radiation Center (SRC) we use ultraviolet photoelectron emission spectroscopy and ultraviolet fluorescence spectroscopy to probe atomic energy levels and understand scintillation mechanisms, while at Lawrence Berkeley Laboratory (LBL), we make more detailed measurements on the most promising compounds.

2 Method and Results

The apparatus used at SSRL, shown in Figure 1, is able to rapidly (within a few minutes per sample) measure the scintillation properties of powdered samples, avoiding the costly and time consuming task of preparing optical quality crystals. A nanosecond burst of X-rays from SSRL passes through a thin aluminum window, and a portion of the beam is absorbed by a powdered sample in a quartz cuvette. The resulting fluorescent emanations (if any) are observed by a quartz photomultiplier tube whose output is measured by a fast (1 ns rise/fall time) oscilloscope. The oscilloscope is triggered by a plastic scintillator attached to a second photomultiplier tube, which is excited by the remainder of the X-ray beam after it exits the chamber. This apparatus is able to measure the decay time with 5 ns resolution and the scintillation light output within an order of magnitude.

During four shifts of SSRL beam time in the Fall of 1987, we tested over one hundred compounds for scintillation. Of these, we discovered one major new scintillator, Cerium Fluoride (CeF_3), and reported its discovery in the IEEE Transactions on Nuclear Science NS-36. Its scintillation properties are listed as the final entry in Table 1. The short lifetime, high density, and reasonable light output of Cerium Fluoride suggest that it would be useful for applications where high counting rates, good stopping power, and nanosecond timing are important, such as medical imaging and nuclear science.

	NaI	BGO	BaF_2	CeF_3
Density (g/cm^3)	3.7	7.1	4.9	6.2
Decay time (ns)	230	300	0.8/620	27
Luminance (ph/keV)	40	4.8	2.0/6.5	2.5
Emission λ (nm)	410	480	225/310	340
Hygroscopic	yes	no	little	no

Table 1: Properties of Common Scintillators

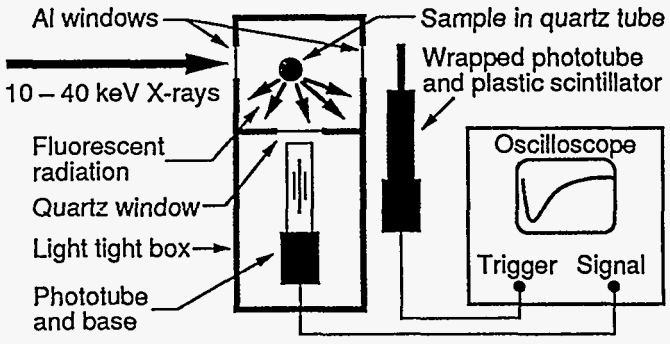

Figure 1: Apparatus for Screening Powdered Samples

Acknowledgments

This work was supported in part by the U.S. Department of Energy, under contract No. DE-AC03-76SF00098, and in part by Public Health Service Grant numbers P01 HL25840 and R01 CA38086. Work partially done at SSRL which is funded by the DOE under contract No. DE-AC03-82ER-13000, Office of Basic Energy Sciences, Division of Chemical Sciences and the NIH, Biotechnology Resource Program, Division of Research Resources.

SHIFT OF THE RESONANCE ENERGY OF A SYSTEM OF MÖSSBAUER NUCLEI DURING NUCLEAR BRAGG DIFFRACTION OF X-RAYS

J. Arthur, G.S. Brown, S.L. Ruby, and D.E. Brown
Stanford Synchrotron Radiation Laboratory, Stanford, CA 94309

The spectroscopy of the 14.4 keV Mössbauer resonance in ^{57}Fe is often used as a probe of the internal fields in a solid. Absorption experiments using standard radioactive sources and Doppler-shifting velocity drives are the common means for carrying out such spectroscopy. However, information about the effects of internal fields on resonance energy levels can also be obtained from the beat pattern that results when a short, broad-band pulse of radiation from a synchrotron light source is used to coherently excite the hyperfine-split Mössbauer levels in a sample in Bragg diffraction geometry.[1]

In the course of studying the beat pattern of the (002) reflection from a crystal of yttrium iron garnet (YIG), we have observed changes in the pattern that depend sensitively on the deviation of the incidence angle of the radiation from the Bragg angle. These changes are due to small shifts in the energies of peak reflectivity for the collection of Fe nuclei in the crystal lattice, an effect of dynamical diffraction rather than internal fields.

Analysis of the dynamical diffraction theory for simple resonant nuclei by Kagan, et al.[2] shows that the resonance energy plays a role analogous to that of the diffracting wave vector in conventional, non-resonant dynamical theory. There is a small shift in the effective resonance energy for each branch of the dispersion surface, and the magnitudes of these shifts become larger as the deviation between the incidence angle and the Bragg angle decreases. The magnitudes of the shifts are proportional to the transition probability amplitudes and to the crystal structure factors. The new tiny energy splitting that is introduced, between the two branches of the dispersion surface, tends to broaden the frequency width of the effective resonance and decrease the effective lifetime, an effect known as speed-up.

The energy shifts are quite small (typically 10^{-8} eV for YIG), and would be difficult to observe directly. However, since hyperfine fields in YIG produce an ^{57}Fe spectrum consisting of several resonances split by about 10^{-7} eV, the small shifts can have an important effect on the beat pattern resulting from the split resonances.

We observed the time distribution of photons diffracted from the YIG (002) planes in symmetric Bragg geometry, when illuminated by short (<1 ns) pulses of synchrotron X-rays from the 1B undulator at the PEP storage ring. A silicon (111) premonochromator was used to produce an incident beam with bandwidth of about 2 eV at 14.4 keV. An alignment field (of about 100 G) nearly parallel to the incident beam oriented the internal moments and provided a quantization axis, so that the hyperfine structure consisted of two resonances excited by the left-hand-circular polarization (LHC) component of the incident light, and two resonances excited by the right-hand-circular (RHC) component. The incident radiation was highly linearly polarized, providing equal amounts or LHC and RHC light. The transition probability amplitudes of the various resonances differ, such that the energy shifts due to deviations of the incident angle from the Bragg angle caused the effective energy values for the LHC resonances to move closer together when the effective values for the RHC resonances moved farther apart, and vice versa. The observed time distribution of the scattered radiation thus consisted of a superposition of an intensity pattern with beats from the LHC component, and an intensity pattern with beats from the RHC component. The periods of the two overlapping beat patterns could be changed relative to each other by adjusting the deviation angle.

Figure 1 shows the time distribution obtained when the deviation angle $\delta\theta=(\theta-\theta_B)$ was very small.

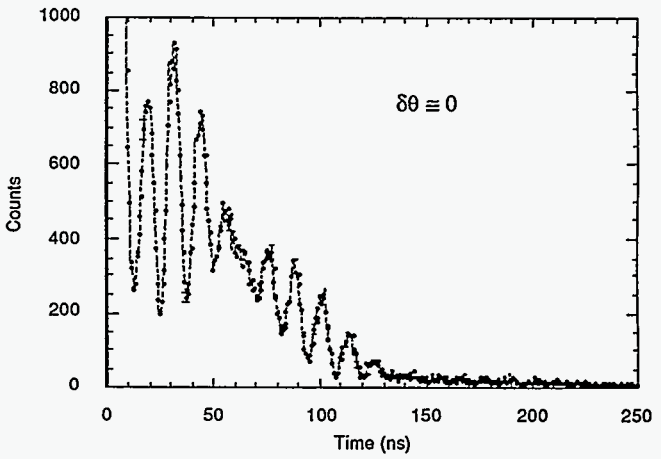

Figure 1
Time distribution of resonantly scattered X-rays from YIG(002) in symmetric Bragg geometry. The line through the experimental points is a guide for the eye.

The most prominent features of this distribution are the very large peak at t=0, due to non-resonant electronic scattering, the large speed-up giving very little intensity after about 140 ns, and the fast beat structure due to the interference of the hyperfine-split resonances. No background or other corrections have been made to this data, which was collected in 11 minutes.

Figures 2 and 3 show the time distributions obtained when the YIG crystal was slightly rotated, introducing a deviation angle. With such deviation angles, the overall intensity is much reduced, the

speed-up effect is smaller, and a slow beat pattern with period of about 130 ns, due to electric quadrupole terms in the hyperfine interaction, is clearly visible. Moreover, there are striking differences in the fast beat pattern. The energy shifts in the +34 μrad case are such that the LHC and RHC beat patterns have peaks and valleys that nearly coincide during the time period 10-100 ns, whereas in the -34 μrad case the peaks of the LHC beat pattern tend to fall upon the valleys of the RHC pattern during this time period. In Figs. 2 and 3 the solid curves are calculations based on the dynamical theory of Kagan, et al.[2]

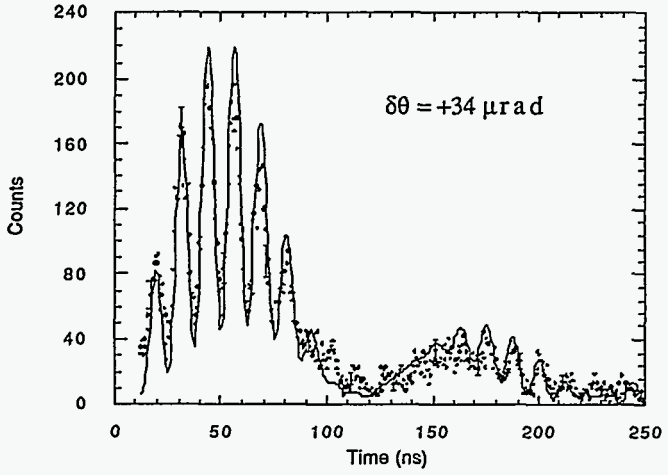

Figure 2
Time distribution with YIG crystal slightly rotated away from the Bragg angle. The solid curve is a dynamical theory calculation. This data was collected in 10 minutes.

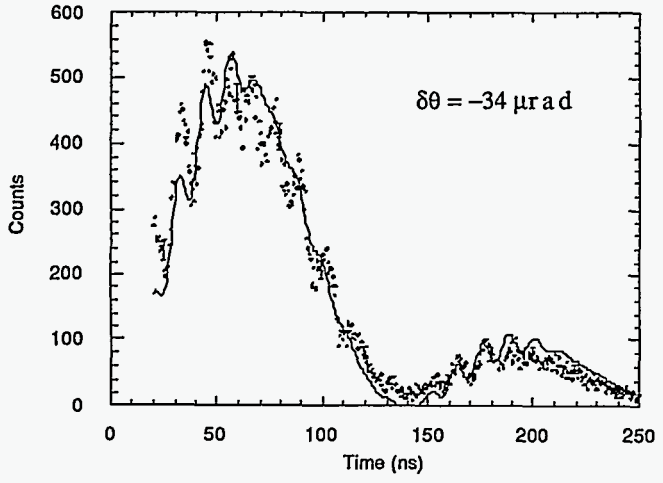

Figure 3
Time distribution data and dynamical theory calculation for the case where the YIG crystal has been rotated off Bragg in the other direction. This data was collected in 20 minutes.

The agreement with the experimental data is quite good; the small discrepancies are probably due to the fact that the calculation neglects the effects of 16 of the 40 Fe nuclei in the YIG unit cell. These 16 nuclei have a vanishing structure factor for the (002) reflection, but their forward scattering amplitude does not vanish, and in the dynamical calculation would cause slight additional shifts in the effective resonance energies for scattering. (Because this effect should be stronger at smaller deviation angles, and because of the computational difficulty of properly averaging over the divergence of the incident beam, which becomes important at small deviation angles, no attempt was made to calculate a time distribution for the data in Fig. 1) The fast beat patterns of the two polarization states have periods of about 12.3 and 12.8 ns in Fig. 2, whereas in Fig. 3 the periods are about 12.0 and 13.1 ns. The small changes in the periods, due to the small shifts in effective resonance energies, have a clearly visible effect on the time distribution.

This experiment benefitted immensely from the characteristics of PEP beam line 1B. With an electron energy of 13.5 GeV and a typical current of 15 mA, we found that about 10^{12} photons/s were selected by the Si(111) premonochromator at 14.4 keV, a slightly lower rate than was found using the high-power wiggler beam line 10 at the SPEAR storage ring, running in dedicated mode with 80 mA at 3.0 GeV. However, the reduced emittance of the PEP beam line, along with some improvements in experimental procedure, resulted in a resonantly scattered signal rate increase of a factor of 100 compared to the SPEAR beam line, and a background rate decrease of about a factor of 10. With rates of resonantly scattered photons of up to 500/s, and a background rate of less than 1/s, we were able to collect a time distribution with excellent statistics in 10 minutes, rather than the hours such a measurement required at the SPEAR beam line. This represents a fundamental change in the nature of resonant nuclear scattering experiments. We hope to continue to explore the new possibilities in the near future.

This research was performed at SSRL, which is operated by the Department of Energy, Office of Basic Energy Sciences, Division of Chemical Sciences. That Office's Divison of Materials Sciences has provided support for this research.

---

1 E. Gerdau, R. Rüffer, R. Hollatz, and J.P. Hannon, Phys. Rev. Lett. **57**, 1141 (1986). A general review of this field is to be published by J.P. Hannon and G.T. Trammel in Physica B.

2 Yu. Kagan, A.M. Afanas'ev, and V.G. Kohn, J. Phys. **C12**, 615 (1979).

3d Metal Ions Substitution in $YBa_2Cu_3O_7$ Superconductors

Joe Wong*, E. M. Larson*, R. B. Greegor** and F. W. Lytle**

*Lawrence Livermore National Laboratory, Livermore, CA 94550
**The Boeing Company, Seattle, WA 98124

We have investigated the local atomic structure and coordination geometry of 3d transition metals from Ti to Zn substituted for 10% Cu in $YBa_2Cu_3O_7$ (YBC) using a combination of EXAFS and XANES. The samples are represented by $YBa_2(Cu_{0.9}M_{0.1})_3O_7$, where M=Ti, V, Cr, Mn, Fe, Co, Ni, and Zn. The samples have been investigated previously by Xiao et al. (Phys. Rev. B 36, 8782 (1987) using x-ray diffraction, resistance, magnetization and magnetic susceptibility (above T_c) measurements. The measurements showed that T_c was depressed for all the 3d metals, particularly for Zn, Co and Fe. Preliminary x-ray diffraction revealed that all the samples were single phase, with the same perovskite-like structure as undoped YBC.

The ionic size of the 3d metals are comparable to Cu, and so it is expected that some fraction of the added elements will occupy either the Cu(1) or Cu(2) sites. Indeed, the effect on T_c indicates that some degree of some kind of substitution occurred although this could not be quantified by the previous work. To examine the extent and nature of this substitution we have used XAS to examine the Y, Cu and 3d metal local electronic and structural environment. In addition to analyzing the XAS of each 3d element to determine its lattice site(s) and valence(s) which will be averaged over all the sites it occupies, we used the EXAFS-derived radial structure function of Y and Cu in each sample to sense the degree of substitution from the perspective of their lattice positions. We believe this approach to be particularly useful when a major fraction of the added element does not substitute into a normal lattice site but forms a separate phase. As long as this phase is not commensurate with the lattice it will be essentially invisible from the perspective of the Y and Cu sites because of the averaging that would occur with a randomly dispersed impurity phase. This Y/Cu radial structure function analysis was also sensitive to the varying degree of Y/Cu antisite disorder induced by the 3d metal substitution.

The results indicate that Ti, Mn, Fe and Co are incorporated into the YBC planar, four-fold coordinated, Cu(1) site. The V goes into the Cu(2) site while Ni appears to be substituting for Cu in both the Cu(1) and Cu(2) sites. The added 3d elements also affect the degree of anti-site Cu/Y disorder. At a 10% level of substitution there appears to be an additional segregated oxide phase for each of the above 3d metals with the majority of the Cr in a chromate phase and the Ni in a NiO-like phase. The segregation is clearly indicated in the XANES spectra shown in Fig. 1.

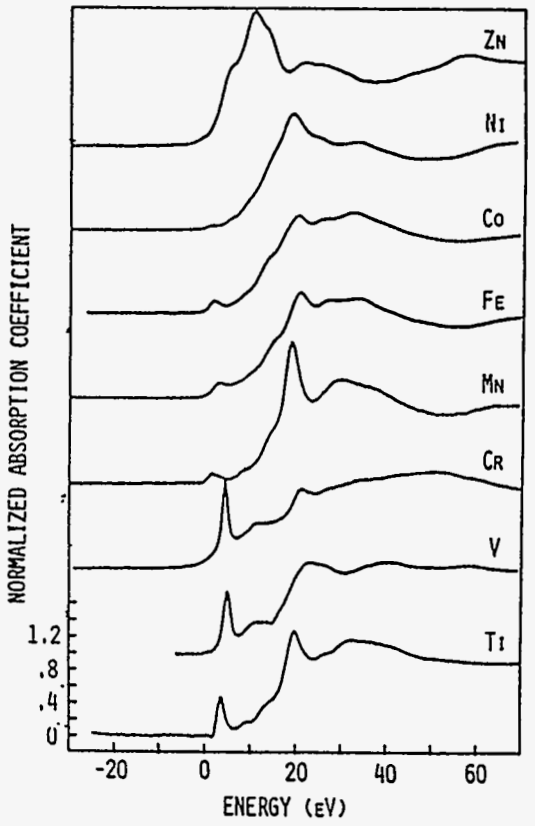

Figure 1 - Normalized XANES spectra of Ti to Zn substituted for 10% Cu in YBC

ANOMALOUS SCATTERING OF X-RAYS

David H. Templeton and Lieselotte K. Templeton

Department of Chemistry, University of California, Berkeley, CA 94720

INTRODUCTION

In this project we are seeking basic information about anomalous scattering of X-rays to provide a foundation for applications of synchrotron radiation in the study of chemical structure. The emphasis is on the large resonance effects near absorption edges and how they depend on photon polarization.

K-EDGE ANOMALOUS SCATTERING OF ZINC(2+)

Anomalous scattering terms for Zn(2+) near the K edge were derived from diffraction experiments with zinc tartrate crystals and from absorption spectra (1). This cation is the chemical state of zinc most likely to be used to help solve the phase problem for a macromolecular crystal. The effects (Fig. 1) are as much as 9.2(2) for f'' and down to -11.6(1) for f'. For the metallic state (2) the maximum of f'' is only about 4.6, and f' fails to reach -9. Cromer & Liberman theory (3), which omits the resonance line, gives 3.9 as the maximum of f''. When corrected for level width, it gives -9.3 as the minimum f' (Fig. 1).

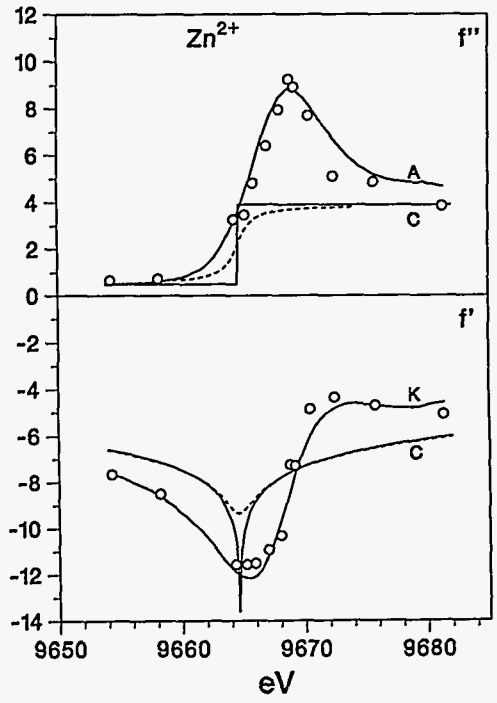

Figure 1. Anomalous scattering of Zn(2+) from diffraction (circles). Curve A: f'' from absorption; K: f' from Kramers-Kronig transformation of A; C: f' and f'' from Cromer's program before (solid lines) and after correction (broken lines) for level width.

K-EDGE ANOMALOUS SCATTERING OF RUBIDIUM(1+)

Similar experiments with rubidium hydrogen tartrate yielded a maximum of 4.7(1) for f'' and a minimum of -9.7(1) for f'. The open circles in Fig. 2 indicate results of diffraction experiments with R = 0.019 to 0.030 which agree well with values from absorption spectra (lines). The solid circles indicate data from another crystal for which there were problems with absorption corrections.

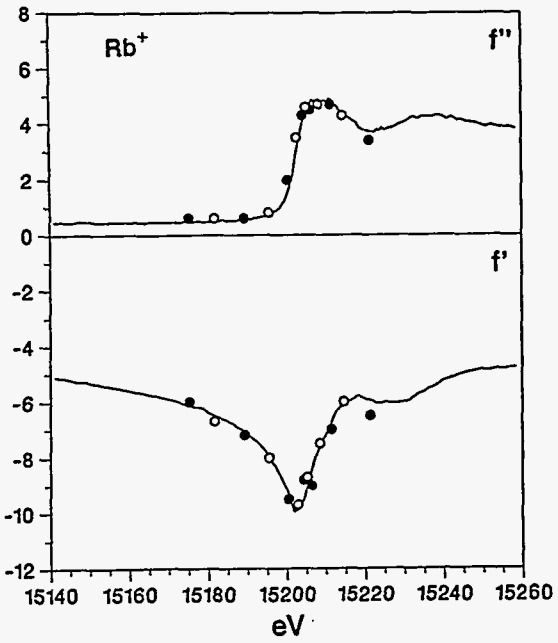

Figure 2. Anomalous scattering of Rb(1+) from diffraction (circles) and absorption (curves).

OTHER PUBLICATIONS

Publications this year included a study of the degree of polarization of radiation at SSRL (4) and the determination of biaxial tensors for selenium K-edge anomalous scattering in selenolanthionine (5).

ACKNOWLEDGEMENTS

This research was supported by National Science Foundation Grant CHE-8515298 and was done at SSRL which is supported by the Department of Energy, Office of Basic Energy Sciences; and the National Institutes of Health, Biotechnology Resource Program, Division of Research Resources. It used some facilities of the Lawrence Berkeley Laboratory, supported by DOE Contract DE-AC03-76SF00098.

REFERENCES

1. L.K. Templeton & D.H. Templeton, J. Appl. Cryst. 21, 558-561 (1988).
2. J.P. Simon, J.J. Hoyt, O. Lyon, R. Pro, B.E.C. Davis, D. De Fontaine & W.K. Warburton, J. Appl. Cryst. 18, 181-183 (1985); P. Goudeau, A. Fontaine, A. Naudon & C.E. Williams, ibid., 19, 19-24 (1986); R. Begum, M. Hart, K.R. Lea & D.P. Siddons, Acta Cryst. A42, 456-464 (1986).
3. D.T. Cromer, J. Appl. Cryst. 16, 437 (1983).
4. D.H. Templeton and L.K. Templeton, J. Appl. Cryst. 21, 151-153 (1988).
5. L.K. Templeton & D.H. Templeton, Acta Cryst. A44, 1045-1051 (1988).

SULFUR K XAS OF THE IRON-MOLYBDENUM COFACTOR FROM A. vinelandii NITROGENASE: LIGAND EXCHANGE, AND XAS WITH in situ ELECTROCHEMICAL CONTROL

Britt Hedman[1], Patrick Frank[2], Benjamin Feldman[3], Stephen F. Gheller[3], William E. Newton[3] and Keith O. Hodgson[2]

[1]SSRL, SLAC, Bin 69, P.O. Box 4349, Stanford, CA 94309, USA
[2]Department of Chemistry, Stanford University, Stanford, CA 94305, USA
[3]Western Regional Research Center, USDA-ARS, Albany, CA 94710; and Department of Agronomy and Range Sciences, University of California, Davis, CA 95616, USA

We have continued our study of the electronic and structural nature of S and Mo in the iron-molybdenum cofactor (FeMoco) isolated from the MoFe protein of A. vinelandii nitrogenase. The study is performed using x-ray absorption edge and near-edge spectroscopy at the sulfur K and molybdenum L_3 and L_2 edges. In the 2.4-3.0 keV region, the energy resolution is significantly improved, resulting in higher sensitivity to changes in electronic and structural environment at the absorbing atom.

The experiments were performed using beam line 6-2 at low fields (~1.5-5 kG; with 250, 125 and 25 μm Be windows and no graphite filters in the beam line) during dedicated conditions (3.0 GeV, 40-80 mA, focused, Si(111) double-crystal monochromator).

Results. In the cofactor isolation process, dithionite is normally added to maintain FeMoco in its semi-reduced (s-r) state. Since the S K edge spectrum of dithionite (and its oxidation/decomposition products) obscures that of FeMoco, an anaerobic column chromatographic method of purification was developed. Spectra were thus obtained for dithionite-free FeMoco(ox), as reported previously [1]. These measurements showed the presence of an unprecedented form of sulfur, a thiosulfate ($-S-SO_3$) moiety bound through its terminal sulfur as an integral part of FeMoco.

It is likely that this moiety derives from disproportionation of dithionite to thiosulfate (and sulfite) which binds FeMoco during extraction from the protein. We have therefore measured S K edge spectra (Fig. 1) of samples where the presence of dithionite was carefully regulated. They show that the presence of thiosulfate is directly correlated to the presence of dithionite in the isolation process, as well as the time over which the FeMoco is incubated with dithionite. It further indicates that ligand exchange is taking place on FeMoco, the details of which is the next step of our study.

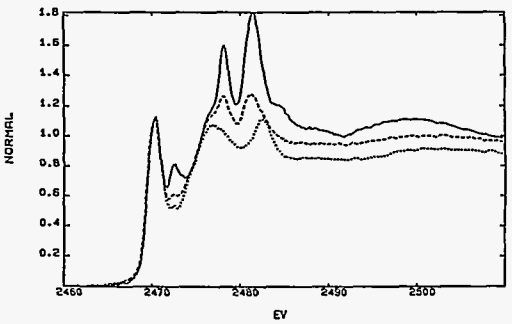

Fig. 1. Sulfur K edge spectra of column-purified FeMoco: dithionite present for several months (—); ~3 hours (- -); not present in the isolation process (···). The presence of bound thiosulfate correlates with the time over which FeMoco has been treated with dithonite, as indicated by the ~2478 and ~2481 eV transitions.

Enzyme-bound FeMoco is an active catalytic center. Insight into potentials and numbers of electrons for two of the redox processes for FeMoco have come from cyclic voltammetry (CV) studies [2]. Each process (ox→s-r→red) involves the transfer of approximately one electron as determined by controlled potential coulometry [3] and CV. In order to study FeMoco with stringent control over the redox state, and in the absence of dithionite, we have developed, built and extensively tested an anaerobic electrochemical cell, which is compatible with XAS measurements at these low energies. It consists of two compartments separated by a Nafion membrane. The front compartment contains the sample, an RVC (reticular vitreous carbon) working electrode, a miniature Ag/AgCl reference electrode, and the rear chamber a reference solution and a Pt-wire auxiliary electrode. The cell is not stirred but, in the millimolar range, sample electrolysis is completed rapidly due to the extremely high surface area of the RVC electrode.

We are thus extending our XAS studies to utilize this in situ electrochemical control to produce and monitor specific oxidation state species in solution. Through the use of bulk coulometry, a given sample oxidation state can be prepared. The solution resting potential will indicate the redox state of the sample, which can be dynamically maintained. CV measurements before, during and after the experiment will directly query sample integrity (which will also be monitored by activity assays and EPR). The cell has been bench tested with both model compounds and FeMoco, and will be used with x-ray beam at the earliest possible opportunity.

Acknowledgements. This research was supported by NSF grant CHE 88-17702 and was done at SSRL which is supported by the Department of Energy, Office of Basic Energy Science, and the National Institutes of Health, Division of Research Resources, Biotechnology Resource Program.

References.

[1] B. Hedman, P. Frank, S.F. Gheller, A.L. Roe, W.E. Newton, K.O. Hodgson, J. Am. Chem. Soc. 110 (1988) 3798.
[2] F.A. Schultz, S.F. Gheller, B.K. Burgess, S. Lough, W.E. Newton, J. Am. Chem. Soc. 197 (1985) 5364; W.E. Newton, F.A. Schultz, S.F. Gheller, S. Lough, J.W. McDonald, S.D. Conradson, B. Hedman, K.O. Hodgson, Polyhedron 5 (1986) 567.
[3] F.A. Schultz, S.F. Gheller, W.E. Newton, Biochem. Biophys. Res. Comm. 152 (1988) 629.

A STRUCTURAL STUDY OF BLUE MEMBRANES

Soichi Wakatsuki[1], Yoshiaki Kimura[2], W. Stoeckenius[2],
K.O. Hodgson[1], and S. Doniach[3]

[1]Department of Chemistry, Stanford University, Stanford, CA, 94305
[2]Cardiovascular Research Institute, University of California,
San Francisco, CA, 94134
[3]Department of Applied Physics, Stanford University, Stanford, CA, 94305

Introduction

Spectroscopic studies of the deionized form of the purple membranes in bacteriorhodopsin, which are called blue membranes because of their color, have indicated that the purple-to-blue transition accompanies a conformational change. However, the change of x-ray diffraction has not been investigated in great detail due to its liable nature giving rise to loss of the lattice structure. So far contradictory descriptions of the structures of the blue membranes have appeared: one claiming a well-preserved lattice[1,2] and one a distortion of the lattice[3]. Because of the lower surface pH of the blue membranes, it has been suggested that their lattice structure is largely disordered in the ultracentrifuged samples thus preventing structure determination using x-ray diffraction. The blue form of bacteriorhodopsin lacks some intermediates and does not function as a proton pump. Therefore, the determination of the conformational change during purple-to-blue transition may give insights as to how the deionization stops the pump. As an addition to our ongoing project on cation binding sites of bR, we are investigating the diffraction patterns of the blue form and comparing them to the ones for native purple membranes.

Experimental

The blue membranes were prepared as described[1] and ultracentrifuged at 45000 rpm for 3 hours followed by partial drying on a mica substrate. The data were collected on beamline 4-2 at SSRL in February 1989 using the SSRL Biotechnology Laboratory Small Angle X-ray Scattering Camera. The x-ray beam was in the plane of the membranes in order to obtain in-plane diffraction patterns.

Results

Preliminary experiments on the blue form showed that the lattice structure of the blue membrane can be observed and is comparable in quality to that of the purple membrane (Fig.1). The blue membrane has a slightly different unit cell dimension. After dehydration for a few hours, however, the blue membrane lattice structure disordered and its diffraction pattern deteriorated drastically (profile B in Fig.1). The diffraction pattern still shows lower index reflections such as (1,1) and (2,0) although its higher index peaks have lost their fine structures. This may be related to a change of CD spectrum seen in a reversible transition of the purple membrane between lattice and distorted one at around 80°C[4]. The diffraction pattern B in Fig.1 after a few hours of further dehydration also shows a broad peak at around 0.1Å which corresponds to inter monomer distance of 10Å. Our data clearly show that the fresh blue membranes have their lattice well preserved (profile A in Fig.1) and that the later disruption of the lattice is due to further dehydration (profile B in Fig.1).

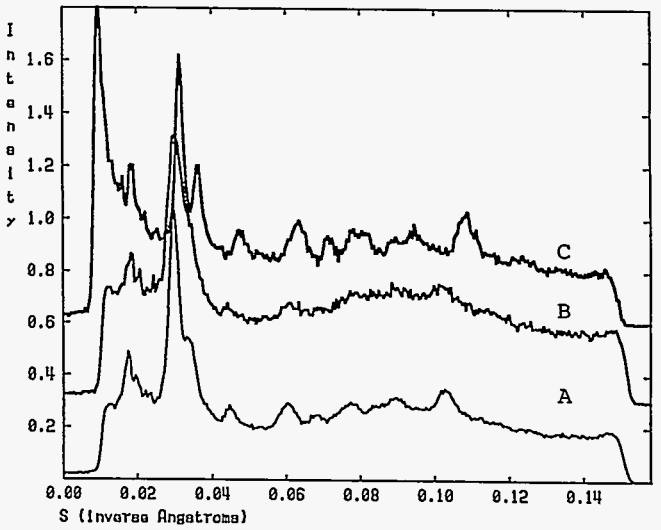

Figure. 1 Calibrated diffraction patterns of the purple and the deionized blue membranes. Intensities were scaled to give about the same heights for all of the three patterns. A) Partially hydrated blue membranes. B) Dehydrated blue membranes after 2 to 3 hours of drying. C) Partially hydrated Purple membranes. Exposure times were about 10 minutes for each sample and the sample to detector distance was 15cm.

REFERENCES:

1. Kimura, Y., Ikegami, A. and Stoeckenius, W. (1984), Photochem. Photobiol., 40, 641-646.
2. Katre, N.V., Kimura, Y. and Stroud, M. (1986), Biophysics J., 50, 277-284.
3. Mowery, P.C., Lozier, R.H., Quae, C., Tseng, Y.-W., Taylor, M., and Stoeckenius, W. (1979), Biochemistry, 18, 4100-4107.
4. Hirake, K., Hamanake, T., Mitsui, T., and Kito, Y. (1981), Biochim. Biophys. Acta, 647, 18-28.

ACKNOWLEDGEMENTS This research was supported by NIH Grant RR 1209 and data were recorded at SSRL which is supported by the DOE's Office of Basic Energy Science.

X-RAY ABSORPTION SPECTROSCOPY OF PROTEIN A OF METHANE MONOOXYGENASE

Jane DeWitt, Britt Hedman, Agneta Ericson and Keith O. Hodgson
Department of Chemistry and Stanford Synchrotron Radiation Laboratory
Stanford University, Stanford, CA 94305, USA

James Bentsen, Robert Beer and Stephen J. Lippard
Department of Chemistry, Massachussetts Institute of Technology
Cambridge, MA 02139, USA

Jeffrey Green and Howard Dalton
Department of Biological Sciences, University of Warwick
Coventry CV4 7AL, England

Introduction

Methane monooxygenase (MMO) is a non-heme iron-containing protein which activates dioxygen for incorporation into a remarkable variety of substrates including methane [1]. We report the use of x-ray absorption Fe K edge and EXAFS analysis to characterize structurally the active center of this protein. We have collected data for the semimet form of Protein A of MMO from *Methylococcus capsulatus* (Bath) and *Methylosinus trichosporium* (OB3b), and of the reduced form of Protein A of MMO from *Methylococcus capsulatus* (Bath).

All data were measured at 10 K during dedicated conditions on the wiggler beam lines 4-2 and 7-3 at the Stanford Synchrotron Radiation Laboratory (SSRL). Model compounds were measured as powders, mixed with BN, in transmission mode, while all protein data were measured as glasses in fluorescence mode.

Results and discussion

Both *semimet* samples were prepared in their oxidized form, but were photoreduced to the mixed-valence state by the x-ray beam, as demonstrated by a shift in the Fe K edge of ~ 1.5 eV to lower energy. The photoreduction took place within about 4 hours, after which no further reduction of the sample occured during exposure to the x-ray beam. The fully reduced protein was prepared by chemical reduction of oxidized protein A using dithionite reduced methyl viologen. The *reduced* form of the protein showed no edge shift, and its edge appears ~ 2.7 eV to lower energy relative to the semimet edge. In Figure 1, a summation of the first edge scan of the initially oxidized protein with a scan of the reduced sample is compared to the edge spectrum of the actual semimet sample. The sum and the semimet edge show good agreement. ESR measurements of the XAS samples confirm the mixed-valence state.

The EXAFS of semimet and reduced MMO from *M. capsulatus* (Bath) differ mainly in phase, and a difference in beat is noticed around $\underline{k} = 8.0$ Å^{-1}. The Fourier transforms of the two samples (Figure 2) differ quite dramatically. There is no well-defined second shell EXAFS contribution for the fully reduced protein. Curve-fitting to the EXAFS for the semimet and fully reduced protein samples indicates that the first coordination shell around iron is composed of approximately six nearest O/N neighbors at an average distance of ~ 2.11 Å in the semimet form, and at a slightly longer distance in the reduced sample. Data analysis of the second-shell filter of semimet MMO shows the presence of a dimeric iron center with an Fe-Fe distance of 3.42 Å. Data analysis of the second-shell and of a wide two-shell Fourier filter of the reduced form of the protein does not suggest such a tightly coupled binuclear iron center. Most importantly, we cannot rule out the dissociation of a reduced binuclear core in this sample. A short μ-oxo bridge is *not* present in either of the protein samples.

Preliminary fits of the EXAFS of semimet *M. trichosporium* (OB3b) suggest the presence of a first coordination shell similar to that of *M. capsulatus* (Bath), as well as a binuclear Fe center with an Fe-Fe distance of about 3.42 Å.

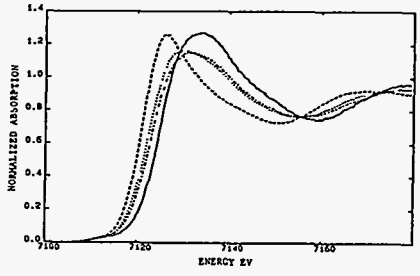

Fig. 1. The Fe edge of the reduced (– –) and the oxidized (—) forms of MMO from *M. capsulatus* (Bath) along with the 1:1 sum of the two spectra (·····). The edge of the semimet protein (–·–) is included.

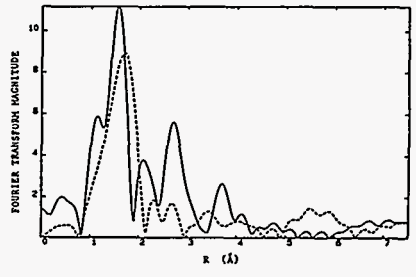

Fig.. 2. The Fourier transforms of semimet (—) (k = 3.5 - 12.2 Å^{-1}) and reduced (– –) (k = 3.5 - 12.5 Å^{-1}) MMO from *M. capsulatus* (Bath).

References

[1] (a) Colby, J.; Dalton, H. *Biochem. J.* **165** 495 (1976). (b) Colby, J.; Stirling, D.I.; Dalton, H. *Biochem. J.* **165** 395 (1977). (c) Colby. J.; Dalton, H. *Biochem. J.* **171** 461 (1978).

[2] A preliminary account of some of this work has appeared: Ericson, A.; Hedman, B.; Hodgson, K.O.; Green, J.; Dalton, H.; Bentsen, J.G.; Beer, J.H.; Lippard, S.J. *J. Am. Chem. Soc.* **110** 2330 (1988).

Acknowledgment

The data were collected at the Stanford Synchrotron Radiation Laboratory, which is supported by the Department of Energy, Office of Basic Energy Sciences, and the National Institutes of Health , Biotechnology Resource Program, Division of Research Resources. Grant Support was provided by the National Science Foundation (CHE 85-12129 to KOH), the Gas Research Institute (5086-260-1209 to HD), and the National Institute of General Medical Sciences (GM 32134 to SJL).

EDGE AND EXAFS STUDIES OF CU COORDINATION IN DEOXY HEMOCYANIN

Grace Tan, Lung-Shan Kau, Keith O. Hodgson and Edward I. Solomon

Department of Chemistry, Stanford University, Stanford, CA 94305, USA.

Introduction

Hemocyanin (Hc) is the oxygen transport protein in the blood of molluscs and arthropods. The active site contains two Cu atoms, each ligated with histidines. In the deoxy form, both Cu atoms are in oxidation state (I), and it is thus very difficult to probe the site by most spectroscopic means in this state. We report the use of x-ray absorption edge and EXAFS analysis to characterize the deoxy Hc state and study its interaction with exogenous ligands.

Experimental

All data were collected at SSRL, on the wiggler beam line 7-3. Data were collected at 5 (or 10) K, 77 (or 80) K and 200 K. Model compounds were measured as powders with BN in transmission mode, while all protein samples were measured as glasses in fluorescence mode. The EXAFS data, obtained by normalization and polynomial spline background removal, was analyzed using curve-fitting techniques. Empirical phases and amplitudes were obtained from and tested on model compounds of known structure.

Edges

We have observed that, for model compounds [1], 2-coordinate Cu(I) compounds with C, N or O ligation all show a sharp spike in the edge at 8983-8984 eV, and this holds true for bond angles varying from 178° to 160°. Three-coordinate Cu(I) compounds normally show a lower intensity in this region. The difference edge methodology (a Cu(II) edge subtracted from a Cu(I) edge) is a helpful way of quantifying the differences between 2-, 3- and 4-coordinate Cu(I) edges. With this method we have ascertained that only the edges of 2- and 3-coordinate Cu(I) compounds show any feature below 8985 eV. Edges of 4-coordinate Cu(I) compounds show features only at or above 8985 eV.

It is very clear from comparison with these model studies that the edge in Panulirus Interruptus (P. I.) deoxy Hc is 3-coordinate in character.

EXAFS

EXAFS analysis of the Fourier-filtered 1st shell signal of deoxy Hc consistently shows a co-ordination of 2, as seen in the Table.

The coordination numbers for deoxy Hc may be reconciled with the edge information by considering the results for the 2 Cu(I) complexes given in the Table. $Cu_2(bpeac)BF_4$ is a bicuprous complex wherein each Cu is 4-coordinate but the 2 Cu atoms are inequivalent. There are thus 8 different scatterers at 1.9-2.2 Å contributing to the EXAFS. $[Cu(timm)_2](BF_4)_2$ has 2 equivalent 3-coordinate Cu, i.e. 3 scatterers at 1.9-2.05 Å contribute to the EXAFS. The results for these model compounds suggest strongly that static disorder in the 1st shell over a range of 0.2-0.3 Å cannot be entirely absorbed into σ^2, but causes a drop in the apparent coordination number. (We cannot account for the reverse trend in σ^2 with temperature for $Cu_2(bpeac)BF_4$.)

Sample	Co-ord. No.	σ^2(Å^2)
P.I. deoxy Hc, pH 4.5, 5 K	2.0	0.01086
P.I. deoxy Hc, pH 4.5, 77 K	1.9	0.01057
P.I. deoxy Hc, pH 7.5, 5 K	2.0	0.01016
P.I. deoxy Hc, pH 7.5, 77 K	2.0	0.01079
P.I. deoxy Hc, pH 9.6, 77 K	2.2	0.01081
Bus. C. deoxy Hc, pH 7.5, 77 K	2.3	0.01170
$Cu_2(bpeac)BF_4$, 10 K	2.1	0.01618
$Cu_2(bpeac)BF_4$, 80 K	2.1	0.01593
$Cu_2(bpeac)BF_4$, 200 K	2.0	0.01562
$[Cu(timm)]_2(BF_4)_2$, 5 K	2.6	0.01324
$[Cu(timm)]_2(BF_4)_2$, 77 K	2.7	0.01359
$[Cu(timm)]_2(BF_4)_2$, 200 K	2.7	0.01423

Binding of thioacetamide to deoxy Hc

The binding of thioacetamide (TA) to deoxy Hc is of interest because TA is one of the very few exogenous ligands that displays charge transfer bands upon binding to the Cu(I)'s.

Edge studies of the binding of TA to Busycon Canaliculatum (Bus. C.) deoxy Hc at pH 7.5, 77 K show that Bus. C. deoxy Hc is 3,3-coordinate, but Bus. C. deoxy Hc + TA is either 3,4- or 4,4-coordinate.

Corresponding EXAFS analysis shows that the 1st shell of Bus. C. deoxy Hc + TA contains 0.8-1.0 S atoms.

These results show that TA clearly does bind, and further suggest that it binds through S.

Conclusion

The Cu atoms in deoxy Hc are most probably 3,3-coordinate, and the lower coordination numbers obtained in EXAFS analysis may be explained as arising from static disorder. Thioacetamide binds to deoxy Hc through S, increasing the coordination number of at least 1 Cu atom in the site.

Reference

1. Kau, L.-S.; Spira-Solomon, D. J.; Penner-Hahn, J. E.; Hodgson, K. O.; Solomon, E. I. J. Am. Chem. Soc. 109, 6433 (1987).

Acknowledgements. This work was supported by the National Science Foundation through Grant CHE-85-12129 to K.O.H. and by the National Institutes of Health through Grant DK-31450 to E.I.S. The Stanford Synchrotron Radiation Laboratory is supported by the Department of Energy, Office of Basic Energy Sciences, and the National Institutes of Health, Division of Research Resources.

A TIME-RESOLVED X-RAY DIFFRACTION STUDY OF PURPLE MEMBRANES IN BACTERIORHODOPSIN

S. Wakatsuki[1,4], U. Spann[2], B. Hedman[2], N. Gillis[3], Y. Amemiya[4], S. Kishimoto[4], T. Matsushita[4], K.O. Hodgson[1], and S. Doniach[3]

[1]Department of Chemistry, Stanford University, Stanford, CA, 94305
[2]SSRL, SLAC, Bin 69, P.O. BOX 4349, Stanford, CA 94305
[3]Department of Applied Physics, Stanford University, Stanford, CA, 94305
[4]The Photon Factory, National Institute for High Energy Physics, Japan

Introduction

Purple membrane is an integral membrane protein of bacteriorhodopsin (bR) which functions as light-driven proton pump. A key step in the photocycle of the bR which can be detected by x-ray diffraction, is the L550 to M412 transformation or reappearance of the ground state bR570. The M412 intermediate has a life time of 5-10 ms at 20°C, which can be extended at lower temperatures (activation energy is 13 kcal/mol). There are apparently at least two classes of conformational changes in the bR on going to M412 state: a local change associated with the primary cis-trans isomerization of the c13-c14 double bond in the retinal, and a much larger scale change involving disruption of the trimer unit cells of the bR lattice[1]. It is therefore pertinent to measure both the optical absorption and the x-ray diffraction of purple membranes during the photo cycle. We have developed a system which consist of time-resolved x-ray diffraction measurement using Rotating Imaging Plate detector[2,3] and optical absorption measurement using photo diode array detectors based on EG&G Reticon's RL0256S chips and CAMAC modules.

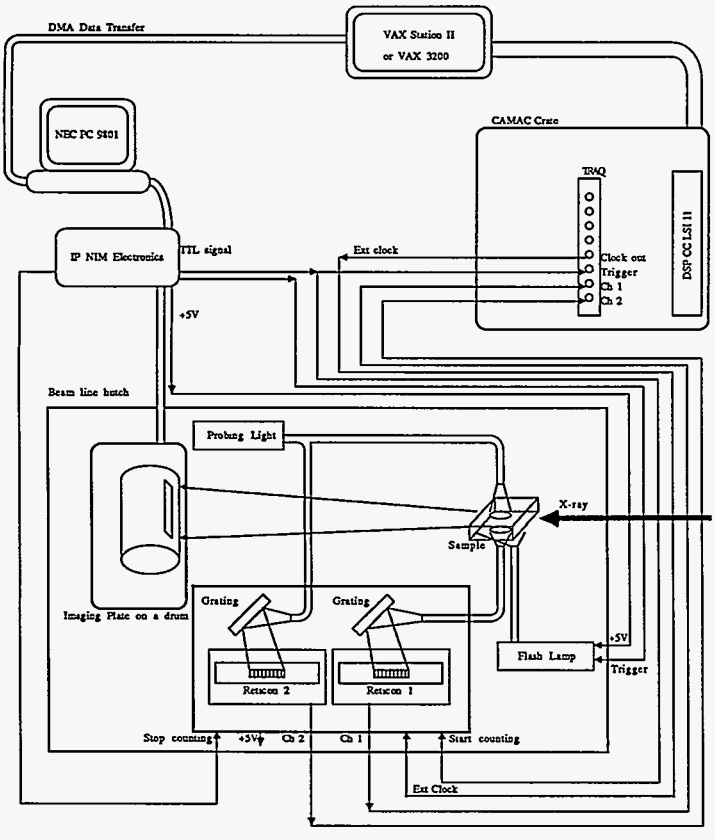

Figure 1. Schematic diagram of the simultaneous measurement of x-ray diffraction and optical absorption of purple membranes.

Experimental

The bacteriorhodopsin samples were first centrifuged for 5 to 10 hours at 50000 rpm then air-dried and in some cases rehydrated. The thickness was chosen to be thin enough for the excitation and probing the optical absorption. The typical optical density was 1 to 4. Both static and dynamic x-ray diffraction data were collected on PEP beamline 1B (December, 1988) and on SPEAR 4-2 (February,1989). A one-dimensional position-sensitive detector was used for alignment of the camera and the samples. Once a sample was aligned, the position sensitive detector was removed and the Imaging Plate detector was pulled forward close to the end of the vacuum path (Fig.1). Distance between the sample and the detector was about 20cm. X-ray energy was 10.0 keV on PEP 1B and 7.5 keV on SPEAR 4-2. During the experiment on PEP 1B, due to the difficulty of having the flash lamp and the probing light close enough to the sample, we could not measure the optical absorption and the x-ray diffraction simultaneously. Instead, we synchronized the flash lamp which illuminated the sample for 20 μsec and the Imaging Plate detector to obtain the time-resolved x-ray diffraction data. On SPEAR beamline 4-2, however, we were able to measure the optical absorption simultaneously with the x-ray exposure. A probing light and the excitation light were perpendicular to each other in order to minimize the image-lag on the photo diode array detector due to the flash lamp and both were perpendicular to the x-ray beam.

Results

Equatorial diffraction patterns were collected using both of the detectors. The signal to noise ratios of the dried samples were significantly better than the ones of hydrated membranes. Even a very thin sample, with the optical density of 1 or smaller which corresponds to about 10 μm thickness, showed a fairly good signal-to-noise ratio, which is important for the experiment because the excitation light can penetrate the sample without being totally absorbed. Thus the whole sample can be excited and the probing light can be detected by the photo-diode array spectrophotometer with a reasonable signal level. The Imaging Plate needed only a few seconds or so of total exposure time to obtain a reasonable diffraction pattern (Fig.2) where as the one-dimensional position-sensitive detector required 1 minute or longer for a pattern of comparable signal-to-noise ratio. The low horizontal angular divergence of the PEP beamline 1B source was very good and we could resolve reflections which could not be separated before. Spacial resolution of the Imaging Plate detector, 25 μm to 100 μm, is also better than that of the position-sensitive detector, about 200 μm. The exposure and the excitation was repeated 3000 to 7000 times to obtain sufficient statistics. The number of repeats were decided according to the current of the beam and the stability (especially on PEP 1B the beam drifted 1 to 3 mm rather often). The time resolution was 0.5 msec and total time was 250 msec. Although further analysis is required, the diffraction pattern did not change significantly after the excitation. More detailed data analysis is in progress.

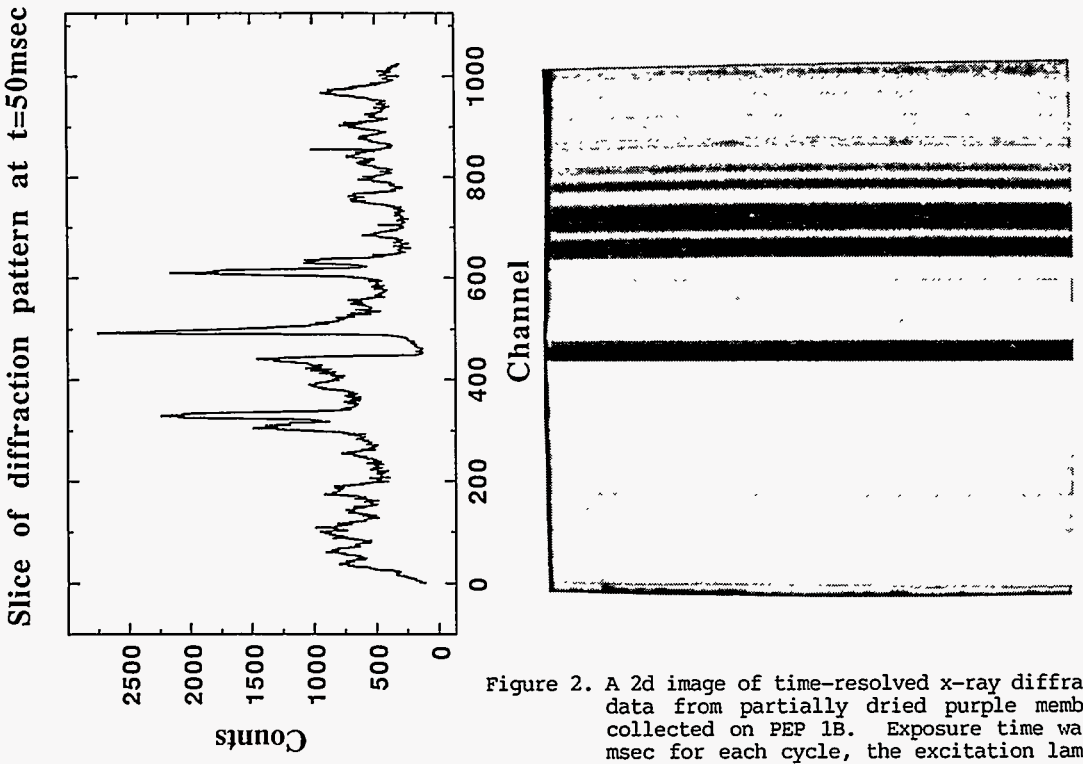

Figure 2. A 2d image of time-resolved x-ray diffraction data from partially dried purple membranes collected on PEP 1B. Exposure time was 250 msec for each cycle, the excitation lamp was flushed at 50 msec, repeated 3000 cycles. On the left is a slice of diffraction pattern at 50 msec. Total exposure time for this slice was 1.5 secs. X-ray energy was 10.0 keV.

REFERENCES

1. Frankel, R.D. and Forsyth, J.M., 1985, Biophysics J., 47:387-393.
2. Amemiya, Y., Wakabayashi, K., Tanake, H., Ueno, Y., and Miyahara, U. 1987. Science, 237:164-168.
3. Amemiya, Y., and Miyahara, U., 1989. Nature, 336:89-90.

ACKNOWLEDGMENTS This research was supported by NIH Grant RR 1209. Data were collected at SSRL which is supported by the DOE's Office of Basic Energy Science. The collaboration on the Imaging Plate detector system is supported by a grant from the U.S.-Japan Cooperative Science Program, NSF INT-87-16096.

Structural Differences of Transforming *ras* p21(Val-12) from the Normal Protein

Liang Tong, Abraham M. de Vos, Michael V. Milburn, Jarmila Jancarik, Shigeru Noguchi*, Susumu Nishimura*, Kazunobu Miura ✪, Eiko Ohtsuka ✪ and Sung-Hou Kim
Department of Chemistry and Lawrence Berkeley Laboratory, University of California, Berkeley, CA 94720 U.S.A.;
*Biology Division, National Cancer Center Research Institute, Tokyo, Japan; and
✪Faculty of Pharmaceutical Sciences, Hokkaido University, Sapporo, Japan

Introduction

One of the most commonly found transforming *ras* oncogenes in human tumors has a valine codon replacing the glycine codon at position 12 (1). To understand the structural reasons for cell transformation by this single amino acid substitution, we have determined the crystal structure of the GDP bound form of this mutant, p21(Val-12). One of the major differences between this structure and that of the normal protein (2) is that the loop that binds the ß-phosphate of the guanine nucleotide is enlarged. Such a change in the "catalytic site" conformation could explain the reduced GTPase activity of the mutant (3), which keeps the protein in the GTP bound "signal on" state for a prolonged period of time, ultimately causing cell transformation. We report here the overall structure of p21(Val-12) at 2.2Å resolution and compare it with the structure of the normal c-H-*ras* protein (2). Structural comparison of normal and transforming *ras* proteins provides a basis for understanding cell transformation at the molecular level.

The diffraction data for p21(Val-12, 1-171) was collected on an Enraf Nonius rotation camera installed on the 8-pole wiggler line at the Stanford Synchrotron Radiation Laboratory, Palo Alto, California. The x-ray wavelength used for data collection was 1.08Å, the crystal-to-film distance was 85mm, and 2° rotation was used for each exposure. One set of data was collected from one crystal, at 4°C, on a total of 32 films (16 film packs).

Results and Discussion

The overall structure of the transforming p21(Val-12) is similar to that of the normal protein (2). It contains six ß-strands, four α-helices, and nine connecting loops. Both structures appear to consist of two recognizable domains: the N-terminal domain, containing the first 75 residues (including the first three ß-strands and one α-helix), is the "phosphate binding domain" , and the C-terminal domain, containing the remaining residues (including the last three ß-strands and three α-helices), is the "guanine recognition domain". There is only a short stretch of hydrogen-bonding between the two domains. This separation of domains is also manifested by the distribution of the residue temperature factors in each domain. The residues in the N-terminal domain have higher temperature factors (an average of 42Å^2), and thus are more mobile than those in the C-terminal domain (an average of 33Å^2). This high mobility of the N-terminal domain may have a functional significance in that it is in this domain where the catalytic site of GTP hydrolysis, the putative effector region (4) and the GTPase activating protein binding region (residues 30-40) (5) are located.

The differences between the two structures are mainly localized in the loops in the N-terminal half of the molecule. The root-mean-square difference in Cα between p21(Val-12) and the normal protein is 1.26Å for residues in the N-terminal domain (residues 1-75) and 0.56Å for residues in the the C-terminal domain (residues 76-171). At the current stage of the refinement, the two regions with the largest differences are located in two loops shown in black in the figure below.

The most clear and largest structural differences were found in loop L1, corresponding to residues 9 through 18, which wraps around the ß-phosphate of the bound GDP molecule (2). The current refinement results of the normal protein as well as the transforming p21(Val-12) reveal that there are several unusual aspects about this loop. First, there appear to be no side chains, except that of Lys-16, involved in binding to the phosphate.Second, the backbone amide groups are pointing toward the ß-phosphate, making hydrogen bonds to the phosphate oxygens and thus fixing the orientation of the ß-phosphate, which is presumably important for GTPase activity. Third, there is a metal ion (probably Mg^{++} or Ca^{++}) coordinated to the oxygen atoms of the ß-phosphate.

The simplest description of the structural differences in loop L1 is that the size of this loop in p21(Val-12) is much larger than that in the normal protein, resulting in the loss of two hydrogen bonds (from the backbone NH groups of residues 12 and 13) to the ß-phosphate. We have suggested (2) that this loop would have straddled the phosphodiester bond between the ß- and γ-phosphates of GTP, and therefore is the prime candidate to be the catalytic site for GTP hydrolysis in the normal p21 protein. The loss of two hydrogen bonds may alter the orientation of the ß-phosphate either when presented to the attacking group, or as a leaving group after the γ-phosphate is attacked, thus changing the GTP hydrolysis rate. The position of the bound metal ion is such that it is a reasonable candidate for providing the attacking group (probably one of its bound water molecules) to the ß-phosphate, perhaps for the on-line displacement of the γ-phosphate, or the cation may be participating in fixing the ß-phosphate in collaboration with backbone NH groups, with an as yet unidentified water molecule attacking the ß-phosphate. An alternative mechanism, similar to that proposed for elongation factor Tu, is that the γ-phosphate (which is not present in our structure) is attacked, possibly by a water molecule. This could explain the autophosphorylation activity of the viral *ras* proteins, because in that case the hydroxyl group of Thr-59, located near the presumed γ-phosphate site, could be the attacking group.

Acknowledgement

This work was supported by grants from the National Institute of Health, the Department of Energy, the Japanese Ministry of Health and Welfare, and a gift from Merck, Sharp and Dohme to the University of California-Berkeley. Sh.N. was supported by a fellowship from the Foundation for Promotion of Cancer Research.

References

1. Barbacid, M. *Ann.Rev.Biochem.* **56,** 779-828 (1987).

2. De Vos, A.M. *et al. Science* **239,** 888-893 (1988).

3. Gibbs, J.B., Sigal, I.S., Poe, M. & Scolnick, E.M. *Proc.Nat.Acad.Sci.USA* **81,** 5704-5708 (1984).

4. Sigal, I.S., Gibbs, J.B., D'Alonzo, J.S. & Scolnick, E.M. *Proc.Nat.Acad.Sci.USA* **83,** 4725-4729 (1986).

5. Adari, M., Lowy, D.R., Willumsen, B.M., Der, C.J. & McCormick, F. *Science* **240,** 518-521 (1988).

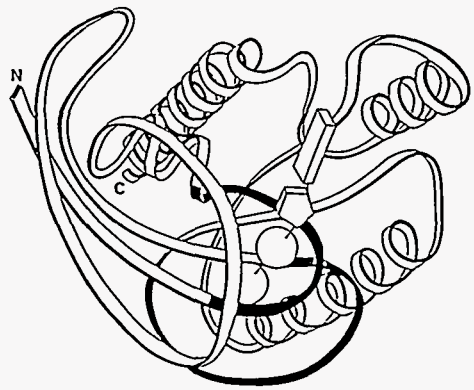

CRYSTALLOGRAPHIC STUDIES ON INTACT RIBOSOMAL PARTICLES

A. Yonath *#, K. von Bohlen #, I. Makowski**, S. Weinstein* **,

H. Hope + and H.G. Wittmann **

*Department of Structural Chemistry, Weizmann Institute, Rehovot,Israel.

#Max Planck Research Unit for Structural Molecular Biology,Hamburg,FRG

**Max Planck Institute for Molecular Genetics, Berlin (West).

Crystallographic studies, aimed at the determination of the three-dimensional structure of ribosomes (see Annual report, 1987) have been continued along the following lines:

a. Crystallization:

We were able to improve the crystals of 50S ribosomal subunits from Halobacteria marismortui as well as to obtain crystals of 30S subunits from Thermus thermophilus and a new form of 50S ribosomal subunits from Bacillus stearothermophilus and its mutant, in which one protein is missing. Furthermore, we could crystallize a complex of 50S subunits together with some components of protein biosynthesis, namely a fragment of the newly synthesized polypeptide and a tRNA molecule

b. Crystallographic studies

(i) Ribosomal subunits from Halobacterium marismortui

Crystals of 50S subunits with size of 0.6x0.6x0.1mm, diffract to a resolution of about 4.5Å, are packed densely with one particle in an asymmetric unit in cells with symmetry &C222, and dimensions: 214 x 300 x 581 &ansg. At cryo-temperature irradiated crystals, presoaked in 18% ethylene-glycol hardly show radiation damage for days in the synchrotron beam. complete data sets could be collected from single crystals. The usefulness of the crystallographic data depends strongly on the orientation of the crystals in respect to the beam. Therefore we have designed multidirectional and differently shaped spatulas for mounting crystals in a variety of orientations. Data collected from crystals mounted on perpendicular spatulas have been evaluated. Representative results are: (i) native crystals, data to 13Å resolution: 1256 measurements, 851 included from which 707 are independent, have R-scale (for intensities) of 5.53%; (ii) crystals of undecagold soaked crystals to 18Å resolution: 1512 measurements, 1078 included of which 868 are independent with R-scale (for intensities) of 3.6% and R-anomalous of 8%.

(ii) 50S subunits from B. stearothermophilus

Diffracting crystals from wild-type and mutated (lacking protein BL11) 50S subunits from these bacteria have been obtained by using a low concentration of polyethylene glycol in the presence of the cations essential for integrity of ribosomes (Mg^{++} and NH^{+}) at slightly higher concentrations than needed for storage of ribosomes from eubacteria. Preliminary crystallographic measurements show that these crystals diffract better than 11 Å, are packed with a C2 symmetry and unit cell dimensions of 294, 542 and 712 Å and an angle of 112°. They are somewhat loosely packed and contain 4 subunits in an asymmetric unit. The ribosomes from B. stearothermophilus are well characterized biochemically and we have taken advantage of this in our studies. In particular, we were able to detach selected proteins by genetic and biochemical methods. We could crystallize the depleted particles and also were able to bind to the detached proteins and incorporate the modified ones into the core particles. A detailed description of this work is given below.

(iii) The small (30S) ribosomal subunits.

Small ribosomal subunits form Thermus thermophilus and from Halobacteria marismortui have been crystallized. The crystals of the first are packed in a tetragonal space group ($P42_12$) with dimensions of 406 X 406 X 171 Å and diffract to 8.5 Å Data from native as well as from soaked ones (in solutions of: iridium and gold clusters, various compounds of multi(6-12)-wolfram, tetra-platinum salts, and TAMM (a tetra mercury compound) have been collected. Most of these data are of similar quality to those obtained from crystals of of the large ribosomal subunits from Halobacteria (e.g. R scale factor of 5-6% on intensities).

One of the cell axis of this form (171Å) is of dimensions similar to that of the 30S particle. We have reconstructed a model for the 70S ribosome as well as for the large ribosomal subunit. By subtracting the large subunit from the whole particle, we were able to approximate the shape of the small subunit. Using this model we initiated a molecular search for possible packing diagrams. This work is now in progress.

c. Preparation of Heavy-Atom Derivatives

For specific derivatization, two heavy-atom clusters, undecagold and tetra iridium, were modified chemically, so that they could be used as monofunctional reagents. (Weinstein et al., 1989). We also have developed chemical and genetic procedures for obtaining particles in which one or a few selected proteins are missing. As mentioned above, a mutant of Bacillus stearothermophilus which lacks one ribosomal protein (BL11) in the large subunits has been grown. Incorporation of this protein into the depleted core particles resulted in regaining the original activity of the wild-type particles. The mutated subunits could be crystallized under the same conditions as the particles from the wild type. Moreover, the two crystal forms obtained from the mutated subunits are isomorphous to the corresponding forms of the same particles from the wild-type bacteria. This shows that for both crystal forms, the missing protein, BL11, is not involved in the crystal forces networks. BL11 has one sulfhydryl group which is accessible on the surface of the 50S particle. Binding of N-ethylmaleamid, gold and iridium clusters to BL11, when isolated from the ribosome, was possible under denaturing conditions (6M urea). therefore, that the conformation of the isolated protein is different from its conformation when it is a part of the ribosome. Derivatized BL11 was fully reconstituted with the 50S subunits of the mutant to form modified 50S particles.

It is interesting that the products of the incorporation of derivatized or of native BL11 into the mutated 50S subunits are biologically active and could be crystallized in two or three dimensions under the same conditions as used for crystallization of the 50S particles from the wild type of Bacillus stearothermophilus.

Crystallographic experiments showed that the crystals of the modified 50S subunits with both clusters are isomorphous to the native ones. Diffraction data were collected using synchrotron radiation at 85 K. These data are currently being examined.

Resonant Photoemission from the Ni-GaAs(110) Interface

T. Kendelewicz, R. Cao, K. Miyano, I. Lindau, and W. E. Spicer
Stanford Electronics Laboratories
Stanford University, Stanford, CA 94305

We report the results of a study on the use of resonant photoemission (PES) to better understand better reactions at the transition metal semiconductor interfaces. The data were taken on Ni/GaAs(110) interfaces and compared with results from NiAs crystals fractured in vacuum.

The resonant PES close to the 3p → 3d absorption threshold was first detected experimentally by Guillot et al. for metallic Ni [1] and explained in an atomic like picture in which direct PES from $3d^n$ leaving the Ni atom in the $3d^{n-1}$ final configuration:

$$3p^6 3d^n 4s \rightarrow 3p^6 3d^{n-1} 4s + \text{elecron}$$

(for metallic Ni the ground state configuration is $3d^8 4s$) leads to the same final state as the process:

$$3p^6 3d^n 4s \rightarrow 3p^5 3d^{n+1} 4s \rightarrow 3p^6 3d^{n-1} 4s + \text{electron}$$

in which absorption is followed by photoionization (direct recombination). Because the same final state can be obtained in two distinct ways, in order to obtain probabilities, one has to square the sum of amplitudes of both individual processes. This leads to the characteristic Fano-type enhancements known as resonant PES. The observation of Fano resonances in the satellite rather than in the main line (where an interference dip is detected) has forced the reinterpretation of PES data for long studied NiO and related transition metal insulators. The role of d-hole screening by the ligand in the main line has been recognized.

As stated above, in this work, we are mostly interested in to what extent resonant PES can be useful in an interface chemistry study. For this purpose, we have chosen the Ni/GaAs interface for which a reference crystal of NiAs was available to us. As reported in our earlier core level PES study [3], NiAs is one of the phases believed to be formed as a result of interfacial reaction. The Ni/GaAs interfaces were grown *in situ* in an UHV chamber (base pressure in 10^{-11} Torr range) by incremental deposition of Ni onto freshly cleaved GaAs(110) surfaces. After each step, the interface was characterized with core level and valence band (VB) photoemission. The interface with 25 Å of Ni was stepwise annealed to 250°C and 380°C to promote the otherwise kinetically limited chemical reaction.

In this work, we studied in detail the angle integrated valence band spectra close to the Ni 3p → 3d threshold from the Ni/GaAs interfaces and NiAs crystals. The energy of the photoabsorption threshold was determined with the constant final state (CFS) spectra to occur just above 64 eV for all the studied interfaces and NiAs crystals. Fig. 1a presents a set of the VB spectra from the Ni/GaAs interfaces for a photon energy of 64 eV, i.e. just below the photoabsorption threshold.

A shift of the main line originating mostly from the Ni 3d states moving to lower binding energy with increasing Ni coverage is observed. These changes are typical for the interface of a transition metal with a nearly filled d shell [4]. At 25 Å the spectrum is very similar to that from metallic Ni which is consistent with the conclusion of limited reaction obtained on the basis of the core level data. The shift back of the maxima and the characteristic change of the lineshape with a knee close to the Fermi level upon annealing give clear cut evidence for increased reaction of extra Ni with the substrate. This behavior is characteristic of p-d hybridization as discussed by us for the related Pd interfaces [4]. At least qualitatively, the shape of this spectra is similar to that of NiAs which was shown to agree fairly well with one electron band calculations [1]. It is obvious

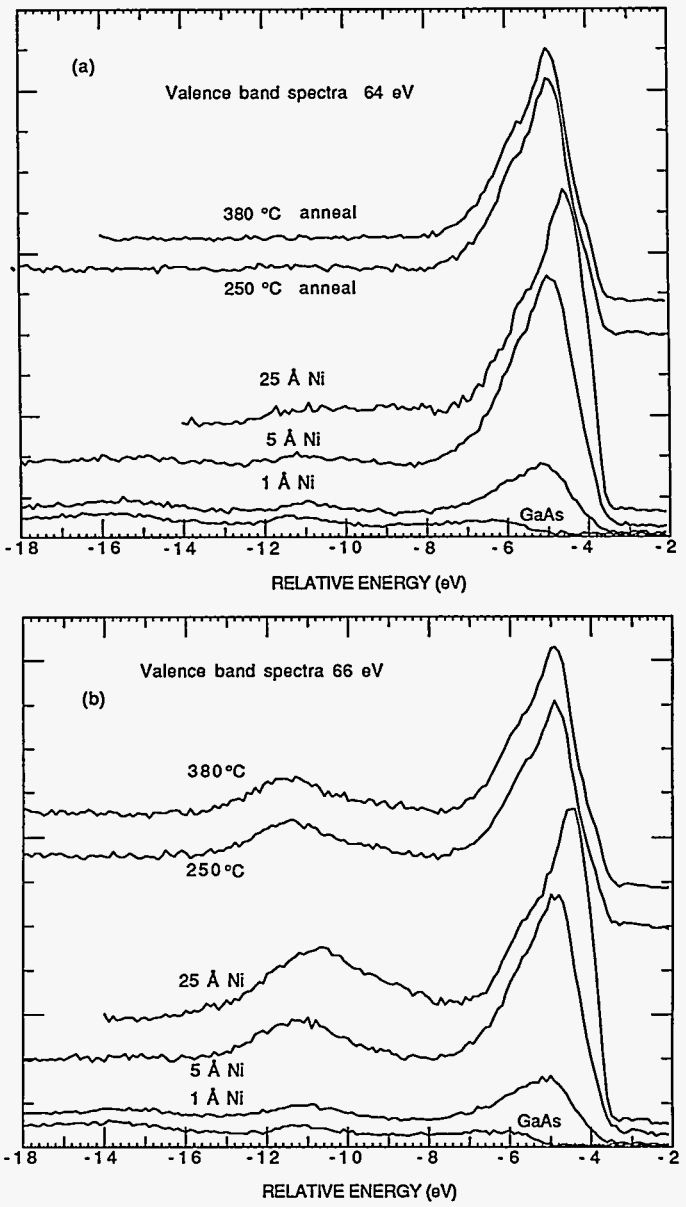

Fig 1. Valence band PES spectra from the Ni/GaAs interfaces taken a) just below (64 eV) and b) just above (66 eV) Ni 3p threshold

that band calculations fail to account for many body features such as satellites. In Fig. 1b, we present a set of the VB spectra for 66 eV, i.e. just above 3p → 3d absorption threshold. A strong new feature is clearly seen 6.5 eV below the main photoemission peak. Note that the energy of these satellites, which show strong resonant behavior, follows the position of the main line.

To get a better insight into what is going on, we took flux normalized constant initial state (CIS) spectra at several initial state energies. All features around the main peak show an interference dip, while the satellite shows a pronounced

resonance at the 3p → 3d threshold. Very similar CIS results were obtained for all other annealed and unannealed interfaces studied in this work. We find that, whenever Ni is present, the satellite resonates in a very similar way. The same conclusion is reached for the main line, where an interference dip of similar shape is always observed.

This leads us to the conclusion that resonant PES for the interfaces studied in this work is not very dependent on the details of chemistry at different stages of the interface development. From this data alone, one may conclude that either the resonant effects are atomic in nature and are not strongly affected by bonding in solid or that the type of bond of all phases formed at the interface are very much alike and little affected by resonant behavior.

ACKNOWLEDGMENT

We would like to thank Jim Allen for providing the NiAs crystal used in this study. This work was supported by the DARPA and ONR under Contract N00014-83-K-0073.

REFERENCES

1. C. Guillot, Y. Ballu, J. Paigne, J. Lecante, K. P. Jain. P. Thiry, R. Pinchaux, Y. Petroff, and L. M. Falicov, Phys. Rev. Lett. 39, 1632 (1977).

2. W. P. Ellis, R. C. Alberts, J. W. Allen, Y. Laissailly, J. S. Kang, B. B. Pate, and I. Lindau, Solid State Commun. 62, 591 (1987).

3. T. Kendelewicz, M. D. Williams, W. G. Petro, I. Lindau, and W. E. Spicer, Phys. Rev. B 32, 3758 (1985).

4. T. Kendelewicz, R. S. List, K. A. Bertness, M. D. Williams, I. Lindau, and W. E. Spicer, J. Vac. Sci. Technol. B 4, 959 (1986).

UNIQUE BAND BENDING AT THE Sb/InP(110) INTERFACE

T. Kendelewicz, R. Cao, K. Miyano, I. Lindau, and W. E. Spicer
Stanford Electronics Laboratories
Stanford University, Stanford, CA 94305

The Sb monolayers on GaAs and InP are of special interest due to their epitaxial growth in the form of zig-zag chains in which Sb atoms are bonded alternately to the Ga(In) and As(P) atoms of the unrelaxed surface [1]. The well understood morphology makes these interfaces ideal model systems for which experimental data can be checked against theory. Indeed, several interesting investigations have been performed in the past for the Sb/GaAs interface. The data base for InP is smaller. A recent electrical study of the Sb/InP(110) interfaces showed that the Sb overlayers form Ohmic contacts to n-InP(110) and large barriers for the p-type doping [2].

The experiments on the Sb/InP interface were performed on the grasshopper monochromator beam lines at SSRL. The In 4d and P 2p spectra were monitored for the cleaved InP(110) surface and after each calibrated Sb deposition. The data have been reduced with a computer-aided fitting routine using a convolution of Lorentzian and Gaussian line shapes.

The examples of the In 4d and P 2p spectra from the Sb/n-InP interface are presented in Fig. 1. The data show that the interface is completely unreactive for all studied coverages. After an initial shift to the higher kinetic energy indicating band bending typical of the overlayer on n-doped InP, an unusual shift in the opposite direction is observed. At around 1 ML (2.56 Å), the line width considerably narrows for both core levels indicating complete attenuation of the surface component and lack of any new components. The simple growth morphology allows precise evaluation of the surface core level shifts and of the band bending. Some results on the band bending remain, however, puzzling. In principle, one expects equal band bending shifts of all substrate core levels. As shown in Fig. 2, this proved not to be the case for the uniquely simple system studied. This observation perhaps questions the precision of the band bending determinations from the photoemission experiments and warrants further investigation. Despite the described technical problem in the quantitative determination of the band bending, the results in Fig. 3 show some definite trends. The initially pronouced band bending is reversed at around 0.5 ML, and the interface Fermi level moves toward the CBM. Both core levels show reversal of the shift which without doubt is dominated by band bending. At saturation, the Fermi level is placed 0.1 eV or 0.2 eV below CBM depending on the core level chosen for the analysis. This value of the band bending corroborates the conclusions of previous workers which reported Ohmic contacts for this interface with thicker Sb layers [10]. Our result indicates that the Ohmic behavior is an intrinsic property of the Sb/InP system which is established in monolayer coverage regime.

ACKNOWLEDGMENTS

This work was supported by the DARPA and ONR under contract N00014-83-K-0073.

REFERENCES

1 P. Skeath, C. Y. Su, W. A. Harrison, I. Lindau, and W. E. Spicer, Phys. Rev. B 27, 6246 (1983), and references therein; C. B. Duke, A. Patton, W. K. Ford, A. Kahn, and J. Carelli, Phys. Rev. B 26, 803 (1982); C. Mailhiot, C. B. Duke, and D. J. Chadi, J. Vac. Sci. Technol. A 3, 915 (1985); Phys. Rev. Lett. 53, 2114 (1984); Phys. Rev. B 31, 2213 (1985); F. Schäffler, R. Ludeke, A. Taleb-Ibrahimi, G. Hughes, and D. Rieger, Phys. Rev. B 36, 1328 (1987); J. Vac. Sci. Technol. B 5, 1048 (1987).

2. D. R. Zahn, A. B. McLean, R. H. Williams, N. Esser, and W. Richter, Appl. Phys. Lett. 52, 739 (1988).

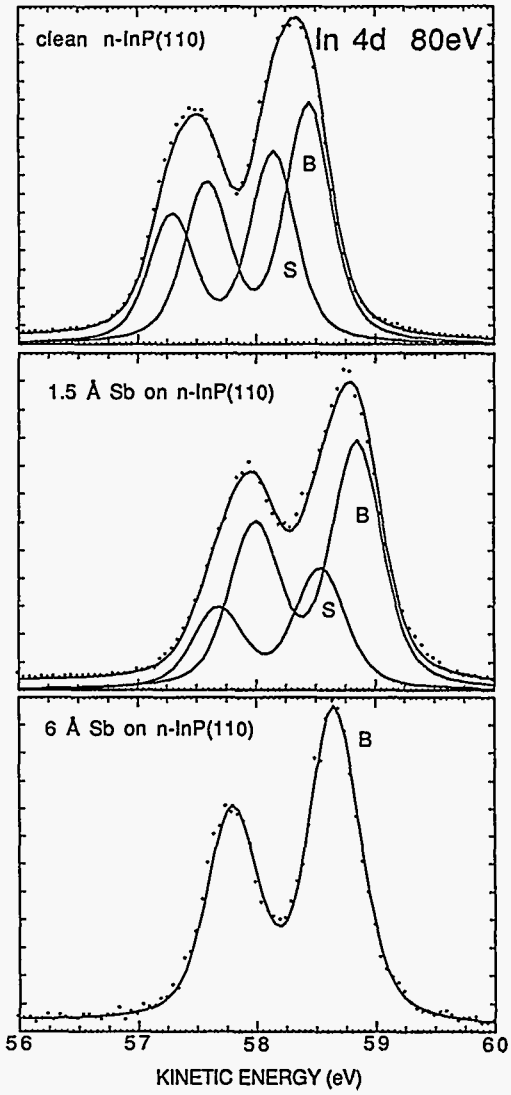

Fig 1 a. Curve fitted In 4d core level spectra for various coverages of Sb on InP(110)

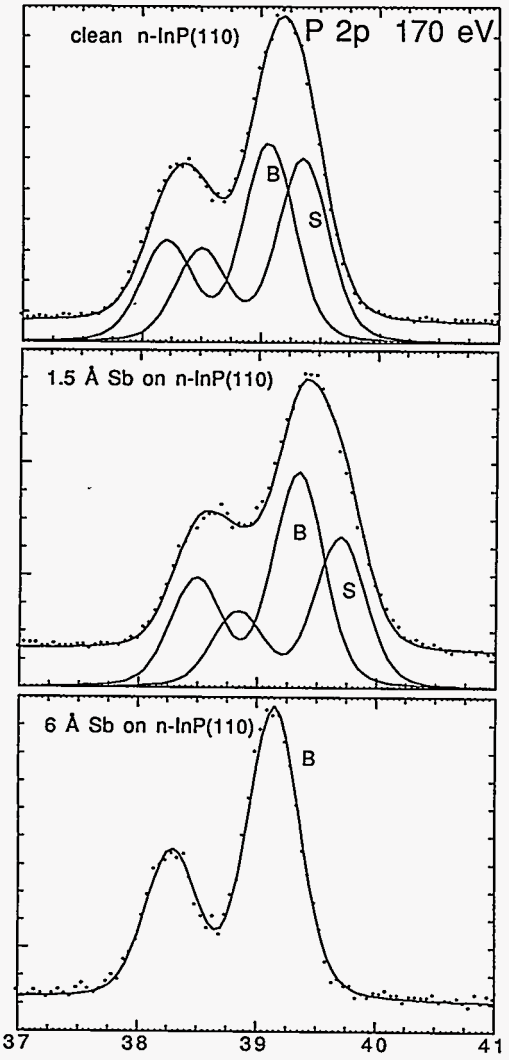

Fig 1 b. Curve fitted P 2p core level spectra for various coverages of Sb on InP(110)

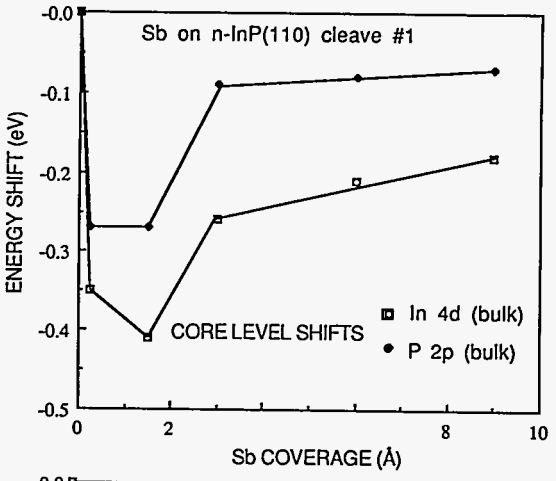

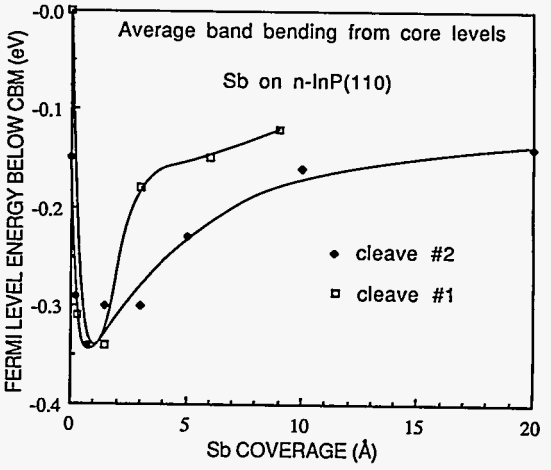

fig 2 and 3

PHOTOEMISSION STUDY OF THE ELECTRONIC STRUCTURE OF HIGH Tc SUPERCONDUCTORS

Z.-X. Shen, P. A. P. Lindberg, K. Shih, I. Lindau, and W. E. Spicer
Stanford Electronics Laboratories
StanfordUniversity, Stanford, CA 94305

I. INTRODUCTION

The discovery of the high Tc superconductors has drawn a lot of attention mainly because of the potential impact these materials may have. The unusually high critical temperature raises the question of whether the traditional theory of superconductivity is sufficient to describe the mechanism behind the superconductivity. At present, the lack of understanding of the electronic structure poses a major obstacle for the theoretical understanding of the origin of high temperature superconductivity.

As a very powerful tool for exploring the electronic structure of these materials, photoemission has been used to study the electronic structure of high-Tc superconductors. Last year, the focus of our study was on the earlier discovered superconductors $YBa_2Cu_3O_7$ and $La_{2-x}Sr_xCuO_4$ [1,2]. The results suggested that a two band Anderson model, which takes the correlation effect and the Cu-O charge transfer interaction into account at the same time, gives the most realistic description of the electronic structures of high Tc superconductors. This year our research program is focused on $La_{3-x}Ba_{3+x}Cu_6O_{14}$ and the $Y_{1-x}Pr_xBa_2Cu_3O_7$ system [4-8]. In the following sections, we discuss our most recent research efforts done at SSRL.

II. STUDIES OF REPLACEMENT OF Y BY Pr; $Y_{1-x}Pr_xBa_2Cu_3\ O_{7-\delta}$

It is found that the superconductivity in the $Y_{1-x}Pr_xBa_2Cu_3O_7$ system is quenched as Y is replaced by Pr. This result is unusual because most of the $RBa_2Cu_3O_7$ compounds, where R is a rare earth element, are superconducting with T_c near 90 K, except for the cases of Ce, Pr and Tb. (For Ce and Tb, the 1-2-3 compounds do not form.) $Y_{1-x}Pr_xBa_2Cu_3O_7$ compounds form the same orthorhombic crystal structure as $YBa_2Cu_3O_7$, but the degree of orthorhombic distortion relative to the corresponding tetragonal structure is diminished with the increasing substitution of Pr. A model for the Tc quenching could be that the valence of Pr is 4+, so that extra charge is transferred to the Cu-O planes and fills the holes that are widely believed to be the superconducting carriers. We have performed XPS, Bremsstrahlung isochromat spectroscopy (BIS) and RESPES studies near the Cu (3p-->3d), Pr (4d-->4f) and O (2s-->2p) thresholds [5, 6]. Figure 1 shows the Pr 4f spectrum of the Pr ions in the $Y_{1-x}Pr_xBa_2Cu_3O_7$ compounds in comparison with that of the Pr metal. It is clear that the Pr 4f states of the Pr ions in $Y_{1-x}Pr_xBa_2Cu_3O_7$ are changed considerably. Our data imply that Pr 4f/O2p/Cu 3d hybridization alters the electronic or the magnetic structure of the x = 0 material, which results in the quenching of the superconductivity.This result is consistent with conclusions drawn from the pressure dependence of the transport properties of these alloys.

III. STUDIES OF NiO AND OTHER "MOTT INSULATORS'

The other aspect of our work which should be mentioned is the study of the electronic structure of simpler materials which are sufficiently highly correlated to be difficult to describe by band theory. We have studied NiO using PES techniques, including those of angle resolved PES (ARPES) [7]. The prime reason for using ARPES is to look for k dependent dispersion of the photoemission peaks. Stoffel et al. and Takahashi et al. [9,10] have studied HTSC single crystal and report no significant dispersion effects, except perhaps the bands very close to the

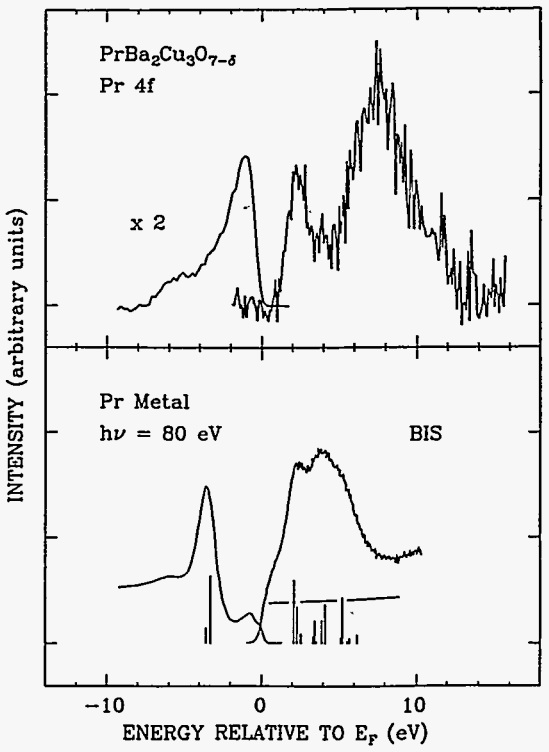

Fermi level. This is attributed to the large number of bands per unit energy and to the importance of correlation effects.

However, due to their simple electronic structure, materials like NiO, CuO, etc. provide an opportunity to examine the dispersion and other aspects of the electronic structure for materials in which correlation is important. NiO has a partially filled set of Ni 3d states and filled oxygen 2p states. Figure 2 shows dispersion (i.e., E vs k) as predicted by band theory and observed in these experiments. However, it must be emphasized that in Figure 2 the d-bands of Ni have been moved down in energy by about 2 eV from their calculated positions.

The valence states lying below the 3d states are predominantly oxygen derived. The band calculations predict strong dispersion in these states, and as Figure 2 indicates this is seen experimentally. Due to the localized nature of these strong Ni 3d states, one might expect no dispersion; however, as Figure 2 shows, a small amount of dispersion is observed, which is probably mainly derived from the Ni/O hybridization.

This exploratory study of NiO indicates that some features of band calculation correlate with experiments, whereas other features need a description which contains correlation and thus goes beyond band theory. For example, Lee et al. [11], using the so-called "slave boson" mean field theory, have found that in copper oxide superconductors the renormalized d-bands show significant shifts toward the oxygen p-bands relative to the band picture which is very similar to our experimental findings in NiO. Thus, we look upon this exploratory study of NiO as important to develop a theoretical understanding of the effects of strong correlations within the context of a periodic potential. As we outline in more

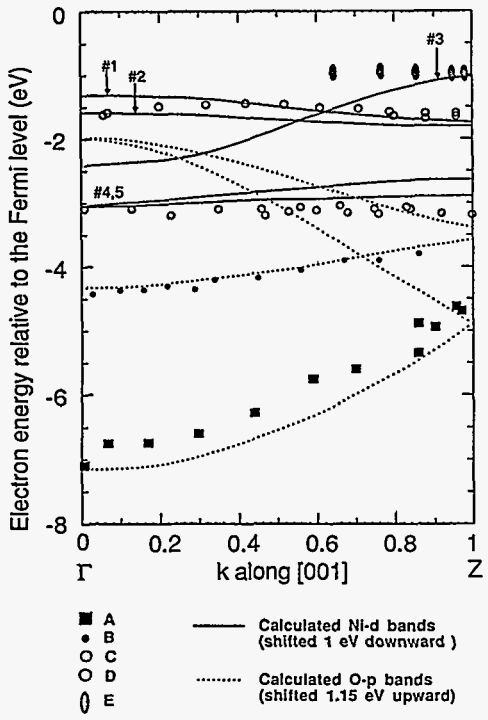

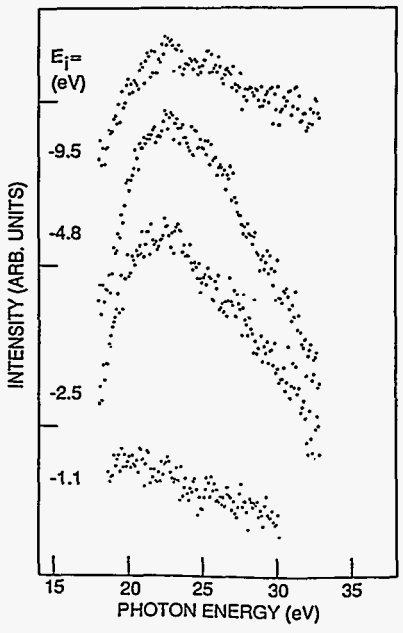

detail in the next section, we will propose here an experimental program which emphasizes strong interaction with a wide range of theorists in order to try to address these complex questions which may be critical to obtaining a better understanding of the phenomena responsible for high temperature superconductivity.

IV. THE $La_{1+x}Ba_{2-x}Cu_3O_{7+\delta}$ SYSTEM

Photoemission experiments using the 18 degree beam line at SSRL were also conducted on the $La_{1+x}Ba_{2-x}Cu_3O_{7+\delta}$ system which, similarly to the $Y_{1-x}Pr_xBa_2Cu_3O_7$ compound, exhibits superconductivity around 90 K for small values of x ($x < 0.1$) and a gradual decrease of the transition temperature as x increases [11]. The valence band features showed features strikingly similar to those previously observed on other "123" compounds of the copper-oxide superconductors, although evidence of a slightly different chemical environment of the Ba atoms was obtained by measuring Ba5p core level spectra (core level shifts). The tunability of the synchrotron radiation was used to identify the chemical origin of the valence band features. By scanning the photon energy through the O2s --> O2p absorption threshold around 20 eV, oxygen-related resonant intensity variations were observed for most of the features in the valence band (Figure 3). The stability of the in situ scraped pellets in ultrahigh vacuum as a function of time and temperature were also studied and reported [11].

REFERENCES

1. Z.-X. Shen, J. W. Allen, J.-J. Yeh, J.-S. Kang, W. Ellis, W. E. Spicer, I. Lindau, M. B. Maple, Y. D. Dalichaouch, M. S. Torikachvili, J. Z. Sun, and T. H. Geballe, "Anderson Hamiltonian Description of the Experimental Electronic Structure and Magnetic Interactions of Copper Oxide Superconductors," Phys. Rev. B, Vol. **36**, 8414 (1987).

2. Z.-X. Shen, J.-J. Yeh, I. Lindau, W. E. Spicer, J. Z. Sun, K. Char, N. Missert, A. Kapitulnik, T. H. Geballe, and M. R. Beasley, "Photoemission Study of the Surface Chemistry and the Electronic Structure of Copper Oxide Superconducting Thin Films," SPIE Symp. Proc., Vol. **948-10** (1987).

3. Z.-X. Shen, J. W. Allen, J.-J. Yeh, J.-S. Kang, W. Ellis, W. E. Spicer, I. Lindau, M. B. Maple, Y. D. Dalichaouch, M. S. Torikachvili, J. Z. Sun, and T. H. Geballe, "Photoemission Study of the Electronic Structure of Copper Oxide Superconductors," MRS Symp. Proc., Vol. **99**, 349 (1987).

4. Z.-X. Shen, P. A. P. Lindberg, W. E. Spicer, I. Lindau, and J. W. Allen, "Photoemission Study of High Temperature Superconductors," to be published in the AIP/AVS Conference Proceedings, 1988.

5. J.-S. Kang, J. W. Allen, Z.-X. Shen, W. P. Ellis, J.-J. Yeh, B.-W. Lee, M. B. Maple, W. E. Spicer, and I. Lindau, "Electronic Structure of the Quenched Superconductivity Materials $Y_{1-x}Pr_xBa_2Cu_3O_{7-d}$" Journal of Less Common Metals **24** & **25**, (1988).

6. J.-S. Kang, J.W. Allen, B.-W. Lee, M. B. Maple, Z.-X. Shen, J.-J. Yeh, W. P. Ellis, W. E. Spicer, and I. Lindau, to appear in "The Proceedings of the International Symposium on the Electronic Structure of High Tc Superconductors," Rome, October 1988, "Electronic Spectroscopy Studies of High Temperature Superconductors: $Y_{1-x}Pr_xBa_2Cu_3O_{7-\delta}$."

7. C. K Shih, Z.-X. Shen, P.A.P. Lindberg, I. Lindau, W.E. Spicer, S.Doniach, and J.W. Allen, " Dispersion of One Hole Excitation in an Antiferromagnetic Mott-Insulator: An Angle-Resolved Photoemission Study," submitted to Phys. Rev. Lett.

8. P. A. P. Lindberg, Z.-X. Shen, J. Hwang, C. K. Shih, I. Lindau, W. E. Spicer, D. B. Mitzi, and A. Kapitulnik, "Electronic Structure of the $La_{1+x}Ba_{2-x}Cu_3O_{7+d}$ System Studied by Photoelectron Spectroscopy," to be published in Solid State Commun.

9. N. G. Stoffel, P. A. Morris, W. A. Bonner, D. Lagraffe, Ming Tang, Y. Chang, G. Margaritondo, and M. Onellion, Phys. Rev. B **37**, 7952.

10. T.Takahashi et al., Nature, Vol. **334**, 691 (1988).

11. P.A.P. Lee, preprint.

Reaction and Barrier Formation at Metal/GaP (110) Interfaces

K. Miyano, R. Cao, T. Kendelewicz, I. Lindau, and W. E. Spicer
Stanford Electronics Laboratories
Stanford University, Stanford, CA 94305

The room temperature growth of the interfaces between UHV-cleaved GaP (110) and overlayers of Ga, In, Al, Ag, Au, Ni, and Pd has been studied using soft x-ray photoemission spectroscopy. Of the column III overlayers, Ga and In display strong clustering and little reactivity with the substrate, but the interface with Al shows a cation replacement reaction similar to that seen at Al / GaAs (110). Of the noble metals, Ag shows little reactivity with GaP, whereas the formation of a Au-Ga alloy is observed at Au coverages of one monolayer and above. The transition metals Ni and Pd react with the substrate to form phosphides in which Ga is segregated.

Despite these differences in reactivity between the various interfaces with GaP, the surface Fermi level position is seen to stabilize at high coverage near 0.8 eV above VBM with little dependence on the type of overlayer (see figure). Hence, the barrier height shows a much weaker dependence on the overlayer work function than reported previously.[1] The one exception is In, but this overlayer needs to be taken to higher coverage. It has been reported previously that In exhibits unusually slow kinetically-limited band bending on n-GaAs (110).[2] As with GaAs, the GaP Fermi level stabilization position is in the range of both the defect levels as created by irradiation and the theoretical charge neutrality level toward which Metal Induced Gap States should move the surface Fermi level. The influence of overlayer morphology and metallicity, as well as reactivity on the barrier development in relation to these two potential sources of interface states, will be discussed in an upcoming paper.

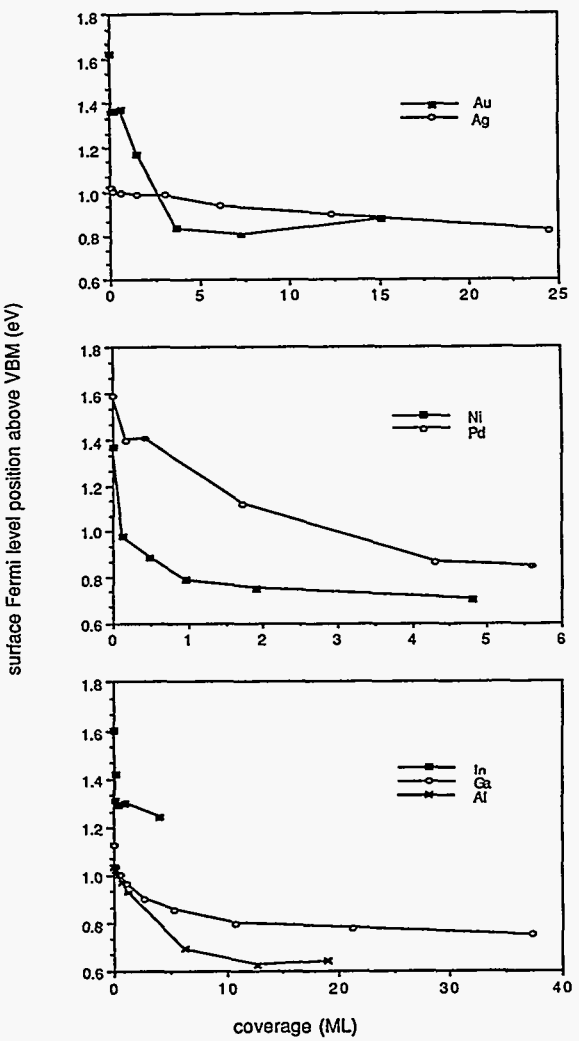

REFERENCES

1. P. Chiaradia, L. J. Brillson, M. Slade, R. E. Viturro, D. Kilday, N. Tache, M. Kelly, and G. Margaritondo, J. Vac. Sci. Technol. B **5**, 1075 (1987).

2. R. R. Daniels, T.-X. Zhao, and G. Margaritondo, J. Vac. Sci. Technol. A **2**, 831 (1984).

Ag Clustering on GaAs(110) Surface

T. T. Chiang, C. J. Spindt, A. K. Wahi, G. P. Carey, I. Lindau, and W. E. Spicer
Stanford Electronics Laboratories
Stanford University, Stanford, CA 94305

Previously, we have seen that high temperature anneal (around 500°C) of the Ag/GaAs(110) interface unpins the surface Fermi level and causes the Ag to form clusters [1]. However, the Ag clustering results in the Ag covering a much smaller fraction of the GaAs surface. Hence, we expect a dramatically reduced Ag4d photoemission signal, which is observable only if we tune the photon energy for maximum Ag4d photoionization cross section. This is achieved by using 70 eV photons from the Grasshopper monochromator of beam line 1-1. The 70 eV photons allowed one to clearly see a small remnant Ag4d signal after the 500°C anneal.

This result was also confirmed by scanning electron microscopy (SEM) and scanning Auger microscopy (SAM). SEM results showed that high temperature anneals of the Ag/GaAs interface formed hemispherical-like islands with a size distribution up to ~500 Å in diameter. The average island separation is about a few thousand angstroms (~2000 Å). SAM demonstrated that these islands are largely Ag.

In summary, our experimental findings confirm that high temperature anneal induces Ag clustering on GaAs. However, the kinetics of this clustering is not well known, so work is underway to investigate the temperature dependence of this Ag clustering. Furthermore, there is also the question of the relationship of the Ag clustering to the Fermi level unpinning. This issue is also under further investigation.

ACKNOWLEDGEMENT

This work was supported by the U.S. Defense Advanced Research Projects Agency (DARPA) and the U.S. Office of Naval Research (ONR) under Contract No. N00014-83-K-0073. The SEM (scanning electron microscopy) and SAM (scanning Auger microscopy) experiments were performed at the Center for Integrated Systems (Stanford University) by Dr. R. Browning.

REFERENCES

1. T. T. Chiang, C. J. Spindt, W. E. Spicer, I. Lindau, and R. Browning, "Reversibility of Fermi Level Pinning," J. Vac. Sci. Technol. **B6**, 1409 (1988), Proceedings of the 15th Conference on the Physics and Chemistry of Semiconductor Interfaces, Asilomar, CA 1988.

Photoemission Study of the Ga/InP(110) Interfaces

R. Cao, K. Miyano, T. Kendelewicz, I. Lindau, and W. E. Spicer
Stanford Electronics Laboratories
Stanford University, Stanford, CA 94305

INTRODUCTION

Study of column III metals on III-V semiconductors is of particular interest in understanding the interfacial properties at the metal/III-V semiconductor interfaces. Ga/InP is an important member of this family. This interface has been studied before[1]. However, some important issues still remain unanswered. For instance, it is generally agreed that the dominant growth mode of Ga on the InP(110) surface is Ga metallic island formation at high coverages; whereas the growth at low coverages is not clear. Moreover, a replacement reaction has been suggested to take place at the Ga/InP interface, but the mechanism is unknown. We notice that all the studies of this interface were conducted using photoemission (PES) with photon energy around 80 eV (synchrotron radiation) or 40.8 eV (He discharge lamp). Overlap of Ga 3d and InP core level spectra at these photon energies prevents one from getting detailed information about this interface, in particular in a low metal coverage range. Here, we performed a PES study of this interface taking the advantage of tunability of synchrotron radiation. The photon energy was tuned to 150 eV, at which In 4d Cooper minimum occurs. As a result, the relative intensity of Ga 3d to that of In 4d is largely enhanced, which is crucial in this study. The experiment was performed at the Stanford Synchrotron Radiation Laboratory (SSRL) at Beam Line I-1 with a grasshopper monochrometer. The Ga/InP interfaces were prepared by cleaving a InP single crystal in (110) orientation followed by Ga deposition.

RESULTS AND DISCUSSIONS

Figure 1 shows the Ga 3d and In 4d core level spectra of the Ga/n-InP(110) interface taken at the In 4d Cooper minimum ($h\nu$ = 150 eV). In the low Ga coverage regime, In 4d undergoes a shift towards low kinetic energy direction, representing a substrate band bending induced by Ga deposition. Meanwhile, another peak appears on the low kinetic energy side. This feature (marked by small bars) is the Ga 3d from the chemisorbed Ga on the InP(110) surface. With increasing Ga coverage, one peak emerges around 127.3 eV kinetic energy. This peak has been identified as Ga 3d of bulk Ga. This establishes that the growth of Ga on the InP(110) surface has two modes: chemisorption at low coverage and metallic island formation at high coverages[2].

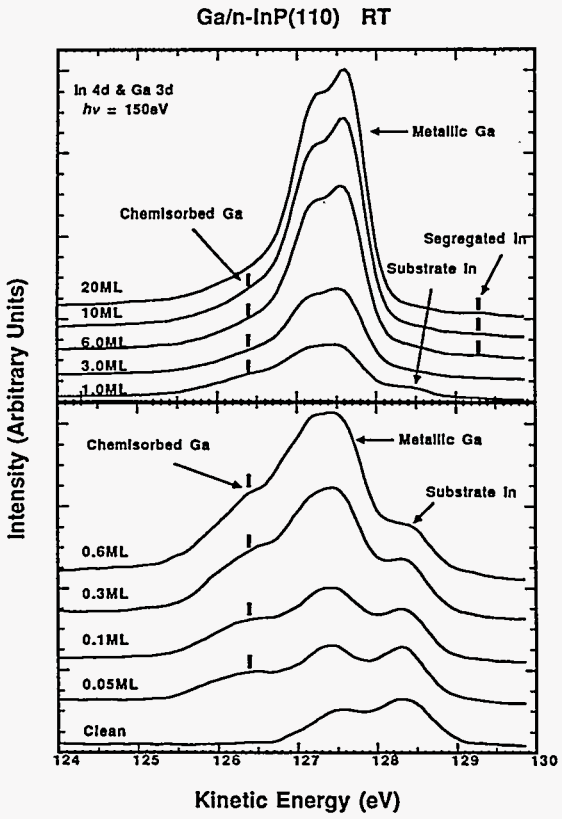

Figure 1. In 4d and Ga 3d core levels taken at the In 4d Cooper minimum ($h\nu$ = 150 eV) as a function of Ga coverages. Different features are marked. The spectra at low Ga coverages are magnified and shown in the bottom panel, and those at high Ga coverages are shown in the top panel.

Also, in this figure, a segregated In component is observed. This can be used as a fingerprint that a replacement reaction is taking place at the interface. The reaction starts being seen at the coverage where metallic Ga island formation becomes dominant. This is more pronounced in the PES spectra taken at 80 eV. (The spectra are not shown here for sake of brevity.) The product of this reaction is most likely GaP. However, the reacted P component has never been observed either in this work or previous studies. This indicates that the reaction occurs underneath the metallic islands. Since the probing depth of the surface sensitive PES is extremely short (~5Å), it is not surprising that the reacted P is not seen when it remains underneath the islands.

The heat of formation of GaP is close to that of InP. This immediately urges one to find a mechanism to initiate such reaction. In the previous studies (mainly concentrated on Al/GaAs), exothermic cluster formation was suggested to release large amounts of energy and provides a driving force for the replacement reaction[3]. However, in our case, applicability of this model is questionable. The crucial difference is the growth mode of the deposited metal on the semiconductor surfaces. In the case of Al/GaAs, a clear transition from chemisorbed Al to small cluster formation was reported [4]; whereas, in our case, such a transition is missing[2]. There may be only gradual formation of clusters. It has been proven that not enough energy would be released during this process. On the other hand, the reaction is closely correlated with metallic island formation. The metal screening will weaken the substrate bonds and enhance the interface reaction. This model has been successfully used in the metal/Si[5] interface and appears to be applicable in our case too.

ACKNOWLEDGEMENT

This work is supported by DARPA and ONR under contract No. N00014-83-K-0073 and by ONR under contract No. N00014-86-K-0736. The experiment was performed at the SSRL which is supported by the Department of Energy under contract No. DE-AC03-82ER-13000, Office of Basic Energy Sciences, Division of Chemical/Material Sciences.

REFERENCES

1. T. Kendelewicz, M. D. Williams, W. G. Petro, I. Lindau, and W. E. Spicer, Phys. Rev. B **31**, 6503 (1985).

2. R. Cao, K. Miyano, T. Kendelewicz, I. Lindau, and W. E. Spicer, Mat. Res. Soc. Symp. Proceed. (to be published).

3. A. Zunger, Phys. Rev. B **24**, 4372 (1981).

4. R. R. Daniels, A. D. Katnani, T. -X. Zhao, G. Margaritondo, and A. Zunger, Phys. Rev. Lett. **49**, 895 (1982).

5. A. Hiraki, Surf. Sci. Rep. **3**, 357 (1984).

E. Puppin, I. Lindau
Stanford Electronics Laboratories, Stanford University
Stanford CA 94305

M. Sancrotti, I. Abbati, L. Braicovich
Istituto di Fisica, Politecnico di Milano, P.za Leonardo da Vinci 32,
20133 Milano ITALY

R. Eggenhoffner
Dipartimento di fisica, Universita' di Genova, Via Dodecaneso
16100 Genova ITALY

A. Iandelli, G. L. Olcese, A. Palenzona
Istituto di Chimica Fisica, Universita' di Genova, Corso Europa,
16132 Genova ITALY

The effect produced on valence by introducing different atomic species in a CeRh matrix has been investigated. In particular we focused our interest on the value of Ce valence studied via X-rays absorption spectroscopy. The polycristalline samples, prepared by arc melting, were scraped in situ with a diamond file in a vacuum system whose base pressure was in the 10^{-10} Torr range. Ce L_{III} edges were measured on beam line II-3 equipped with a Si(220) crystal. The spectra were collected by measuring the total photocurrent with an electron multiplier (total yield mode). Three compounds were studied: CeRh, $Ce_{0.8}Y_{0.2}$ Rh and $CeRh_{0.8}Ag_{0.2}$. Reference spectra from metallic Ce were also collected.

The L_{III} edges we measured are shown in figure. The effect of introducing Y impurities in the CeRh matrix has a minor effect compared to the case of Ag substitution, as clearly shown in the figure. Due to the relevance of final state effect induced by high energy spectroscopies in Ce and its compounds [1], it is not possible to extract in a simple way any physical information from the spectra shown in figure. Work is in progress to analyze the data in terms of the Gunnarsson and Schonammer model [2]. Magnetic susceptibility data will be also collected in order to extend the set of experimental informations on these compounds.

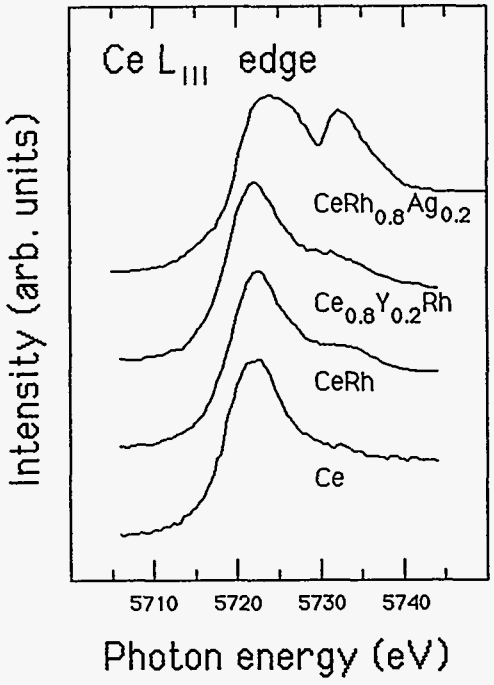

References

1) "Handbook on the Physics and Chemistry of Rare Earths", Vol. 10, editors K. A. Gschneider Jr., L. Eyring and S. Hufner (North-Holland, Amsterdam, 1988).

2) O. Gunnarsson and K. Schonammer, Phys. Rev. B 28, 4315 (1983).

Observation of Correlation Effects in Zero Kinetic Energy Electron Spectra Near the N1s and C1s Thresholds in N_2, CO, C_6H_6, and C_2H_4 *

L.J. Medhurst, T.A. Ferrett,[1] P.A. Heimann, D.W. Lindle,[2] S.H. Liu,[3] and D.A. Shirley

Materials and Chemical Sciences Division
Lawrence Berkeley Laboratory
and
Department of Chemistry
University of California
Berkeley, California 94720

Zero kinetic energy (ZKE) spectra of N_2, CO, C_2H_4, and C_6H_6 were taken across the N1s (N_2) and C1s ionization thresholds. Discrete resonances at sub-threshold photon energies were observed and were found to become more intense as threshold is approached relative to the same peaks in absorption spectra. For N_2 the satellite/main line branching ratios at threshold are: 11(1)% for the 419.7(1) eV binding energy satellite, and 2.3(1.0)% for the 426.5(1) eV binding energy satellite. For CO, the branching ratio for the 304.6(1) eV binding energy satellite is 15(2)% at its threshold (see Fig. 1). Branching ratios at threshold are also determined for the satellites of C_6H_6 and C_2H_4. Decay characteristics and assignments of the continuum features of C_6H_6 and C_2H_4 are also discussed.

*This work was supported by the Director, Office of Energy Research, Office of Basic Energy Sciences, Chemical Sciences Division of the U.S. Department of Energy under Contract No. DE-AC03-76SF00098. It was performed at the Stanford Synchrotron Radiation Laboratory, which is supported by the Department of Energy's Office of Basic Energy Sciences.

---

[1]Present address: Department of Chemistry, Swarthmore College, Swarthmore, PA 19081.

[2]Present address: National Bureau of Standards, Gaithersburg, MD 20899.

[3]Permanent address: Institute of Chemistry, Academia Sinica, People's Republic of China.

Reference

1. U. Gelius, J. Electron Spectros. Relat. Phenom. 5, 985 (1974).

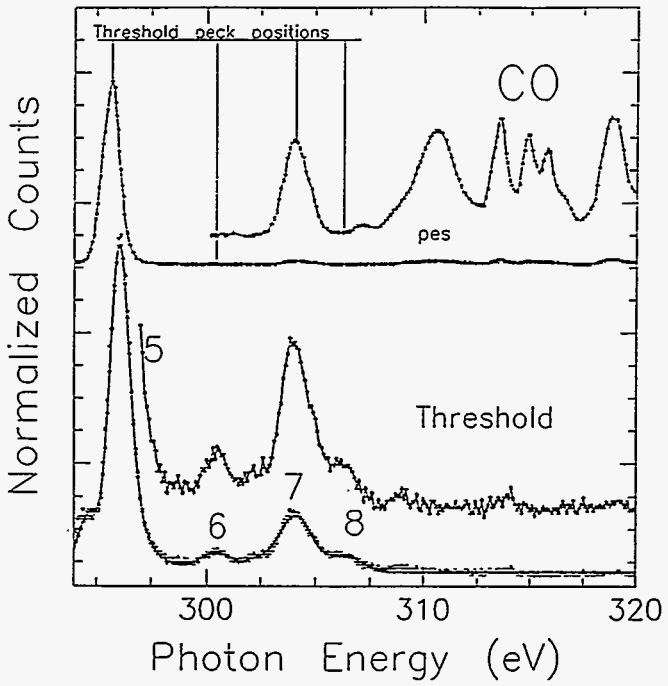

Figure 1. ZKE scan of CO above the C1s threshold. The solid line is a least-squares fit to the spectrum. Included for comparison is the PES spectrum of Gelius et al.[1]

Surface Bonding Geometry of (2x1)S/Ge(001) by Normal Emission Angle-Resolved Photoemission Extended Fine Structure*

K.T. Leung,[1] L.J. Terminello,[2] Z. Hussain,[3] X.S. Zhang,[4] T. Hayashi,[5] and D.A. Shirley

Materials and Chemical Sciences Division
Lawrence Berkeley Laboratory
and
Department of Chemistry
University of California
Berkeley, California 94720

The surface structure of (2x1)S/Ge(001) was determined using Angle-Resolved Photoemission Extended Fine Structure (ARPEFS) in the normal emission direction. By comparing the experimental data with curved-wave, multiple-scattering calculations, quantitative information about the local adsorption geometry was obtained. In particular, adsorption in a two-fold bridge site, with a S-Ge bond length of 2.36 ± 0.05 Å, was found. The two-fold S bridge appears most likely to occur between two partially intact symmetric Ge-Ge dimers, with the Ge dimer laterally displaced by 0.10 ± 0.05 Å from the bulk position. This result therefore provides evidence for S bonding to strong dangling bonds in the original dimers of the clean Ge(001) surface (Fig.1). There is, however, no evidence of significant surface contraction or expansion in the substrate layers, in contrast to the (2x2)S/Ge(111) case.

*This work was supported by the Director, Office of Energy Research, Office of Basic Energy Sciences, Chemical Sciences Division of the U.S. Department of Energy under Contract No. DE-AC03-76SF00098. It was performed at the Stanford Synchrotron Radiation Laboratory, which is supported by the Department of Energy's Office of Basic Energy Sciences.

---

[1]Present address: Department of Chemistry, University of Waterloo, Waterloo, Ontario N2L 3G1, Canada.
[2]Present address: IBM, T.J. Watson Research Center, Yorktown Heights, NY 10598.
[3]Permanent address: Department of Physics, University of Petroleum & Minerals, Dhahran, Saudi Arabia.
[4]Permanent address: Department of Physics, Zhejiang University, Hangzhou, People's Republic of China.
[5]Permanent address: Material Evaluation Section, NTT Electrical Communications Laboratories, Tokyo 180, Japan.

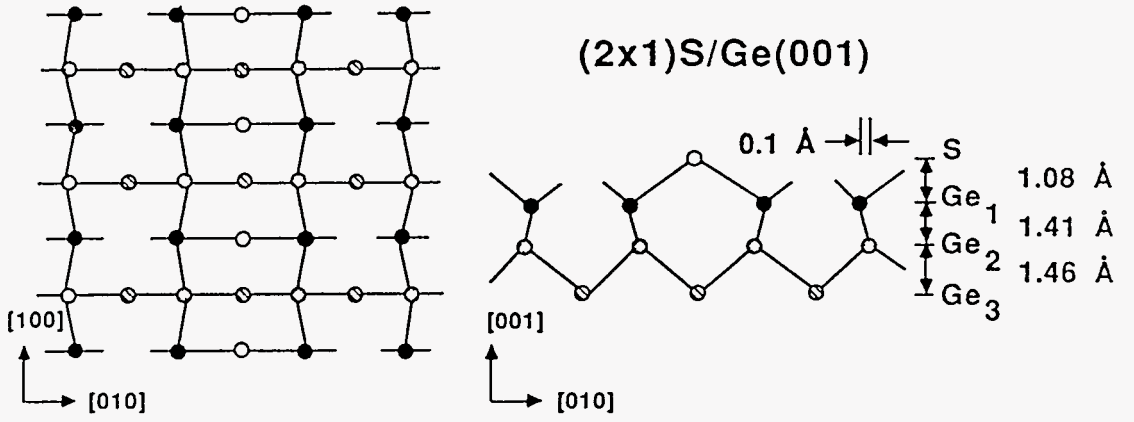

Figure 1. The surface bonding geometry of (2x1)S/Ge(001) determined by ARPEFS. Note that the result does not give information about the planarity of the Ge layers. Therefore only interlayer distances and the lateral displacement from the bulk position are indicated and are rounded off to the nearest 0.01 Å.

Angle-Resolved Photoemission From the Ar 2p Subshell *

D.W. Lindle,[1] L.J. Medhurst, T.A. Ferrett,[2] P.A. Heimann, M.N. Piancastelli,[3] S.H. Liu,[4]
D.A. Shirley, T.A. Carlson,[5] P.C. Deshmukh,[6] G. Nasreen,[7] and S.T. Manson[7]

Materials and Chemical Sciences Division
Lawrence Berkeley Laboratory
and
Department of Chemistry
University of California
Berkeley, California 94720

The angular distribution for Ar 2p photoionization has been measured from just above threshold to 400 eV photon energy, and calculated in the same energy range using the relativistic random-phase approximation (see Fig. 1). The present experimental and theoretical results are in good agreement, but disagree somewhat with earlier Hartree-Fock (HF) calculations. The HF values are found to be significantly higher in the near-threshold region. Possible reasons for this discrepancy are discussed with relevance to the general understanding of inner-shell photoionization phenomena.

*This work was supported by the Director, Office of Energy Research, Office of Basic Energy Sciences, Chemical Sciences Division of the U.S. Department of Energy under Contract No. DE-AC03-76SF00098. It was performed at the Stanford Synchrotron Radiation Laboratory, which is supported by the Department of Energy's Office of Basic Energy Sciences.

[1]Present address: National Bureau of Standards, Gaithersburg, MD 20899.
[2]Present address: Department of Chemistry, Swarthmore College, Swarthmore, PA 19081.
[3]Permanent address: Department of Chemistry, Second University of Rome, 00100 Rome, Italy.
[4]Permanent address: Institute of Chemistry, Academia Sinica, People's Republic of China.
[5]Permanent address: Chemistry Division, Oak Ridge National Laboratory, Oak Ridge, TN 37831-6201.
[6]Permanent address: Department of Physics, Indian Institute of Technology, Madras 600036, India.
[7]Permanent address: Department of Physics and Astronomy, Georgia State University, Atlanta, GA 20202.

Reference

1. D.J. Kennedy and S.T. Manson, Phys. Rev. A 5, 227 (1972).

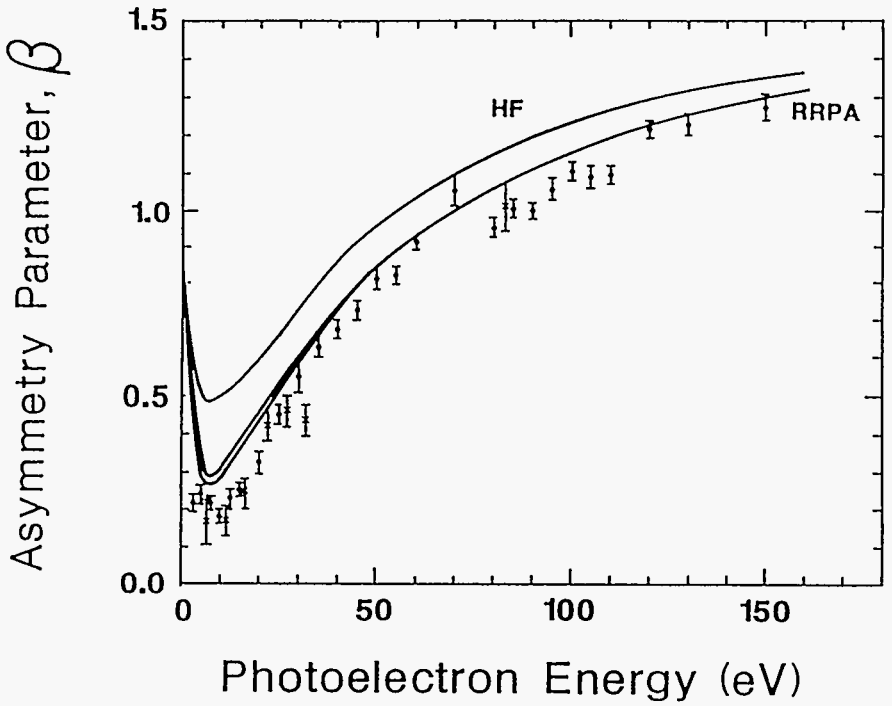

Figure 1. Angular-distribution asymmetry parameter for Ar 2p photoionization as a function of energy above the $2p_{3/2}$ ionization threshold at 248.4 eV. All of the β_{2p} results are unresolved with respect to the 2p spin-orbit components. Experimental results are from the Berkeley group (solid circles) and the ORNL group (X). Theoretical curves represent the present relativistic random-phase approximation (RRPA) 5- and 14-channel calculations (upper and lower, respectively) and Hartree-Fock (HF) calculations from Ref. 1.

Resonant Processes Above the Carbon 1s Ionization Threshold in Benzene and Ethylene *

M.N. Piancastelli,[1] T.A. Ferrett,[2] D.W. Lindle,[3] L.J. Medhurst, P.A. Heimann, S.H. Liu,[4] and D.A. Shirley

Materials and Chemical Sciences Division
Lawrence Berkeley Laboratory
and
Department of Chemistry
University of California
Berkeley, California 94720

Resonant photoemission has been studied above the carbon 1s ionization thresholds in gas-phase benzene and ethylene. The experimental data for both molecules include relative partial cross-section and asymmetry-parameter measurements for the C 1s main line and asymmetry-parameter measurements for one C1s shake-up statellite in each system (see Fig. 1). Resonances above the C K edge have been analyzed on the basis of their decay to either the C 1s main-line or valence-hole states, and have been tentatively assigned as either shape resonances or doubly excited states according to their observed one-electron or many-electron decay, respectively. The importance of determining the resonant behavior of all available photoemission channels in the proximity of a resonance is thus illustrated.

*This work was supported by the Director, Office of Energy Research, Office of Basic Energy Sciences, Chemical Sciences Division of the U.S. Department of Energy under Contract No. DE-AC03-76SF00098. It was performed at the Stanford Synchrotron Radiation Laboratory, which is supported by the Department of Energy's Office of Basic Energy Sciences.

[1]Permanent address: Department of Chemistry, Second University of Rome, 00100 Rome, Italy.
[2]Present address: Department of Chemistry, Swarthmore College, Swarthmore, PA 19081.
[3]Present address: National Bureau of Standards, Gaithersburg, MD 20899.
[4]Permanent address: Institute of Chemistry, Academia Sinica, People's Republic of China.

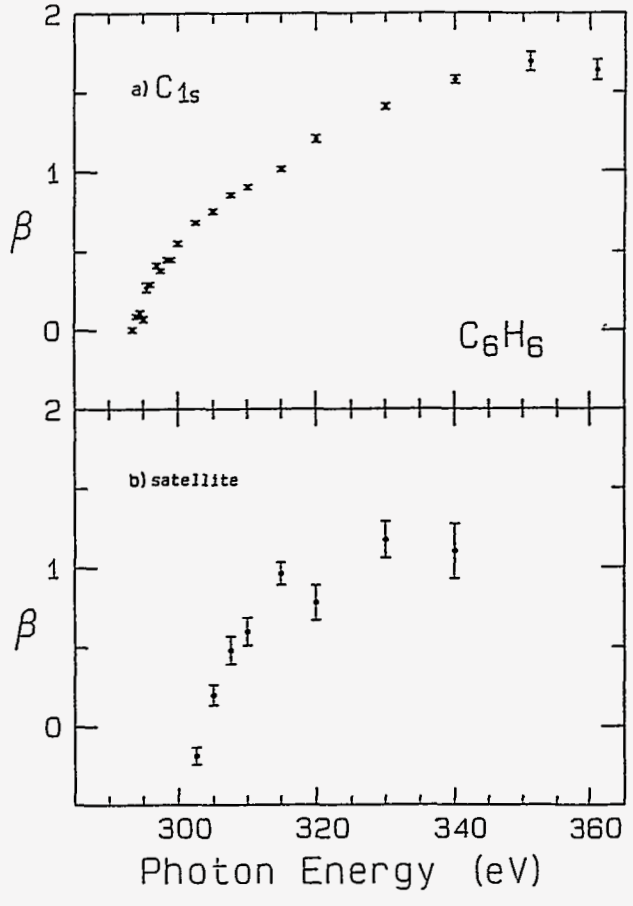

Figure 1. Angular-distribution parameter for the C 1s main line and the 297 eV satellite in benzene (XBL 885-1788).

Surface Geometry of (1x1)PH_x/Ge(111) Determined with Angle-Resolved Photoemission Extended Fine Structure *

L.J. Terminello,[1] K.T. Leung,[2] Z. Hussain,[3] T. Hayashi,[4] X.S. Zhang,[5] and D.A. Shirley

Materials and Chemical Sciences Division
Lawrence Berkeley Laboratory
and
Department of Chemistry
University of California
Berkeley, California 94720

Angle-resolved photoemission extended fine structure (ARPEFS) obtained from the phosphorous 1s core level was studied to determine the chemisorption geometry of (1x1)PH_x/Ge(111), prepared by partial dissociation of PH_3 adsorbed on Ge(111). The most likely composition of the adsorbate dissociation product is PH_2. We determined that the phosphorous adsorbs 2.26 Å above a first layer germanium atom, and preferentially tilts toward the second layer germanium atom with a 0.63 Å lateral displacement from a true atop position. Other geometrical parameters determined from the multiple-scattering, spherical-wave analysis (Fig 1) of the ARPEFS include the first to second layer germanium Ge(1)-Ge(2) spacing (0.68 Å) and the second to third layer germanium Ge(2)-Ge(3) spacing (2.68 Å). This represents a 17% contraction for Ge(1)-Ge(2) and a 9% expansion for Ge(2)-Ge(3) (Fig. 2). The importance of adsorbate scattering and how it affects data interpretation is also discussed. Comparison of this chemisorption system with other systems is made.

*This work was supported by the Director, Office of Energy Research, Office of Basic Energy Sciences, Chemical Sciences Division of the U.S. Department of Energy under Contract No. DE-AC03-76SF00098. It was performed at the Stanford Synchrotron Radiation Laboratory, which is supported by the Department of Energy's Office of Basic Energy Sciences.

[1]Present address: IBM, T.J. Watson Research Center, Yorktown Heights, NY 10598.
[2]Present address: Department of Chemistry, University of Waterloo, Waterloo, Ontario N2L 3G1, Canada.
[3]Permanent address: Department of Physics, University of Petroleum & Minerals, Dhahran, Saudi Arabia.
[4]Permanent address: Material Evaluation Section, NTT Electrical Communications Laboratories, Tokyo 180, Japan.
[5]Permanent address: Department of Physics, Zhejiang University, Hangzhou, People's Republic of China.

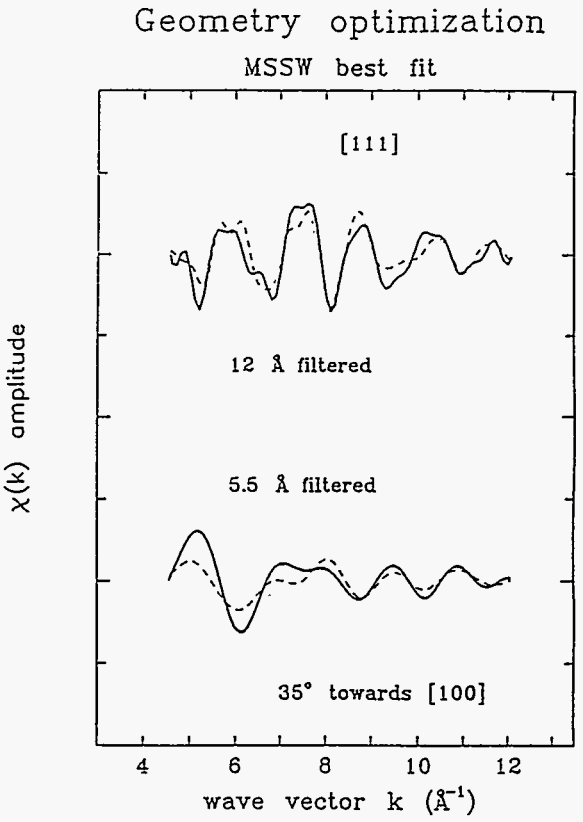

Figure 1. Fourier-filtered experimental data (solid lines) are shown with the best-fit MSSW calculation (dashed lines).

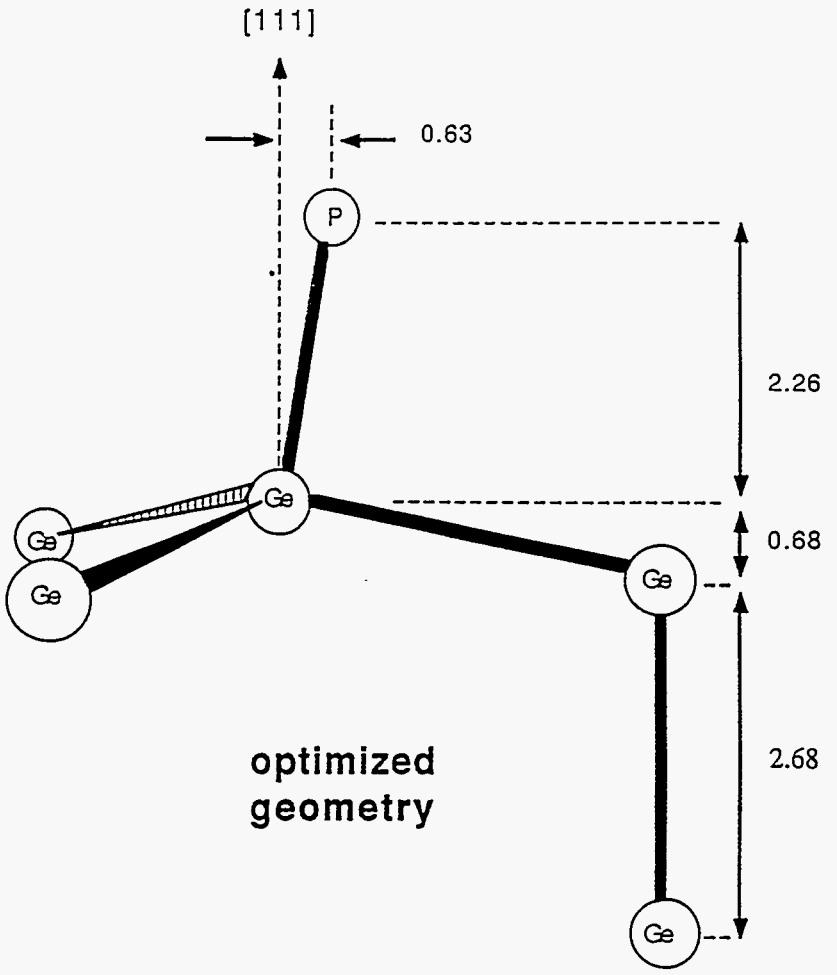

Figure 2. This figure illustrates the local adsorption geometry including the reconstructed Ge(111) surface and the tilted atop site (not drawn to scale).

Adsorption and Surface Reactions of H_2S and SO_2 on Cu(100) Studied by Electron Energy Loss Spectroscopy*

K.T. Leung,[1] X.S. Zhang,[2] and D.A. Shirley

Materials and Chemical Sciences Division
Lawrence Berkeley Laboratory
and
Department of Chemistry
University of California
Berkeley, California 94720

The adsorption of H_2S and SO_2 on Cu(100) were investigated using electron energy loss spectroscopy as a function of coverage, temperature and scattering angles. In particular, irreversible dissociation of H_2S and the formation of sulfhydryl (SH) species at low and intermediate coverage on Cu(100) were observed at low temperature. This was followed by molecular physiadsorption at higher coverage. In the case of SO_2 on Cu(100), decomposition of SO_2 and the formation of SO_3 surface species at room temperature were observed (Fig. 1). A surface reaction involving pre-adsorbed SO_2 on Cu(100) with H_2S is discussed.

*This work was supported by the Director, Office of Energy Research, Office of Basic Energy Sciences, Chemical Sciences Division of the U.S. Department of Energy under Contract No. DE-AC03-76SF00098. It was performed at the Stanford Synchrotron Radiation Laboratory, which is supported by the Department of Energy's Office of Basic Energy Sciences.

[1]Present address: Department of Chemistry, University of Waterloo, Waterloo, Ontario N2L 3G1, Canada.
[2]Permanent address: Department of Physics, Zhejiang University, Hangzhou, People's Republic of China.

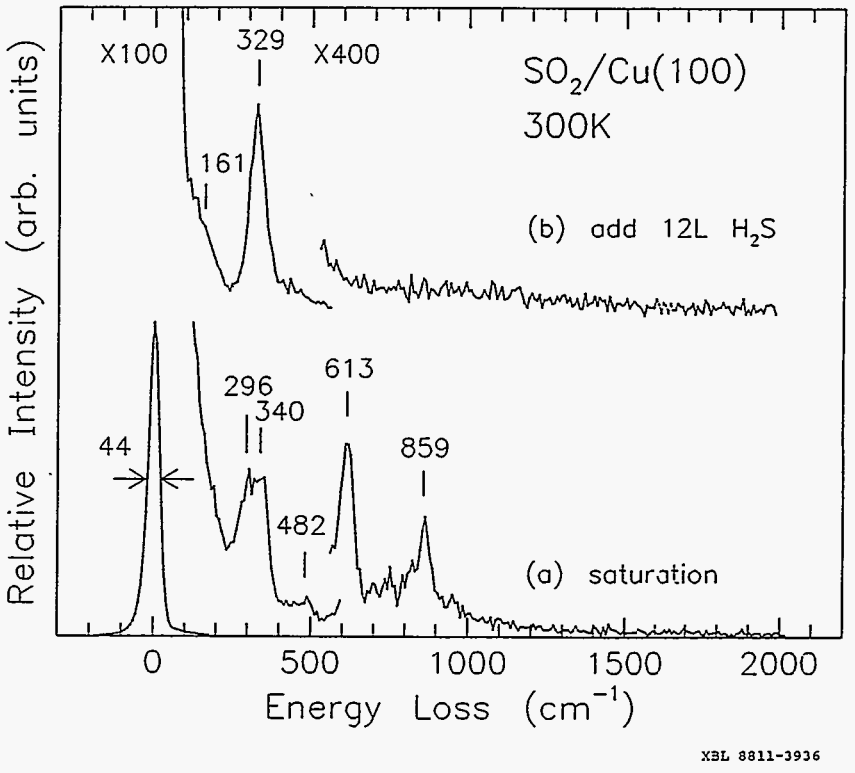

Figure 1. Electron energy loss spectra of a saturation coverage of SO_2 on Cu(100) at 300 K before (a) and after (b) exposing an additional 12 L of H_2S.

ELECTRON SPECTROSCOPY STUDIES OF HIGH TEMPERATURE SUPERCONDUCTORS: $Y_{1-x}Pr_xBa_2Cu_3O_{7-\delta}$

J.W. Allen[1], J.-S. Kang[1,2], B.-W. Lee[2], M.B. Maple[2], Z.-X. Shen[3], J.J. Yeh[3,4], W.P. Ellis[5], W.E. Spicer[3], I Lindau[3]

[1] Dept. of Physics, University of Michigan, Ann Arbor, MI. 48109-1120

[2]Dept. of Physics, University of California at San Diego, La Jolla, CA. 92093

[3]Stanford Electronics Laboratories, Stanford, CA. 94305

[4]AT&T Bell Laboratories, Murray Hill, NJ. 07974

[5]Los Alamos National Laboratory, Los Alamos, NM. 87545

The superconductivity is quenched with increasing x in the isostructural alloy system $Y_{1-x}Pr_xBa_2Cu_3O_{7-\delta}$[1]. We describe the results of an electron spectroscopy study and impurity Anderson Hamiltonian analysis of the Pr 4f spectrum of $Y_{1-x}Pr_xBa_2Cu_3O_{7-\delta}$. The 4f spectra determined experimentally by a combination of synchrotron-excited resonant photoemission spectroscopy[2] (PES) and bremsstrahlung isochromat spectroscopy[3] (BIS) are largely independent of x. The PES and BIS spectra for x=1 are shown by the dotted curves in panels (a) and (b), respectively, of Fig. 1. The impurity Anderson Hamiltonian models the Pr 4f state as a 14-fold degenerate local orbital, characterized by its binding energy ϵ_f relative to E_F, and its Coulomb interaction U_{ff}. The orbital is hybridized to a continuum density of states, with strength characterized by a parameter Δ_{av}. The Gunnarsson/Schönhammer calculation[4] for Ce has been adapted approximately to Pr, as described by them, with the 4f spin-orbit and multiplet splittings included only in simulating the BIS final states.

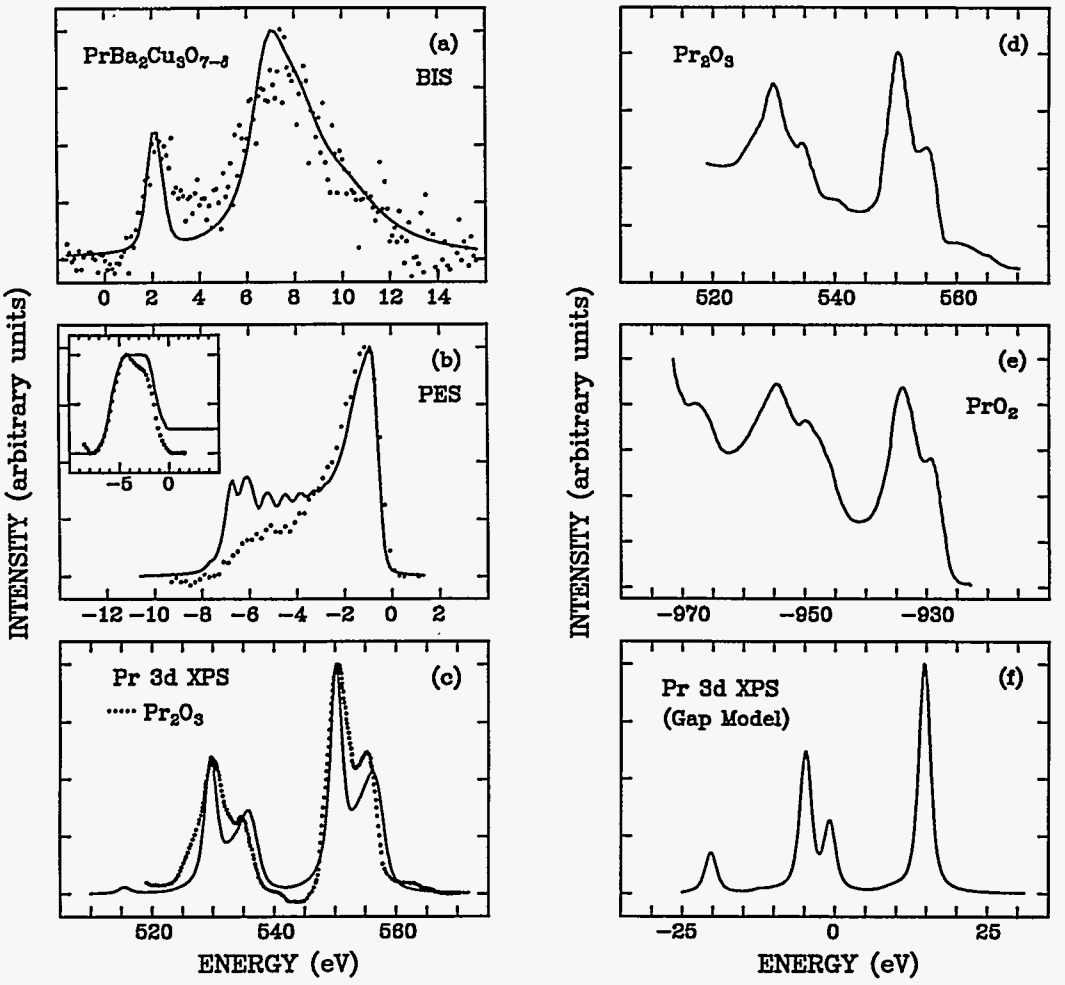

Fig. 1

The solid lines of panels (a) through (c) of Fig. 1 show, respectively, the 4f BIS, 4f PES, and 3d XPS spectra of a metallic mixed valence model. The inset of (b) shows the continuum density of states, with the important part below E_F essentially the same as the Pr 4f off-resonance spectrum shown, where the Cu 3d emission dominates, but with an increased intensity between –2 eV and E_F to account for the contribution from oxygen p-states. We note that interatomic spacings from Pr to both Cu and O permit strong hybridization, and Δ_{av} = 0.16 eV, intermediate between smaller values for α-like Ce intermetallics and larger values for cerium oxides. The other model parameters are $\epsilon_f = E(f^2 \rightarrow f^1) = -3$ eV, U_{ff} = 8.45 eV, and the 4f-3d Coulomb interaction U_{fc} = 12.1 eV. As discussed further below, the theoretical PES and BIS spectra have been shifted away from E_F by 0.6 eV and 2 eV, respectively, and superposed on experimetnal spectra. Although the Pr 3d spectrum is obscured in $PrBa_2Cu_3O_{7-\delta}$ by the Cu 2p spectrum, and is therefore unknown, we can guess that it should resemble that of Pr_2O_3, and be different from that of PrO_2, from the finding that the Pr L-edge XAS spectrum is very much like that of Pr_2O_3 and very much different from that of PrO_2. Panels (d) and (e) show the 3d XPS spectra of Pr_2O_3[5] and PrO_2[6], respectively. The Pr_2O_3 spectrum, with its inelastic background and non-monochromatic-source satellites at 540 eV and 561 eV (incompletely) removed numerically, is also shown in panel (c), and it is indeed much like that of our theory curve.

The metallic continuum model reproduces the various 3d and 4f spectral signatures generally thought to measure the Pr 4f valence and hybridization strength. The calculated ground state is 4.2% f^1, 89.9% f^2 and 5.9% f^3, giving 2.02 f-electrons. If we assume hybridization to a metallic density of states, the weights of the BIS and PES peaks near E_F relative to those far from E_F can be reproduced rather well with only a modest departure from trivalence. However, our fitting results are only partially successful. The theoretical spectra perforce show BIS and PES peaks meeting at E_F, whereas our experimental peaks lie away from E_F somewhat, requiring the theory curves to be shifted as mentioned above. We can produce a 4f spectrum with a gap by introducing a gapped continuum model, but the hybridization strength and valence mixing required to fit the the weights of the two peaks in the BIS spectrum is then so large that other spectra are not reproduced. For example, panel (f) of Fig. 1 shows the calculated 3d spectrum for the gapped-continuum model and it is obvious that it looks much different from that of Pr_2O_3 due to the strong f^2/f^3 valence mixing. Our present inclination is to give credence to the metallic-model characterization of the Pr valence and hybridization strength, while making further experiments to ascertain if the gap could be extrinsic, e.g., a charging phenomenon of some sort.

To summarize, we have found that the Pr valence is close to 3+ for all x. In addition, the extracted Pr 4f spectral lineshape indicates much hybridization to other valence band states. The Cu valence is essentially unchanged with x. From these findings, it is natural to speculate that the extensive hybridization between Pr 4f and other valence band states may have disrupted some features of the electronic or magnetic structure of the x=0 material which is essential for superconductivity. We suggest that it is the Pr magnetic degrees of freedom that are most important. From the view of the metallic model, there occur Kondo spin fluctuations with an associated energy scale of T_K. Although our model calculation is very unrealistic for T_K in neglecting spin-orbit and multiplet splittings, it is suggestive that the value of T_K obtained is about 125 K, the same order of magnitude as T_c. $T_c \sim T_K$ is the condition for maximum suppression of T_c by a magnetic impurity in a BCS superconductor with singlet pairing[7] and may have generic significance in the present case.

REFERENCES

1. Y.D. Dalichaouch, M.S. Torikachvili, E.A. Early, B.-W. Lee, C.L. Seaman, K.N. Yang, H. Zou, and M. B. Maple, Solid State Commun. **65**, 1001 (1987).
2. J.-S. Kang, J.W. Allen, Z.-X. Shen, W. Ellis, J.J. Yeh, B.W. Lee, M.B. Maple, W.E. Spicer, and I. Lindau, J. Less. Common. Metals **148 & 149**, to be published (1988).
3. J.-S. Kang, J.W. Allen, B.-W. Lee, M.B. Maple, Z.-X. Shen, J.J. Yeh, W.P. Ellis, W.E. Spicer, and I. Lindau, in Proceedings of the International Symposium on the Electronic Structure of High T_c Superconductors, edited by A. Bianconi, Oct. 5–7, 1988, Rome (Pergamon, 1989) to be published.
4. O. Gunnarsson and K. Schönhammer, Phys. Rev. **B 31**, 4815 (1985): In: *Handbook on the Physics and Chemistry of Rare Earths* (K.A. Gschneidner, L. Eyring, and S. Hüfner, ed.), Vol. **10**, Chap. 64, pp. 103-163. North-Holland, Amsterdam.
5. P. Burroughs, A. Hamnett, A. F. Orchard, and G. Thornton, J. Chem. Soc., Dalton Trans. **17**, 1686 (1976).
6. A. Bianconi, A. Kotani, K. Okada, R. Giorgi, A. Gargano, A. Marcelli, and T. Miyahara, Phys. Rev. **B 38**, 3433 (1988).
7. E. Muller-Hartmann and J. Zittartz , Z. Physik **234**, 58 (1970).

VIII ACTIVE PROPOSALS

As of December 31, 1988 there were 180 active SSRL proposals. Proposals remain active for two years after their initial rating by the Proposal Review Panel. Since October 1974 SSRL has received a total of 2076 proposals. The Spokesperson for each proposal is underlined and their institution shown in parentheses. The letter suffix appended to the proposal number indicates the sub-panel of the Proposal Review Panel to which the proposal is assigned: Materials (M), Biology (B) or Vacuum Ultra-Violet (V). The small (p) indicates a program proposal.

No.	Received	Experimenters	Title
100Mp	9/7/83	**DARYL CROZIER** ROBERT L INGALLS FARREL W LYTLE ANDREW J SEARY ROBERT B GREEGOR P VIRAN NEIL ALBERDING J E WHITMORE K R BAUCHSPIESS *(SIMON FRASER UNIVERSITY)*	**X-ray Absorption Studies of Disordered Systems**
882Mp	3/1/84	**MATI BLOCH** PETER M EISENBERGER *(ARGONNE NATIONAL LABORATORY)*	**Structural Studies of Organic Thin Films on the Solid Gas and Liquid Gas Interface**
897Vp	4/3/84	**GERALD M ROTHBERG** MARTIN L DENBOER INGOLF LINDAU *(STEVENS INSTITUTE OF TECHNOLOGY)*	**Spin Polarized Photoelectron Studies of Magnetism in Solids (SPEXAFS)**
898Mp	5/3/84	**L D GIBBS** KEVIN L D'AMICO JOHN D AXE DAVID MONCTON JAKOB BOHR *(BROOKHAVEN NATIONAL LABORATORY)*	**Magnetic X-Ray Scattering from Ho**
906Bp	8/29/84	**DALE E SAYERS** PAULINE HARRISON E A STERN ELIZABETH C THEIL KENNETH RAYMOND *(NORTH CAROLINA STATE UNIVERSITY)*	**X-Ray Absorption Studies of the Protein-Iron Interaction in Ferritin**
908Vp	8/31/84	**ROSS D BRINGANS** ROBERT Z BACHRACH ROGER I G UHRBERG J E NORTHRUP *(XEROX)*	**Influence of Surface Reconstruction on Electronic Properties of Semiconductor Surfaces**

910 Mp	8/31/84	**CHARLES E BOULDIN** M I BELL R A FORMAN *(NATIONAL INSTITUTE OF STANDARDS AND TECHNOLOGY)*	**Structural Studies of Ion Implants in III-V Semiconductors with Reflectance EXAFS**
922Bp	9/6/84	**RICHARD C ELDER** KATHERINE TEPPERMAN *(UNIVERSITY OF CINCINNATI)*	**Gold-Based Antiarthritis and Anticancer Drugs and Metabolites: XAS, WAXS, DAS**
928 Mp	9/11/84	**PETER M EISENBERGER** KENG S LIANG *(EXXON RESEARCH & ENGINEERING)*	**Grazing-Incidence X-ray Scattering Program**
935Vp	9/20/84	**INGOLF LINDAU** C BOWMAN K K CHIN M D WILLIAMS J J YEH TOMAS F KENDELEWICZ JOE WOICIK WILLIAM E SPICER S LIST K SHIH C MCCANTS T CHIANG JUN NOGAMI CARLO R CARBONE DANIEL FRIEDMAN KRISTINE BERTNESS S J EGLASH JOEL SILBERMAN EZIO PUPPIN N NEWMAN *(SSRL)*	**Electronic Structure, Chemistry, and the Fermi Level at Semiconductor Surfaces and Interfaces**
941Vp	9/26/84	**LUCIO BRAICOVICH** STEFANO NANNARONE O BISI IVANO ABBATI CARLO CALANDRA MASSIMO SANCROTTI Z SHEN EZIO PUPPIN WILLIAM E SPICER INGOLF LINDAU UMBERTO DEL PENNINO *(POLITECNICO DI MILANO)*	**Study of the Formation of Rare Earth/Elemental Semiconductor (Ge, Si) Interfaces and Compounds**

943Vp	9/6/84	**DAVID A SHIRLEY** DENNIS W LINDLE ERNESTO PAPARAZZO LOUIS J TERMINELLO SEHUN KIM LAISHING WANG TRICIA FERRETT JOHN J BARTON SHIHONG LIU TONG LEUNG BAOHUA NIU LAURA MEDHURST PHILIP A HEIMANN ALEXIS SCHACH V WITTENAU STEVEN W ROBEY ALLEN L JOHNSON ZHENG-QING HUANG MARIA NOVELLA PIANCASTELLI XUN-SHENG ZHANG CHARLES C BAHR *(LAWRENCE BERKELEY LABORATORY)*	**Electron Spectroscopy of Gases, Solids, and Surfaces**
947V	10/15/84	**PAUL H CITRIN** FABIO COMIN *(AT&T BELL LABORATORIES)*	**Proposal to Perform SEXAFS from Substrate Surfaces**
956Mp	2/27/84	**G P HUFFMAN** FARREL W LYTLE ROBERT B GREEGOR F E HUGGINS R G JENKINS NARESH SHAH *(UNIVERSITY OF KENTUCKY)*	**Applications of EXAFS Spectroscopy in the Steel and Coal Industries**
957Bp	2/28/84	**DAVID H TEMPLETON** L K TEMPLETON *(LAWRENCE BERKELEY LABORATORY)*	**Anomalous Scattering of X-rays**
959Vp	3/1/85	**ROBERT Z BACHRACH** ROSS D BRINGANS *(XEROX)*	**Core Level and Near Edge Structure Study of Interface Formation**
963Vp	3/6/85	**JOACHIM STOHR** *(IBM RESEARCH LABORATORY)*	**NEXAFS and SEXAFS Studies by Means of X-ray Fluorescence Detection: Local Structure Around Low-Z Atoms**
969Bp	3/14/85	**ROBERT A SCOTT** STEPHEN P CRAMER *(UNIVERSITY OF GEORGIA)*	**X-ray Absorption Spectroscopic Studies of Nickel-Containing Metalloenzymes**

973M	4/12/85	**CHARLES E BOULDIN** M I BELL R A FORMAN G K HUBLER E D DONOVAN *(NATIONAL INSTITUTE OF STANDARDS AND TECHNOLOGY)*	**EXAFS Study of Damage and Annealing of Ion Implanted Semiconductors**
981Bp	9/3/85	**JAMES O ALBEN** ALLAN A CROTEAU STEPHEN P CRAMER FRANK G FIAMINGO KIMBERLY A POWELL CRAIG F HEMANN *(OHIO STATE UNIVERSITY)*	**High Resolution EXAFS Spectroscopy of Iron and Copper Proteins**
991Bp	9/4/85	**RICHARD C ELDER** EDWARD A DEUTSCH *(UNIVERSITY OF CINCINNATI)*	**Technetium and Rhenium Imaging Agents and Therapeutic Radiopharmaceuticals**
994Mp	9/5/85	**GLENN A WAYCHUNAS** GORDON E BROWN, JR *(STANFORD UNIVERSITY)*	**High Temperature EXAFS Study of Fe and Ca in Silicate Crystals and Melts**
995Mp	9/6/85	**GORDON E BROWN, JR** KEITH O HODGSON GEORGE A PARKS GLENN A WAYCHUNAS JAMES O LECKIE KIM F HAYES *(STANFORD UNIVERSITY)*	**XAS Study of Cation Adsorption at Aqueous/Oxide Interface**
997Mp	9/10/85	**I K ROBINSON** P J ESTRUP M ALTMAN ROBERT J BIRGENEAU *(AT&T BELL LABORATORIES)*	**The Surface Phase Transition of Clean W(100)**
998M	9/10/85	**KENG S LIANG** PETER M EISENBERGER G J HUGHES *(EXXON RESEARCH & ENGINEERING)*	**Order-Disorder Transition of Adsorbates on Nickel**
999Mp	9/10/85	**GORDON E BROWN, JR** C W PONADER GLENN A WAYCHUNAS W A JACKSON S ROTHFUS *(STANFORD UNIVERSITY)*	**EXAFS Study of Trace Element Environments in Quenched Silicate Melts of Geochemical Interest**
1008Mp	10/4/85	**WILLIAM K WARBURTON** ARTHUR BIENENSTOCK KARL F LUDWIG *(X-RAY INSTRUMENTATION ASSOCIATES)*	**Binary Liquid Structures Determined by Anomalous X-ray Scattering**

1010M	10/14/85	C R SAFINYA BILL VARADY N A CLARK *(EXXON RESEARCH & ENGINEERING)*	**Synchrotron Studies of Freely Suspended Discotic and Ordered Microemulsion Strands**
1012Bp	11/4/85	ROBERT H FAIRCLOUGH STEVEN R HUBBARD KEITH O HODGSON SEBASTIAN DONIACH D RICHMAN *(UNIVERSITY OF CHICAGO)*	**Membrane X-Ray Diffraction Studies of the Acetylcholine Receptor**
1013Vp	11/18/87	FRANCESCO SETTE J E ROWE JOHN M POATE *(AT&T BELL LABORATORIES)*	**NEXAFS and EXAFS Studies of Shallow Inpurities in Semiconductors by Soft X-ray Fluorescence**
1015Vp	2/28/86	JOHN L GLAND FRANCISCO ZAERA DANIEL A FISCHER *(EXXON RESEARCH & ENGINEERING)*	**The Structure and Reactivity of Adsorbed Intermediates Using NEXAFS and SEXAFS**
1017M	3/3/86	JAMES B BOYCE FRANK G BRIDGES J C MIKKELSON *(XEROX)*	**Local Structure of Icosahedral Materials**
1018Mp	3/3/86	D DE FONTAINE B E C DAVIS JEFF J HOYT M KRAITCHMAN B CLARK *(UNIVERSITY OF CALIFORNIA)*	**Diffusion in Ternary Multilayer Thin Films**
1019B	3/3/86	F SCOTT MATHEWS R PAUL PHIZACKERLEY LOUIS LIM ETHAN A. MERRITT *(WASHINGTON UNIVERSITY)*	**Crystallographic Study of Amicyanin by Anomalous Scattering Using Synchrotron Radiation**
1021Mp	3/3/86	WILLIAM PARRISH TING C HUANG GEORGE WILL MAURIZIO BELLOTTO CURT ERICKSON MICHAEL HART *(IBM RESEARCH LABORATORY)*	**Synchrotron X-ray Polycrystalline Diffractometry**
1022Vp	3/3/86	EDWARD I SOLOMON KRISTINE BUTCHER STEVE V DIDZIULIS JIAN-YI LIN *(STANFORD UNIVERSITY)*	**UPS Studies of the Coordination Chemistry of Metal Oxides, Chlorides and Sulfides**

1025M	3/4/86	**S C WEAVER** M CHEN LEI ANTHONY D COX P ZIA J V ACRIVOS *(CALIFORNIA STATE UNIVERSITY)*	**Structure of Multiple Valence Compounds such as Prussian Blue vs Temperature**
1026M	3/4/86	**DONALD R SANDSTROM** FARREL W LYTLE *(BOEING COMPANY)*	**Transition Metal Ion Complexes in the Gas Phase**
1027Bp	3/5/786	**STEVE D CONRADSON** BASIL SWANSON WILLIAM WOODRUFF *(LOS ALAMOS NATIONAL LABORATORY)*	**Dispersive XAS Development: Time Resolved and Diamond Anvil Applications**
1028Vp	3/5/86	**JIM ALLEN** INGOLF LINDAU *(UNIVERSITY OF MICHIGAN)*	**High-Photon Flux Photoemission Studies of Narrow Band Materials**
1029B	3/5/86	**MICHAEL SEUL** SRIRAM SUBRAMANIAM *(AT&T BELL LABORATORIES)*	**X-ray Diffraction by Molecular Films on Solid Substrates in Aqueous Environment**
1030Bp	3/17/86	**STEPHEN P CRAMER** M WW ADAMS B E SMITH EDWARD I STIEFEL V MINAK J ENEMARK L S SOLMONSON W CLELAND GRAHAM N GEORGE *(BROOKHAVEN NATIONAL LABORATORY)*	**Soft X-ray Spectrocopy of Molybdenum Enzymes, Cofactors and Model Compounds**
1032M	3/19/86	**CHARLES E BOULDIN** P BOOLCHAND *(NATIONAL INSTITUTE OF STANDARDS AND TECHNOLOGY)*	**EXAFS Study of Local Chemical Coordination of Cation and Anion Sites in Chalcogenide Glass**
1033M	3/27/86	**JAMES E PENNER-HAHN** ROBERT MK CARLSON GEOFFREY WALDO *(UNIVERSITY OF MICHIGAN)*	**XAS Determination of the Chemical Forms of Sulfur in Petroleums**
1034Mp	3/486	**L B SORENSEN** ERIC SIROTA SUZANNE AMADOR *(UNIVERSITY OF WASHINGTON)*	**Structure and Phase Transitions of Hexatic Phases in Thin Liquid Crystal Films**

1035B	4/14/86	JAMES E PENNER-HAHN DAVID P BALLOU CHRISTOPHER J BATIE HIM-TAI TSANG JAMES A FEE *(UNIVERSITY OF MICHIGAN)*	**XAS Investigations of Rieske-Like Iron Sulfur Centers**
1037M	5/19/86	TIMOTHY M HAYES G KRAUSS D L WILLIAMSON *(COLORADO SCHOOL OF MINES)*	**Grain Boundary Segregation of Impurities in Iron and Steel**
1039B	6/3/86	STEPHEN P CRAMER ROGER C PRINCE ROBERT A SCOTT GRAHAM N GEORGE TERRENCE G FREY *(BROOKHAVEN NATIONAL LABORATORY)*	**Polarized XANES and EXAFS of Cytochrome Oxidase in Hydrated, Oriented Mitochondria I Multilayers**
1040B	6/3/86	RUSSELL HILLE STEPHEN P CRAMER *(OHIO STATE UNIVERSITY)*	**X-Ray Absorption Spectroscopy of Xanthine Oxidase**
1041B	9/3/86	ROBERT A SCOTT MARLY EIDSNESS *(UNIVERSITY OF GEORGIA)*	**Measurement of Metal-Metal Distances in Proteins by X-ray Anomalous Scattering**
1042B	9/3/86	BRITTON CHANCE BARTON HOLMQUIST JAMES RIORDAN MARK CHANCE DAVID AULD LINDA S POWERS B VALLEE *(UNIVERSITY OF PENNSYLVANIA)*	**Studies of Intermediates in the Mechanism of Carboxypeptidase-a**
1043B	9/3/86	BRITTON CHANCE GRANT BUNKER PETER REICHARD S M KHALID GUANG ZHANG BRITT-MARIE SJOBERG ALI NAQUI *(UNIVERSITY OF PENNSYLVANIA)*	**X-Ray Absorption Spectroscopy of Iron-Iron Interactions: Ribonucleotide Reductase**
1044M	9/3/86	MATTHEW A MARCUS CHING-LONG TSAI J BEVK *(AT&T BELL LABORATORIES)*	**Structural Effects of Ultrahigh Strains and Dislocation Densities**
1045M	9/3/86	MATTHEW A MARCUS CHING-LONG TSAI *(AT&T BELL LABORATORIES)*	**Multiple and Unusual Siting in Dilute Solid Solutions**

1046M	9/3/86	EDWARD RUBENSTEIN HERBERT D ZEMAN DONALD C HARRISON ROBERT HOFSTADTER GEORGE S BROWN W THOMLINSON ALBERT C THOMPSON ROBERT KERNOFF JOHN OTIS *(STANFORD UNIVERSITY)*	**Iodine Dichromography with Monochromatic X-ray Beams for Angiography**
1047M	9/3/86	ROBERT L INGALLS J FREUND DARYL CROZIER *(UNIVERSITY OF WASHINGTON)*	**High Pressure Transition Mechanisms via EXAFS**
1048M	9/11/86	CAROLINE STAHLE SEAN BRENNAN ARTHUR BIENENSTOCK *(STANFORD UNIVERSITY)*	**High Resolution Compton Profiles of Iron and Silicon**
1049Mp	9/11/86	ROBERT B GREEGOR FARREL W LYTLE B C CHAKOUMAKOS R C EWING *(BOEING COMPANY)*	**X-ray Spectroscopic Investigation of Radiation Damaged Materials**
1050Mp	9/11/86	GLENN A WAYCHUNAS MICHAEL J APTED GREG J EXARHOS JAMES E PENNER-HAHN *(STANFORD UNIVERSITY)*	**X-ray Anomalous Scattering and EXAFS Study of Heavy Metal Complexes in Aqueous Solutions**
1051M	9/11/86	GLENN A WAYCHUNAS LAWRENCE R BERNSTEIN *(STANFORD UNIVERSITY)*	**Crystal and Aqueous Chemistry of Germanium in Geochemically Important Systems**
1052M	9/11/86	IVAN SELLIN D A CHURCH S B ELSTON C S O H CEDERQUIST J LEVIN *(OAK RIDGE NATIONAL LABORATORY)*	**Measurement of Recoil Energies of Multiply Charged Recoil Ions and Molecular Fragments**
1053B	9/15/86	ROBERT A SCOTT DAVID M DOOLEY *(UNIVERSITY OF GEORGIA)*	**Copper EXAFS Spectroscopy of Non-Blue Copper Proteins. Amine Oxidases**

1054M	9/15/86	RICHARD W RYON HARRY E MARTZ SUZANNE FLETCHER ROBERT A DAY JOHN H KINNEY *(LAWRENCE LIVERMORE NATIONAL LABORATORY)*	**X-Ray Induced Photoacoustic Emission**
1055B	9/15/86	KEITH O HODGSON BRITT HEDMAN STEPHEN F GHELLER FRANK A SCHULTZ W E NEWTON *(SSRL)*	**XAS of Iron-Molybdenum Cofactor of Nitrogenase under Electrochemical Control**
1056Mp	9/16/86	S R STOCK B COULMAN Y H CHUNG ZOPHIA U REK *(GEORGIA INSTITUTE OF TECHNOLOGY)*	**Section Topographic Strain Mapping Using Synchrotron White Radiation**
1058M	9/16/86	PAUL M HORN GLENN HELD *(IBM RESEARCH LABORATORY)*	**Roughening Transition of Metal Surfaces**
1059M	9/16/86	MURLI H MANGHNANI L C MING *(UNIVERSITY OF HAWAII)*	**In Situ High P-T Equation-of-State, Phase Transformations and Kinetics Studies on Mantle Mineral Phases using Synchrotron Radiation**
1060Mp	9/16/86	MARYBETH RICE ARTHUR BIENENSTOCK *(STANFORD UNIVERSITY)*	**Structural Investigations of Layered Synthetic Microstructures and Binary Amorphous Alloys**
1061Bp	9/16/86	JAMES Q ALBEN ALLAN A CROTEAU FRANK G FIAMINGO KIMBERLY A POWELL CRAIG F HEMANN *(OHIO STATE UNIVERSITY)*	**Iron Porphyrin Models for EXAFS Analysis**
1062Vp	10/1/86	DONALD C LORENTS R L SHARPLESS *(SRI INTERNATIONAL)*	**Spectroscopy and Kinetics of Excited Gases**
1063M	11/24/86	JOSEPH G GORDON LESSER BLUM OWEN MELROY M SAMANT *(IBM RESEARCH LABORATORY)*	**In Situ SEXAFS Study of the Compact Layer at an Electrode/Electrolyte Interface**

1064M	3/3/87	J AKELLA H K MAO G S SMITH L C MING MURLI H MANGHNANI QUINTIN C JOHNSON *(LAWRENCE LIVERMORE NATIONAL LABORATORY)*	**Statis High Pressure and High Temperature X-Ray Diffraction Studies of Some Rare-Earth Elements Using Diamond-Anvil Apparatus**
1065Mp	3/1/87	MICHEL BOUDART R J DAVIS *(STANFORD UNIVERSITY)*	**Characterization of Supported Pd/Au Alloys by X-RayAbsorption Spectroscopy**
1066Mp	3/1/87	RICHARD C ELDER WILLIAM R HEINEMAN *(UNIVERSITY OF CINCINNATI)*	**X-Ray Spectroscopy of Electrochemically Generated Species**
1067Bp	3/1/87	ROBERT A SCOTT SUNNEY I CHAN P MARK LI *(UNIVERSITY OF GEORGIA)*	**Active Site Structures of Cytochrome c Oxidase**
1068Bp	3/1/87	R H FELTON E A STERN *(GEORGIA INSTITUTE OF TECHNOLOGY)*	**Structure of Transients in the Catalytic Cycle of Dioxygenases**
1069M	3/1/87	NOLAN MANGELSON MAX W HILL FARREL W LYTLE *(BRIGHAM YOUNG UNIVERSITY)*	**Characterization of Vanadium, Chromium, Nickel and Arsenic in Particulate Matter**
1070M	3/1/87	THOMAS BEIN KARIN MOLLER *(UNIVERSITY OF NEW MEXICO)*	**Anchoring Chemistry of Transition Metal Complexes and Clusters to Intrazeolite Surfaces**
1071M	3/1/87	MICHEL BOUDART G P VALENCA *(STANFORD UNIVERSITY)*	**Characterization of Clusters of Pt/Y-Zeolite and Rh/ -A1 O by X-Ray Absorption Spectroscopy**
1072M	3/1/87	STEVE M HEALD HEATHER CHEN *(BROOKHAVEN NATIONAL LABORATORY)*	**Glancing Angle EXAFS and Reflectivity of Aluminum-Metal Interfaces**
1073M	3/1/87	STEVE M HEALD J M TRANQUADA M SUENAGA *(BROOKHAVEN NATIONAL LABORATORY)*	**X-Ray Absorption Study of La CuO Based Superconductors**
1074M	3/1/87	STEVE M HEALD DALE E SAYERS JIM VICCARO ERIC ZIEGLER *(BROOKHAVEN NATIONAL LABORATORY)*	**X-Ray Absorption and Reflectivity Studies of Interfaces in Multilayer Optics**

1076B	3/1/87	SEBASTIAN DONIACH KEITH O HODGSON S WAKATSUKI ROBERT M STROUD *(STANFORD UNIVERSITY)*	**Study of Conformational Changes in Bacteriorhodopsin using Time-Resolved Small Angle X-Ray Diffraction**
1077M	3/1/87	KRISHNA M CHOUDHARY *(UNIVERSITY OF NOTRE DAME)*	**Photoemission EXAFS Studies of Surfaces and Interfaces in Compound Semiconductors**
1078M	3/1/87	N S LEWIS BRUCE J TUFTS KEITH O HODGSON *(CALIFORNIA INSTITUTE OF TECHNOLOGY)*	**X-Ray Absorption Studies of Metal Ion at Semiconductor Surfaces**
1079M	3/1/87	JAMES B BOYCE T CLAESON FRANK G BRIDGES THEODORE H GEBALLE *(XEROX)*	**Local Atomic Structure of High-T_c Superconductors**
1080Vp	3/1/87	ROBERT J MADIX C M FRIEND J SOLOMON PAUL STEVENS J T ROBERTS A C LIU B FACTOR *(STANFORD UNIVERSITY)*	**Adsorption Structure of Heteroatom-Containing Molecules on Transition Metal Surfaces**
1081M	3/1/87	DAVID P POPE JOHN E BENCI *(UNIVERSITY OF PENNSYLVANIA)*	**A Study of Creep Damage Using Microradiography**
1082B	3/24/87	DAVID A LARSON CLIFF LING THEODORE L PHILLIPS DENNIS SHRIEVE MICHAEL SCHELL TERESA TROXEL *(UNIVERSITY OF CALIFORNIA)*	**Contribution of Auger Electrons to Radiation Sensitization with IUdR**
1083B	3/1/87	M IKEDA-SAITO ROGER C PRINCE GRAHAM N GEORGE *(UNIVERSITY OF PENNSYLVANIA)*	**X-Ray Absorption Spectroscopy of and Lactoperoxidase**
1084Bp	3/1/87	GRAHAM N GEORGE STEPHEN P CRAMER ROGER C PRINCE *(EXXON RESEARCH & ENGINEERING)*	**Polarized X-Ray Spectroscopy of the Oriented Chloroplast Water-Oxidizing Complex**

1085Bp	3/1/87	**JAMES E PENNER-HAHN** W D FRASCH V L PECORARO HIM-TAI TSANG C F YOCUM D GHANOTAKIS J T GROVES M STERN *(UNIVERSITY OF MICHIGAN)*	**X-Ray Absorption Spectroscopic Characterization of the Manganese in Biological Systems**
1086V	3/1/87	**RICHARD D DESLATTES** PAUL L COWAN DENNIS W LINDLE SEAN BRENNAN *(NATIONAL INSTITUTE OF STANDARDS AND TECHNOLOGY)*	**Polarization in Molecular X-Ray Flourescence**
1087Bp	3/1/87	**WAYNE A HENDRICKSON** CRAIG OGATA R PAUL PHIZACKERLEY STEVEN R HUBBARD WILLIAM E ROYER ARNO PAHLER MARIANNE CUFF HM KRISHNA MURTHY WEI YANG JOHN HORTON *(COLUMBIA UNIVERSITY)*	**Anomalous-scattering Studies of Protein Crystal Structures**
1088M	3/1/87	**JAMES E PENNER-HAHN** GEOFFREY WALDO RICHARD FRONKO SHENGKE WANG GLENN A WAYCHUNAS *(UNIVERSITY OF MICHIGAN)*	**Polarized X-Ray Absorption Near Edge Structure**
1089M	3/1/87	**JAMES HOWARD** JULIA PECK WILLIAM MURPHY STEPHEN P CRAMER GRAHAM N GEORGE *(SCHLUMBERGER DOLL RESEARCH)*	**X-Ray Absorption of Iridium in K-T Boundary Samples and Meteorites**
1090Mp	6/9/87	**T E FURTAK** TIMOTHY M HAYES *(COLORADO SCHOOL OF MINES)*	**Electrolyte-Metal Interfaces**
1091Mp	6/9/87	**D L WILLIAMSON** TIMOTHY M HAYES F M KUSTAS *(COLORADO SCHOOL OF MINES)*	**Characterization of Ion-Implanted Aluminum and Titanium**

1092M	6/19/87	**JAMES HOWARD** S WHITTINGHAM N WADA D R HINES STEPHEN P CRAMER *(SCHLUMBERGER DOLL RESEARCH)*	**Structural Investigation of Interlayer Potassium and Sodium in Phyllosilicates**
1093 Mp	8/7/87	**STEPHEN LADERMAN** THEODORE H GEBALLE ALICE FISCHER-COLBRIE J MOLL J Z SUN N MISSERT A D KENT B OH K CHAR *(HEWLETT PACKARD LABORATORIES)*	**Structure of Superconducting Thin Films**
1094 M	8/20/87	**JAKOB BOHR** H H ANDERSEN L SARHOLT-KRIST L F GRAABAEK E JOHNSON A JOHANSEN I K ROBINSON *(RISO NATIONAL LABORATORY)*	**X-Rays Studies of Rare Gas Inclusions in Single Crystal Aluminium**
1095 Mp	8/7/87	**PAUL H FUOSS** LAURA NORTON D W KISKER *(AT&T BELL LABORATORIES)*	**EXAFS and NEXAFS Investigation of OMPVE Growth of II-VI Compounds**
1096 Mp	8/20/87	**PAUL H FUOSS** D W KISKER LAURA NORTON *(AT&T BELL LABORATORIES)*	**In-Situ X-Ray Scattering Studies of OMVPE Growth of II-VI Compounds**
1097 Mp	8/20/87	**FARREL W LYTLE** ROBERT B GREEGOR *(BOEING COMPANY)*	**Anti-Site Disorder in High T_c Superconductors**
1098 M	9/1/87	**DANIEL A SCHERSON** PHILIP N ROSS *(CASE WESTERN RESERVE UNIVERSITY)*	**In-Situ EXAFS Transition Metal Macrocycles Absorbed on Electrode Surfaces**
1099M	9/15/87	**J V ACRIVOS** S S P PARKIN D HELMOLDT J SATCHER R ITHNIN S ARNOLD C BUSTILLO M CHEN LEI *(LAWRENCE BERKELEY LABORATORY)*	**Study of Organic Metals**

2000M	9/15/87	**J V ACRIVOS** MELVIN P KLEIN S S P PARKIN M CHEN LEI S ARNOLD R ITHNIN C BUSTILLO D HELMOLDT J SATCHER *(LAWRENCE BERKELEY LABORATORY)*	**Study of Cation, Anion X-Ray Edges in S Intercalated Perovskites $[Y_1Ba_2Cu(O/S)_{7+\delta}]n$**
2001M	9/15/87	**JEFFREY R LINCE** PAUL D FLEISCHAUER *(THE AEROSPACE CORPORATION)*	**Extended X-Ray Absorption Fine Structure of Transition Metal Dischalcogenide Materials**
2002Mp	9/15/87	**J D BROCK** ROBERT J BIRGENEAU J D LITSTER *(MIT)*	**Bond Orientational Order in Tilted Hexatic Liquid Crystal Films**
2003M	9/15/87	**MIKE TONEY** W H SMYRL OWEN MELROY *(IBM RESEARCH LABORATORY)*	**In-Situ X-Ray Scattering Study of the Structure of Passive Oxides on Single Crystal Ti**
2005M	9/15/87	**ROBERT L INGALLS** B HOUSER DARYL CROZIER J M TRANQUADA E A STERN *(UNIVERSITY OF WASHINGTON)*	**X-Ray Absorption Studies of Perovskites as a Function of Pressure**
2006Mp	9/15/87	**D DE FONTAINE** JEFF J HOYT M KRAITCHMAN S SPOONER M WIEDENMEIR *(UNIVERSITY OF CALIFORNIA)*	**Kinetics of Phase Separation in Al-Li**
2007B	9/15/87	**JAMES PHILLIPS** *(BROOKHAVEN NATIONAL LABORATORY)*	**Protein Folding Studied by Synchrotron X-Ray Scattering**
2008B	9/15/87	**DOUGLAS S CLARK** GREGG A MARG R MARK GUINN *(UNIVERSITY OF CALIFORNIA)*	**EXAFS of Active-Site Metals in Glucose Isomerase and Methane Monooxygenase**

2009Vp 9/17/87 **JOACHIM STOHR** — **Structural Studies of Thin Polymer Films on Surfaces**
THOMAS P RUSSELL
(IBM RESEARCH LABORATORY)

2010Bp 9/17/87 **MELVIN P KLEIN** — **X-Ray Spectroscopy of Manganese and Iron in Chloroplasts**
R GUILES
SUSAN DEXHEIMER
ANN MCDERMOTT
KENNETH SAUER
J L ZIMMERMANN
VICKIE DEROSE
(LAWRENCE BERKELEY LABORATORY)

2011V 9/17/87 **DON KANIA** — **Synchrotron Based Studies of X-Ray Induced Photoconductivity**
J TREBES
PIERO PIANETTA
(LAWRENCE LIVERMORE NATIONAL LABORATORY)

2012M 9/17/87 **E E ALP** — **Electronic Structure of High T_c Oxide Superconductors by X-Ray Absorption Spectroscopy**
L SODERHOLM
GOPAL K SHENOY
PEDRO A MONTANO
(ARGONNE NATIONAL LABORATORY)

2013M 9/17/87 **DAVE WARK** — **Photoelectron Spectrometry of Correlation Satellites in KR**
RICH MARTIN
JOHN HENDERSON
DAVE KNAPP
WALTER J. TRELA
TOM BOWLES
HAMISH ROBERTSON
JOHN WILKERSON
S B WHITFIELD
S L SORENSEN
BERND CRASEMANN
ROGER J BARTLETT
GEORGE S BROWN
(LOS ALAMOS NATIONAL LABORATORY)

2014M 9/17/87 **ROBERT M SUTER** — **Melting of Xe/TiS_2: Structure and Thermodynamics**
R F HAINSEY
J D SHINDLER
(CARNEGIE MELLON UNIVERSITY)

2015Mp 9/17/87 **S R STOCK** — **In-Situ Synchrotron Microradiography of Delamination in Graphite/Epoxy Composites**
G WEBB
S D ANTOLOVICH
ZOPHIA U REK
(GEORGIA INSTITUTE OF TECHNOLOGY)

2016M	9/17/87	GEORGE KWEI JOYCE A GOLDSTONE ROBERT B VON DREELE ART WILLIAMS ANDREW C LAWSON *(LOS ALAMOS NATIONAL LABORATORY)*	**Anomalous X-Ray Powder Diffraction Studies of the Structure of Materials**
2017Mp	9/17/87	BENJAMIN OCKO DAVID M ZEHNER S G J MOCHRIE L D GIBBS *(BROOKHAVEN NATIONAL LABORATORY)*	**Structure and Stability of Metal Surfaces: A Proposal for X-Ray Scattering Experiments**
2018M	9/21/87	JEFFREY B KORTRIGHT ROSS D BRINGANS JONATHAN DENLINGER MARJORIE OLMSTEAD *(LAWRENCE BERKELEY LABORATORY)*	**Structural Study of Hetero-Epitaxial CaF_2 on Si(111) Using Standing Wave Fluorescence**
2019V	9/21/87	MARJORIE OLMSTEAD JONATHAN DENLINGER ROSS D BRINGANS *(UNIVERSITY OF CALIFORNIA)*	**Heteroepitaxial Interface Formation Between Insulators and Semiconductors**
2020Mp	9/21/87	S H LIN T GROY J R SCHOONOVER *(ARIZONA STATE UNIVERSITY)*	**X-Ray Diffraction of Solid State Reactions and Phase Transitions**
2021M	9/21/87	NOLAN MANGELSON MAX W HILL ROBERT B GREEGOR FARREL W LYTLE *(BRIGHAM YOUNG UNIVERSITY)*	**Structures of Silver (I)-Crown Complexes in Liquid and Solid Phases**
2022B	9/21/87	BRITTON CHANCE GRANT BUNKER HIROYUKI OYANAGI S G SLIGAR KE ZHANG *(UNIVERSITY OF PENNSYLVANIA)*	**Structural Features of Low Temperature Recombination of Hemoproteins, Carbon Monoxide and Oxygen**
2023Mp	9/21/87	STEVE D CONRADSON ANTONIO REDONDO ZACHARY FISK IAN D RAISTRICK *(LOS ALAMOS NATIONAL LABORATORY)*	**High T_c Superconducting Materials: Their Structural and Electronic Characterization by XAS**
2024Mp	9/21/87	STEVE D CONRADSON ALFRED SATTLEBERGER BASIL SWANSON *(LOS ALAMOS NATIONAL LABORATORY)*	**XAS Studies of Quasi-One-Dimensional Halide-Bridged Mixed Valence Platinum Compounds**

2025B	9/21/87	**BRITTON CHANCE** GRANT BUNKER TSOO E KING EDGAR DAVIDSON ROBERT POYTON KE ZHANG *(UNIVERSITY OF PENNSYLVANIA)*	**Altered Structures of Cytochrome Oxidase**
2026Mp	9/21/87	**PIERO PIANETTA** JEFF NELSON JENNCHANG HWANG GLENN KUBIAK RICHARD H STULEN *(SSRL)*	**The Bonding Behaviour in Strained Semiconductor Heterostructures**
2027M	9/22/87	**SEAN BRENNAN** ARTHUR BIENENSTOCK ROLAND TIMSIT B FACTOR *(SSRL)*	**Structural Studies of Co-Sputtered Amorphous AlTa Thin Films**
2028M	9/29/87	**HOWARD OCKEN** ZOPHIA U REK FARREL W LYTLE *(EPRI)*	**Characterization of Cobalt-Bearing Passive Oxides on Stainless Steel by EXAFS**
2029Bp	9/29/87	**KEITH O HODGSON** BRITT HEDMAN BARBARA K BURGESS STEVEN A VAUGHN *(SSRL)*	**Mo and Se XAS Studies of Small-Molecule Binding to Nitrogenase**
2030Bp	9/29/87	**KEITH O HODGSON** BRITT HEDMAN STEPHEN J LIPPARD ROBERT H BEER JAMES G BENTSEN *(SSRL)*	**XAS Structural Characterization of the Binuclear Iron-Center in Methane Monooxygenase**
2031Bp	9/29/87	**KEITH O HODGSON** BRITT HEDMAN GRACE TAN EDWARD I SOLOMON *(SSRL)*	**X-Ray Absorption Studies of Coupled Binuclear Copper Sites in Proteins**
2032Bp	9/29/87	**KEITH O HODGSON** BRITT HEDMAN MASANORI SONO JOHN H DAWSON *(SSRL)*	**XAS Studies of Heme-Iron Enzymes: Cytochrome P-450 and Peroxidases**

2033Mp	9/29/87	**TERESA A SMITH** KEITH O HODGSON BRITT HEDMAN *(EASTMAN KODAK RESEARCH LABORATORY)*	**Sulfur K Edge XAS Studies of Photographic Sensitizing Centers**
2034M	9/29/87	**KEITH O HODGSON** BRITT HEDMAN MATTHEW B ZISK HITOSHI ASAHINA JAMES P COLLMAN *(SSRL)*	**XAS Studies of Liquid Crystalline Ruthenium Phthalocyanines and Porphyrins**
2035B	9/29/87	**SEBASTIAN DONIACH** ROBERT M STROUD S WAKATSUKI U W SPANN KEITH O HODGSON *(STANFORD UNIVERSITY)*	**X-Ray Diffraction Studies of Helix Linking Regions of Bacteriorhodopsin**
2037Vp	9/29/87	**PIERO PIANETTA** DANIEL SELIGSON PAUL KING LAWRENCE PAN *(SSRL)*	**X-Ray Lithography Process Development**
2038M	10/1/87	**P G ELLER** ROBERT B GREEGOR FARREL W LYTLE E M LARSON J D PURSON *(LOS ALAMOS NATIONAL LABORATORY)*	**EXAFS Study of Actinide and Fission Product Speciation in Nuclear Waste Storage Media**
2039Vp	10/1/87	**JON ERICKSON** WAYNE WIEMER CAREY SCHWARTZ SANDY LANGSJOEN PHILLIP LAROE TSU-WIE NEE AROLD K GREEN VICTOR REHN *(NAVAL WEAPONS CENTER)*	**Superconductor-Semiconductor Heterostructure Research**
2040M	10/4/87	**FRANK G BRIDGES** JAMES B BOYCE *(UNIVERSITY OF CALIFORNIA)*	**EXAFS Study of Off-Center Behavior and Aggregation in Dilute Immissible Systems**
2041B	10/4/87	**JOHN P LANGMORE** MICHAEL F SMITH SHAWN WILLIAMS BRIAN D ATHEY *(UNIVERSITY OF CALIFORNIA)*	**Synchrotron Studies of Ordered Chromatin Fibers for Model Calculations**

2042M	10/12/87	**ERIC SIROTA** GREG S SMITH N A CLARK C R SAFINYA *(EXXON RESEARCH & ENGINEERING)*	**Synchrotron Scattering Studies of Dilute Membrane Systems**
2043V	10/12/87	**PIERO CHIARADIA** L J BRILLSON GIORGIO MARGARITONDO *(ISTITUTO DI STRUTTURA DELLA MATERIA)*	**Schottky Barrier Formation in GaP Single Crystals**
2044Mp	11/5/87	**PAUL H FUOSS** LAURA NORTON SEAN BRENNAN ARTHUR BIENENSTOCK J KAHN *(AT&T BELL LABORATORIES)*	**Direct Scattering Studies of Surface Premelting**
2045M	11/5/87	**MARYBETH RICE** PAUL H FUOSS ARTHUR BIENENSTOCK LANE C WILSON *(STANFORD UNIVERSITY)*	**Grazing Incidence X-Ray Scattering Study of Ge Epitaxy on Mo**
2046M	11/5/87	**R COLELLA** Q ZHAO *(PURDUE UNIVERSITY)*	**X-Ray Study of Charge Density Waves (CDW's) in Layer Compounds**
2047B	11/16/87	**JAMES E PENNER-HAHN** HIM-TAI TSANG THOMAS V O'HALLORAN RICHARD FRONKO DIANA RALSTON JEFF WRIGHT *(UNIVERSITY OF MICHIGAN)*	**X-Ray Absorption Spectroscopy of the MER-R Gene Product**
2048B	11/16/87	**JAMES E PENNER-HAHN** RICHARD FRONKO JAMES D WHITTAKER ROBERT KERTAYASA *(UNIVERSITY OF MICHIGAN)*	**X-Ray Absorption Spectroscopy of Galactose Oxidase**
2049Mp	3/1/88	**FARREL W LYTLE** ROBERT B GREEGOR EDWARD C MARQUES *(THE BOEING COMPANY)*	**Catalyst Characterization by X-ray Absorption Spectroscopy**
2050B	3/1/88	**R PAUL PHIZACKERLEY** MICHAEL SOLTIS JANOS HADJU *(SSRL)*	**Laue Diffraction Trials with Protein Crystals on PEP**

2051Bp 3/1/88 **BRIAN J HALES** — **X-Ray Absorption of Vanadium and Tungsten Nitrogenases and Storage Proteins**
STEPHEN P CRAMER
GRAHAM N GEORGE
CATHEY COYLE
(LOUISIANA STATE UNIVERSITY)

2052M 3/1/88 **FRANK L GALEENER** — **X-Ray Induction of Charge Trapping Defects in Amorphous SiO_2**
DAVID B KERWIN
(COLORADO STATE UNIVERSITY)

2053Mp 3/10/88 **G MEITZNER** — **Physical and Electronic Structure of Support Bimetallic Catalysts**
FARREL W LYTLE
JOHN H SINFELT
GRAYSON H VIA
(EXXON RESEARCH & ENGINEERING)

2054B 3/11/88 **S A COLLETT** — **The Crystal Structure of Metallothionein**
R PAUL PHIZACKERLEY
ETHAN A MERRITT
(RESEARCH INSTITUTE OF SCRIPPS)

2055M 3/15/88 **TIMOTHY M HAYES** — **Shallow and Deep Donors in $Ga_{1-x}Al_xAs$ Semiconducting Alloys**
P GIBART
D L WILLIAMSON
(COLORADO SCHOOL OF MINES)

2056Mp 3/15/88 **H K MAO** — **Measurements in the Terapascal Range and Hydrogen Metallization**
ALBERT C THOMPSON
R J HEMLEY
A P JEPHCOAT
J H UNDERWOOD
Y WU
(CARNEGIE INSTITUTE)

2057M 3/15/88 **WILLIAM W MOSES** — **Search for Ultra-Fast Heavy Atom Scintilliators**
STEPHEN E DERENZO
(LAWRENCE BERKELEY LABORATORY)

2058M 3/15/88 **DANIEL A SCHERSON** — **In-Situ EXAFS Transition Metal Macrocycles Adsorbed on Electrode Surfaces**
PHILIP N ROSS
(CASE WESTERN RESERVE UNIVERSITY)

2059M 3/15/88 **MIKE TONEY** — **X-Ray Scattering of Amorphous and Hydrogenated Amorphous Carbon Thin Films**
PAUL H FUOSS
SEAN BRENNAN
(IBM RESEARCH LABORATORY)

2060Bp 3/15/88 **LINDA S POWERS** — **Structure-Function Studies of the Active Site of Lignases, Peroxidases, and Models**
S AUST
J BUMPUS
J LI
M TIEN
(UTAH STATE UNIVERSITY)

2061M	3/17/88	OWEN MELROY MIKE TONEY *(IBM RESEARCH LABORATORY)*	**Electrochemically Deposited Metal Monolayers: Structure, Compressibility and Growth**
2062Mp	3/17/88	WILLIAM K WARBURTON EDWARD FRANCO PAUL PLAG *(X-RAY INSTRUMENTATION ASSOCIATES)*	**Structural Improvements in Multilayers for Instrumentation Applications**
2063Mp	3/17/88	HOWARD D DEWALD *(OHIO UNIVERSITY)*	**Characterization of Electrochemical Processes by X-Ray Absorption Spectroscopy**
2064M	3/21/88	IAN D RAISTRICK STEVE D CONRADSON ANTONIO REDONDO *(LOS ALAMOS NATIONAL LABORATORY)*	**X-Ray Absorption Studies or Bimetallic Electrocatalysts for C_1 Oxidation**
2065M	3/24/88	ALBERT C THOMPSON Y WU J H UNDERWOOD ROBERT D GIAUQUE *(LAWRENCE BERKELEY LABORATORY)*	**Elemental X-Ray Imaging with PEP Using an X-Ray Microscope**
2067M	4/21/88	JAMES E PENNER-HAHN I-WEI CHEN T Y TIEN *(UNIVERSITY OF MICHIGAN)*	**X-Ray Absorption Spectroscopy of Transformation-Toughened Zirconia Ceramics**
2068Bp	5/7/88	JAMES E PENNER-HAHN DIMITRI COUCOUVANIS MAX O FUNK DAVID P BALLOU CHRISTOPHER J BATIE HIM-TAI TSANG *(UNIVERSITY OF MICHIGAN)*	**X-Ray Absorption Spectroscopy of Phthalate Dioxygenase and Soybean Lipoxygenase**
2069Mp	5/7/88	JAMES E PENNER-HAHN DAVID CURTIS *(UNIVERSITY OF MICHIGAN)*	**XAS of Metal-Sulfur Clusters Supported on Metal Oxide Surfaces**
2070B	9/2/88	MARTHA LUDWIG CARL C CORRELL ETHAN A MERRITT HENRY BELLAMY R PAUL PHIZACKERLEY *(UNIVERSITY OF MICHIGAN)*	**Multiple-Wave Length X-Ray Diffraction Analysis of Phthalate Oxygenase Reductase**
2071Bp	9/13/88	E A STERN PETERIS LIVINS DAN THIEL AARON LEWIS *(UNIVERSITY OF WASHINGTON)*	**Measurements on Focussed X-Rays for use with Microsecond Resolved XAFS**

2072M	9/13/88	**J KRIM** MIKE TONEY R CHIARELLO C L WANG *(NORTHEASTERN UNIVERSITY)*	**Surface Melting of Xenon Adsorbed on Au(111)**
2073Mp	8/31/88	**JEFF J HOYT** F A GARNER K C RUSSELL *(WASHINGTON STATE UNIVERSITY)*	**Phase Separation in Fe-Ni**
2074Vp	9/13/88	**BRAD PATE** J WU WILLIAM E SPICER INGOLF LINDAU *(SSRL)*	**Electronic and Geometric Properties of Impurities ON/IN Carbon**
2075M	9/13/88	**GLENN A WAYCHUNAS** BRIGID A REA CHRISTOPHER A FULLER JAMES A DAVIS *(STANFORD UNIVERSITY)*	**Characterization of Ferrihydrite Reactive Surface Sites and Structure**
2076Mp	9/13/88	**GLENN A WAYCHUNAS** RICHARD J REEDER CHARLES R ROS WAYNE A DOLLASE *(STANFORD UNIVERSITY)*	**Investigation of Short Range Order in Mineralogical Solid Solutions**

LETTERS OF INTENT

9034	6/1/90	**JOE WOICIK** FABIO COMIN TOM F KENDELEWICZ PIERO PIANETTA *(STANFORD UNIVERSITY)*	**In-Situ Surface EXAFS Studies of Ge/Si(111), Ge/Mo(110), and Model Metal Semiconductor Interfaces**
9035	6/1/90	**THOMAS P RUSSELL** BRAD FACTOR *(IBM RESEARCH LABORATORY)*	**Glancing Angle Diffraction Studies of Polymer Films**
9036	6/1/90	**S R STOCK** QUINTIN C JOHNSON ULRICH BONSE MONTE NICHOLS ZOPHIA U REK JOHN H KINNEY *(GEORGIA INSTITUTE OF TECHNOLOGY)*	**Microtomography of Damage in Cu-1% Sb Deformed at Elevated Temperatures**

9037	6/1/90	R COLELLA Q ZHAO STEPHEN M DURBIN *(PURDUE UNIVERSITY)*	**Overhauser's Theory of Charge Density Waves**
9038	6/1/90	STUART RICE *(UNIVERSITY OF CHICAGO)*	**Properties of Liquid Surfaces and Ampiphile Monolayers Supported on Liquid Surfaces**
9039	6/1/90	J JAKLEVIC *(LAWRENCE BERKELEY LABORATORY)*	**EXAFS III-V Compounds Semiconductors**
9040	6/1/89	TROY W BARBEE, JR. *(LAWRENCE LIVERMORE NATIONAL LABORATORY)*	**Multilayer Structures and Multilayer X-ray Optics**
9041	3/17/89	THOMAS P RUSSELL *(IBM RESEARCH LABORATORY)*	**Testing of 1-4 Detector as Replacement Polymers**
9042	3/17/89	ALICE P GAST *(STANFORD UNIVERSITY)*	**Polymer and Colloidal Structure in Solution**
9043	3/17/89	JOHN C BILELLO ZOPHIA U REK *(CALIFORNIA STATE UNIVERSITY)*	**Characterization of Thin Metallic Layers**
9044	3/17/89	JOHN C BILELLO ZOPHIA U REK *(CALIFORNIA STATE UNIVERSITY)*	**Crack Propagation in Refractory Metals**

ROTATION CAMERA PROPOSALS

Access to the rotation camera facility for protein crystallography is through the submittal of a brief application which is reviewed by the Biology Sub-panel of the PRP on a short turnaround basis. The 23 rotation camera proposals active in 1988 are listed below.

1A57B	2/1/87	BRIAN W MATTHEWS STEVE RODERICK LARRY WEAVER *(UNIVERSITY OF OREGON)*	**Structural Studies of Luciferase and other Proteins**
1A62B	7/8/87	C D STOUT ARTHUR ROBBINS S A COLLETT *(RESEARCH INSTITUTE OF SCRIPPS)*	**High Resolution Data Collection on Ferredoxin**
1A63B	7/8/87	JANUSZ M SOWADSKI GORDON GILL SUSAN TAYLOR *(UNIVERSITY OF CALIFORNIA)*	**Catalytic Subunit of Protein Kinase (cAMP dependent)**

1A66B	8/14/87	**IAN WILSON** JAMES RINI JAIRO AREVALO GUY LAMBERT ENRICO STURA *(RESEARCH INSTITUTE OF SCRIPPS)*	**The Structure of Antibodies, Antigens and Antibody-Antigen Complexes**
1A68B	8/5/87	**MICHAEL G ROSSMANN** KLAUS PIONTEK JOHN BADGER S KRISHNASWAMY PHILIPPE DUMAS SANGSOO KIM THOMAS J SMITH *(PURDUE UNIVERSITY)*	**Virus Structure**
1A71B	9/23/87	**MARCOS H HATADA** BRADFORD GRAVES JULANN MILLER *(HOFFMANN-LA ROCHE INC.)*	**Interleukin 2**
1A72B	9/23/87	**MARCOS H HATADA** BRADFORD GRAVES JULANN MILLER *(HOFFMANN-LA ROCHE INC.)*	**Interleukin 2: Interleukin 2 Receptor**
1A73B	9/23/87	**MARCOS H HATADA** BRADFORD GRAVES JULANN MILLER *(HOFFMANN-LA ROCHE INC.)*	**Interleukin 1 Δ**
1A74B	9/23/87	**C D STOUT** ARTHUR ROBBINS S A COLLETT *(RESEARCH INSTITUTE OF SCRIPPS)*	**High Resolution Data Collection on Aconitase**
1A75B	9/23/87	**ROBERT M STROUD** V RAMALINGAM CYNTHIA WOLBERGER MICHAEL SHUSTER MICHAEL MCCARTHY THOMAS EARNEST KATHY KANTARDJIEFF *(UNIVERSITY OF CALIFORNIA)*	**Crystal Structure of Colicin Ia**
1A76B	11/5/87	**IVAN RAYMENT** *(UNIVERSITY OF WISCONSIN)*	**Crystallographic Studies of Myosin Subfragment-1**

1A78B	12/17/87	**ADA YONATH** ILONA MAKOWSKI FELIX FROLOW KLAUS BARTELS HAKON HOPE KLAUS V BOEHLEN *(WEIZMANN INSTITUTE)*	**Crystallographic Studies on Ribosomal Particles**
1A79B	12/28/87	**SUNG-HOU KIM** BART DE VOS MIKE MILBURM LIANG TONG CHULHEE KANG *(UNIVERSITY OF CALIFORNIA)*	**Redesignal Sweet Protein**
1A80B	1/1/88	**THOMAS EARNEST** MICHAEL SHUSTER JULIE EARNEST CYNTHIA WOLBERGER MICHAEL MCCARTHY ROBERT M STROUD *(UNIVERSITY OF CALIFORNIA)*	**Crystal Structure of Transmembrane Ion Channels: Colicin Ia and the Nicotinic Acetylcholine Receptor**
1A81B	1/1/88	**DOUGLAS C REES** *(UNIVERSITY OF CALIFORNIA)*	**Structures of Electron-Transfer Proteins**
1A82B	3/1/88	**MICHAEL N G JAMES** *(UNIVERSITY OF ALBERTA)*	**High Resolution Crystal Structure of Human Kidney Renin**
1A83B	3/1/88	**F SCOTT MATHEWS** LONGYIN CHEN *(WASHINGTON UNIVERSITY)*	**Methylamine Dehydrogenase-Amicyanin Complex**
1A84B	3/1/88	**WILLIAM J RAY** MAQSUD RAHMAN MICHAEL G ROSSMANN *(PURDUE UNIVERSITY)*	**Structure of an Enzyme Substrate Analog Complex**
1A85B	3/1/88	**HANS E PARGE** JOHN A TAINER ELIZABETH D GETZOFF *(RESEARCH INSTITUTE OF SCRIPPS)*	**Heavy Atom Screening and Data Collection on Pilin**
1A86B	3/1/88	**LI LIANG** DONGSHENG LIU R PAUL PHIZACKERLEY *(IHEP)*	**Diffraction Data Collection of R-Phycoerythrin**

1A87B	3/21/88	**JOHN E JOHNSON** JEAN-PIERRE WERY JEAN CAVARELLI ZHONGGUO CHEN PAUL SEHNKE *(PURDUE UNIVERSITY)*	**Data Collection from Plant Viruses (with partially ordered RNA) and Insect Viruses**
1A88B	4/1/88	**MING LUO** S V L NARAYANA GILLIAN M AIR PAT BOSSART *(UNIVERSITY OF ALABAMA-BIRMINGHAM)*	**Structures of Viruses and Virus Proteins**
1A89B	5/9/88	**S C HARRISON** DON C WILEY *(HARVARD UNIVERSITY)*	**Studies of the CD4 Glycoprotein**

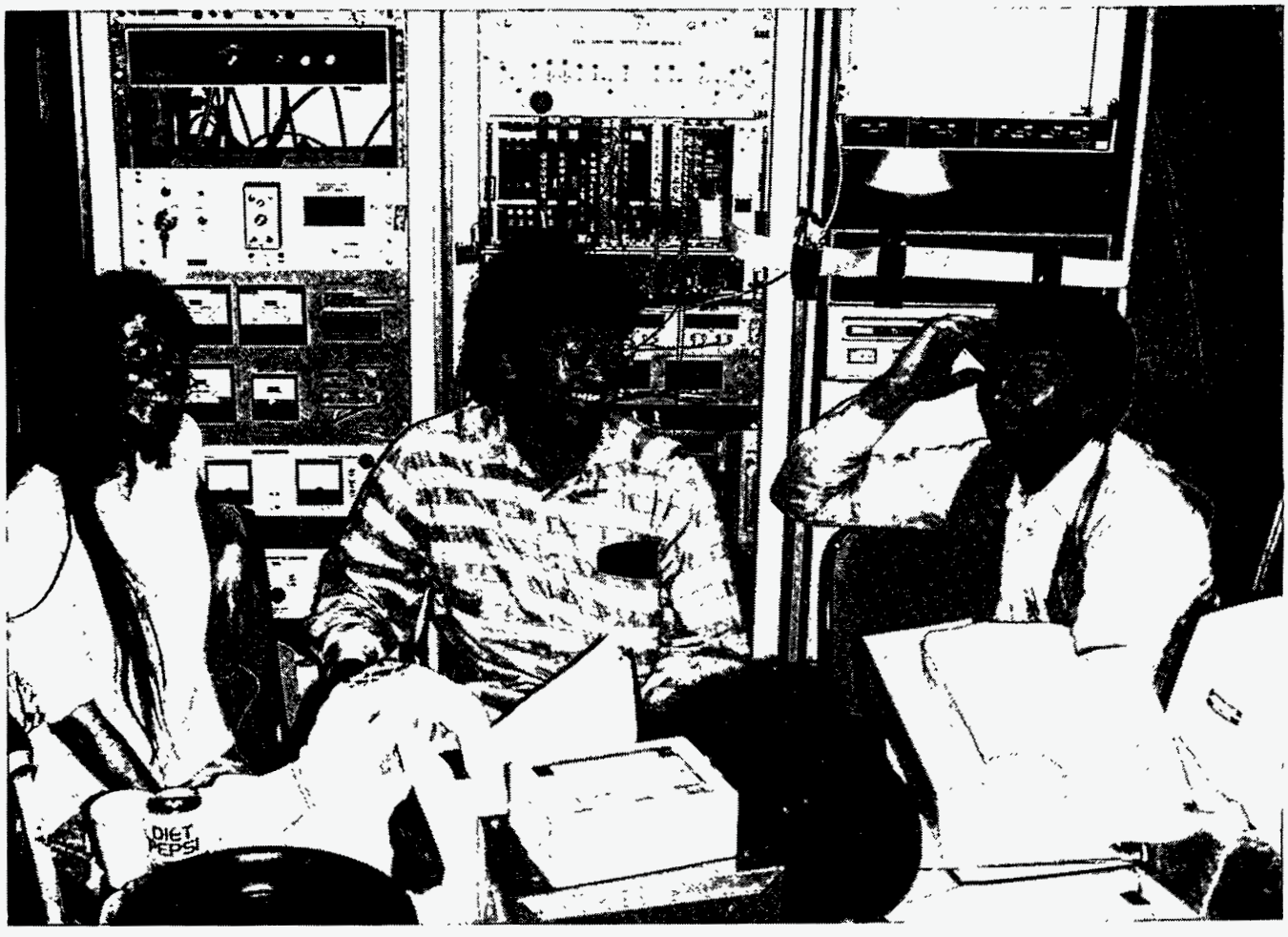

Mary Beth Rice (Stanford University), Soichi Wakatsuki (Stanford University), and Bob Fairclough (University of Chicago) collaborating on station 4-2.

IX SSRL EXPERIMENTERS AND PROPOSALS BY INSTITUTIONS

As of December 31, 1988 there were 688 experimenters from 130 institutions officially involved with active proposals at SSRL. In addition, over a 100 others (graduate students, etc.) participated in work at the laboratory in collaboration with these scientists. The 99 United States Institutions included 62 Universities, 23 private companies and 14 government laboratories.

U.S. COMPANIES: 3M CENTRAL RESEARCH LABORATORY, ARACOR, AT&T BELL LABORATORIES, BECTON DICKINSON & CO. RSCH. CNTR., BOEING COMPANY, CHEVRON OIL FIELD RESEARCH COMPANY, CHEVRON RESEARCH COMPANY, EASTMAN KODAK RESEARCH LABORATORY, EPRI, EXXON RESEARCH & ENGINEERING, HEWLETT PACKARD LABORATORIES, HOFFMANN-LA ROCHE INC., IBM RESEARCH LABORATORY, INTEL CORPORATION, MARTIN MARIETTA, MINERAL SEARCH, MONSANTO COMPANY, SCHLUMBERGER DOLL RESEARCH, SIGNETICS CORPORATION, SRI INTERNATIONAL, THE AEROSPACE CORPORATION, X-RAY INSTRUMENTATION ASSOCIATES, XEROX

U.S. LABORATORIES: ARGONNE NATIONAL LABORATORY, BROOKHAVEN NATIONAL LABORATORY, LAWRENCE BERKELEY LABORATORY, LAWRENCE LIVERMORE NATIONAL LABORATORY, LOS ALAMOS NATIONAL LABORATORY, NATIONAL INSTITUTE OF STANDARDS AND TECHNOLOGY, NAVAL RESEARCH LABORATORY, NAVAL WEAPONS CENTER, OAK RIDGE NATIONAL LABORATORY, PACIFIC NORTHWEST LABORATORY, SANDIA NATIONAL LABORATORY, STANFORD SYNCHROTRON RADIATION LABORATORY, US GEOLOGICAL SURVEY, WESTERN REGIONAL RSCH. CTR.

U.S. UNIVERSITIES: AMHERST COLLEGE, ARIZONA STATE UNIVERSITY, BOSTON UNIVERSITY, BRIGHAM YOUNG UNIVERSITY, BROWN UNIVERSITY, CALIFORNIA INSTITUTE OF TECHNOLOGY, CALIFORNIA STATE UNIVERSITY, CARNEGIE INSTITUTE, CARNEGIE MELLON UNIVERSITY, CASE WESTERN RESERVE UNIVERSITY, CITY UNIVERSITY OF NEW YORK, COLORADO SCHOOL OF MINES, COLORADO STATE UNIVERSITY, COLUMBIA UNIVERSITY, CORNELL UNIVERSITY, FLORIDA-ATLANTIC UNIVERSITY, GEORGIA INSTITUTE OF TECHNOLOGY, HARVARD MEDICAL SCHOOL, HARVARD UNIVERSITY, HUNTER COLLEGE CUNY, LOUISIANA STATE UNIVERSITY, MASSACHUSETTS INSTITUTE OF TECHNOLOGY, NORTH CAROLINA STATE UNIVERSITY, NORTHEASTERN UNIVERSITY, NORTHWESTERN UNIVERSITY, OHIO STATE UNIVERSITY, OHIO UNIVERSITY, PENNSYLVANIA STATE UNIVERSITY, PRINCETON UNIVERSITY, PURDUE UNIVERSITY, RESEARCH INSTITUTE OF SCRIPPS CLINIC, STANFORD UNIVERSITY, STATE UNIVERSITY-NEW YORK, STEVENS INSTITUTE OF TECHNOLOGY, TEXAS A&M UNIVERSITY, UNIVERSITY CITY SCIENCE CENTER, UNIVERSITY OF ALABAMA-BIRMINGHAM, UNIVERSITY OF ARIZONA, UNIVERSITY OF CALIFORNIA, UNIVERSITY OF CHICAGO, UNIVERSITY OF CINCINNATI, UNIVERSITY OF COLORADO, UNIVERSITY OF GEORGIA, UNIVERSITY OF HAWAII, UNIVERSITY OF ILLINOIS, UNIVERSITY OF KENTUCKY, UNIVERSITY OF MICHIGAN, UNIVERSITY OF MINNESOTA, UNIVERSITY OF MISSISSIPPI, UNIVERSITY OF NEW MEXICO, UNIVERSITY OF NOTRE DAME, UNIVERSITY OF OREGON, UNIVERSITY OF PENNSYLVANIA, UNIVERSITY OF PUERTO RICO, UNIVERSITY OF SOUTH CAROLINA, UNIVERSITY OF SOUTH FLORIDA, UNIVERSITY OF TOLEDO, UNIVERSITY OF WASHINGTON, UNIVERSITY OF WISCONSIN, UTAH STATE UNIVERSITY, WASHINGTON STATE UNIVERSITY, WASHINGTON UNIVERSITY

FOREIGN: ALCAN INTERNATIONAL LIMITED, CHALMERS INSTITUTE OF TECHNOLOGY, CNRS, ELECTROTECHNICAL LABORATORY, EUROPEAN SYNCHROTRON RADIATION FACILITY, HC ORSTED INSTITUTE, IHEP, ISTITUTO DI FISICA DEL POLITECNICO, ISTITUTO DI STRUTTURA DELLA MATERIA, KAROLINSKA INSTITUTE, KING'S COLLEGE, LINKOPING UNIVERSITY, MAX-PLANCK INSTITUTE FUR MED FORSCH, MEDICAL NOBEL INSTITUTE, MITSUBISHI PETROCHEMICAL CO., LTD., MPG HAMBURG, OXFORD UNIVERSITY, POLITECNICO DI MILANO RISO NATIONAL LABORATORY, SIMON FRASER UNIVERSITY, UNIVERSITA DI BRESCIA, UNIVERSITA DI MODENA, UNIVERSITA DI ROMA, UNIVERSITAT BAYREUTH, UNIVERSITAT BONN, UNIVERSITY OF ALBERTA, UNIVERSITY OF DORTMUND, UNIVERSITY OF SHEFFIELD, UNIVERSITY OF SUSSEX, WEIZMANN INSTITUTE, ZHEJIANG UNIVERSITY

SSRL EXPERIMENTERS AND PROPOSALS BY INSTITUTION
UNITED STATES INSTITUTIONS

AMHERST COLLEGE

D.M. DOOLEY	1053

ARACOR

E. FRANCO	2062
P. PLAG	2062

ARGONNE NATIONAL LABORATORY

E.E . ALP	2012
M. BLOCH	882
D. MONCTON	898, 1001
G.K. SHENOY	2012
L. SODERHOLM	2012
J. VICCARO	1074

ARIZONA STATE UNIVERSITY

T. GROY	2020
S.H. LIN	2020
J.R. SCHOONOVER	2020

AT&T BELL LABORATORIES

J. BEVK	1044
M. CHANCE	1042
P.H. CITRIN	947
P.H. FUOSS	1095, 1096, 2044, 2045, 2059
D.W. KISKER	1095, 1096
M.A . MARCUS	1044, 1045
S.G.J. MOCHRIE	2017
L. NORTON	1095, 1096, 2044
J.M. POATE	1013
I.K. ROBINSON	997, 1094
J.E. ROWE	1013
F. SETTE	1013
M. SEUL	1029
J.J. YEH	935

BECTON DICKINSON & COMPANY RESEARCH CENTER

A. NAQUI	1043

BOEING COMPANY

R.B. GREEGOR	100, 956, 1049, 1097, 2021, 2038, 2049
F.W. LYTLE	100, 956, 1026, 1049, 1069, 1097, 2021, 2028, 2038, 2049, 2053
E.C. MARQUES	2049
D.R. SANDSTROM	1026

BROOKHAVEN NATIONAL LABORATORY

J.D . AXE	898
H. CHEN	1072
S.P. CRAMER	969, 981, 1030, 1039, 1040, 1084, 1089, 1092, 2051
D.A. FISCHER	1015
L.D. GIBBS	898, 2017
S.M. HEALD	1072, 1073, 1074
S.M. KHALID	1043
B. OCKO	2017
J. PHILLIPS	2007
M. SUENAGA	1073
W. THOMLINSON	1046
J.M. TRANQUADA	1073, 2005

BOSTON UNIVERSITY

K.F. LUDWIG	1008

BRIGHAM YOUNG UNIVERSITY

M.W. HILL	1069, 2021
N. MANGELSON	1069, 2021

BROWN UNIVERSITY

M. ALTMAN	997
P.J. ESTRUP	997

CALIFORNIA INSTITUTE OF TECHNOLOGY

S.I. CHAN	1067
N.S. LEWIS	1078
P.M. LI	1067

CALIFORNIA STATE UNIVERSITY

S. ARNOLD	1099, 2000
C. BUSTILLO	1099, 2000
D. HELMOLDT	1099, 2000
R. ITHNIN	1099, 2000
M.C. LEI	1025, 1099, 2000
J. SATCHER	1099, 2000
S.C. WEAVER	1025
P. ZIA	1025

CARNEGIE INSTITUTE

R.J. HEMLEY	2056
A.P. JEPHCOAT	2056
H. K. MAO	1064, 2056

CARNEGIE MELLON UNIVERSITY

R.F. HAINSEY	2014
J.D. SHINDLER	2014
R.M. SUTER	2014
J.D. WHITTAKER	2048

CASE WESTERN RESERVE UNIVERSITY

D.A. SCHERSON	1098, 2058

CHEVRON OIL FIELD RESEARCH COMPANY

R.M.K. CARLSON	1033

CHEVRON RESEARCH COMPANY

G. ZHANG	1043

CITY UNIVERSITY OF NEW YORK

P.A. MONTANO	2012

COLORADO SCHOOL OF MINES

T.E. FURTAK	1090
T.M. HAYES	1037, 1090, 1091, 2055
G. KRAUSS	1037
D.L. WILLIAMSON	1037, 1091, 2055

COLORADO STATE UNIVERSITY

F.L. GALEENER	2052
D.B. KERWIN	2052

COLUMBIA UNIVERSITY

M. CUFF	1087
W.A. HENDRICKSON	1087
J. HORTON	1087
S.R. HUBBARD	1012, 1087
S.J. LIPPARD	2030
H.M.K. MURTHY	1087
A. PAHLER	1087
W.E. ROYER	1087
W. YANG	1087

CORNELL UNIVERSITY

A. LEWIS	2071
D. THIEL	2071

EASTMAN KODAK RESEARCH LABORATORY

T.A. SMITH	2033

EPRI

H. OCKEN	2028

EXXON RESEARCH & ENGINEERING

M.W.W. ADAMS	1030
C. COYLE	2051
K.L. D'AMICO	898
P.M. EISENBERGER	882, 928, 998, 1001
G.N. GEORGE	1030, 1039, 1083, 1084, 1089, 2051
J.L. GLAND	1015
G.J. HUGHES	998
K.S. LIANG	928, 998, 1001
G. MEITZNER	2053
V. MINAK	1030
J.M . NEWSAM	1001
R.C. PRINCE	1039, 1083, 1084
C.R. SAFINYA	1001, 1010, 2042
J. H. SINFELT	1001, 2053
S.K. SINHA	1001
E. SIROTA	1034, 2042
G.S. SMITH	2042
E.I. STIEFEL	1030
B. VARADY	1010
G.H. VIA	1001, 2053

FLORIDA-ATLANTIC UNIVERSITY

F.A . SCHULTZ	1055

GEORGIA INSTITUTE OF TECHNOLOGY

S.D. ANTOLOVICH	2015
Y.H. CHUNG	1056
R.H. FELTON	1068
S.R. STOCK	1056, 2015, 9036
G. WEBB	2015

HARVARD MEDICAL SCHOOL

D. AULD	1042
B. HOLMQUIST	1042
J. RIORDAN	1042
B. VALLEE	1042

HARVARD UNIVERSITY

S. AMADOR	1034
C.M. FRIEND	1080
S.C. HARRISON	1A89
A.C. LIU	1080
J.T. ROBERTS	1080
D.C. WILEY	1A89

HEWLETT PACKARD LABORATORIES

A. FISCHER-COLBRIE	1093
S. LADERMAN	1093
J. MOLL	1093

HOFFMANN-LA ROCHE INC.

B. GRAVES	1A71, 1A72, 1A73
M.H. HATADA	1A71, 1A72, 1A73
J. MILLER	1A71, 1A72, 1A73

HUNTER COLLEGE CUNY

M.L . DENBOER	897

IBM RESEARCH LABORATORY

C. ERICKSON	1021
J.G. GORDON	1063
G. HELD	1058
P.M. HORN	1058
T.C. HUANG	1021
O. MELROY	1063, 2003, 2061
S.S.P. PARKIN	1099, 2000
W. PARRISH	1021
T.P. RUSSELL	2009, 9035
M. SAMANT	1063
J. STOHR	963, 2009
M. TONEY	2003, 2059, 2061, 2072

INTEL CORPORATION

D. SELIGSON	2037

LAWRENCE BERKELEY LABORATORY

J.V. ACRIVOS	1025, 1099, 2000
C.C. BAHR	943
J.J. BARTON	943
S.E. DERENZO	2057
V. DEROSE	2010
S. DEXHEIMER	2010
T. FERRETT	943
R.D. GIAUQUE	2065
R. GUILES	2010
P.A. HEIMANN	943
A.L. JOHNSON	943
M.P. KLEIN	2000, 2010
J.B. KORTRIGHT	2018, 9900
A. MCDERMOTT	2010
W.W. MOSES	2057
E. PAPARAZZO	943
M.N. PIANCASTELLI	943
S.W. ROBEY	943
P. N. ROSS	1098, 2058
K. SAUER	2010

LAWRENCE BERKELEY LABORATORY - *(Continued)*

D.A. SHIRLEY	943
D.H. TEMPLETON	957
L.K. TEMPLETON	957
L.J. TERMINELLO	943
A.C. THOMPSON	1046, 2056, 2065
J.H. UNDERWOOD	2056, 2065
A. SCHACH V WITTENAU	943
Y. WU	2056, 2065
J.L. ZIMMERMANN	2010

LAWRENCE LIVERMORE NATIONAL LABORATORY

J. AKELLA	1064
T.W. BARBEE, JR.	9040
R.A. DAY	1054
N. DEL GRANDE	9901
S. FLETCHER	1054
J. HENDERSON	2013
Q.C. JOHNSON	1064, 9036
D. KANIA	2011
J.H. KINNEY	1054, 9036
D. KNAPP	2013
E. M. LARSON	2038
H.E . MARTZ	1054
R.W. RYON	1054
G.S. SMITH	1064
G. TIRSELL	9901
J. TREBES	2011
M.J. WEBER	9901, 9902
L.C. WILSON	2045, 9902

LOS ALAMOS NATIONAL LABORATORY

R.J. BARTLETT	2013
T. BOWLES	2013
S.D. CONRADSON	1027, 2023, 2024, 2064
P.G. ELLER	2038
J.A. FEE	1035
Z. FISK	2023
J.A. GOLDSTONE	2016
G. KWEI	2016
A.C. LAWSON	2016
R. MARTIN	2013
J.D. PURSON	2038
I.D. RAISTRICK	2023, 2064
A. REDONDO	2023, 2064
H. ROBERTSON	2013
A. SATTLEBERGER	2024
B. SWANSON	1027, 2024

LOS ALAMOS NATIONAL LABORATORY - *(Continued)*

W.J. TRELA	2013
R.B. VON DREELE	2016
D. WARK	2013
J. WILKERSON	2013
A. WILLIAMS	2016
W. WOODRUFF	1027

LOUISIANA STATE UNIVERSITY

B.J. HALES	2051

3M CENTRAL RESEARCH LABORATORY

C.- L. TSAI	1044, 1045

MARTIN MARIETTA

F. M. KUSTAS	1091

MINERAL SEARCH

L.R. BERNSTEIN	1051

MIT

R.H. BEER	2030
J.G. BENTSEN	2030
R.J. BIRGENEAU	997, 2002
J.D. BROCK	2002
J.D. LITSTER	2002
K.C. RUSSELL	2073
S. SUBRAMANIAM	1029

MONSANTO COMPANY

L. LIM	1019

NATIONAL INSTITUTE OF STANDARDS AND TECHNOLGOY

M.I. BELL	910, 973
C.E. BOULDIN	910,973, 1032
P.L. COWAN	1086
R.D. DESLATTES	1086
R.A. FORMAN	910, 973
D.W. LINDLE	943, 1086

NAVAL RESEARCH LABORATORY

E.D. DONOVAN	973
G.K. HUBLER	973

NAVAL WEAPONS CENTER

J. ERICKSON	2039
A.K. GREEN	2039
S. LANGSJOEN	2039

NAVAL WEAPONS CENTER - *(Continued)*

P. LAROE	2039
T.- W. NEE	2039
V. REHN	2039
C. SCHWARTZ	2039
W. WIEMER	2039

NORTH CAROLINA STATE UNIVERSITY

D.E. SAYERS	906, 1074
E.C. THEIL	906

NORTHEASTERN UNIVERSITY

R. CHIARELLO	2072
J. KRIM	2072
C.L. WANG	2072

NORTHWESTERN UNIVERSITY

T.V. O'HALLORAN	2047
D. RALSTON	2047
J. WRIGHT	2047

OAK RIDGE NATIONAL LABORATORY

H. CEDERQUIST	1052
B.C. CHAKOUMAKOS	1049
S.B. ELSTON	1052
J. LEVIN	1052
C.S. O	1052
I. SELLIN	105
S. SPOONER	2006
D.M. ZEHNER	2017

OHIO STATE UNIVERSITY

J. O. ALBEN	981, 1061
A. A . CROTEAU	981, 1061
F.G. FIAMINGO	981, 1061
C.F. HEMANN	981, 1061
R. HILLE	1040
K.A . POWELL	981, 1061

OHIO UNIVERSITY

H.D. DEWALD	2063

PACIFIC NORTHWEST LABORATORY

M.J. APTED	1050
G.J. EXARHOS	1050
F.A. GARNER	2073

PENNSYLVANIA STATE UNIVERSITY

R.G. JENKINS	956
M. TIEN	2060

PRINCETON UNIVERSITY

J.T. GROVES	1085
M. STERN	1085

PURDUE UNIVERSITY

J. BADGER	1A68
J. CAVARELLI	1A87
Z. CHEN	1A87
R. COLELLA	2046, 9037
P. DUMAS	1A68
S.M. DURBIN	9037
J.E. JOHNSON	1A87
S. KIM	1A68
S. KRISHNASWAMY	1A68
K. PIONTEK	1A68
M. RAHMAN	1A84
W.J. RAY	1A84
M.G. ROSSMANN	1A68, 1A84
P. SEHNKE	1A87
T.J . SMITH	1A68
J.-P. WERY	1A87
Q. ZHAO	2046, 9037

RESEARCH INSTITUTE OF SCRIPPS CLINIC

J. AREVALO	1A66
S.A. COLLETT	1A62, 1A74, 2054
E.D. GETZOFF	1A85
G. LAMBERT	1A66
H.E. PARGE	1A85
J. RINI	1A66
A. ROBBINS	1A62, 1A74
C.D. STOUT	1A62, 1A74
E. STURA	1A66
J.A . TAINER	1A85
I. WILSON	1A66

SANDIA NATIONAL LABORATORY

G. KUBIAK	2026
J. NELSON	2026
M. NICHOLS	9036
R.H. STULEN	2026

SCHLUMBERGER DOLL RESEARCH

D.R. HINES	1092
J. HOWARD	1089, 1092
W. MURPHY	1089
J. PECK	1089
N. WADA	1092

SIGNETICS CORPORATION

B. COULMAN	1056

SRI INTERNATIONAL

D.C. LORENTS	1062
R.L. SHARPLESS	1062

SSRL

H. BELLAMY	2070
A. BIENENSTOCK	1008, 1048, 1060, 2027, 2044, 2045
S. BRENNAN	1048, 1086, 2027, 2044, 2059
G.S. BROWN	1046, 2013
A.D. COX	1025
B. HEDMAN	1055, 2029, 2030, 2031, 2032, 2033, 2034
K.O. HODGSON	995, 1012, 1055, 1076, 1078, 2029, 2030, 2031, 2032, 2033, 2034, 2035
I. LINDAU	897, 935,941, 1028, 2074
B. PATE	2074
R.P. PHIZACKERLEY	1019, 1087, 1A86, 2050, 2054, 2070
P. PIANETTA	2011, 2026, 2037, 9034
Z.U. REK	1056, 2015, 2028, 9036
M. SOLTIS	2050
U.W. SPANN	2035
T. TROXEL	1082
J. WU	2074

STANFORD UNIVERSITY

K. BERTNESS	935
M. BOUDART	1065, 1071
C. BOWMAN	935
G.E. BROWN, JR	994, 995, 999
K. BUTCHER	1022
K. CHAR	1093
T. CHIANG	935
J.P. COLLMAN	2034
R.J. DAVIS	1065
S.V. DIDZIULIS	1022
S. DONIACH	1012, 1076, 2035
S.J. EGLASH	935
B. FACTOR	1080, 2027, 9035
D. FRIEDMAN	935
T.H. GEBALLE	1079, 1093
D.C. HARRISON	1046
K.F. HAYES	995
R. HOFSTADTER	1046
J. HWANG	2026
W.A . JACKSON	999
J. KAHN	2044

STANFORD UNIVERSITY - *(Continued)*

T.F. KENDELEWICZ	935, 9034
A.D. KENT	1093
R. KERNOFF	1046
P. KING	2037
J.O. LECKIE	995
J.-Y. LIN	1022
R.J. MADIX	1080
C. MCCANTS	935
N. MISSERT	1093
N. NEWMAN	935
J. NOGAMI	935
B. OH	1093
J. OTIS	1046
L. PAN	2037
G.A . PARKS	995
C.W. PONADER	999
E. PUPPIN	935, 941
M. RICE	1060, 2045
S. ROTHFUS	999
E. RUBENSTEIN	1046
Z. SHEN	941
K. SHIH	935
J. SILBERMAN	935
E.I. SOLOMON	1022, 2031
J. SOLOMON	1080
W.E. SPICER	935, 941, 2074
C. KILBOURNE	1048
J.Z. SUN	1093
G. TAN	2031
B.J. TUFTS	1078
G.P. VALENCA	1071
S. WAKATSUKI	1076, 2035
G.A. WAYCHUNAS	994, 995, 999, 1050, 1051, 1088, 2075, 2076
M.D. WILLIAMS	935
J. WOICIK	935, 9034
H.D. ZEMAN	1046
M.B. ZISK	2034

STATE UNIVERSITY-NEW YORK

R.J. REEDER	2076
S. WHITTINGHAM	1092

STEVENS INSTITUTE OF TECHNOLOGY

G.M. ROTHBERG	897

TEXAS A&M UNIVERSITY

D.A. CHURCH	1052

THE AEROSPACE CORPORATION

P.D. FLEISCHAUER	2001
J.R. LINCE	2001

UNIVERSITY CITY SCIENCE CENTER

G. BUNKER	1043, 2022, 2025
T.E. KING	2025
K. ZHANG	2022, 2025

UNIVERSITY OF ALABAMA-BIRMINGHAM

G.M. AIR	1A88
P. BOSSART	1A88
M. LUO	1A88
S.V.L. NARAYANA	1A88

UNIVERSITY OF ARIZONA

J. ENEMARK	1030

UNIVERSITY OF CALIFORNIA

F.G. BRIDGES	1017, 1079, 2040
B.K. BURGESS	2029
B. CLARK	1018
D.S. CLARK	2008
B.E.C. DAVIS	1018
D. DE FONTAINE	1018, 2006
B. DE VOS	1A79
J. DENLINGER	2018, 2019
W.A. DOLLASE	2076
J. EARNEST	1A80
T. EARNEST	1A75, 1A80
G. GILL	1A63
R.M. GUINN	2008
H. HOPE	1A78
Z.-Q. HUANG	943
C. KANG	1A79
K. KANTARDJIEFF	1A75
S. KIM	943
S.-H. KIM	1A79
M. KRAITCHMAN	1018, 2006
D. A. LARSON	1082
T. LEUNG	943
C. LING	1082
S. LIU	943
G.A. MARG	2008
M. MCCARTHY	1A75, 1A80
L. MEDHURST	943
M. MILBURM	1A79
B. NIU	943
C. OGATA	1087
M. OLMSTEAD	2018, 2019

UNIVERSITY OF CALIFORNIA - *(Continued)*

T.L. PHILLIPS	1082
V. RAMALINGAM	1A75
K. RAYMOND	906
D.C. REES	1A81
M. SCHELL	1082
D. SHRIEVE	1082
M. SHUSTER	1A75, 1A80
J.M. SOWADSKI	1A63
R.M. STROUD	1076, 1A75, 1A80, 2035
S. TAYLOR	1A63
L. TONG	1A79
S.A . VAUGHN	2029
L. WANG	943
M. WIEDENMEIR	2006
C. WOLBERGER	1A75, 1A80
F. ZAERA	1015

UNIVERSITY OF CHICAGO

R.H. FAIRCLOUGH	1012
S. RICE	9038
D. RICHMAN	1012

UNIVERSITY OF CINCINNATI

P. BOOLCHAND	1032
E.A. DEUTSCH	991
R.C. ELDER	922, 991, 1066
W.R. HEINEMAN	1066
K. TEPPERMAN	922

UNIVERSITY OF COLORADO

N.A . CLARK	1010, 2042
R. POYTON	2025

UNIVERSITY OF GEORGIA

M. EIDSNESS	1041
R.A. SCOTT	969, 1039, 1041, 1053, 1067

UNIVERSITY OF HAWAII

M.H. MANGHNANI	1059, 1064
L.C. MING	1059, 1064

UNIVERSITY OF ILLINOIS

S.G. SLIGAR	2022

UNIVERSITY OF KENTUCKY

G.P. HUFFMAN	956
F.E. HUGGINS	956
N. SHAH	956

UNIVERSITY OF MICHIGAN

J. ALLEN	1028
B.D. ATHEY	2041
D.P. BALLOU	1035, 2068
C.J. BATIE	1035, 2068
I.- W. CHEN	2067
C.C. CORRELL	2070
D. COUCOUVANIS	2068
M.D. CURTIS	2069
W.D. FRASCH	1085
R. FRONKO	1088, 2047, 2048
D. GHANOTAKIS	1085
R. KERTAYASA	2048
J.P. LANGMORE	2041
M. LUDWIG	2070
V.L. PECORARO	1085
J.E. PENNER-HAHN	1033, 1035, 1050, 1085, 1088, 2047, 2048, 2067, 2068, 2069
M.F. SMITH	2041
T.Y. TIEN	2067
H.-T. TSANG	1035, 1085, 2047, 2068
G. WALDO	1033, 1088
S. WANG	1088
S. WILLIAMS	2041
C.F. YOCUM	1085

UNIVERSITY OF MINNESOTA

W.H. SMYRL	2003

UNIVERSITY OF MISSISSIPPI

W. CLELAND	1030

UNIVERSITY OF NEW MEXICO

T. BEIN	1070
R.C. EWING	1049
K. MOLLER	1070

UNIVERSITY OF NOTRE DAME

K.K. CHIN	935
K. CHOUDHARY	1077

UNIVERSITY OF OREGON

B. CRASEMAN	2013
B. W. MATTHEWS	1A57
S. RODERICK	1A57
S.L. SORENSEN	2013
L. WEAVER	1A57
S.B. WHITFIELD	2013

UNIVERSITY OF PENNSYLVANIA

J.E. BENCI	1081
B. CHANCE	1042, 1043, 2022, 2025
E. DAVIDSON	2025
T.G. FREY	1039
M. IKEDA-SAITO	1083
D.P. POPE	1081

UNIVERSITY OF PUERTO RICO

L. BLUM	1063

UNIVERSITY OF SOUTH CAROLINA

J.H. DAWSON	2032
M. SONO	2032

UNIVERSITY OF SOUTH FLORIDA

L.S. SOLMONSON	1030

UNIVERSITY OF TOLEDO

M.O. FUNK	2068

UNIVERSITY OF WASHINGTON

J. FREUND	1047
B. HOUSER	2005
R. L. INGALLS	100, 1047, 2005
P. LIVINS	2071
E.A. MERRITT	2070
L.B. SORENSEN	1034
E.A . STERN	906, 1068, 2005, 2071
P. VIRAN	100
J.E. WHITMORE	100

UNIVERSITY OF WISCONSIN

G. MARGARITONDO	2043
I. RAYMENT	1A76

US GEOLOGICAL SURVEY WATER RESOURCES DIVISION

J.A. DAVIS	2075
C.A. FULLER	2075
B.A. REA	2075

UTAH STATE UNIVERSITY

S. AUST	2060
J. BUMPUS	2060
J. LI	2060
L.S. POWERS	1042, 2060

WASHINGTON STATE UNIVERSITY

J.J. HOYT	1018, 2006, 2073

WASHINGTON UNIVERSITY

L. CHEN	1A83
F.S. MATHEWS	1019, 1A83

WESTERN REGIONAL RESEARCH CENTER

S.F. GHELLER	1055
W.E. NEWTON	1055

X-RAY INSTRUMENTATION ASSOCIATES

W.K. WARBURTON	1008, 2062

XEROX

R.Z. BACHRACH	908, 959
J.B. BOYCE	1017, 1079, 2040
L.J. BRILLSON	2043
R.D. BRINGANS	908, 959, 2018, 2019
J.C. MIKKELSON	1017
J.E. NORTHRUP	908

SSRL EXPERIMENTERS AND PROPOSALS BY INSTITUTIONS
FOREIGN INSTITUTIONS

ALCAN INTERNATIONAL LIMITED *(Canada)*
R. TIMSIT 2027

ELECTROTECHNICAL LABORATORY *(Japan)*
H. OYANAGI 2022

MITSUBISHI PETROCHEMICAL CO., LTD. *(Japan)*
H. ASAHINA 2034

MPG HAMBURG *(West Germany)*
K.V. BOEHLEN 1A78

ZHEJIANG UNIVERSITY *(People's Republic of China)*
X.-S. ZHANG 943

CNRS *(France)*
P. GIBART 2055

EUROPEAN SYNCHROTRON RADIATION FACILITY *(France)*
E. ZIEGLER 1074

IHEP *(People's Republic of China)*
L. LIANG 1A86
D. LIU 1A86

MAX-PLANCK INSTITUTE FUR MED FORSCH *(West Germany)*
K. BARTELS 1A78

RISO NATIONAL LABORATORY *(Denmark)*
J. BOHR 898, 1094

CHALMERS INSTITUTE OF TECHNOLOGY *(Sweden)*
T. CLAESON 1079

HC ORSTED INSTITUTE *(Denmark)*
H.H. ANDERSEN 1094
L.F. GRAABAEK 1094
A. JOHANSEN 1094
E. JOHNSON 1094
L. SARHOLT-KRIST 1094

ISTITUTO DI FISICA DEL POLITECNICO *(Italy)*
I. ABBATI 941
M. SANCROTTI 941

ISTITUTO DI STRUTTURA DELLA MATERIA *(Italy)*
P. CHIARADIA 2043
F. COMIN 947, 9034

KAROLINSKA INSTITUTE *(Sweden)*
B.- M. SJOBERG 1043

LINKOPING UNIVERSITY *(Sweden)*
R.I.G. UHRBERG 908

MEDICAL NOBEL INSTITUTE *(Sweden)*
P. REICHARD 1043

OXFORD UNIVERSITY *(England)*
J. HADJU 2050

POLITECNICO DI MILANO *(Italy)*
L. BRAICOVICH 941

SIMON FRASER UNIVERSITY *(Canada)*
N. ALBERDING 100
K.R. BAUCHSPIESS 100
D. CROZIER 100, 1047, 2005
A. J. SEARY 100

UNIVERSITA DI BRESCIA *(Italy)*
M. BELLOTTO 1021

UNIVERSITA DI MODENA *(Italy)*
O. BISI 941
C. CALANDRA 941
U. DEL PENNINO 941

UNIVERSITA DI ROMA *(Italy)*
S. NANNARONE 941

UNIVERSITAT BAYREUTH *(West Germany)*
C.R. ROSS 2076

UNIVERSITAT BONN *(West Germany)*
G. WILL 1021

UNIVERSITY OF ALBERTA *(Canada)*
M.N.G. JAMES 1A82

UNIVERSITY OF DORTMUND *(West Germany)*
U. BONSE 9036

UNIVERSITY OF MANCHESTER *(England)*
M. HART 1021

UNIVERSITY OF SHEFFIELD *(England)*
P. HARRISON 906

UNIVERSITY OF SUSSEX *(England)*
B.E. SMITH 1030

WEIZMANN INSTITUTE *(Israel)*
F. FROLOW 1A78
I. MAKOWSKI 1A78
A. YONATH 1A78

X SSRL PUBLICATIONS

The following is a partial list of papers published or submitted in 1988 based on work at SSRL. The list represents 195 publications.

S.T. Ahn, H.W. Kennel, J.D. Plummer, W.A. Tiller, Z.U. Rek and S.R. Stock, **Effect of Oxygen Precipitation on Phosphorus Diffusion in Czochralski Silicon:** Appl. Phys. Lett. 53, 34 (1988)

N. Alberding, K.R. Bauchspiess, J.M. Tranquada, R. Ingalls and E.D. Crozier, **High Pressure EXAFS Study of High T_c Superconductors:** accepted Physica B.

J. Akella, Q. Johnson, G.S. Smith and L.C. Ming, **Diamond-Anvil Cell High Pressure X-Ray Studies on Thorium to 100 GPa:** High Pressure Rsch 1, 91 (1988)

M.R. Antonio, J.F. Brazil, L.C. Glaeser, M. Mehicic and R.G. Teller, **Structural Environments and Oxidation States of Metal Cations in Bismuth Cerium Molydate Solid Solutions by X-ray Absorption Spectroscopy:** J. Phys. Chem. 92, 2338 (1988)

M.R. Antonio, R.G. Teller, D.R. Sandstrom, M. Mehicic and J.F. Brazdil, **Structural Characterization of Bismuth Molybdates by X-ray Absorption Spectroscopy and Powder Neutron Diffraction Profile Analysis:** J. Phys. Chem. 92, 2939 (1988)

M. Ardehali and I. Lindau, **Measurement of the Partial Photoionization Cross-Section and the Asymmetry Parameter of Ag Valence Band Near the 4d Threshold:** submitted to Phys. Rev. B

J. Arthur, **The Use of Simultaneous Reflections for Precise Absolute Energy Calibration of X-Rays:** submitted to Rev. Sci. Instrum.

H. Asahina, M.B. Zisk, B. Hedman, J.T. McDevitt, J.P. Collman and K.O.Hodgson, **X-Ray Absorption Spectroscopic Studies of Rutheniumoctaethylporphyrin Dimers:** submitted to J. Chem. Soc.

H. Asahina, M.B. Zisk, B. Hedman, J.T. McDevitt, J.P. Collman and K.O. Hodgson, **XAS Studies of Ruthenium Octaethylporphyrin Dimers:** accepted for publication in Phys. B

R.Z. Bachrach, R.D. Bringans, L. Swartz, I. Lindau, B.B. Pate, R.G. Carr, N. Hower, B. Youngman, H. Morales and P. Pianetta, **Multi-Undulator Beam Line V at SSRL: A Progress Report:** Nucl. Instrum. & Methods A266, 83 (1988)

K.R. Bauchspiess, N. Alberding and E.D. Crozier, **Comment on Simple Method for the Evaluation of Bond Length from EXAFS Data:** Phys. Rev. Lett. 60, 468 (1988)

K. R. Bauchspiess, E.D. Crozier and R. Ingalls, **The Valence Transition in SmSe:** accepted Physica B.

U. Becker, B. Langer, H.G. Kerkhoff, M. Kupsch, D. Szostak, R. Wehlitz, P.A. Heimann, S.H. Liu, D.W. Lindle, T.A. Ferrett and D.A. Shirley, **Observation of Many New Argon Valence Satellites Near Threshold:** Phys. Rev. Lett. 60, 1490 (1988)

A. Bienenstock, **Synchrotron Radiation Studies: Anomalous Scattering, Grazing Incidence Scattering EXAFS:** J. Non-Crys. Solids 106, 17 (1988)

A. Bienenstock, G. Brown, H. Wiedemann and H. Winick, **PEP as a Synchrotron Radiation Source:** submitted to Rev. Sci. Instrum.

A. Bienenstock, **SSRL Development – Recent and Planned:** Nucl. Instrum. & Methods A266, 13 (1988)

A. Bienenstock and S. Brennan, **Grazing Incidence X-ray Scattering:** to be published in Res. & Dev.

J.B. Boyce, F. Bridges, T. Claeson, J.M. Trarascon and M. Nygren, **X-ray Absorption Edges of Transition-Metal Doped $Y_1Ba_2Cu_3O_{7-\delta}$:** Intl. J. Mod. Phys. 1, 1153 (1988)

J.B. Boyce, F. Bridges, T. Claeson, and T.H. Geballe, **Second Neighbor Shells Around Cu in Oxygen-Deficient and Transition-Metal Doped $Y_1Ba_2Cu_3O_{7-\delta}$:** accepted Physica B.

J.B. Boyce, F. Bridges, T. Claeson, R.S. Howland and T.H. Geballe, **X-Ray Absorption Study of $Y_1Ba_2Cu_3O_7$ and $Gd_1Ba_2Cu_3O_7$ Superconductors:** Mat. Res. Soc. Symp. Proc. 99, 943 (1988)

J.B. Boyce, F. Bridges, T. Claeson, R.S. Howland, T.H. Geballe and M. Nygren, **X-Ray Absorption Study of Oxygen-Deficient and Transition Metal-Doped $Y_1Ba_2Cu_3O_{7-\delta}$:** accepted for publication in Phys. Rev. B

J.B. Boyce, F. Bridges, T. Claeson, T.H. Geballe, G.W. Hull, N. Kitamura and F. Weiss, **X-Ray Absorption Fine Structure Study of the A15 Superconductors $Nb_3(Sn,Sb)$:** Phys. Rev. B37, 54 (1988)

J.B. Boyce, F. Bridges, T. Claeson and T.M. Geballe, **Extended X-Ray Absorption Fine Structure of High T_c Ceramic Superconductors:** Physica Scripta 37, 912 (1988)

S. Brennan, A. Bienenstock and J.E. Keem, **Fluorescence Extended X-Ray Absorption Fine Structure Study of Silicon in Neodymium Iron Boron Rare-Earth Magnets:** J. Appl. Phys. 65, 697 (1988)

R. Carr and J. Yang, **Current to Frequency Converter for Electron Multiplier:** accepted for publication in Rev. Sci. Instrum.

R. Carr, **A New Ultrahigh Vacuum Cleaver for Brittle Materials:** Rev. Sci. Instrum. 56, 989 (1988)

R. Carr, **Finite Element Analysis of PZT Tube Scanner Motion for Scanning Tunneling Microscopy:** accepted for publication in J. Micro.

T.-Y. Chan, H. Gaw, D. Seligson, L. Pan, P.L. King and P. Pianetta, **New Energy-Dependent Soft X-ray Damage in MOS Devices:** SPIE 923, 63 (1988)

G. Comelli, J. Stöhr, W. Jark and B.B. Pate, **Extended X-ray-Absorption Fine-Structure Studies of Diamond and Graphite:** Phys. Rev. B37, 4383 (1988)

S.D. Conradson, A.P. Sattelberger and W.H. Woodruff, **X-ray Absorption Study of Octafluorodirhenate(III): EXAFS Structures and Resonance Raman Spectroscopy of Octahalodirhenates:** J. Amer. Chem. Soc. 110, 1390 (1988)

S.D. Conradson, I.D. Raistrick and G.H. Kwei, **Analysis and Interpretation of EXAFS Data for $YBa_2Cu_3O_{7-\sigma}$ and Related Materials:** accepted for publication in Phys. Rev. B

P.L. Cowan and S. Brennan, **Self-Filtering Crystal Monochromators for Synchrotron X-Radiation:** submitted to Rev. Sci. Instrum.

C.L. Coyle, M.A. Harmer, G.N. George and E.I. Stiefel, **The Conversion of MoS_4^{2-} to $Mo_2S_8^{2-}$ by Organic Disulfides: The Mechanism of an Induced Redox Reaction:** in press Inorg. Chem.

S.P. Cramer, M. Siskin, L.D. Brown and G.N. George, **Characterization of Arsenic in Oil Shale and Oil Shale Derivatives by X-Ray Absorption Spectroscopy:** J. Energy & Fuels 2, 175 (1988)

S.P. Cramer, O. Tencho, M. Yocum and G.N. George, **A 13-Element Ge Detector for Fluorescence EXAFS:** Nucl. Instrum. & Methods A266, 586 (1988)

E.D. Crozier, **Recent Topics in EXAFS Data Analysis:** accepted Physica B.

A.M. DeVos, L. Tong, M.V. Milburn, P.M. Matias, J. Jancarik, S. Noguchi, S. Nishimura, K. Miura, E. Ohtsuka and S-H. Kim, **Three-Dimensional Structure of an Oncogene Protein: Catalytic Domain of Human c-H-ras p21:** Science 239, 888 (1988)

J. DeWitt, B. Hedman, A. Ericson, K.O. Hodgson, J. Bentsen, R. Beer, S.J. Lippard, J. Green and H. Dalton, **X-ray Absorption Spectroscopy of Protein A of Methane Monooxygenase:** accepted for publication in Phys. B

S.V. Didziulis, K.D. Butcher, S.L. Cohen and E.I. Solomon, **The Chemistry of Copper Overlayers on Zinc Oxide Single Crystal Surfaces: Model Active Sites for Cu/ZnO Methanol Synthesis Catalysts:** submitted to J. Am. Chem. Soc.

S.V. Didziulis, S.L. Cohen, K.D. Butcher and E.I. Solomon, **Variable Photon Energy Photoelectron Spectroscopic Studies of Covalent Bonding in $3d^{10}$ Transition Metal Compounds:** Inorg. Chem. 27, 2238 (1988)

S.V. Didziulis, S.L. Cohen, A.A. Gerwirth and E.I. Solomon, **Variable Photon Energy Photoelectron Spectroscopic Studies of Copper Chlorides: An Experimental Probe of Metal-Ligand Bonding and Changes in Electronic Structure on Ionization:** J. Am. Chem. Soc. 110, 250 (1988)

Y.S. Ding, R.A. Register, S.L. Cooper, S.R. Hubbard and K.O. Hodgson, **Anomalous Small-Angle X-ray Scattering from a Sulfonated Polystyrene Ionomer:** in press PMSE Reprints

Y.S. Ding, S.R. Hubbard, K.O. Hodgson, R.A. Register and S.L. Cooper, **Anomalous Small-Angle X-Ray Scattering from a Sulfonated Polystyrene Ionomer:** Macromolecules 21, 1698 (1988)

M.F. Doerner and S. Brennan, **Strain Distribution in Thin Aluminum Films using X-ray Depth Profiling:** J. Appl. Phys. 63, 126 (1988)

M. Dormiani, **Finite Element Analysis of a SiC Mirror Receiving Synchrotron Radiation:** Nucl. Instrum. & Methods A266, 507 (1988)

R.C. Elder, C.E. Lunte, A.F.M.M. Rahman, J.R. Kirchhoff, H.D. Dewald and W.R. Heineman, **In Situ Observation of Copper Redox in a Polymer Modified Electrode Using EXAFS Spectroelectrochemistry:** J. Electroanal. Chem. 240, 361 (1988)

A. Ericson, B. Hedman, K.O. Hodgson, J. Green, H. Dalton, J.G. Bentsen, R.H. Beer and S.J. Lippard, **Structural Characterization by EXAFS Spectroscopy of the Binuclear Iron Center in Protein A of Methane Monooxygenase from Methylococcus capsulatus (Bath):** J. Am. Chem. Soc. 110, 2330 (1988)

R.H. Fairclough, R.M. Stroud, R.C. Miake-Lye, K.O. Hodgson and S. Doniach, **Terbium-Calcium Binding Sites on the Acetylcholine Receptor:** Ann. NY Acad. Sci. 505, 752 (1988)

T.A. Ferrett, D.W. Lindle, P.A. Heimann, M.N. Piancastelli, P.H. Kobrin, H.G. Kerkhoff, U. Becker, W.D. Brewer and D.A. Shirley, **Shape-resonant and Many-electron Effects in the S 2p Photoionization of SF_6:** J. Chem. Phys. 89, 4726 (1988)

T.A. Ferrett, M.N. Piancastelli, D.W. Lindle, P.A. Heimann and D.A. Shirley, **Si 2p and 2s Resonant Excitation and Photoionization in SiF_4:** Phys. Rev. A38, 701 (1988)

A. Fischer-Colbrie, A. Bienenstock, P.H. Fuoss and M.A. Marcus, **Structure and Bonding in Photo-diffused Amorphous Ag-$GeSe_2$ Thin Films:** Phys. Rev. B23, 12388 (1988)

P.H. Fuoss and A. Fischer-Colbrie, **Structure of α-$GeSe_2$ from X-Ray Scattering Measurements:** Phys. Rev. B38, 1875 (1988)

P.H. Fuoss, D.W. Kisker, S. Brennan and J.L. Kahn, **In Situ X-ray Scattering Studies of Organometallic Vapor Phase Epitaxy:** submitted to Mat. Res. Soc. Proc.

P.H. Fuoss, L.J. Norton, S. Brennan and A. Fischer-Colbrie, **X-ray Scattering Studies of the Si-SiO_2 Interface:** Phys. Rev. Lett. 60, 600 (1988)

G.N. George, C.L. Coyle, B.J. Hales and S.P. Cramer, **X-ray Absorption of Azotobacter Vinelandii Vanadium Nitrogenase:** J. Am. Chem. Soc. 110, 4057 (1988)

G.N. George, W.E. Cleland Jr., J.H. Enemark, B.E. Smith, C.A. Kipke, S.A. Roberts and S.P. Cramer, **L-Edge Spectroscopy of Molybdenum Compounds and Enzymes:** submitted to J. Am. Chem. Soc.

G.N. George, J. Byrd and D.R. Winge, **X-ray Absorption Studies of Yeast Copper Metallothionein:** J. Biol. Chem. 263, 8199 (1988)

G.N. George, R.C. Prince, C.A. Kipke, J.H. Enemark and S.P. Cramer, **X-Ray Absorption of Sulfite Oxidase:** in press Biochem. J.

G.N. George, N.A. Turner, R.C. Bray, D.H. Boxer, F.F. Morpeth and S.P. Cramer, **X-Ray Absorption and Electron Paramagnetic Resonance Studies of the Molybdenum Environment in Escherichia coli Nitrate Reductase:** in press Biochem. J.

J. Gland, F. Zaera, D. Fischer, R. Carr and E. Kollin, **Ethylidine Formation Rates on the Pt(111) Surface:** submitted to Chem. Phys. Lett.

R.B. Greegor, F.W. Lytle, R.J. Livak and F.W. Clinard, **X-Ray Spectroscopic Investigation of Pu Substituted Zirconolite:** J. Nucl. Materials 152, 270 (1988)

R.B. Greegor, F.W. Lytle, B.C. Chatoumakos, R.C. Ewing, R. J. Livak, F. W. clinard, E.D. Crozier, N. Alberding, A.J. Seary, G.W. Arnold, M.J. Wever, J. Wong and W.J. Weber, **Application of Various EXAFS Techniques to the Investigation of Structurally Damaged Materials:** accepted Physica B.

M. Green, M. Richter, X. Xing, D. Scherson, K.J. Hanson, P.N. Ross, R. Carr and I. Lindau, **In-Situ Scanning Tunneling Microscopy Studies of the Underpotential Deposition of Lead on Au(111):** accepted for publication in J. Phys. Chem. Lett.

M. Green, J. Kortright, T. Barbee, R. Carr and I. Lindau, **Scanning Tunneling Microscopy of X-Ray Optics:** J. Vac. Sci. Technol. A6, 428 (1988)

M.A. Green, M.K. Kelly, B. Lai, R.A. Otte, E.M. Rowe, J.P. Stott, W.S.Trzeciak, D.J. Wallace, W.R. Winter, F. Cerrina and H. Winick, **First Undulator Operation at SRC:** Nucl. Instrum. & Methods A266, 91 (1988)

D.M. Gualtieri, W. Lavender and S.L. Ruby, **^{57}Fe-YIG: Narrow X-Ray Linewidth Epitaxial Layers on $Gd_3Ga_5O_{12}$:** J. Appl. Phys. 63, 3795 (1988)

J.M. Guss, E.A. Merritt, R.P. Phizackerley, B. Hedman, M. Murata, K.O. Hodgson and H.C. Freeman, **Phase Determination by Multiple-Wavelength X-Ray Diffraction: Crystal Structure of a Basic "Blue" Copper Protein from Cucumbers:** Science 241, 806 (1988)

S. Hahn, M. Arst, K.N. Ritz, S. Shatas, H.J. Stein, Z.U. Rek and W.A. Tiller, **Effects of High Carbon Concentration Upon Oxygen Precipitation and Related Phenomena in CzSi:** J. Appl. Phys. 64, 849 (1988)

F.D. Hardcastle, I.E. Wachs, J.A. Horsley and G.H. Via, **The Structure of Surface Rhenium Oxide on Alumina from Laser Raman Spectroscopy and X-ray Absorption Near-Edge Spectroscopy:** J. Molecular Catalysis 46, 15 (1988)

M. Hart, W. Parrish, M. Bellotto and G.S. Lim, **The Refractive Index Correction in Powder Diffraction:** Acta. Cryst. A44, 193 (1988)

C.R. Hartzell, H. Beinert, G.T. Babcock, S.I. Chan, G. Palmer and R.A. Scott, **Heterogeneity in an Isolated Membrane Protein. Has the 'Authentic Cytochrome Oxidase' been Identified?:** FEBS Lett. 236, 1 (1988)

B. Hedman, P. Frank, S.F. Gheller, A.L. Roe, W.E. Newton and K.O. Hodgson, **New Structural Insights into the Iron-Molybdenum Cofactor from Azotobacter vinelandii Nitrogenase through Sulfur K and Molybdenum L X-Ray Absorption Edge Studies:** J. Am. Chem. Soc. 110, 3798 (1988)

B. Hedman, P. Frank, S.F. Gheller, W.E. Newton, E.I. Solomon and K.O. Hodgson, **Low Energy X-Ray Absorption Edge Spectroscopy: Applications to the Nitrogenase Cofactor and Electronic Structure of S and Cl in Inorganic Solids:** accepted for publication in Phys. B

W.A. Hendrickson and W.E. Royer, **Molecular Symmetry of Lumbricus Erythrocruorin:** J. Biol. Chem. 263, 13762 (1988)

W.A. Hendrickson, J.L. Smith, R.P. Phizackerley and E.A. Merritt, **Crystallographic Structure Analysis of Lamprey Hemoglobin from Anomalous Dispersion of Synchrotron Radiation:** Proteins 4, 77 (1988)

R.O. Hettel, **Beam Steering and Stabilizing Systems: Present Status and Considerations for the Future:** Nucl. Instrum. & Methods A266, 155 (1988)

R. Hille, G.N. George, M.K. Eidsness and S.P. Cramer, **EXAFS Analysis of Xanthine Oxidase Complexes with Alloxanthine, Violapterin, and 6-Pteridylaldehyde:** submitted to Inorg. Chem.

H. Hiraoka, A. Patlach, K.N. Chiong, D. Seligson and P. Pianetta, **Aqueous Developable, Negative-working Resist Made of Chlorinated Novolac Resin:** SPIE 920, 128 (1988)

J.J. Hoyt, B. Clark, D. DeFontaine, J.P. Simon and O. Lyon, **A Synchrotron Radiation Study of Phase Separation in Al-Zn Alloys. I. Kinetics:** accepted for publication in Acta Metall.

J.J. Hoyt and D. DeFontaine, **A Synchrotron Radiation Study of Phase Separation in Al-Zn Alloys. II. Scaling:** accepted for publication in Acta Metall.

S.R. Hubbard, K.O. Hodgson and S. Doniach, **Small-angle X-ray Scattering Investigation of the Solution Structure of Troponin C:** J. Biol. Chem. 263, 4151 (1988)

F.E. Huggins, G.P. Huffman, N. Shah, R.G. Jenkins, F.W. Lytle and R.B. Greegor, **Further EXAFS Examination of the State of Calcium in Pyrolysed Char:** Fuel 67, 938 (1988)

J. Hwang, C.K. Shih, P. Pianetta, G.D. Kubiak, R.H. Stulen, L.R. Dawson, Y.-C. Pao and J.S. Harris Jr., **Effect of Strain on the Band Structure of GaAs and $In_{0.2}Ga_{0.8}As$:** Appl. Phys. Lett. 52, 308 (1988)

J. Hwang, Y.C. Pao, C.K. Shih, Z.-X. Shen, P.A.P. Lindberg and R. Chow, **K-Resolved Alloy Bowing in Pseudobinary $In_xGa_{1-x}As$ Alloys:** Phys. Rev. Lett. 61, 877 (1988)

J.S. Iwanczyk, N. Dorri, M. Wang, M. Szawlowski, W.K. Warburton, B. Hedman and K.O. Hodgson, **Advances in Mercuric Iodide Energy Dispersive X-ray Array Detectors and Associated Miniaturized Processing Electronics:** submitted to Rev. Sci. Instrum.

J.S. Iwanczyk, W.K. Warburton, A.J. Dabrowski, B. Hedman, K.O. Hodgson and B.E. Patt, **Development of Mercuric Iodide Energy Dispersive X-ray Array Detectors:** IEEE Trans. Nucl. Sci. NS-35, 93 (1988)

J.S. Iwanczyk, W.K. Warburton, B. Hedman, K.O. Hodgson and A. Beyerle, **The HgI_2 Array Detector Development Project:** Nucl. Instrum. & Methods A266, 619 (1988)

D. Jiang, N. Alberding, A.J. Seary and E.D. Crozier, **An Angular Scanning Stage for Glancing-Incidence Surface EXAFS:** Rev. Sci. Instrum. 59, 60 (1988)

D. Jiang, N. Alberding, A.J. Seary, B. Heinrich and E.D. Crozier, **A Glancing-incidence Surface EXAFS Study of Epitaxially Grown Al/Ni/Fe(001):** accepted Physica B.

G.W. Johnson, D.E. Brodie and E.D. Crozier, **EXAFS Analysis of Vacuum Deposited Amorphous Germanium:** accepted for publication in Can. J. Phys.

J.-S. Kang, J.W. Allen, M.B. Maple, M.S. Torikachvili, W.P. Ellis, B.B. Pate, Z.-X. Shen, J.J. Yeh, and I. Lindau, **Counter-intuitive 5f Spectral Weight Shift in $Y_{1-x}U_xPd_3$:** submitted to Phys. Rev. Lett.

J.-S. Kang, J.W. Allen, Z.-X. Shen, W.P. Ellis, J.J. Yeh, B.-W. Lee, M.B. Maple, W.E. Spicer and I. Lindau, **Electronic Structure of the Quenched Superconductivity Materials $Y_{1-x}Pr_xBa_2Cu_3O_{7-\sigma}$:** J. Less. Common Metals 24 & 25 (1988)

J.-S. Kang and J.W. Allen, **Reply to Comments of "Spectral Evidence for the Importance of Single-Site Effects in Heavy-Fermion Uranium Materials:** Phys. Rev. Lett. 61, 651 (1988)

J.-S. Kang, J.W. Allen, B.-W. Lee, M.B. Maple, Z.X. Shen, J.J. Yeh, W.P. Ellis, W.E. Spicer and I. Lindau, **Electron Spectroscopy Studies of High Temperature Superconductors: $Y_{1-x}Pr_xBa_2Cu_3O_{7-\sigma}$:** J. Less Common Metals 148 & 149 (1988)

V. Karpenko, J.H. Kinney, S. Kulkarni, K. Neufeld, C. Poppe, K.G. Tirsell, J. Wong, J. Cerino, T. Troxel, J. Yang et al, **Beam Line 10 - A Multipole Wiggler Beam Line at SSRL:** submitted to Rev. Sci. Instrum.

L.-S. Kau, K.O. Hodgson and E.I. Solomon, **X-Ray Absorption Edge and EXAFS Study of the Copper Sites in ZnO Methanol Synthesis Catalysts:** submitted to J. Am. Chem. Soc.

T. Kendelewicz, P. Soukiassian, R.S. List, J.C. Woicik, P. Pianetta, I. Lindau and W.E. Spicer, **Bonding at the K/Si(100) 2x1 Interface: A Surface Extended X-Ray Absorption Fine-Structure Study:** Phys. Rev. B37, 7115 (1988)

P.L. King, L. Pan, P. Pianetta, A. Shimkunas, P. Mauger and D. Seligson, **Radiation Damage in Boron Nitride X-ray Lithography Masks:** J. Vac. Sci. Technol. B6, 162 (1988)

D.W. Kisker, P.H. Fuoss, K.L. Tokuda and S. Brennan, **In-Situ X-Ray Scattering Studies of OMVPE Growth of ZnSe:** accepted for publication in Mat. Res. Soc.

J.B. Kortright and A. Bienenstock, **X-ray Structural Study of Amorphous Mo-Ge Films:** Phys. Rev. B37, 2979 (1988)

C. Kumar, A. Naqui, L. Powers, Y.-C. Ching and B. Chance, **Does the Peroxide Compound of Cytochrome Oxidase Contain a Ferryl Iron?:** J. Biol. Chem. 263, 7159 (1988)

F.P. Larkins, W. Eberhardt, I.-W. Lyo, R. Murphy and E.W. Plummer, **The Core Hole Decay of N_2O Following Core to Bound State Excitations:** J. Chem. Phys. 88, 2948 (1988)

E.M. Larson, P.G. Eller, J.D. Purson, C.F. Pace, M.P. Eastman, R.B. Greegor and F.W. Lytle, **Synthesis and Structural Characterization of $CaTiO_3$ Doped with 0.5 - 7.5 Mole Percent Gadolinium(III):** J. Solid State 73, 408 (1988)

K.T. Leung, L.J. Terminello, Z. Hussain, X.S. Zhang, T. Hayashi and D.A. Shirley, **Surface Bonding Geometry of (2x1)S/Ge(001) by Normal-Emission Angle-Resolved Photoemission Extended Fine Structure Technique:** Phys. Rev. B38, 8241 (1988)

K. Libson, M. Woods, J.C. Sullivan, J. W. Watkins II, R.C. Elder and E. Deutsch, **Electron-Transfer Reactions of Technetium and Rhenium Complexes. 2. Relative Self-Exchange Rate of the M(I)/M(II) Couples $[M(DMPE)_3]^{+/2+}$, Where M=Tc or Re and DMPE=1,2-Bis(dimethylphosphino) ethane:** Inorg. Chem. 27, 999 (1988)

D.W. Lindle, T.A. Ferrett, P.A. Heimann and D.A. Shirley, **Photoemission from Xe in the Vicinity of the 4d Cooper Minimum:** Phys. Rev. A37, 3808 (1988)

D.W. Lindle, L.J. Medhurst, T.A. Ferrett, P.A. Heimann, M.N. Piancastelli, S.H. Liu, D.A. Shirley, T.A. Carlson, P.C. Deshmukh, G. Nasreen and S.T. Manson, **Angle-Resolved Photoemission from the Ar 2p Sub Shell:** Phys. Rev. A38, 2371 (1988)

R.Z. Liu and H. Winick, **A Missing-Bending-Magnet Scheme for PEP:** Nucl. Instrum. & Methods A266, 32 (1988)

F.W. Lytle, E.C. Marques, R.B. Greegor, H.G. Ahlstrom, E.M. Larson, D.E. Peterson and A.J. Panson, **Crystal Lattice Measurements in Superconducting Materials:** SPIE 879, 142 (1988)

F.W. Lytle, R.B. Greegor and A.J. Panson, **Discussion of X-Ray Absorption Near Edge Structure: Application to Cu in the High T_c Superconductors $La_{1.8}Sr_{0.2}CuO_4$ and $YBa_2Cu_3O_7$:** Phys. Rev. B37, 1550 (1988)

R.J. Madix, J.L. Solomon and J. Stöhr, **The Orientation of the Carbonate Anion on Ag(110):** Surf. Sci. 197, L253 (1988)

A. McDermott, V.K. Yachandra, R.D. Guiles, R.D. Britt, S.L. Dexheimer, K. Sauer and M.P. Klein, **Low Potential Membrane Bound Iron-Sulfur Centers in Photosystem I: An X-Ray Absorption Spectroscopy Study:** Biochem. 27, 4013 (1988)

A.E. McDermott, V.K. Yachandra, R.D. Guiles, J.L. Cole, S.L. Dexheimer, R.D. Britt, K. Sauer and M.P. Klein, **Characterization of the Manganese O_2-Evolving Complex and the Iron-Quinone Acceptor Complex in Photosystem II from a Thermophilic Cyanobacterium by Electron Paramagnetic Resonance and X-Ray Absorption Spectroscopy:** Biochem. 27, 4021 (1988)

L.J. Medhurst, T.A. Ferrett, P.A. Heimann, D.W. Lindle, S.H. Liu and D.A. Shirley, **Observation of Correlation Effects in Zero Kinetic Energy Electron Spectra Near the N1s and C1s Thresholds in N_2, CO, C_6H_6, and C_2H_4:** J. Chem. Phys. 89, 10 (1988)

G. Meitzner, G.H. Via, F.W. Lytle, S.C. Fung and J.H. Sinfelt, **Extended X-ray Absorption Fine Structure (EXAFS) Studies of Platinum-Tin Catalysts:** J. Phys. Chem. 92, 2925 (1988)

W.W. Moses and S.E. Derenzo, **Cerium Fluoride, A New Fast, Heavy Scintillator:** submitted to Nucl. Sci.

H.M.K. Murthy, W.A. Hendrickson, W.H. Orme-Johnson, E.A. Merritt and R.P. Phizackerley, **Crystal Structure of Clostridium acidi-urici Ferredoxin at 5-A Resolution Based on Measurements of Anomalous X-Ray Scattering at Multiple Wavelengths:** J. Biol. Chem. 263, 18430 (1988)

A. Naqui, L. Powers, M. Lundeen, A. Constantinescu and B. Chance, **On the Environment on Zinc in Beef Heart Cytochrome c Oxidase: An X-Ray Absorption Study:** J. Biol. Chem. 263, 12342 (1988)

Z. Otwinowski, R.W. Schevitz, R.-G. Zhang, C.L. Lawson, A. Joachimiak, R.Q. Marmorstein, B.F. Luisi and P.B. Sigler, **Crystal Structure of trp Repressor/ Operator Complex at Atomic Resolution:** Nature 335, 321 (1988)

L. Pan, P.L. King, P. Pianetta, D. Seligson and T.W. Barbee, **Synchrotron-Based X-Ray Lithography at Stanford University:** Nucl. Instrum. & Methods A266, 287 (1988)

W. Parrish, **Advances in Synchrotron X-Ray Polycrystalline Diffraction:** Aust. J. Phys. 41, 101 (1988)

J. Penner-Hahn, M. Murata, K.O. Hodgson and H.C. Freeman, **Low-temperature X-ray Absorption Spectroscopy of Plastocyanin: Evidence for Cu-site Photoreduction at Cryogenic Temperatures:** in press Inorg. Chem.

M.N. Piancastelli, T.A. Ferrett, D.W. Lindle, L.J. Medhurst, P.A. Heimann, S.H. Liu and D.A. Shirley, **Resonant Processes Above the Carbon 1s Ionization Threshold in Benzene and Ethylene:** submitted to J. Chem. Phys.

P. Pianetta and T.W. Barbee, **Applications of Multilayers to Synchrotron Radiation:** Nucl. Instrum. & Methods A266, 441 (1988)

R.C. Prince, G.N. George, J.C. Savas, S.P. Cramer and R.N. Patel, **Spectroscopic Properties of the Hydroxylase of Methane Monooxygenase:** Biochim. Biophys. Acta 952, 220 (1988)

I.K. Robinson, R.T. Tung and R. Feidenhans'l, **X-Ray Interference Method for Studying Interface Structures:** Phys. Rev. B38, 3632 (1988)

I.K. Robinson, A.A. MacDowell, M.S. Altman, P.J. Estrup, K. Evans-Lutterodt, J.D. Brock and R.J. Birgeneau, **Order-Disorder Transition of the W(001) Surface:** submitted to Phys. Rev. Lett.

S. Ruby, **Nuclear Inelastic Bragg Scattering and Synchrotrons: Questions and Some Answers:** Hyperfine Interactions 40, 63 (1988)

T.P. Russell, R. Jerome, P. Charlier and M. Foucart, **The Microstructure of Block Copolymers Formed via Ionic Interactions:** J. Am. Chem. Soc. 21, 1709 (1988)
T.P. Russell, **Investigations of Polymer Mixtures using Synchrotron Radiation:** Polymer News 11, 70 (1988)

J. Safranek, H. Wiedemann, W. Xie and S. Okuda, **Tolerance in Diffraction Limited Synchrotron Light Sources:** Nucl. Instrum. & Methods A266, 177 (1988)

M.G. Samant, M.F. Toney, G.L. Borges, L. Blum and O.R. Melroy, **In-Situ Grazing Incidence X-Ray Diffraction Study of Electrochemically Deposited Pb Monolayers on Ag(111):** Surf. Sci. 193, L-29-L36 (1988)

M.G. Samant, G. Bergeret, G. Meitzner and M. Boudart, **Anomalous Wide-Angle X-Ray Scattering and X-Ray Absorption Spectroscopy of Supported Pt-Mo Bimetallic Clusters. 1. Experimental Technique:** J. Phys. Chem. 92, 3542 (1988)

M.G. Samant, M.F. Toney, G.L. Borges, L. Blum and O.R. Melroy, **Grazing Incidence X-Ray Diffraction of Lead Monolayers at a Silver (111) and Gold (111) Electrode/Electrolyte Interface:** J. Phys. Chem. 92, 220 (1988)

M.G. Samant, G. Bergeret, G. Meitzner, P. Gallezot and M. Boudart, **Anomalous Wide-Angle X-Ray Scattering and X-Ray Absorption Spectroscopy of Supported Pt-Mo Bimetallic Clusters. 2. Atomic and Electronic Structure:** J. Phys. Chem. 92, 3547 (1988)

K. Sauer, R.D. Guiles, A.E. McDermot, J.L. Cole, V.K. Yachandra, J.-L. Zimmermann, M.P. Klein, S.L. Dexheimer, and R.D. Britt, **Spectroscopic Studies of Magnanese Involvement in Photosynthetic Oxygen Evolution:** Chemica Scripta 28A, 87 (1988)

J.R. Schoonover and S.H. Lin, **Time Resolved X-ray Diffraction of the Thermal Decomposition of $CdCO_3$ Powders Using Synchrotron Radiation:** J. Solid State Chem. 76, 143 (1988)

U. Schulze-Gahmen, J.M. Rini, J. Arevalo, E.A. Stura, J.H. Kenten and I.A. Wilson, **Preliminary Crystallographic Data, Primary Sequence, and Binding Data for an Anti-peptide Fab and Its Complex with a Synthetic Peptide from Influenza Virus Hemagglutinin:** J. Biol. Chem. 263, 17100 (1988)

R.A. Scott and M.K. Eidsness, **The Use of X-ray Absorption Spectroscopy for Detection of Metal-Metal Interactions Application to Copper-Containing Enzymes:** Inorg. Chem. 7, 235 (1988)

R.A. Scott, C.E. Cote and D.M. Dooley, **Copper X-ray Absorption Spectroscopic Studies of the Bovine Plasma Amine Oxidase-Sulfide Complex:** Inorg. Chem. 27, 3859 (1988)

R.A. Scott, R.J. Sullivan, W.E., Jr. DeWolf, R.E. Dolle and L.I. Kruse, **The Copper Sites of Dopamine β-Hydroxylase: An X-Ray Absorption Spectroscopic Study:** Biochem. 27, 5411 (1988)

D. Seligson, L. Pan, P. King and P. Pianetta, **Soft X-ray Dosimetry and its Application on the Lithography Beam Line at SSRL:** Nucl. Instrum. & Methods A266, 612 (1988)

Z.-X. Shen, J.W. Allen, J.J. Yeh, J.-S. Kang, W. Ellis, W.E. Spicer, I. Lindau, J.Z. Sun, T.H. Geballe, M.B. Maple and M.S. Torikachvili, **Photoemission Study of the Electronic Structure of Copper Oxide Superconductors:** Mat. Res. Soc. Symp. Proc. 99, 349 (1988)

C.K. Shih, Z.-X. Shen, P.A.P. Lindberg, J. Hwang, W.E. Spicer, S. Doniach and J.W. Allen, **Dispersion of One-Hole Excitation in An Antiferromagnetic Mott-Insulator: An Angle Resolved Photoemission Study:** submitted to Phys. Rev. A

A.R. Siedle, R.A. Newmark, W.B. Gleason, R.P. Skarjune, K.O. Hodgson, A.L. Roe and V.W. Day, **Rhodium and Iridium Oxometallates A New Class of Solid Microporous Materials:** Solid State Ionics 26, 109 (1988)

A.R. Siedle, R.A. Newmark, K.A. Brown-Wensley, R.P. Skarjune, L.C. Haddad, K.O. Hodgson and A.L. Roe, **Solid-State Organometallic Chemistry of Molecular Metal Oxide Clusters: C-H Activation by an Iridium Polyoxometalate:** Organometallics 7, 2078 (1988)

E.F. Skelton, **Microdiffraction with Synchrotron Beams (or Ultra-High Pressure Research):** Adv. X-ray Analysis 31, 1 (1988)

J.L. Solomon, R.J. Madix and J. Stöhr, **PI Bonded Intermediates in Alcohol Oxidation: Orientations of Allyloxy and Propargyloxy on Ag(110) by Near Edge X-Ray Absorption Fine Structure:** J. Chem. Phys. 89, 5316 (1988)

S. Sorenson, R. Carr, S. Schaphorst, S. Whitfield and B. Crasemann, **Coster-Kronig Yields in Silver Measured with Synchrotron Radiation:** submitted to Phys. Rev. A

P.A. Stevens, R.J. Madix and C.M. Friend, **Adsorbate Structural Determination of CO and HCNH using C K-edge NEXAFS on W(100)-(5x1)-C:** Surf. Sci. 205, 187 (1988)

S.R. Stock, Y.H. Chung and Z.U. Rek, **A Multiple-Slit Collimator for Synchrotron White Beam Section Topography:** submitted to J. Appl. Cryst.

G. Tan, L.S. Kau, K.O. Hodgson and E.I. Solomon, **Edge and EXAFS Studies of Cu Coordination in Deoxy Hemocyanin:** accepted for publication in Phys. B

D.H. Templeton and L.K. Templeton, **Polarization of Synchrotron Radiation:** J. Appl. Cryst. 21, 151 (1988)

L.K. Templeton and D.H. Templeton, **K-Edge Anomalous Scattering in Zinc Tartrate Hydrate:** J. Appl. Cryst. 21, 558 (1988)

L.K. Templeton and D.H. Templeton, **Biaxial Tensors for Anomalous Scattering of X-Rays in Selenolanthionine:** Acta Cryst. A44, 1045 (1988)

L.J. Terminello, X.-S. Zhang, Z.-Q. Huang, S. Kim, A.E. Schach von Wittenau, K.T. Leung and D.A. Shirley, **c(2x2)S/Cr(001) Surface and Near-Surface Structure Determined using Angle-Resolved Photoemission Extended Fine Structure:** Phys. Rev. B38, 3879 (1988)

A.C. Thompson, J.H. Underwood, Y. Wu, R.D. Giauque, K.W. Jones and M.L. Rivers, **Elemental Measurements with An X-ray Microprobe of Biological and Geological Samples with Femtogram Sensitivity:** Nucl. Instrum. & Methods A266, 318 (1988)
A.C. Thompson, R. Hofstadter, J.N. Otis, H.D. Zeman, R.S. Kernoff, E. Rubenstein, J.C. Giacomini, H.D. Gordon, G.S. Brown and W. Thomlinson, **Transvenous Coronary Angiography using Synchrotron Radiation:** Nucl. Instrum. & Methods A266, 252 (1988)

K.G. Tirsell, E.J. Berglin, B.A. Fuchs, F.R. Holdener, H.H. Humpal, V.P. Karpenko, S. Kulkarni and S.D. Fantone, **Highly Polished, Grazing Incidence Mirrors Developed for Synchrotron Radiation Beam Lines at Stanford Synchrotron Radiation Laboratory:** Optical Eng. 27, 985 (1988)

M.F. Toney and S. Brennan, **Structural Depth Profiling of Iron Oxide Thin Films Using Grazing Incidence Asymmetric Bragg X-Ray Diffraction:** submitted to J. Appl. Phys.

M.F. Toney, T. Huang, S. Brennan and Z. Rek, **Summary Abstract: Analysis of Co Doped Iron Oxide Thin Films by Grazing Incidence X-ray Diffraction:** J. Vac. Sci. Technol. A6, 1077 (1988)

M.F. Toney and S. Brennan, **Observation of the Effect of Refraction on X-Rays Diffracted in a Grazing Incidence Asymmetric Bragg Geometry:** submitted to Phys. Rev. B

M.F. Toney, T.C. Huang, S. Brennan and Z. Rek, **X-ray Depth Profiling of Iron Oxide Thin Films:** J. Mater. Res. 3, 351 (1988)

T. Troxel, G. Brown, J. Cerino and H. Wiedemann, **Measurement of Electron Beam Profile and Position using Pinhole Optics on SPEAR Beam Line II-3:** Nucl. Instrum. & Methods A266, 182 (1988)

T.A. Tyson, A.L. Roe, P. Frank, K.O. Hodgson and B. Hedman, **Polarized Experimental and Theoretical K-Edge X-Ray Absorption Studies of SO_4^{2-}, ClO_3^-, $S_2O_3^{2-}$ and $S_2O_6^{2-}$:** in press Phys. Rev. B

T.A. Tyson, A.L. Roe, B. Hedman, P. Frank and K.O. Hodgson, **A Study of the Electronic Structure of $S_2O_6^{2-}$ by Polarized K-edge X-ray Absorption Spectroscopy:** accepted for publication in Phys. B

T.A. Tyson, M. Benfatto, C.R. Natoli, B. Hedman and K.O. Hodgson, **Ab Initio EXAFS and Multiple Scattering Analysis of SF_6:** accepted for publication in Phys. B

A. Waldhauer, **Update on VUV and Soft X-ray Facilities at SSRL:** Nucl. Instrum. & Methods A266, 16 (1988)

G.A. Waychunas, G.E. Brown, C.W. Ponader and W.E. Jackson, **Evidence from X-ray Absorption for Network-Forming Fe^{2+} in Molten Alkali Silicates:** Nature 332, 251 (1988)

S.B. Whitfield, G.B. Armen, R. Carr, J.C. Levin and B. Crasemann, **Vacancy Multiplication Following Ni L-Shell Photoionization:** Phys. Rev. A37, 419 (1988)

H. Wiedemann, **An Ultra-Low Emittance Mode for PEP using Damping Wigglers:** Nucl. Instrum. & Methods A266, 24 (1988)

G. Will, M. Bellotto, W. Parrish and M. Hart, **Crystal Structures of Quartz and Magnesium Germanate by Profile Analysis of Synchrotron Radiation High Resolution Powder Data:** J. Appl. Cryst. 21, 182 (1988)

L. Wilson and A. Bienenstock, **Atomic Arrangements in Short Period Mo-Ge Multilayers Determined by Anomalous Scattering and EXAFS:** Mat. Res. Soc. Symp. Proc. 69, 103 (1988)

J. Woicik and P. Pianetta, **Near Edge Structure Study of SiGe:** submitted to Phys. Rev. B

J. Woicik and P. Pianetta, **Core Level Study of SiGe:** submitted to Phys. Rev. B

J. Woicik, R.S. List, B.B. Pate and P. Pianetta, **Epitaxial Growth and Band-structure Effects at the Si/Ge(111) Interface:** Mat. Res. Soc. Symp. 102, 283 (1988)

J.C. Woicik, R.S. List, B.B. Pate and P. Pianetta, **Splitting of the "White Line" 1s Absorption Edge in Crystalline Si, SiGe, and Dilute SiGe:** Solid State Commun. 65, 685 (1988)

C.Y. Yang, S.M. Heald, J.M. Tranquada, A.R. Moodenbaugh and X. Youwen, **Lattice Vibrational Studies of Superconducting $YBa_2Cu_3O_7$ by Polarized Extended X-Ray Absorption Fine-Structure Measurements:** Phys. Rev. B38, 6569 (1988)

B.P. Youngman, **History of Thermal/Stress Analysis Methods used at the Stanford Synchrotron Radiation Laboratory:** Nucl. Instrum. & Methods A266, 525 (1988)

B.P. Youngman and J. Arthur, **Thermal Performance of the SSRL Beam Line 6-2 Upstream Beryllium Window:** Am. Inst. of Phys. 171, 342 (1988)

F. Zaera, D. Fischer, R. Carr, E. Kollin and J. Gland, **Kinetics of Ethylidyne Formation on Pt(111) using NEXAFS:** ACS Symp. Ser. 378 (1988)

F. Zaera, D. Fischer, J. Gland and R. Carr, **Determination of Chemisorption Geometries for Complex Molecules by using NEXAFS: Ethylene on Ni(100):** J. Chem. Phys. 89, 5335 (1988)

Z.S. Zhang, L.J. Terminello, S. Kim, Z.Q. Huang, A. Schach von Wittenau and D.A. Shirley, **Chemisorption Structure of c(2x2)S/Fe(001) Determined by ARPEFS:** J. Chem. Phys. 89, 6538 (1988)

BOOKS AND CONFERENCES

R.Z. Bachrach, R.D. Bringans, and M.A. Olmstead, **Synchrotron Radiation Studies of Surfaces and Interfaces using In-Situ Materials Preparations** in Current Trends in the Physics of Materials, Intl. School of Physics Enrico Fermi Course CVI: Italian Physical Society Proceedings.

A. Bienenstock, S. Brennan, A. Fischer-Colbrie, P.H. Fuoss, K.F. Ludwig, Jr., L. Wilson, and W.K. Warburton, **X-ray Synchrotron Radiation Structural Studies of Amorphous Materials** in R.A. Weeks and D.L. Kinser Effects of Modes of Formation on the Structure of Glasses: (Trans Tech Publications, 1988) pp. 245-253.

G.S. Brown, **A Simple Monochromator for Diagnostic Imaging with Synchrotron Radiation** in Synchrotron Radiation Applications to Digital Subtraction Angiography: Italian Physica Society Conf. Proc, Vol. 10, 1988 pp. 89-94.

P. Frank, S.F. Gheller, B. Hedman, W.E. Newton, and K.O. Hodgson, **Spectroscopic Studies of the Purified FeMoco Cofactor from Azotobacter Vinelandii** in H. Bothe, et al. Nitrogen Fixation: Hundred Years After: (Gustav Fisher, Stuggart) 1988 p. 64.

H. Wiedemann, **Beam Stability and Vacuum Chamber Design in Vacuum Design of Advanced and Compact Synchrotron Light Sources:** Amer Inst of Physics, Conf. Proc. No 171.

H. Wiedemann, **Design of Dedicated Radiation Source for Digital Radiation Angiography** in Synchrotron Radiation Applications to Digital Subtraction Angiography: Italian Physica Soc Conf Proc Vol. 10, 1988 pp. 299-316.

H. Wiedemann, **Low Emittance Storage Ring Design** in Frontiers of Particle Beams: Springer Verlag, Vol. 296 (Berlin, 1988)

H. Wiedemann, **Storage Ring Optimization** in Handbook on Synchrotron Radiation, Vol 3.: North-Holland Physics Publishing, Amsterdam, 1988

H. Winick, **Wiggler Magnets as X-ray Sources for Angiography Studies** in Synchrotron Radiation Applications to Digital Subtraction Angiography: Italian Physica Society Conf. Proc., Vol. 10, 1988 pp. 283-97.

H.D. Zeman, J.N. Otis, R. Hofstadter, A.C. Thompson, G.S. Brown, W. Thomlinson, E. Rubenstein, J.C. Giacomini, H.J. Gordon, and R.S. Kernoff, **The Imaging Technology Used at the Synchrotron Radiation Laboratory** in Synchrotron Radiation Applications to Digital Subtraction Angiography: Italian Physica Society Conf. Proc., Vol. 10, 1988 pp. 75-82.

THESES

Two theses based on work at SSRL were completed in 1988 bringing the total number of completed theses to 129 from 20 different Universities.

L. Hsu	UC-Los Angeles	"Electronic Properties of a $PtGa_2$ Single Crystal and Photoemission Studies of the Electron Correlation Effects in the Ni-Ga and the Ni-In Intermetallic Compounds" (Advisor - R.S. Williams)
W.M. Lavender	Stanford University	"Observation and Analysis of X-ray Undulator Radiation from PEP" (Advisor - G.S. Brown)

Overview of SLAC Site

-Photo by Joe Faust

GPO 687-945/19204